NASA CR-167,763

NASA-CR-167763
19830004868

# A Reproduced Copy

**OF**

NASA CR-167,763

Reproduced for NASA

*by the*

**NASA Scientific and Technical Information Facility**

LIBRARY COPY

APR 6 - 1983

LANGLEY RESEARCH CENTER
LIBRARY NASA
HAMPTON, VIRGINIA

FFNo 672 Aug 65

NF01431

NASA CR 167765
c 1

N83-13139

Unclas
G3/16 01270

(NASA-CR-167763) SPACE OPERATIONS CENTER, SHUTTLE INTERACTION STUDY, VOLUME 1 Final Report (Rockwell International Corp.) 326 P HC A15/MF A01
CSCL 22A

# SPACE OPERATIONS CENTER — SHUTTLE INTERACTION STUDY (NAS9-16153)

SSD 81-0076

FINAL REPORT

VOLUME II, APPENDICES, BOOK II OF II

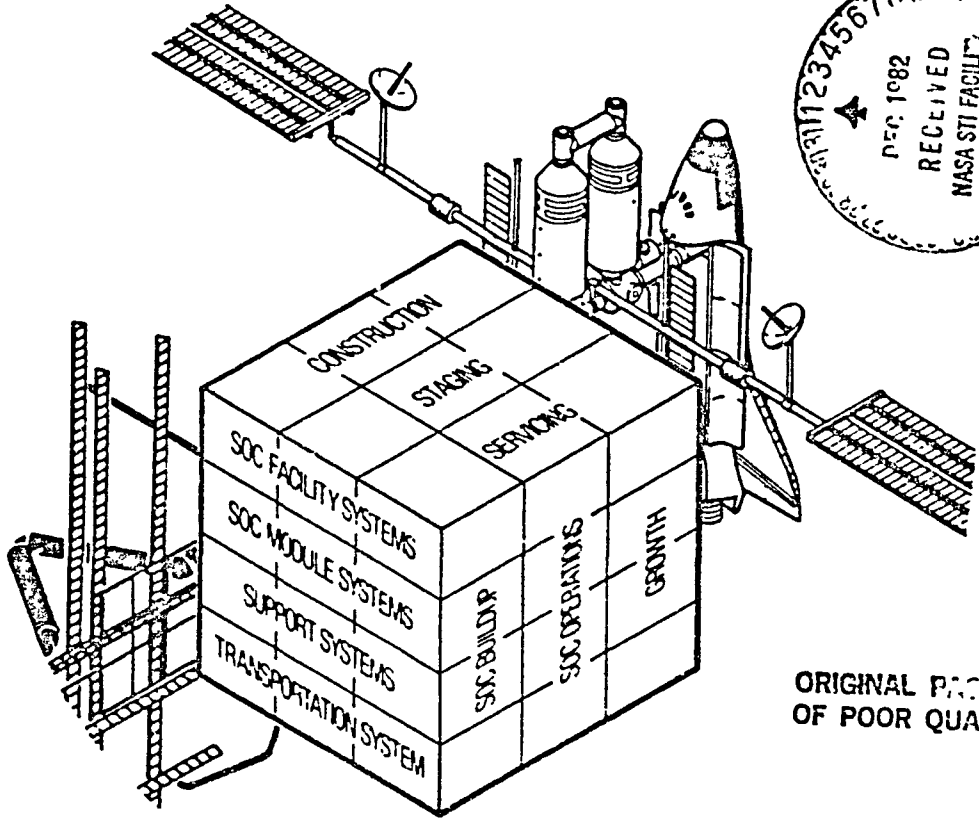


1 2 3 4 5 6 7 8 9 10 11 12
DEC 1982
RECEIVED
NASA STI FACILITY
ACCESS DEPT.

ORIGINAL PAGE IS
OF POOR QUALITY

DRL T-1626

LINE ITEM 3

April 17, 1981

Space Operations and Satellite Systems Division
Rockwell International

N83-13139 #

SSD 81-0076

# SPACE OPERATIONS CENTER/SHUTTLE INTERACTION STUDY

FINAL REPORT, VOLUME II
APPENDIXES (BOOK 2 OF 2)

Contract No. NAS9-16153
DRL T-1626
Line Item 3

April 17, 1981

Rockwell International
Space Operations and
Satellite Systems Division

ORIGINAL PAGE IS
OF POOR QUALITY



## 1.0 INTRODUCTION

The Space Operations Centre (SOC) is a reduced earth dependance facility constructed and serviced in near earth orbit by the Space Shuttle Orbiter.

The SRMS aided SOC/Orbiter berthing is an alternative procedure to the more conventional (using the RCS thrusters) SOC/Orbiter docking.

### 1.1 Objectives and Outline of the Report

This report is a first attempt to evaluate the feasibility of SRMS aided SOC/Orbiter berthing. The very nature of this study together with the limited funding available dictated the rather crude questions this study tries to answer: can The initial relative rates between the SOC and the Orbiter be removed by the arm and what is the best strategy, are the post-capture and manoeuvring loads within the capabilities of the SRMS; can the SOC berthing port be brought in the immediate proximity of the Orbiter berthing port and what is the best way to remove the residual relative motions, etc.

In the remainder of this section various notational conventions are established and various important locations on the Orbiter and SOC structure are defined. The relatively numerous reference frames which will be used throughout this study are also defined here together with the mass properties of both the SOC and the Orbiter.

Section 2.0 deals with the study assumptions and general approach.

Individual descriptions of each of the seven simulation runs performed and comments on the most pertinent results are the subject of Section 3.0.

Section 4.0 contains the general conclusions on the feasibility of SRMS aided SOC/Orbiter berthing and recommendations for future studies.

ORIGINAL PAGE IS
OF POOR QUALITY



Appendix A describes the variables plotted for each of the seven runs and Appendix B contains the plots. Appendix C has a short description of ASAD - the Spar developed SRMS non-real time simulation program.

## 1.2 Notation, Conventions and Definitions

Figure 1-1 shows the Orbiter/RMS/SOC configuration immediately after capture. The axis of the Orbiter berthing port is co-linear with the axis of the SOC berthing port. Figure 1-2 offers a similar view and in addition a side view from the Orbiter starboard. The Orbiter properties and the location of the Orbiter berthing port and of the RMS attach point are shown in Figure 1-3. Finally, Figure 1-4 defines SOC properties, the location of the SOC berthing port and of the grapple fixture.

The following locations are of main interest:

D = Centre of Orbiter berthing port interface

D' = Centre of SOC berthing port interface

G = End effector (EE)/SOC interface

$\oplus$ = SOC centre of mass

$\oplus_{ORB}$ = Orbiter centre of mass with 65 Klbs payload in the cargo bay

A = RMS attach point to the Orbiter

Reference frames are denoted by $\mathcal{F}_2$, where the lower index (1) designates the particular reference frame. The following reference frames will be used throughout this report:

ORIGINAL PAGE IS
OF POOR QUALITY



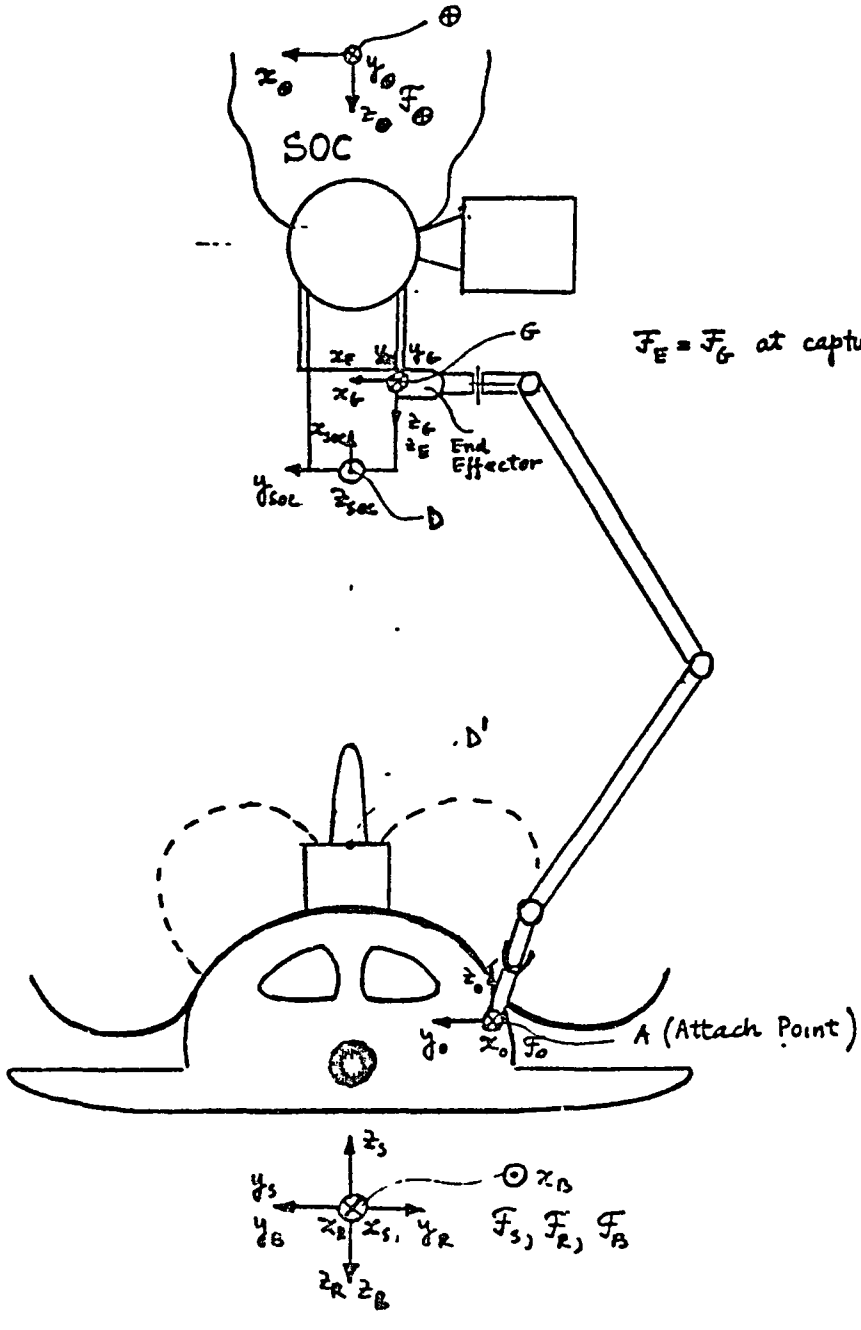


Fig 1-1 Capture geometry and various reference frames

ORIGINAL PAGE IS
OF POOR QUALITY

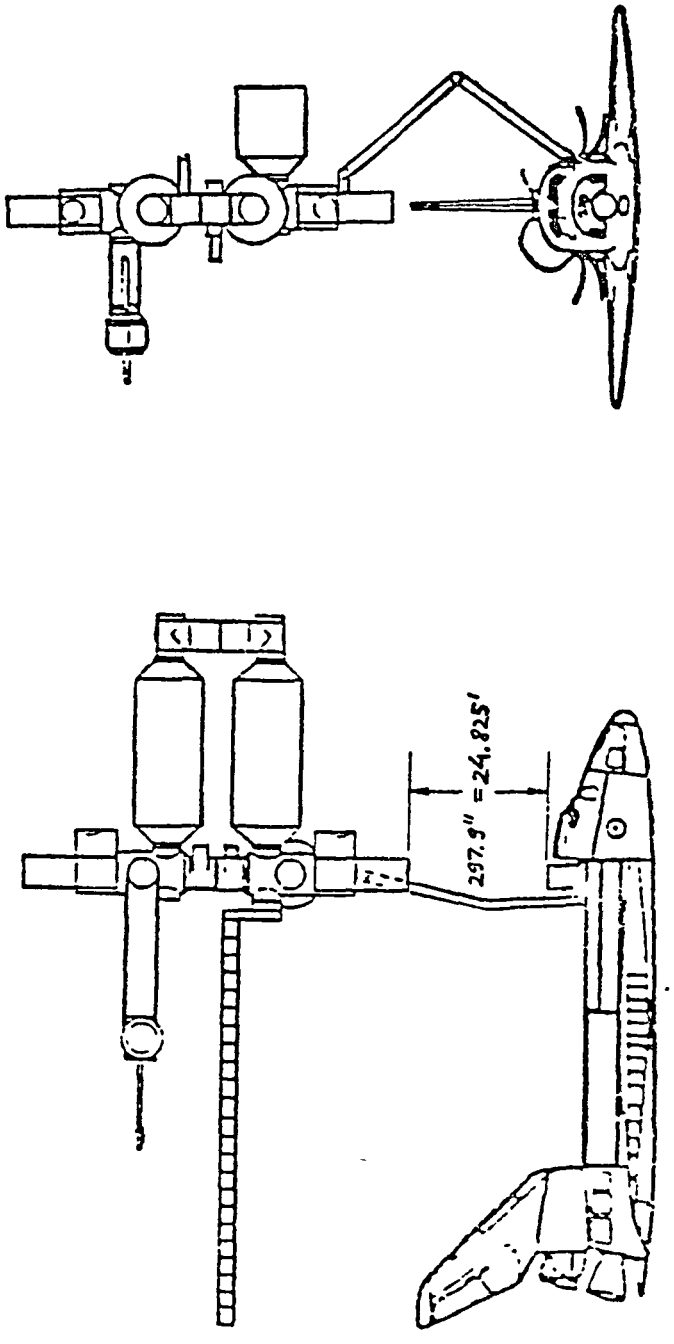


Fig 1-2. Capture geometry ; front and starboard view

ORBITER WITH 65 KLB PAYLOAD

MASS = 271,700 LB

$\oplus_{ORB}$ (IN.) $X_{\oplus ORB}$ = 1129.5
$Y_{\oplus ORB}$ = 0
$Z_{\oplus ORB}$ = 385.6

INERTIAL (SLUG FT$^2$)

| | | |
|---|---|---|
| $I_{XX}$ | = | 977,000 |
| $I_{YY}$ | = | 7,654,000 |
| $I_{ZZ}$ | = | 7,924,000 |
| $I_{XY}$ | = | 2,000 |
| $I_{YZ}$ | = | -2,000 |
| $I_{ZX}$ | = | 272,000 |

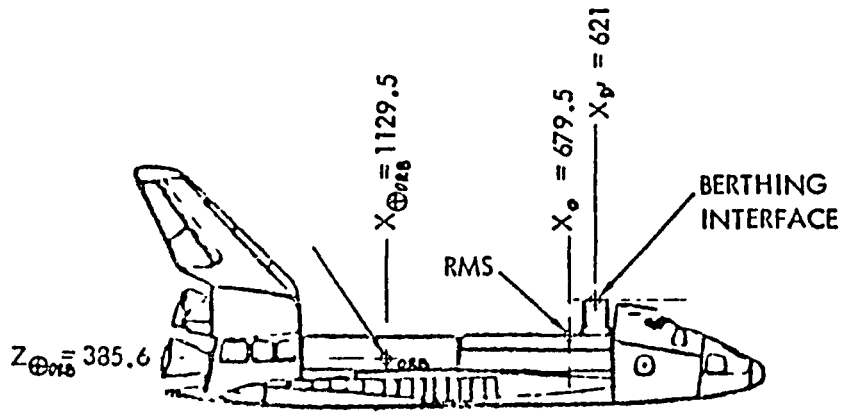


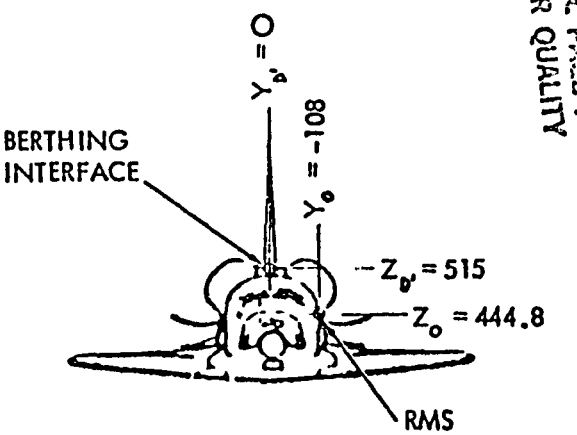


ORIGINAL PAGE IS OF POOR QUALITY



Fig 1-3. Orbiter mass properties and definition of berthing interface.

SOC CONFIGURATION
NO CONSTRUCTION FIXTURE
NO OTV
NO PLANETARY VEHICLE

MASS (LB) = 254,152
$\oplus^{SOC}$ (IN.) $X_\oplus$ = 526.68
$Y_\oplus$ = 2.16
$Z_\oplus$ = 44.28

INERTIAL (SLUG FT$^2$)
$I_{XX}$ = 10.041,413
$I_{YY}$ = 8,269,763
$I_{ZZ}$ = 10,047,094
$I_{XY}$ = +432,403
$I_{YZ}$ = -251,472
$I_{ZX}$ = -648,327

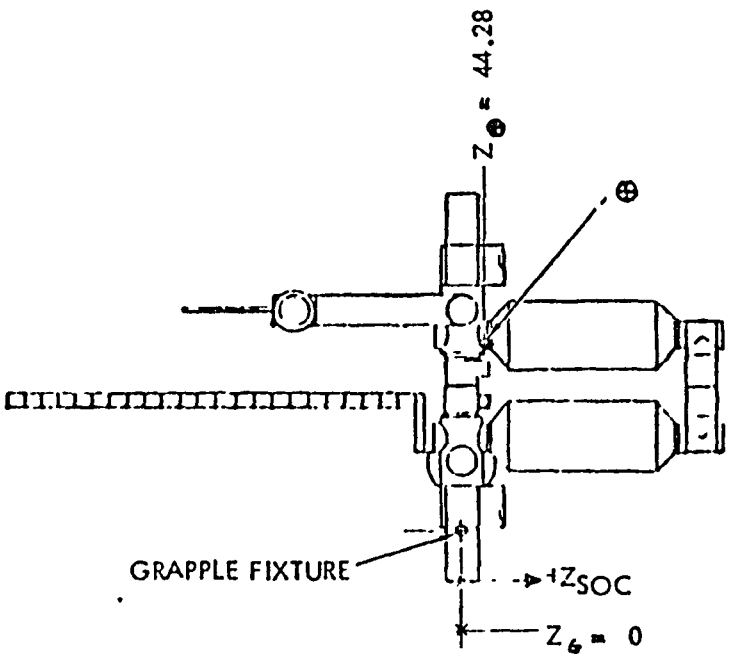


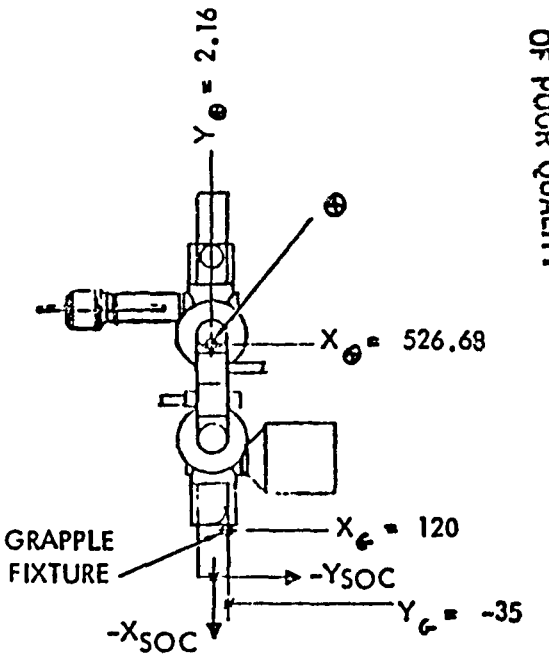


ORIGINAL PAGE IS
OF POOR QUALITY



Fig 1-4 SOC mass properties and definition of grapple fixture and berthing port

ORIGINAL PAGE IS
OF POOR QUALITY



$\mathcal{F}_S$ $(x_S, y_S, z_S)$ = Orbiter Structural Frame

$\mathcal{F}_B$ $(x_B, y_B, z_B)$ = Orbiter Body Frame

$\mathcal{F}_R$ $(x_R, y_R, z_R)$ = Orbiter Rotational Frame

$\mathcal{F}_{SOC}$ $(x_{SOC}, y_{SOC}, z_{SOC})$ = SOC Reference Frame

$\mathcal{F}_E$ $(x_E, y_E, z_E)$ = EE Operating Frame; the origin of $\mathcal{F}_E$ is on the EE/payload interface plane at its very centre. If the arm is swung out and all the other angles are set to zero, then $\mathcal{F}_E$ is parallel to $\mathcal{F}_R$.

$\mathcal{F}_G$ $(x_G, y_G, z_G)$ = The origin of this SOC fixed frame is G. If one rotates $\mathcal{F}_{SOC}$ 90° about $z_{SOC}$ followed by a rotation of -90° about $x_{SOC}$, then $\mathcal{F}_{SOC}$ becomes parallel with $\mathcal{F}_G$. This is enough to define the orientation of $\mathcal{F}_G$.

$\mathcal{F}_\oplus$ $(x_\oplus, y_\oplus, z_\oplus)$ = SOC (fixed) Operating Frame. $\mathcal{F}_\oplus$ is parallel to $\mathcal{F}_G$.

$\mathcal{F}_O$ $(x_O, y_O, z_O)$ = Payload Handling Frame. The origin of $\mathcal{F}_O$ is A. $\mathcal{F}_O$ is parallel to $\mathcal{F}_S$. One more reference frame has to be mentioned. In Figure 4 the inertia of SOC is defined with respect to a reference frame with origin at ⊕ and parallel to $\mathcal{F}_{SOC}$.

ORIGINAL PAGE IS
OF POOR QUALITY



The position of a point is denoted by $\underline{P}_1^u$, where the lower index (1) designates the point while the upper index (u) defines the reference frame relative to which the position vector is computed. For example, $\underline{P}_G^B$ is the position vector of G in $\mathcal{F}_B$. A similar convention applies for linear ($\underline{V}_1^u$) and angular ($\underline{\Omega}_1^u$) velocities. Every underlined variable is a matrix. $\underline{P}$, $\underline{V}$ and $\underline{\Omega}$'s are column matrices whose elements are the vector components in the reference frame indicated by the upper index. If the upper index is missing then the reference frame is $\mathcal{F}_{SOC}$.

Rotation matrices are denoted by $\underline{R}^{ij}$. In general $\underline{R}^{ij}$ is the matrix which transforms the components of a vector in $\mathcal{F}_j$ into the components of the same vector in $\mathcal{F}_i$.

To avoid tedious repetitions, the Euler angles describing the orientation of a SOC (or end effector) embedded reference frame, with respect to another reference frame are defined with the aid of the following column matrix:

$$\underline{\gamma}_1^u = [\gamma_1 \ \gamma_2 \ \gamma_3]^T$$

Where $\gamma_i$ ($i = 1, 2, 3$) are the Euler angles that will bring $\mathcal{F}_u$ into $\mathcal{F}_1$ if the following Euler sequence is followed:

pitch ($\gamma_1$), then yaw ($\gamma_2$), then roll ($\gamma_3$)

For example, $\underline{\gamma}_\phi^R$ defines the orientation of $\mathcal{F}_\phi$ with respect to $\mathcal{F}_R$.

ORIGINAL PAGE IS
OF POOR QUALITY



## 2.0 GENERAL DESCRIPTION OF THE SIMULATION RUNS

### 2.1 Assumptions and Study Approach

It was assumed that the SRMS-aided SOC/Orbiter berthing manoeuvre consists of the following phases:

(a) SOC capture phase*

(b) Stopping phase; this phase starts the moment (SOC) capture has been achieved ($\mathcal{F}_E = \mathcal{F}_G$) and lasts until the relative velocities and motions between SOC and Orbiter reach relatively small values.

(c) Manoeuvring phase; during this phase the SOC berthing port is brought to the proximity of the Orbiter berthing port; once the SOC reaches a certain 'pre-berth' position/ orientation, it is stabilized with respect to the Orbiter.

(d) Final SOC/Orbiter berthing.

---

* During the capture phase the following sequence occurs: the motor current limits are set to zero (i.e., the arm is made 'limp'), the grapple fixture (GF) is snared by the EE cables and is driven towards the centre of the snaring surface, the EE motor drives the whole snare assembly towards the inboard side of the EE, the GF ramps contact the EE, the GF ramps enter the 'roll adjustment cams', the SOC orientation is adjusted by the 'roll adjustment cams'. At this point the EE/GF misalignment should be minimal. In our simulations (runs 1, 2, 3, 4, 7 initial conditions) we assume it to be zero, i.e., $\mathcal{F}_E = \mathcal{F}_G$.

ORIGINAL PAGE IS
OF POOR QUALITY



In its present configuration ASAD does not have the payload capture simulation capability. Furthermore, the last phase (final SOC/Orbiter berthing) is also beyond the present scope and capability of ASAD. The study, therefore, was limited to the two intermediate phases, the stopping phase and the manoeuvring phase.

The major assumptions of the study are:

- Rigid SOC
- Orbiter and SOC attitude control systems are inactive.

Master Parameter List Issue E parameters were used for all the simulations [1]. In particular the following joint rate limits were enforced:

$\dot{\gamma}_{2c}{}^{u}$ = .115 deg/sec

$\dot{\gamma}_{3c}{}^{u}$ = .115 deg/sec

$\dot{\gamma}_{4c}{}^{u}$ = .160 deg/sec

$\dot{\gamma}_{5c}{}^{u}$ = .238 deg/sec

$\dot{\gamma}_{6c}{}^{u}$ = .238 deg/sec

$\dot{\gamma}_{7c}{}^{u}$ = .238 deg/sec

where $\dot{\gamma}_{ic}^{u}$ is the joint rate command limit for the $i^{th}$ joint.

A total of seven simulation runs were performed. The runs were defined through back and forth consultation between Rockwell and Spar. The results of the initial runs influenced the definition of the ensuing ones. Runs 1, 2, 3, 4, 7 simulate the stopping phase and were intended to find the best stopping strategy. Roughly speaking, two possible approaches can be envisaged for stopping the SOC:

(a) Passive approach; in this case the operator is not directly involved. Two strategies can be identified:

i) The normal operating procedure: the Manual Augmented Mode is the mode of operation for capture; once the capture command has been given and capture achieved the operator sets both hand controllers to null deflection (zero commands). It should be noted that in this operating mode and with zero hand controller commands, a switch to the Position Hold Mode will occur once all joint rates are less than some chreshold.

ii) Applying and maintaining zero joint rate commands; this is an emergency procedure since the zero commands are hardwired and bypass the Shuttle GPC (arm safing). However, we can think of no reason this stopping strategy could not be used for SOC/Orbiter berthing.

(b) Active approach; here the operator, using the hand controllers, is directly involved in trying to stop the SOC. For instance, the operator could command the arm to move in the direction of the capture vector but in the opposite sense. The active approach was not simulated in this study as one variation of the much simpler passive approach turned out to be quite successful.

Runs 5 and 6 simulate the manoeuvring phase. In the fifth run the SOC is commanded to approach the Orbiter in the Manual Augmented Mode of operation. The sixth run has the SOC approaching the pre-berth station in the computer controlled Operator Commanded Auto Sequence (OCAS). The accuracy of positioning and the removal of relative motion were the main concerns of this run.

This is probably an appropriate time to say a few words about some of the SRMS operational mode idiosyncracies which are directly relevant to our study.

The Position Hold Mode (PHM) of operation actively seeks to hold the arm configuration close to the 'commanded' configuration. Anticipating the results of this study, with the present PHM gains which were set to control payloads in the design range of 0 to 65000 lbs, the PHM of operation is marginally stable and as such unsuitaole for SOC/Orbiter berthing. On the other hand the Manual Augmented Mode (MAM) turns out to be well suited for both 'stopping' and stabilizing the SOC (with respect to the Orbiter) and for SOC manoeuvring. Now, the way the MAM is currently implemented, an automatic switch to PHM occurs whenever all the joint rates are within a certain threshold ( $\dot{\theta}_{TH}$ = .05 deg/sec) while both hand controlelrs are in neutral (zero linear and angular commands). To use MAM for SOC berthing one could inhibit the automatic engagement to PHM or update the software in the future to make the Position Hold Mode gain payload dependent, thus extending the range of stability of PHM. The automatic engagement to PHM can be inhibited, in principle, simply by making $\dot{\theta}_{TH}$ negative. For further reference we shall call the 'MAM with inhibited switching to PHM' the 'Modified Manual Augmented Mode' (MMAM) of operation.

It should be mentioned that MMAM in conjunction with zero commands is equivalent with 'safing the arm'. There are several ways safing is initiated. The interesting one is the Operator Commanded Safing (also known as Hardwired Safing). Operator Commanded Safing (OCS) is initiated from the D&C panel and it effectively sends hardwired zero joint rate commands to the arm joints. The hardwired signals bypass both the GPC and the MCIU. Clearly, OCS can be used for 'stopping' and stabilizing the SOC in the same way as MMAM is.

ORIGINAL PAGE IS
OF POOR QUALITY



The initial conditions will be discussed next followed by a section in which each run will be defined in detail.

## 2.2 Initial Conditions

### 2.2.1 Initial Configurations

The same initial configuration was used for runs 1, 2, 3, 4 and 7. The Orbiter berthing port is exactly aligned with the SOC berthing port (Figure 1-1 and 1-2). In other words, the capture configuration is such that the following simple manoeuvre will bring SOC to fully berthed position/orientation:

Translation: along $-z_S$ axis only

Rotation: none

The requirement that at capture the elbow joint should be less than -46° [2] in conjunction with the desire to capture the SOC as far away from the Orbiter as possible completed the specification of the initial configuration. The manipulator initial joint angles were generated* for SOC sliding along the $x_{SOC}$ axis. The configuration corresponding to:

---

* Using KINEMAT, a Spar developed SRMS kinematic simulation program. The same simulation revealed that the current tentative definition of the SOC grapple fixture is not quite acceptable; indeed, when SOC is fully berthed the shoulder pitch joint angle is:

$$140.4 < \gamma_3 = 142.3 < 142.4$$

where the lower limit is the reach limit location and the upper limit is the soft stop location. Note that the mechanical stop limit is at 145°.

ORIGINAL PAGE IS
OF POOR QUALITY



maximum $\gamma_4$: $\gamma_4 < -46°$

maximum D'D

was picked as the initial configuration, where $\gamma_4$ is the elbow angle while the distance D'D is defined in Figure 1-1. It was, thus found:

Initial Arm Configuration for Runs 1, 2, 3, 4, 7

| Configuration Space | Task Space |
|---|---|
| $\gamma_2$ = -108.1 deg | $\underline{p}_{\oplus}^{B} = [x_{\oplus}^{B} y_{\oplus}^{B} z_{\oplus}^{B}]^T$ |
| $\gamma_3$ = 93.9 deg | $= [-576.72 \ 2.16 \ -1339.58]^T$ in |
| $\gamma_4$ = -46.12 deg | |
| $\gamma_5$ = -68.19 deg | $\underline{\gamma}_{\oplus}^{B} = [\gamma_1 \ \gamma_2 \ \gamma_3]^T$ |
| $\gamma_6$ = 17.5 deg | $= [0 \ -90 \ 0]^T$ deg |
| $\gamma_7$ = 25.71 deg | Equivalently: |
| | $\underline{p}_{E}^{B} = [x_{E}^{B} \ y_{E}^{B} \ z_{E}^{B}]^T$ |
| | $= [-6.1. \ -35. \ -932.9]^T$ in |
| | $\underline{\gamma}_{E}^{B} = [\gamma_1 \ \gamma_2 \ \gamma_3]^T$ |
| | $= [0 \ -90 \ 0]^T$ deg |

ORIGINAL PAGE IS
OF POOR QUALITY



where $\gamma_2$ is the shoulder yaw, $\gamma_3$ is the shoulder pitch, $\gamma_4$ is the elbow pitch, $\gamma_5$ is the wirst pitch, $\gamma_6$ is the wrist yaw and $\gamma_7$ is the wrist roll.

For the initial configuration of runs 5 and 6 we picked the final configuration of run 3.

Initial Arm Configuration for Runs 5, 6

| Configuration Space | Task Space |
|---|---|
| $\gamma_2$ = -108.1 deg | $\underline{P}^B_{\oplus} = [x^B_{\oplus}\ y^B_{\oplus}\ z^B_{\oplus}]^T$ |
| $\gamma_3$ = 94.58 deg | $= [-574.7\ 11.94\ -1334.]^T$ in |
| $\gamma_4$ = -48 deg | $\underline{\xi}^R_{\oplus} = [\xi_1\ \xi_2\ \xi_3]^T$ |
| $\gamma_5$ = -68.04 deg | $= [-81.66\ -88.99\ -81.93]^T$ deg |
| $\gamma_6$ = 17.07 deg | |
| $\gamma_7$ = 27.54 deg | |

2.2.2 Initial Relative Velocities

In runs 1, 2, 3 and 4 the translational initial relative velocity is predominant while in run 7 it is the rotational velocity that dominates. In run 2 the relative linear velocity is perpendicular to the arm plane (containing the two long booms). In runs 1, 3 and 4 the linear velocity is mainly in the arm plane and towards the Orbiter.

ORIGINAL PAGE IS
OF POOR QUALITY



Initial Velocities for Runs 1, 3, 4

$\underline{V}_{\oplus}^{B} = [-.0108343 \quad .0 \quad .0994]^{T}$ ft/sec

$\underline{\Omega}_{\oplus}^{R} = [.0180276 \quad .0172 \quad .0]^{T}$ deg/sec

Initial Velocities for Run 2

$\underline{V}_{\oplus}^{B} = [-.09506 \quad .0293 \quad -.01036]^{T}$ ft/sec

$\underline{\Omega}_{\oplus}^{R} = [.0 \quad .0172 \quad -.0180276]^{T}$ deg/sec

Initial Velocities for Runs 5 and 6

$\underline{V}_{\oplus}^{B} = \underline{0}$

$\underline{\Omega}_{\oplus}^{R} = \underline{0}$

Initial Velocities for Run 7

$\underline{V}_{\oplus}^{B} = [-.03 \quad .03 \quad .03]^{T}$ ft/sec

$\underline{\Omega}_{\oplus}^{R} = [.1 \quad .1 \quad .1]^{T}$ deg/sec

ORIGINAL PAGE IS
OF POOR QUALITY



## 3.0 DESCRIPTION OF RUNS AND RESULTS

### 3.1 Run 1

#### Description of the Run

This run simulates the stopping phase. At the beginning of the simulation, immediately after capture, there are relative linear and angular motions between SOC and the Orbiter. For the first five seconds of the run the arm is limp (joint motor current limits are set to zero). The joint motor current limits are then (at time $t_r$) raised back to their nominal values in sudden, step-like manner (arm rigidization). Both hand controllers are set to null deflection (zero manual commands).

Initially the operating mode is Manual Augmented (MAM). A switch to Position Hold mode (PHM) occurs (see 2.1 (a) 1)) quite early in the run (at time $t_{sw}$).

#### Initial Configuration

$$\underline{P}^B_{\oplus} = [-576.72 \;\; 2.16 \;\; -1339.58]^T \text{ in}$$

$$\underline{\Upsilon}^R_{\oplus} = [0 \;\; -90 \;\; 0]^T \text{ deg}$$

#### Initial Velocities

$$\underline{V}^B_{\oplus} = [-.0108343 \;\; 0. \;\; .994]^T \text{ ft/sec}$$

$$\|\underline{V}^B_{\oplus}\| = .1 \text{ ft/sec}$$

ORIGINAL PAGE IS
OF POOR QUALITY



$\underline{\Omega}^R_{\oplus} = [.0180276 \quad .0172 \quad .0]^T$ ft/sec

$\|\underline{\Omega}^e_{\oplus}\| = .025$ deg/sec

We chose $\underline{V}^B_{\oplus}$ such that it lies in the arm plane* and its main component is along $Z_B$.

Duration of Simulation

$T_{END} = 800.$ sec

Rigidization Time

$t_r = 5.$ sec

Time of Switch to PHM

$t_{sw} = 6.8$ sec

Mode of Operation

MAM for time $t \in (0, 6.8)$ sec

PHM for time $t \in (6.8, 800)$ sec

Commands

$\underline{V}^B_{\oplus C} = \underline{0}, \quad \underline{\Omega}^R_{\oplus C} = \underline{0}$

throughout MAM mode of operation.

---

* $\underline{V}^{\mathcal{F}_2}_{\oplus} = [-.0349 \quad 0. \quad -.0937]^T$ ft/sec

where reference frame $\mathcal{F}_2$ is defined in Figure A-1.

ORIGINAL PAGE IS
OF POOR QUALITY



Results

In a certain sense the PHM is capable of 'stopping' the SOC (see plot of LINVEL 3/run 1). However, the same mode of operation is not capable of stabilizing the SOC with respect to the Orbiter. The plots show marginal stability or slight instability. Indeed, after 800 seconds, peak to peak excursions of the SOC centre of mass were:

$$\Delta p^{B}_{\delta x} = 16.2 \text{ inches, along } x_B$$

$$\Delta p^{B}_{\delta y} = 6.478 \text{ inches, along } y_B$$

$$\Delta p^{B}_{\delta z} = 1. \text{ inch, along } z_B$$

The PHM gains were designed for a maximum payload of 65,000 lbs. The analysis of the PHM control loop reveals about 6 db gain margin and 30 degrees phase margin for a 65000 lbs payload. It also shows that as the payload mass increases the phase margin decreases. Hence, under the current design the PHM is not suitable for stopping and stabilizing the SOC.

3.2 Run 2

Description of the Run

This run is quite similar with run 1. The only differences are in initial velocities (direction of the capture vector).

Initial Configuration

Same as run 1

ORIGINAL PAGE IS
OF POOR QUALITY



Initial Velocities

$\underline{V}^B_{\oplus} = [-.09506 \quad .0293 \quad -.01036]^T$ ft/sec

$\|\underline{V}^B_{\oplus}\| = .1$ ft/sec

$\underline{\Omega}^R_{\oplus} = [.0 \quad .0172 \quad -.0180276]^T$ deg/sec

$\|\underline{\Omega}^R_{\oplus}\| = .025$ deg/sec

We chose $\underline{V}^B_{\oplus}$ such that it is normal to the arm plane*.

Duration of Simulation

$T_{END} = 800.$ sec

Rigidization Time

$t_r = 5.$ sec

Time of Switch to PHM

$t_{sw} = 5.5$ sec

Mode of Operation

MAM for time $t \in (0, 5.5)$ sec

PHM for time $t \in (5.5$ to $800)$ sec

Commands

Same as run 1

---

* $\underline{V}^{\mathcal{F}_2}_{\oplus} = [0. \quad -.1 \quad 0.]^T$

ORIGINAL PAGE IS
OF POOR QUALITY



Results

PHM not suited for stopping and stabilizing the SOC. The plots show marginal stability. Of the two initial conditions, the capture vector perpendicular to the arm plane seems to exhibit less unstable behaviour. For more details see run 1.

3.3 Run 3

Description of the Run

This run is similar to run 1 except that it uses a different stopping strategy. The automatic engagement to PHM is inhibited; thus the MMAM (with zero commands for both linear and angular velocities) is the mode of operation throughout the run (see 2.1 (a)).

Initial Configuration

Same as run 1

Initial Velocities

Same as run 1

Duration of Simulation

$T_{END}$ = 800. sec

Rigidization Time

$t_r$ = 5. sec

Mode of Operation

MMAM

Commands

$$\underline{V}^{B}_{\oplus C} = \underline{0}; \qquad \underline{\Omega}^{R}_{\oplus C} = \underline{0}$$

ORIGINAL PAGE IS
OF POOR QUALITY



Results

The MMAM mode of operation in conjunction with zero hand controller commands turns out to be an excellent SOC 'stopping' strategy. After 400 seconds, for instance, the SOC centre of mass excursions were withir 1 inch in all three directions and the attitude excursions were within .2 of a degree. Also, after 400 seconds $\|\underline{V}^B_{\mathcal{O}}\| \leq .00162$ ft/sec = .02 inches/sec and $\|\underline{\Omega}^B_{\mathcal{O}}\| \leq .002$ deg/sec. The stopping distance (maximum excursion seen) is within 1.4 feet.

After rigidization some of the loads (torques at the arm hinges) reach relatively high levels for very short periods of time; the loads are, nevertheless, within bounds the arm can handle[3].

3.4 Run 4

Description of the Run

This run is similar with run 3. The only difference is in the inertia of the SOC which was increased about ten million times. The idea was to simulate the 'stopping phase' while (an ideal) SOC attitude control system was active.

Initial Configuration

Same as run 1

Initial Velocities

Same as run 1

Duration of Simulation

$T_{END}$ = 800. sec

Rigidization Time

$t_r$ = 5. sec

ORIGINAL PAGE IS
OF POOR QUALITY



Mode of Operation

MMAM

Commands

$$\underline{V}^{B}_{\oplus C} = 0; \qquad \underline{\Omega}^{R}_{\oplus C} = 0$$

Results

MAMM with zero hand controller commands is confirmed as a good strategy for 'stopping' the SOC. There is little to add to what was said about run 3. Higher frequencies are exhibited and slightly higher loads, the latter still within acceptable levels. Although the stopping distance is slightly larger, it is still less than 1.4 feet.

After 400 seconds $\|\underline{V}^{B}_{\oplus}\| \leq .00211$ ft/sec = .026 in/sec and $\|\underline{\Omega}^{B}_{\oplus}\| \leq .002$ deg/sec.

3.5 Run 5

Description of the Run

This simulation was done to demonstrate the manoeuvrability of SOC in MMAM. The initial configuraton is the one the manipulator had at the very end of run 3. The command is along $z_B$ axis, towards the pre-berth location.

Initial Configuration

$$\underline{P}^{B}_{\oplus} = [-574.7 \ \ 11.94 \ \ -1334.]^{T} \text{ in}$$

$$\underline{\Psi}^{R}_{\oplus} = [-81.66 \ \ -88.99 \ \ -81.93]^{T} \text{ deg}$$

ORIGINAL PAGE IS
OF POOR QUALITY



Initial Velocities

$\underline{V}^B_{\oplus} = \underline{0}$, $\underline{\Omega}^R_{\oplus} = \underline{0}$

Duration of Simulation

$T_{END}$ = 400. sec

Mode of Operation

MMAM

Commands

$\underline{V}^B_{\oplus C}$ = [0. 0. .1]$^T$ ft/sec for $t \in [0 \quad T_{END}]$

$\underline{\Omega}^R_{\oplus C} = \underline{0}$

Results

During the 400 seconds the simulation lasts, the SOC travels almost 15 feet. The 'allowed' command (dependent on the arm configuration and joint rate limits) is slowly increasing from $\|\underline{V}^B_{\oplus C}\|$ = .02393 ft/sec at the beginning of the run to $\|\underline{V}^B_{\oplus C}\|$ = .05062 ft/sec at the end of the run.

During the 15 ft of vertical travel towards the Orbiter the maximum drift (uncommanded motion) of the SOC centre of mass is about 14 inches along $x_B$ and about 10.5 inches along $y_B$ and occurs at the time t = 350 sec.

The overall dynamics is smooth and uneventful, confirming the suitability of the MMAM for SOC manoeuvring.

## 3.6 Run 6

### Description of Run

This run tests the use of the Operator Commanded Auto Sequence (OCAS), an automatic mode of operation of the SRMS, for SOC manoeuvring. A slightly modified version of the OCAS is also used for positioning and stabilizing the SOC at the pre-berth location. The pre-berth position/orientation is entered by the SRMS operator as the target (final) position/orientation (see below).

In OCAS the arm guidance algorithm commands the arm along a 'straight' line trajectory from the initial position/orientation to the desired final position/oreintation at either maximum linear speed or maximum angular speed (whichever speed has the larger corresponding 'time to accomplish'). Inside the so-called 'washout spheres' (target neighbourhood defined by 2 feet distance and .1 rad angular difference) the commanded velocities are decreased ('washed-out') according to an exponential function. The standard OCAS algorithm is such that whenever the arm position/orientation ($\mathcal{T}_{\Phi}$) intersects the so-called 'position-hold' spheres (another target neighbourhood, much smaller than the 'wash-out' spheres) the system switches into PHM. In run 6 the switch to PHM was inhibited as previous simulation already displayed the marginal stability of this operating mode. The position hold mode has constant gains multiplying the joint angular error. The OCAS also uses position measurements and feedback. Indeed the difference between the instantaneous position/orientation and the target position/orientation is used for defining direction of the linear and angular commands. One could think of OCAS as a position hold mode with variable gains. It was hoped that this mode of operation will be effective in stabilizing the SOC in the pre-berth position/orientation.

ORIGINAL PAGE IS
OF POOR QUALITY



Initial Configuration

Same as run 5

Initial Velocities

$\underline{V}_{\mathcal{B}}^{B} = \underline{0}$

$\underline{\Omega}_{\mathcal{B}}^{R} = \underline{0}$

Duration of Simulation

$T_{END}$ = 800. sec

Mode of Operation

OCAS

Commands

The following defines the position/orientation of $\mathcal{F}_{\mathcal{B}}$ corresponding to the pre-berth station (D is 2 feet above D', see Figure 1-1; Orbiter berthing port is perfectly aligned to the SOC berthing port).

$p^{B} = [-576.72 \ 2.16 \ -1065.68]^{T}$ in

$\underline{\Omega}_{f}^{R} = [0 \ -90 \ 0]^{T}$ deg

ORIGINAL PAGE IS
OF POOR QUALITY



Results

As long as the arm is not close to the target the OCAS mode of operation shows smooth and stable dynamics. Even inside the 'wash-out' spheres, for a while at least, the evolution of the arm is uneventful. However as we approach the target the same marginally unstable behaviour is exhibited.

3.7 Run 7

Description of the Run

This run is similar with run 3 except that the initial relative velocities are more severe. Indeed, while the linear relative velocity is about half the one in run 3 (and in a different direction) the angular relative velocity is about seven times larger. (The maximum allowed residual angular velocity according to capture operating procedures [2]).

Initial Configuration

Same as run 1

Initial Velocities

$$\underline{V}_{\mathcal{B}}^{B} = [-.03 \quad .03 \quad .03]^{T} \text{ ft/sec}$$

$$\|\underline{V}_{\mathcal{B}}^{B}\| = .0519615 \text{ ft/sec}$$

$$\underline{\Omega}_{\mathcal{B}}^{R} = [.1 \quad .1 \quad .1]^{T} \text{ deg/sec}$$

$$\|\underline{\Omega}_{\mathcal{B}}^{R}\| = .1732 \text{ deg/sec}$$

ORIGINAL PAGE IS
OF POOR QUALITY



Duration of Simulation

$T_{END}$ = 800. sec

Mode of Operation

MMAM

Commands

$\underline{V}^{B}_{\mathcal{O}C} = \underline{0}$; $\quad \underline{\Omega}^{B}_{\mathcal{O}C} = \underline{0}$

Results

Again, MMAM in conjunction with zero hand controller commands, is confirmed as a good strategy for 'stoping' and stabilizing the SOC (with respect to the Orbiter). The loads reach high values for short periods of time (immediately after rigidization) yet within acceptable levels.

After 400 seconds $\|\underline{V}^{B}_{\mathcal{O}}\| \leq .002596$ ft/sec = .032 inches/sec and $\|\underline{\Omega}^{B}_{\mathcal{O}}\| \leq .003$ deg/sec

SUMMARY OF SRMS BERTHING SIMULATION RUNS

| Run No. | Case Conditions | Summary Results |
|---|---|---|
| 1 | o Arrest initial motion .1 ft/sec, .025°/sec)<br><br>o MAM/controllers in neutral (i.e. zero rate commands) for the first few seconds, PHM afterwards | o PHM automatically engaged few seconds after 'rigidization'<br><br>o System in PHM exhibits marginal stability. After 800 sec:<br>- no appreciable dar ing<br>- SOC cen e of mass peak to peak excursions 1.5 ft<br><br>o PHM not suited for stopping and/or stabilizing the SOC |
| 2 | o Same as above with initial motion perpendicular to the arm plane | o Same as above |
| 3 | o Arrest initial motion (.1 ft/sec, .025°/sec) Motion in the arm plane<br><br>o MMAM/controllers in neutral | o MMAM/controllers in neutral' is a good strategy for stopping and/or stabilizing the SOC. After 400 sec:<br>- SOC centre of mass peak to peak excursions within 1 inch<br>- SOC attitude excursion within .2 deg |

SUMMARY OF SRMS BERTHING SIMULATION RUNS - continued

| Run No. | Case Conditions | Summary Results |
|---|---|---|
| | | o Relatively high loads for short periods immediately after rigidization; levels acceptable |
| 4 | o Same as above with 'huge' SOC inertia; simulate 'stopping phase' while (an ideal) SOC ACS is active | o 'MMAM/controllers in neutral' confirmed as good strategy for stopping and/or stabilizing the SOC<br>o Higher frequencies are exhibited and slightly higher loads, the latter still with acceptable levels |
| 5 | o Manoeuvre SOC in MMAM<br>o Initial conditions from end of run 3<br>o Command towards 'pre-berth' position/ orientation | o MMAM quite suitable for manoeuvring the SOC |
| 6 | o Using slightly modified OCAS:<br>- Manoeuvre the SOC to 'pre-berth' pos/orient<br>- Stabilize the SOC at 'pre-berth' pos/orient | o OCAS quite suitable for manoeuvring the SOC<br>o OCAS not suitable for stabilizing the SOC; marginal stability is exhibited in the neighbourhood of target |

SUMMARY OF SRMS BERTHING SIMULATION RUNS - continued

| Run No. | Case Conditions | Summary Results |
|---|---|---|
| | o Initial condition from end of run 3 | ('pre-berth' position/ orientation) |
| 7 | o Arrest initial motion (.052 ft/sec, .1732°/sec)<br>o MMAM/controlelrs in neutral | o 'MMAM/controllers in neutral' confirmed as the strategy for stopping and/or stabilizing the SOC |

NOTE: MAM = Manual Augmented Mode of Operation

MMAM = Modified Manual Augmented Mode of Operation

PHM = Position Hold Mode of Operation

OCAS = Operator Commanded Automatic Sequence Mode of Operation

# 4.0 CONCLUSION

## 4.1 Feasibility of SRMS Aided Berthing

Within the assumptions of this study, the SRMS-aided SOC/Orbiter berthing appears to be entirely feasible.

Before summarizing the more interesting results let us say a few words about the loads (hinge torques) exhibited by the arm. The largest loads were encountered in the 'stopping phase' simulations. Immediately after 'rigidization' (rise of the joint motor current limits to their nominal values) some hinge torques exhibit, for very short duration, relatively high levels. In no case, however do they reach unacceptable levels.

The simulation results show the Manual Augmented (Rate) Mode of operation eminently suited for manoeuvring the SOC.

The adequate damping and small drift makes the MAM, in conjunction with zero rate commands (MMAM) also quite appropriate for stopping and stabilizing the SOC (with respect to the Orbiter). More needs to be said here. The author had no available information (if indeed there is any) about the nature and sequence of operations during an eventual SRMS-aided SOC/Orbiter berthing. As such, he had to assume a certain scenario. Part of this scenario was the stabilization of SOC with respect to the Orbiter in some designated 'pre-berth' position/orientation. This was considered desirable in order to allow the operator a last inspection and to make the last berthing manoeuvre (proper SOC/Orbiter berthing) a very simple one (for example: a translation along $z_B$ axis). Now it might turn out that this intermediate stage is not necessary, the payload operator feeling comfident he can achieve berthing by continous 'gentle' use of the hand controllers. On the other hand, if 'pre-berth' stabilization is needed

the following question needs to be answered: is the MMAM adequate? The result of the simulations give an afirmative answer. Nevertheless one would feel more confident* if a position hold mode, i.e., an arm control mode of operation which will actively seek to hold the arm in (or very close to) a desired position/oreintation, would be available and effective. In its current implementation the SRMS proper PHM turns out to be marginally unstable (see runs 1 and 2), hence not suited for our purpose. This came as no real surprise since the whole position hold loop was designed for a 65 Klbs maximum payload mass.

The 'targetting' algorithm of the OCAS mode of operation, as implemented within the 'wash-out' spheres, was also tried. The same 'marginal' stability ensued (run 6). It should be noted however, that, outside the 'washout' spheres the OCAS is perfectly stable. It might turn out that a simple change (of the exponent) in the 'washout' algoritnm will result in a perfectly satisfactory position hold algorithm.

Another alternative for SOC pre-berth stabilization is to apply the brakes once the SOC reached the pre-berth position/orientation and the residual velocities are within acceptable limits.

* ASAD is a simulation. Throughout all the simulations performed for this study the SOC structural flexibility has been neglected, both the Orbiter ACS and the SOC ACS were inactive, and no environmental forces or torques were modelled in.

## 4.2 Future Studies

In many cases future studies are recommended to remove doubts introduced by various assumptions. A rigid SOC is a major assumption as it seems that SOC has considerable structural flexibility. Spar has recently begun work aimed at increasing ASAD capabilities such that it can accommodate flexible payloads. It is expected that this relatively major development will be finished in the second quarter of 1982. We recommend that several of the present simulations be repeated with flexible SOC.

Meanwhile, the time can probably be best utilized by redesigning the PHM and/or the OCAS 'targetting/washout' algorithm such that it can handle payloads with mass properties similar to SOC. While either of the envisaged changes might require additional memory (for example load dependent gains in PHM), it is anticipated the additional memory required to be very small and the corresponding software changes rather trivial. Note that neither of the suggested modifications requires hardware changes.

REFERENCES

[1] Simulation procedures for SRMS Verification and Certification Support, SPAR-RMS-TP.240, Issue B, March, 1980, pp. A1-A13.

[2] SRMS Operating Procedures', R.849, Issue C, 1980.

[3] Load Specification SRMS Manipulator Arm, SPAR-SG.409, Issue E.

# APPENDIX A

## DEFINITION OF THE PLOTTED VARIABLES

ORIGINAL PAGE IS
OF POOR QUALITY

| Plotted Variable Symbol | Description |
|---|---|
| THETA 1 | Orbiter roll angle |
| THETA 2 | Orbiter pitch angle |
| THETA 3 | Orbiter yaw angle |
| | The first three variables are Euler angles. Sequence: pitch, then yaw, then roll. This sequence brings $\mathcal{F}_I$ (inertial reference frame) to $\mathcal{F}_B$ at any instant in time. Note that $\mathcal{F}_I = \mathcal{F}_B$ at the very beginning of the simulation. Also read relevant material in Appendix C. |
| | The next three variables are the components of Orbiter angular velocity (relative to $\mathcal{F}_I$) expressed in $\mathcal{F}_0$: |
| WOS 1 | Component along $x_0$ |
| WOS 2 | Component along $y_0$ |
| WOS 3 | Component along $z_0$ |
| | The next three variables are the components of $\underline{P}_{\oplus}^{B}$, the position of $\oplus$ in $\mathcal{F}_B$ |
| POS 1 | Component along $x_B$ |
| POS 2 | Component along $y_B$ |
| POS 3 | Component along $z_B$ |
| | The next three variables are the Euler angles defining the orientation of $\mathcal{F}_\oplus$ with respect to $\mathcal{F}_R$. The seqence is pitch, then yaw, then roll, from $\mathcal{F}_R$ to $\mathcal{F}_\oplus$ |
| ATT/P 1 | Pitch (about y ) |
| ATT/Y 2 | Yaw (about z |
| ATT/R 3 | Roll (about x ) |
| | The next three variables are the components of $\underline{V}_{\oplus}^{B}$, the velocity of $\mathcal{F}_\oplus$ relative to and expressed in $\mathcal{F}_B$ |

ORIGINAL PAGE IS
OF POOR QUALITY



| Plotted Variable Symbol | Description |
|---|---|
| LINVEL 1 | Component along $x_B$ |
| LINVEL 2 | Component along $y_B$ |
| LINVEL 3 | Component along $z_B$ |
| | The next three variables are the components of $\underline{\Omega}_{@}^{R}$, the angular velocity of SOC relative to and expressed in $\mathcal{F}_R$ |
| ANGVEL 1 | Component along $x_R$ |
| ANGVEL 2 | Component along $y_R$ |
| ANGVEL 3 | Component along $z_R$ |
| ABSVT | Magnitude of $\underline{V}_{@}^{B}$ |
| ABOMGT | Magnitude of $\underline{\Omega}_{@}^{R}$ |
| GAM 1 | Swingout joint angle |
| GAM 2 | Shoulder yaw joint angle |
| GAM 3 | Shoulder pitch joint angle |
| GAM 4 | Elbow pitch joint angle |
| GAM 5 | Wrist pitch joint angle |
| GAM 6 | Wrist yaw joint angle |
| GAM 7 | Wrist roll joint angle |
| GAM 8 | Freeplay angle at the grapple point, about the grapple fixture axis |
| GAMDT 1 | Swingout joint rate |
| GAMDT 2 | Shoulder yaw joint rate |
| GAMDT 3 | Shoulder pitch joint rate |
| GAMDT 4 | Elbow pitch joint rate |
| GAMDT 5 | Wrist pitch joint rate |

ORIGINAL PAGE IS
OF POOR QUALITY



| Plotted Variable Symbol | Description |
|---|---|
| GAMDT 6 | Wrist yaw joint rate |
| GAMDT 7 | Wrist roll joint rate |
| GAMDT 8 | Grapple point rate of elastic deformation, about the grapple fixture axis |
| TCM 1 | Joint freeplay torque of elastic deformation at the swingout joint about $\underset{\sim}{1}_1$ , ($\gamma_1$) axis (see Figure A-1) |
| | The next six variables are the gearbox output torques as seen on the joint side (or the joint input torques). |
| TCM 2 | Shoulder yaw |
| TCM 3 | Shoulder pitch |
| TCM 4 | Elbow pitch |
| TCM 5 | Wrist pitch |
| TCM 6 | Wrist yaw |
| TCM 7 | Wrist roll |
| TCM 8 | Torques of elastic deformation (at EE/payload interface( about $\underset{\sim}{1}_8$ ($\gamma_8$) axis (see Figure A-1) |
| | The next eight variables are joint freeplay torques of elastic deformation about $\alpha$-axes at (see Figure A-1). |
| UAFK 1 | Swingout joint |
| UAFK 2 | Shoulder yaw joint |
| UAFK 3 | Shoulder pitch joint |
| UAFK 4 | Elbow pitch joint |
| UAFK 5 | Wrist pitch joint |

ORIGINAL PAGE IS
OF POOR QUALITY



| Plotted Variable Symbol | Description |
|---|---|
| UAFK 6 | Wrist yaw joint |
| UAFK 7 | Wrist roll joint |
| UAFK8 | Grapple point (SOC/end effector interface) |
| | The next eight variables are joint freeplay torques of elastic deformation about $\beta$- axes at (see Figure A-1) |
| UBFK 1 | Swingout joint |
| UBFK 2 | Shoulder yaw joint |
| UBFK 3 | Shoulder pitch joint |
| UBFK 4 | Elbow pitch joint |
| UBFK 5 | Wrist pitch joint |
| UBFK 6 | Wrist yaw joint |
| UBFK 7 | Wrist roll joint |
| UBFK8 | Grapple point (SOC/end effector interface) |

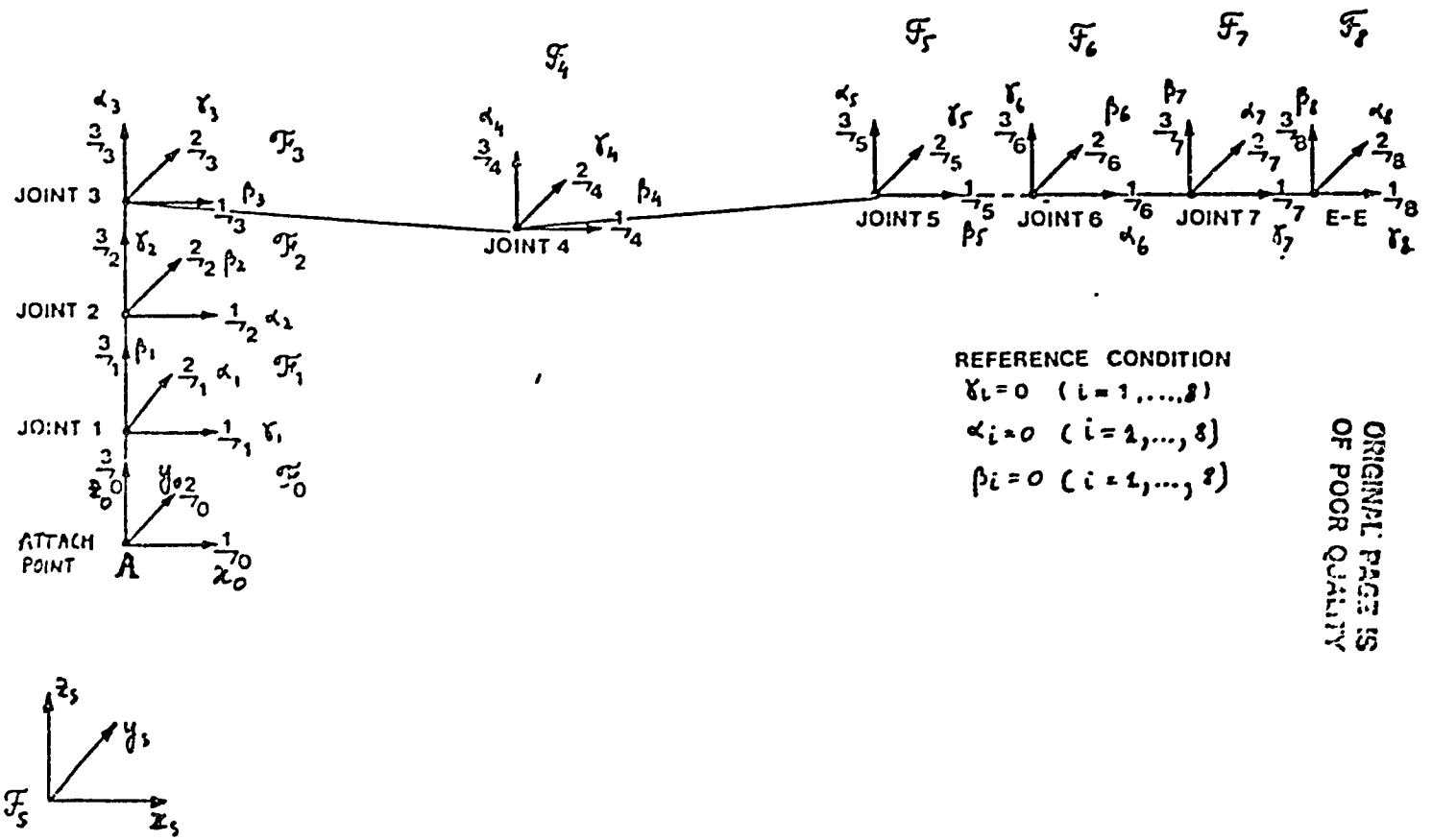


Fig A-1 Arm Control Reference Frames



ORIGINAL PAGE IS OF POOR QUALITY

ORIGINAL PAGE IS
OF POOR QUALITY



# APPENDIX B

## PLOTS

ORIGINAL PAGE IS
OF POOR QUALITY

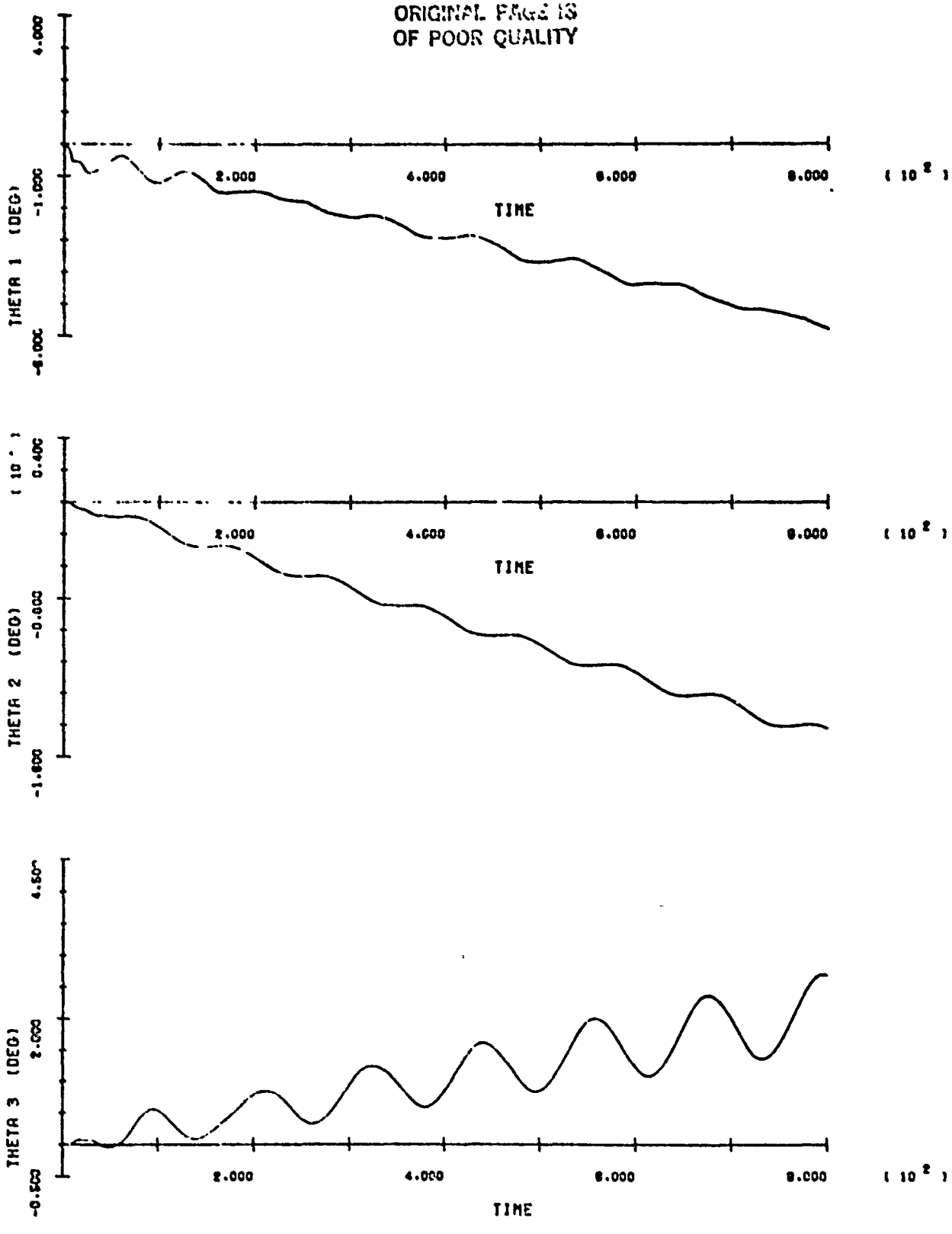


SOC/ORBITER BERTHING RUN 1

ORIGINAL PAGE IS
OF POOR QUALITY

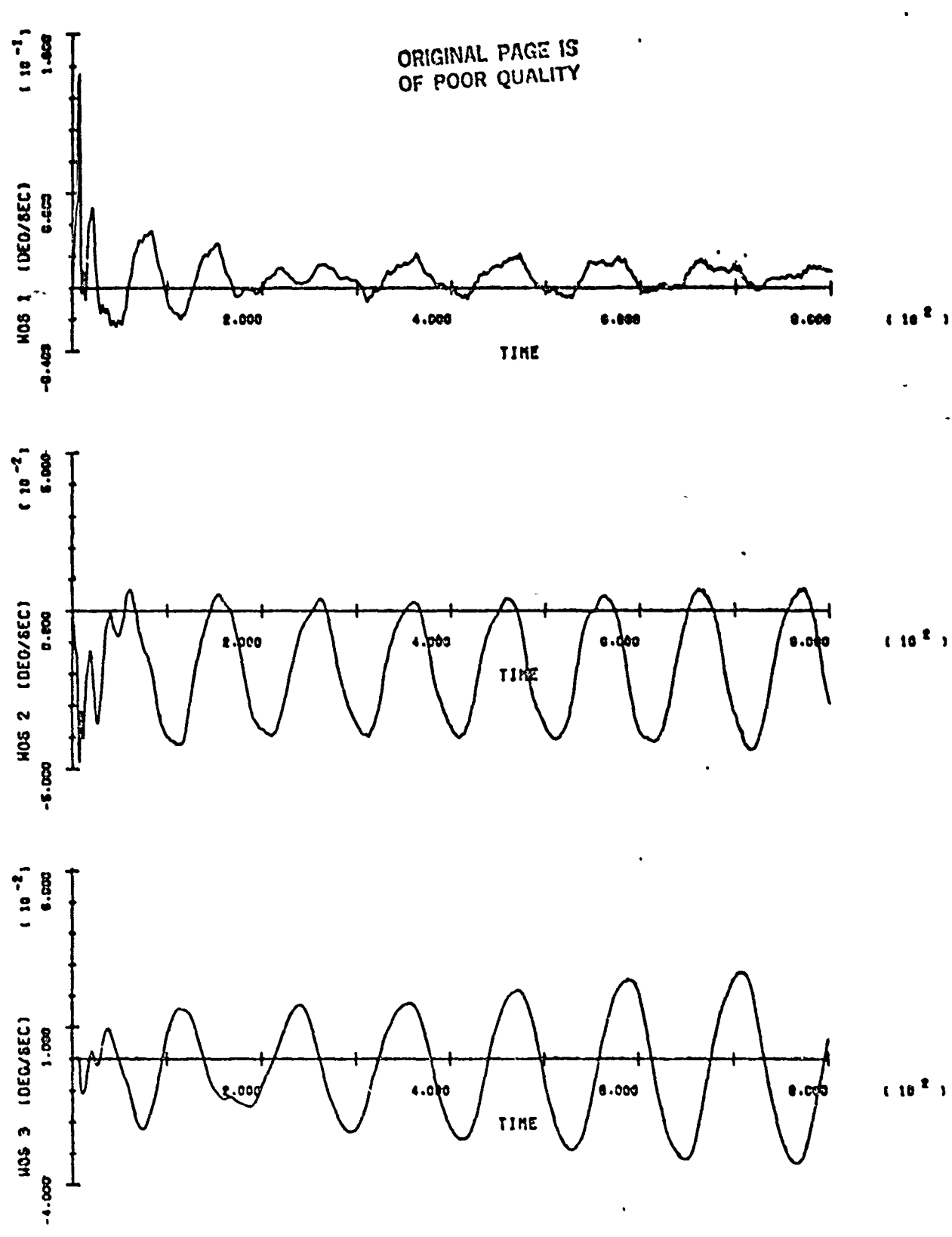


SOC/ORBITER BERTHING RUN 1

ORIGINAL PAGE IS
OF POOR QUALITY

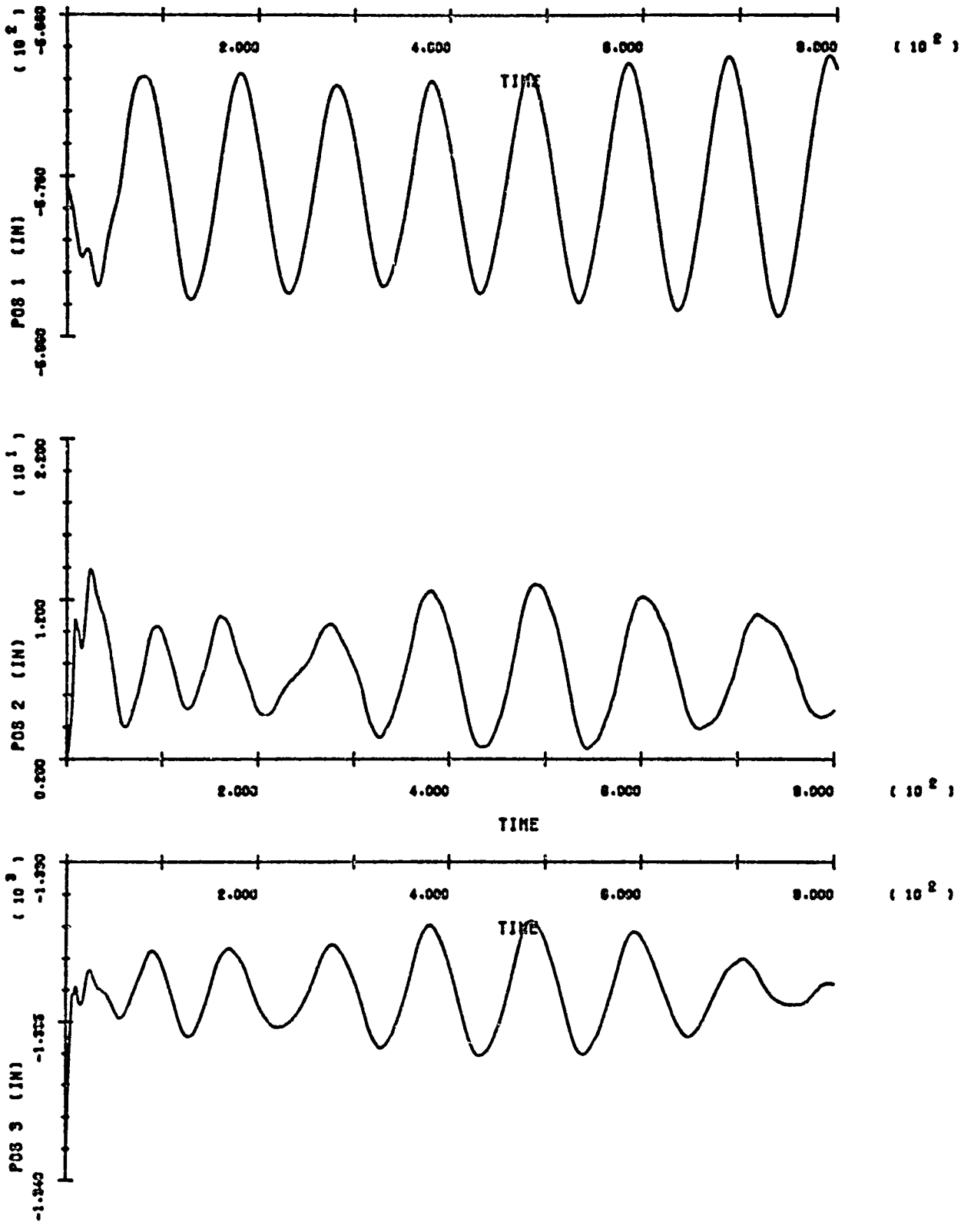


SOC/ORBITER BERTHING RUN 1

ORIGINAL PAGE IS
OF POOR QUALITY

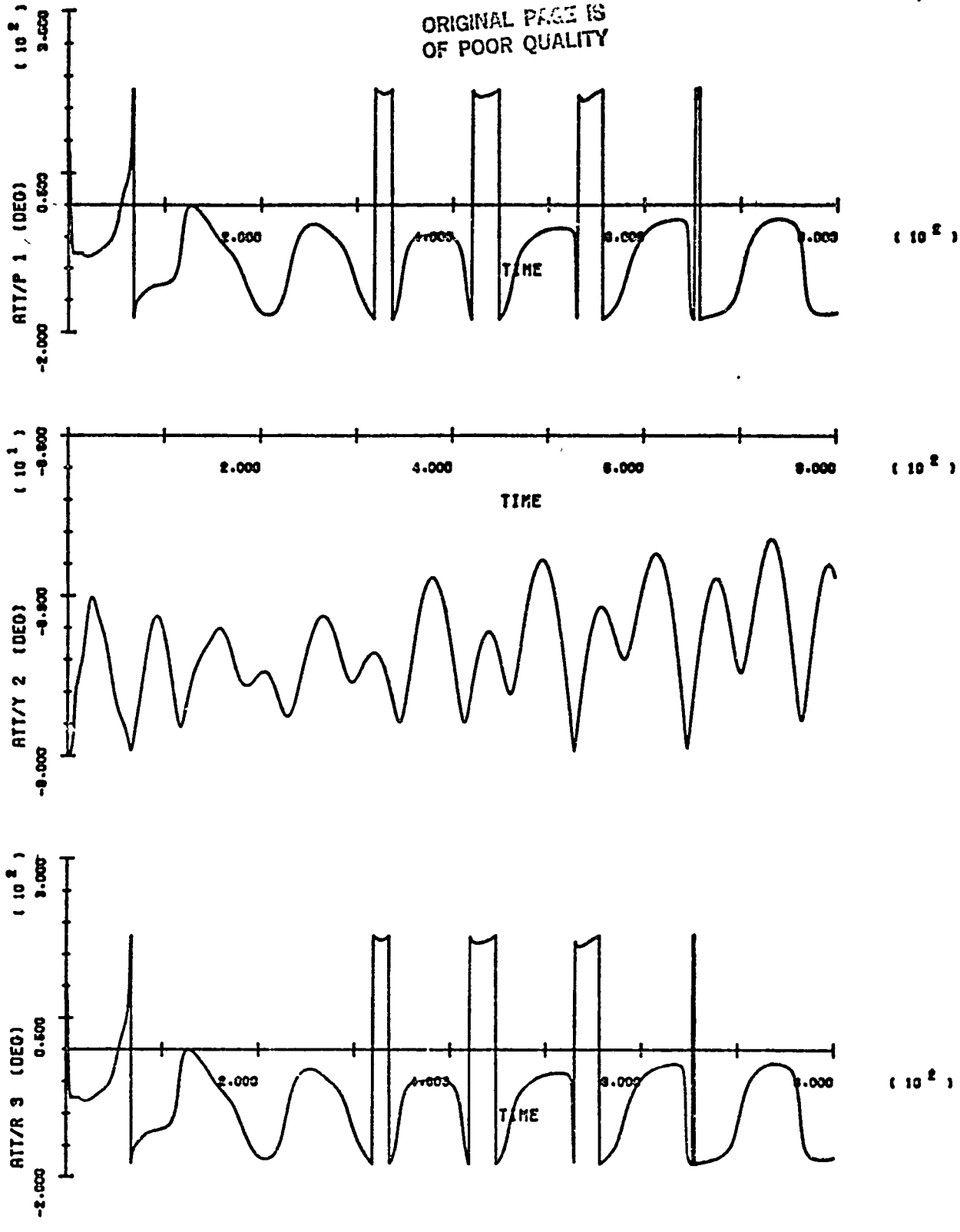


SOC/ORBITER BERTHING RUN 1

ORIGINAL PAGE IS
OF POOR QUALITY

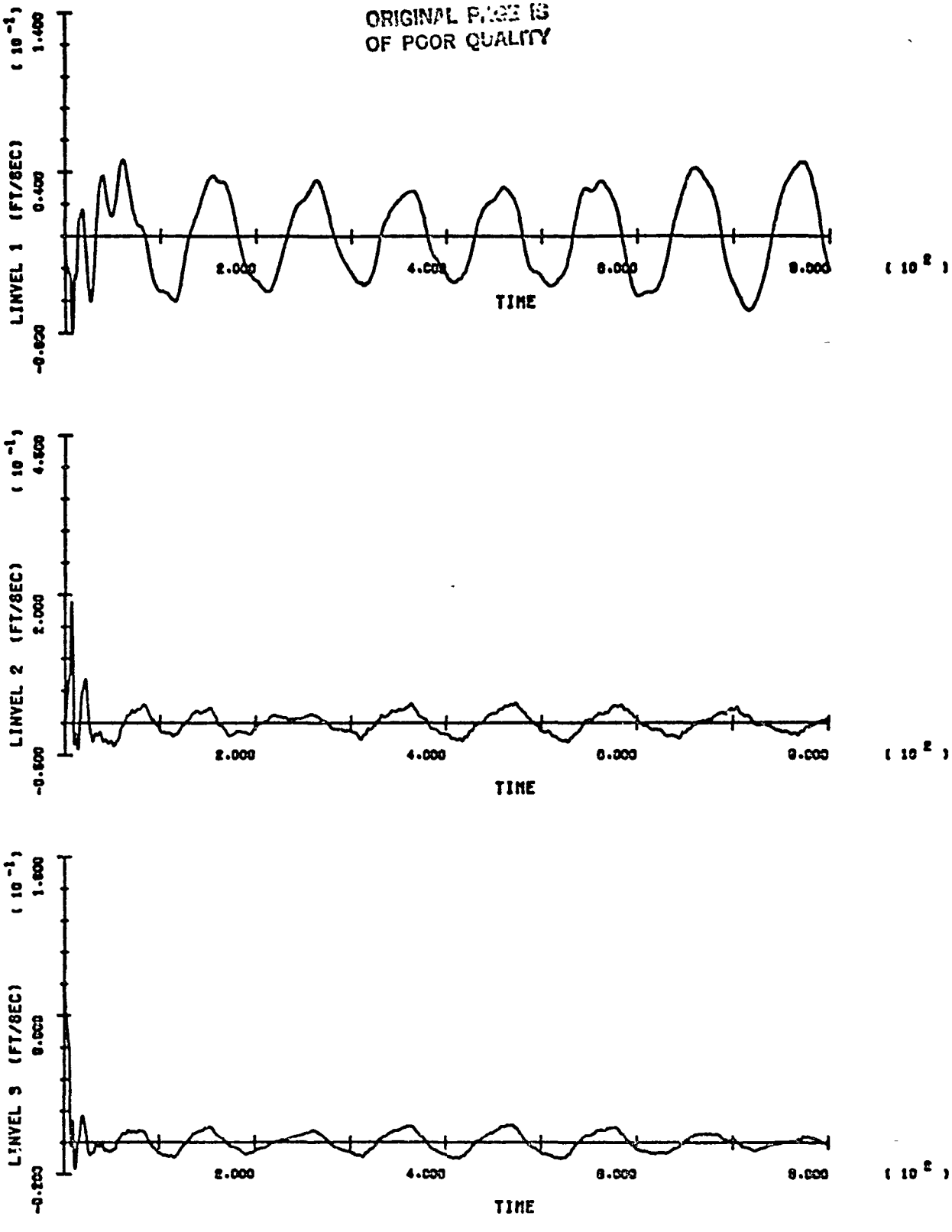


SOC/ORBITER BERTHING RUN 1

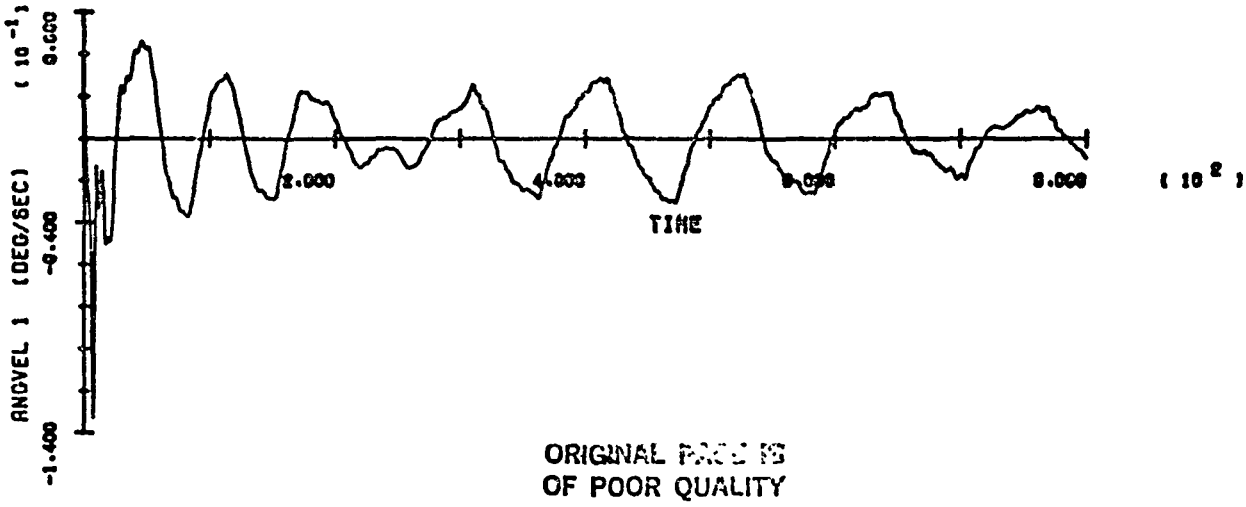


ORIGINAL PAGE IS
OF POOR QUALITY

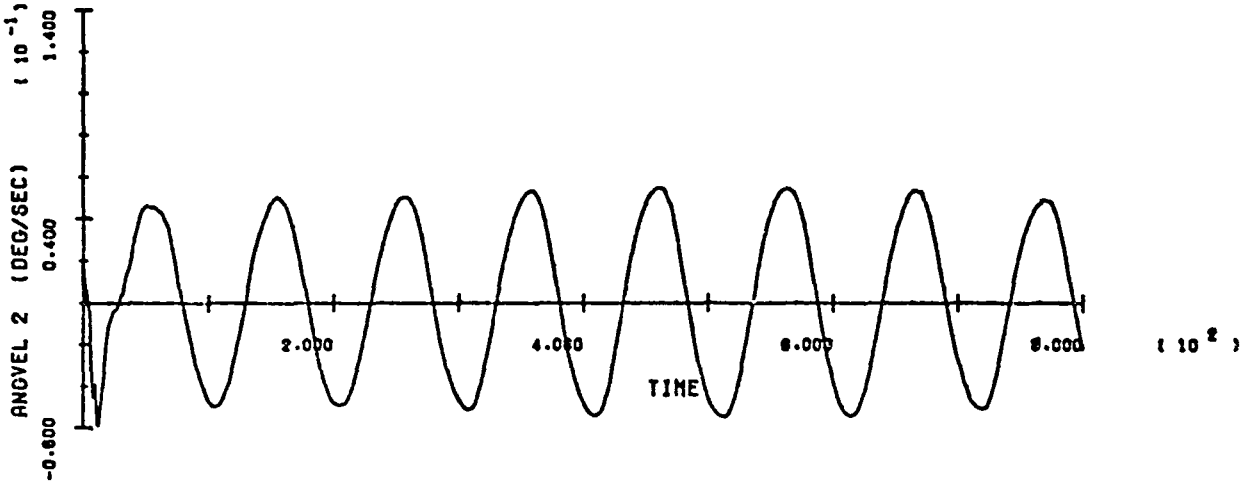


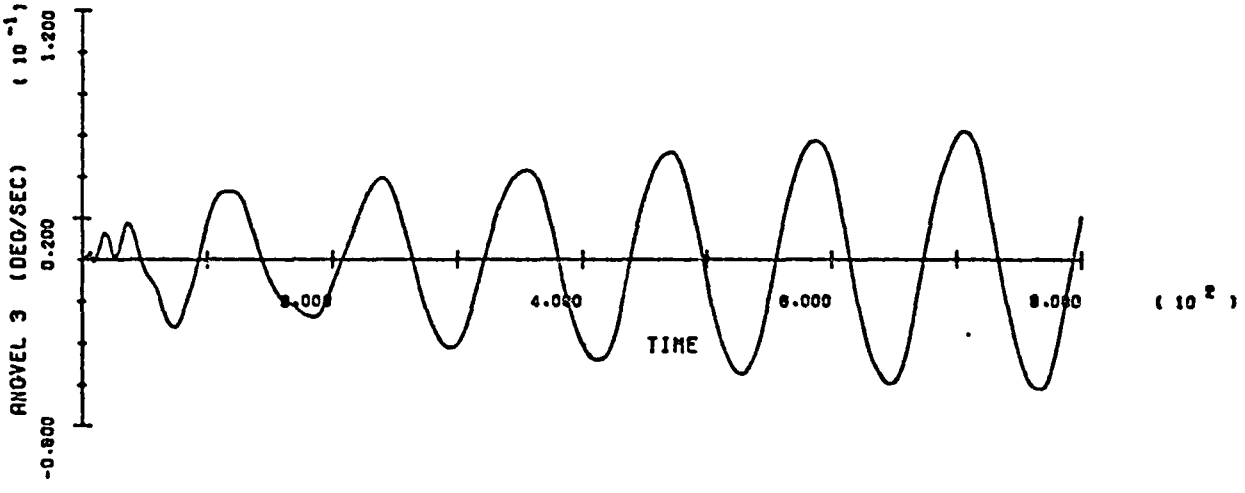


SOC/ORBITER BERTHING RUN 1

ORIGINAL PAGE IS
OF POOR QUALITY

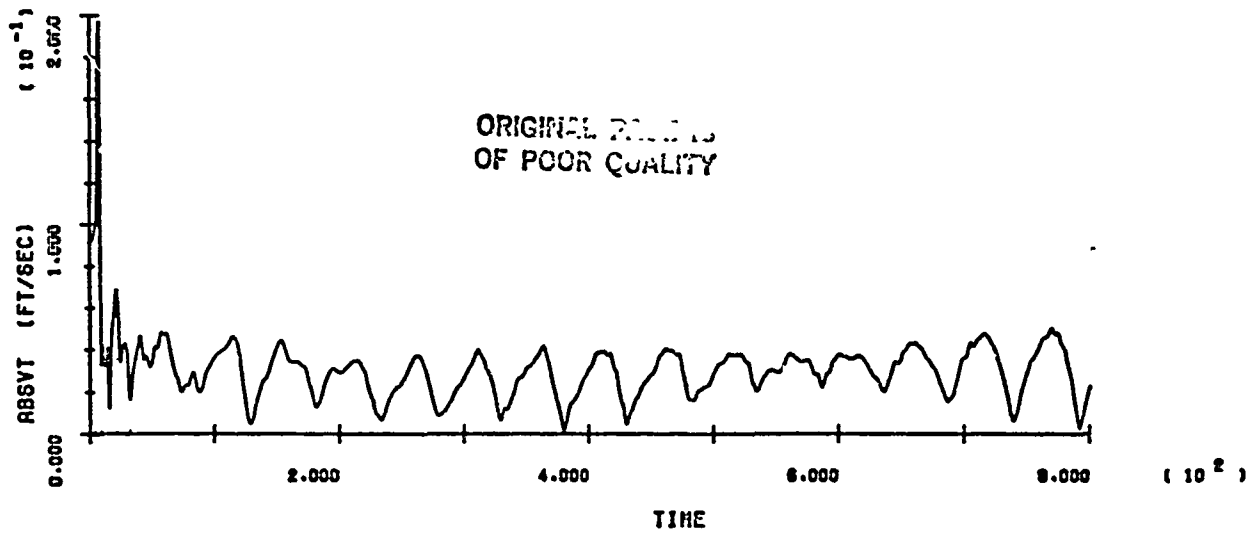


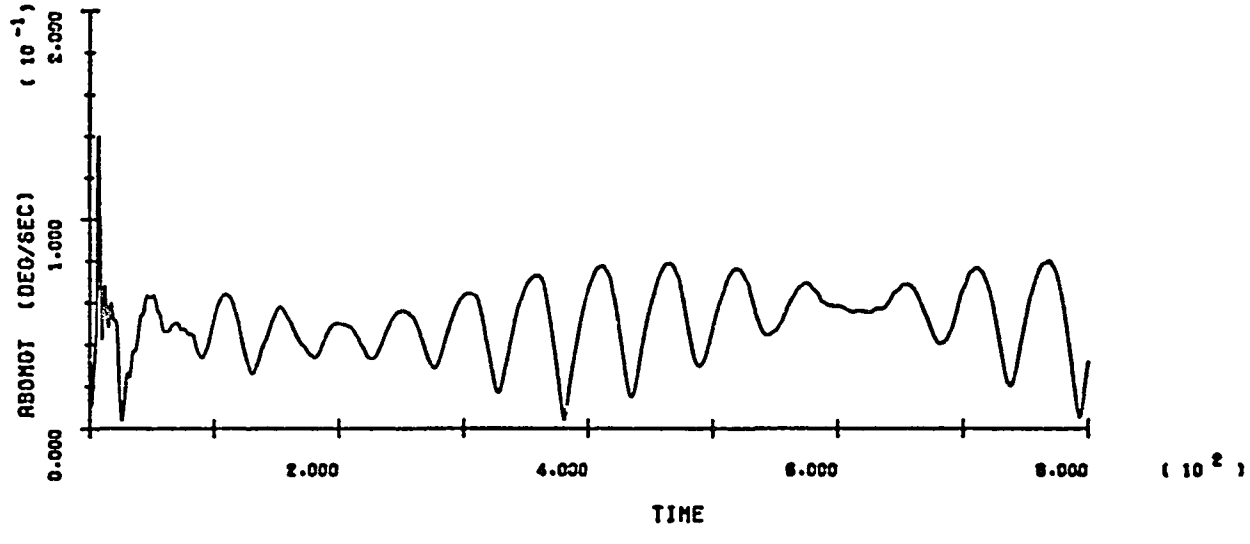


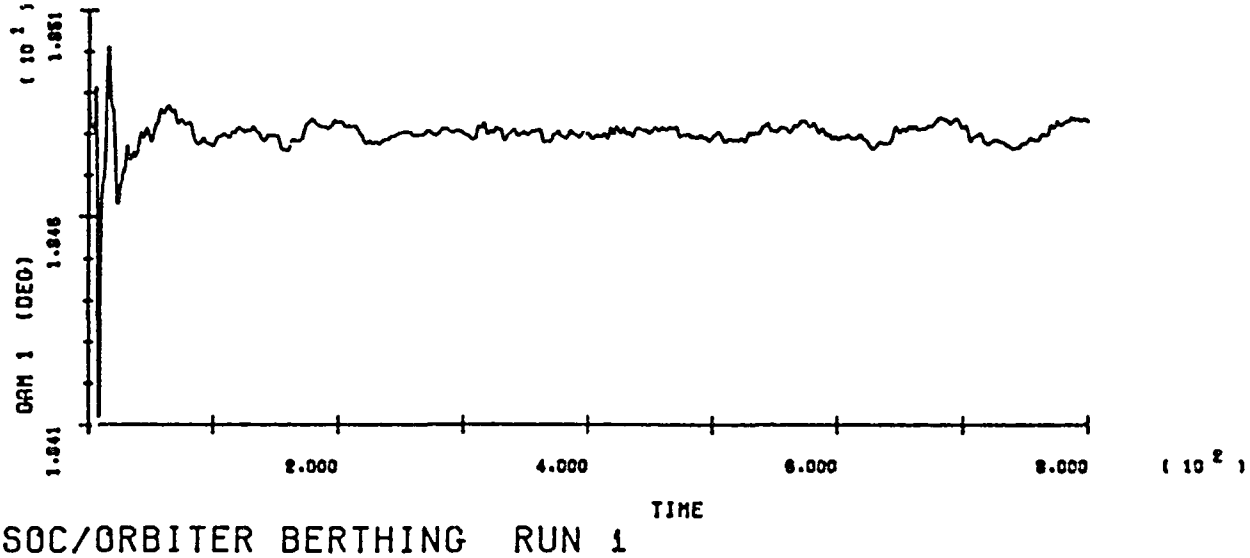


SOC/ORBITER BERTHING RUN 1

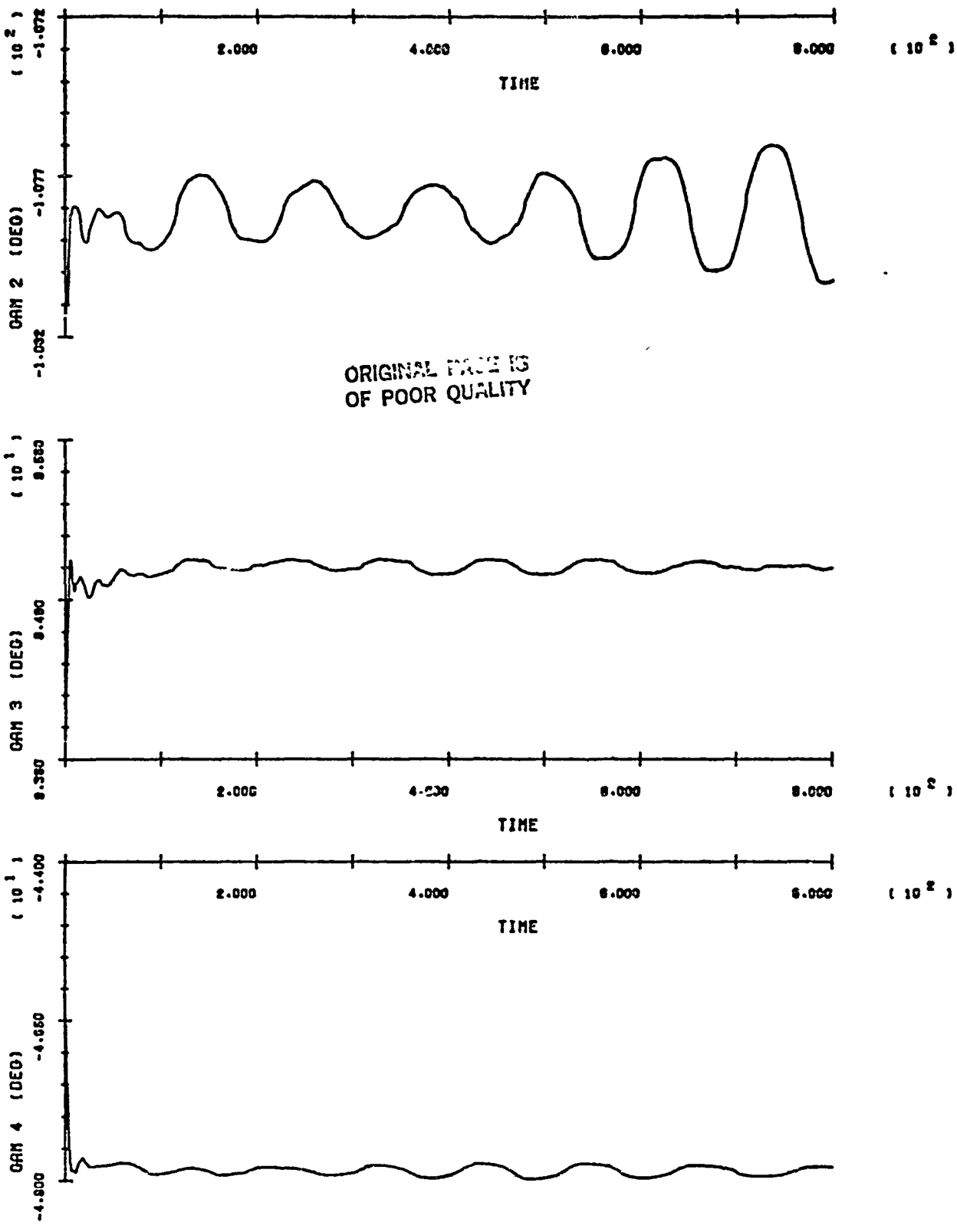


SOC/ORBITER BERTHING RUN 1

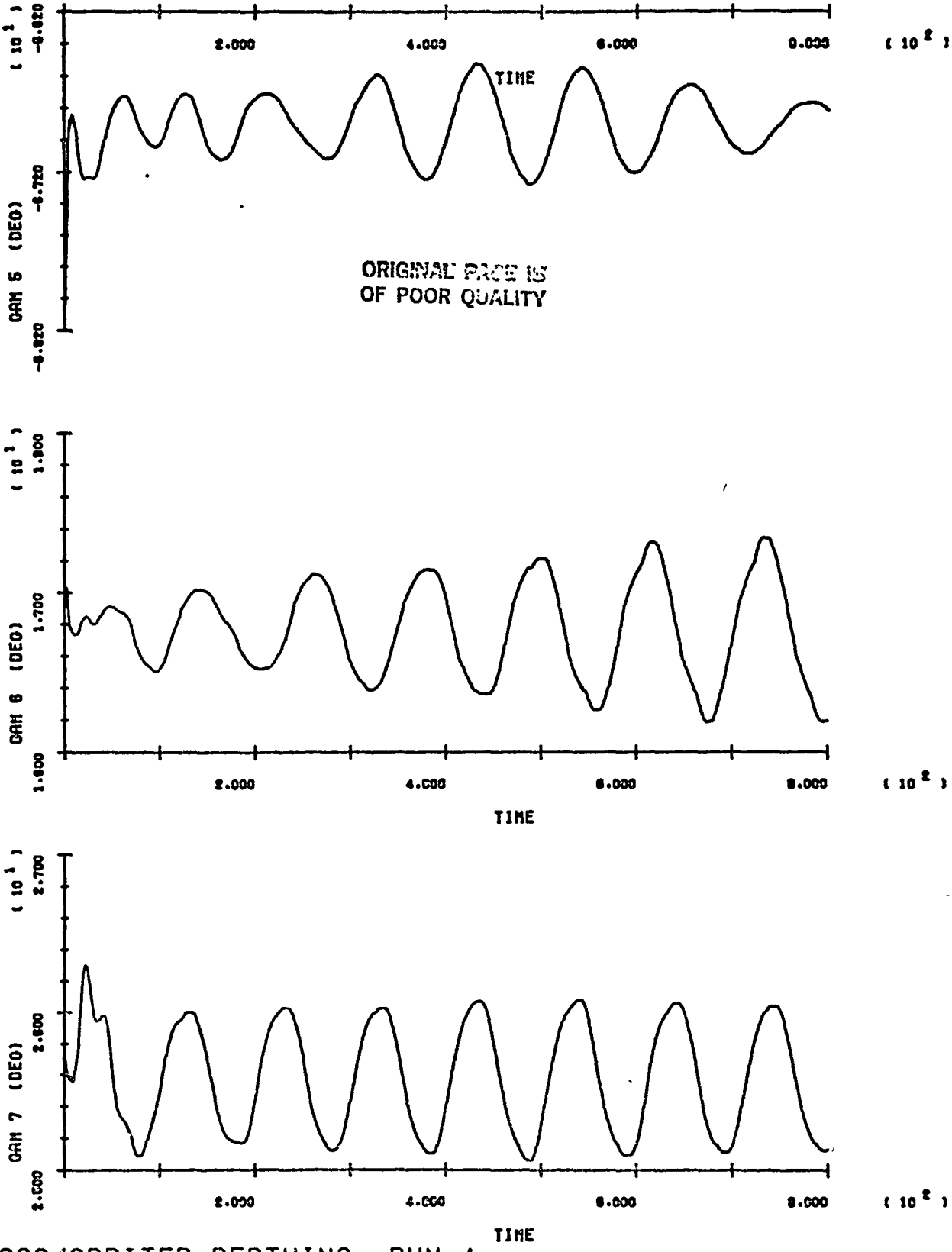


SOC/ORBITER BERTHING RUN 1

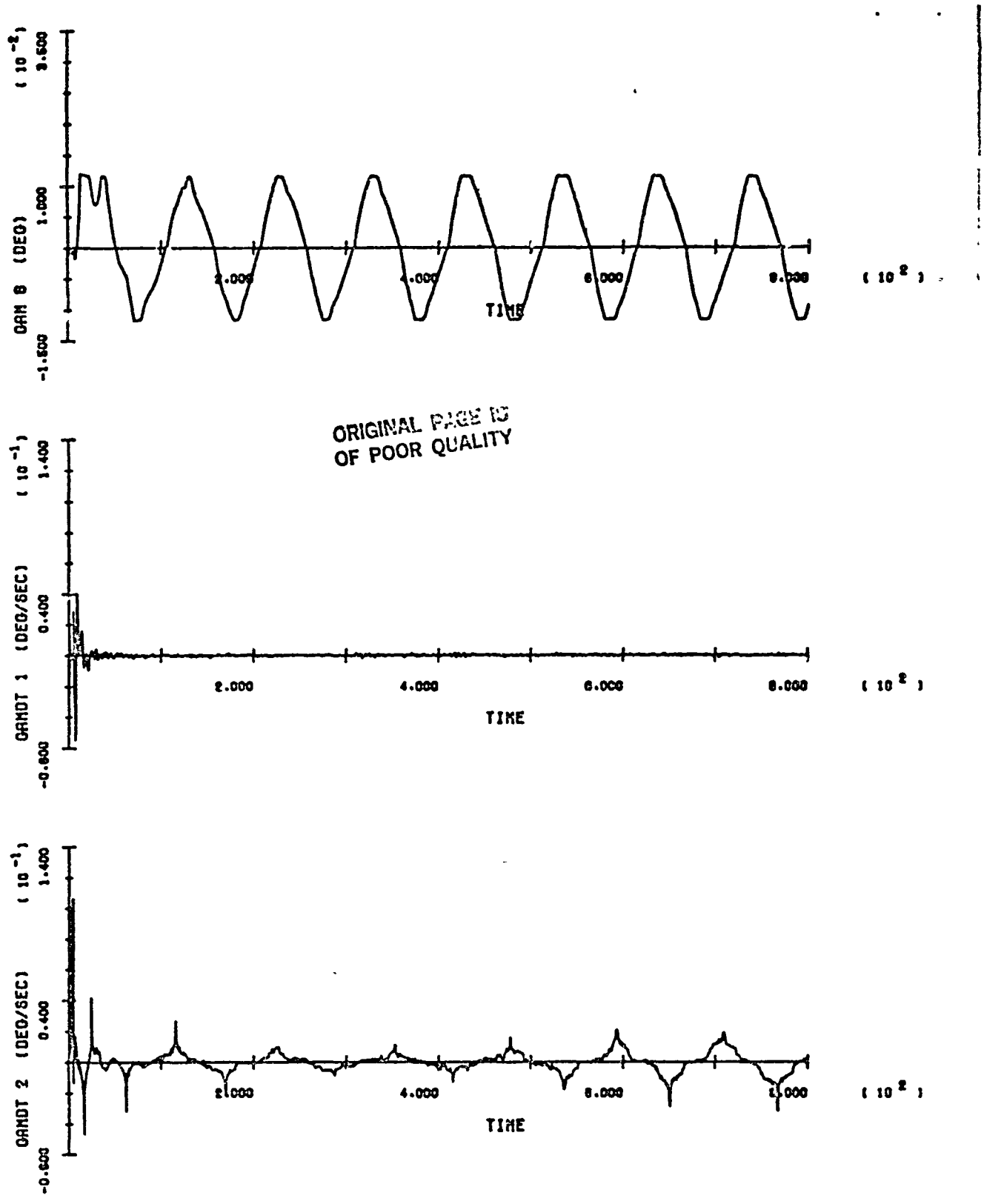


ORIGINAL PAGE IS
OF POOR QUALITY

SOC/ORBITER BERTHING RUN 1

ORIGINAL PAGE IS
OF POOR QUALITY

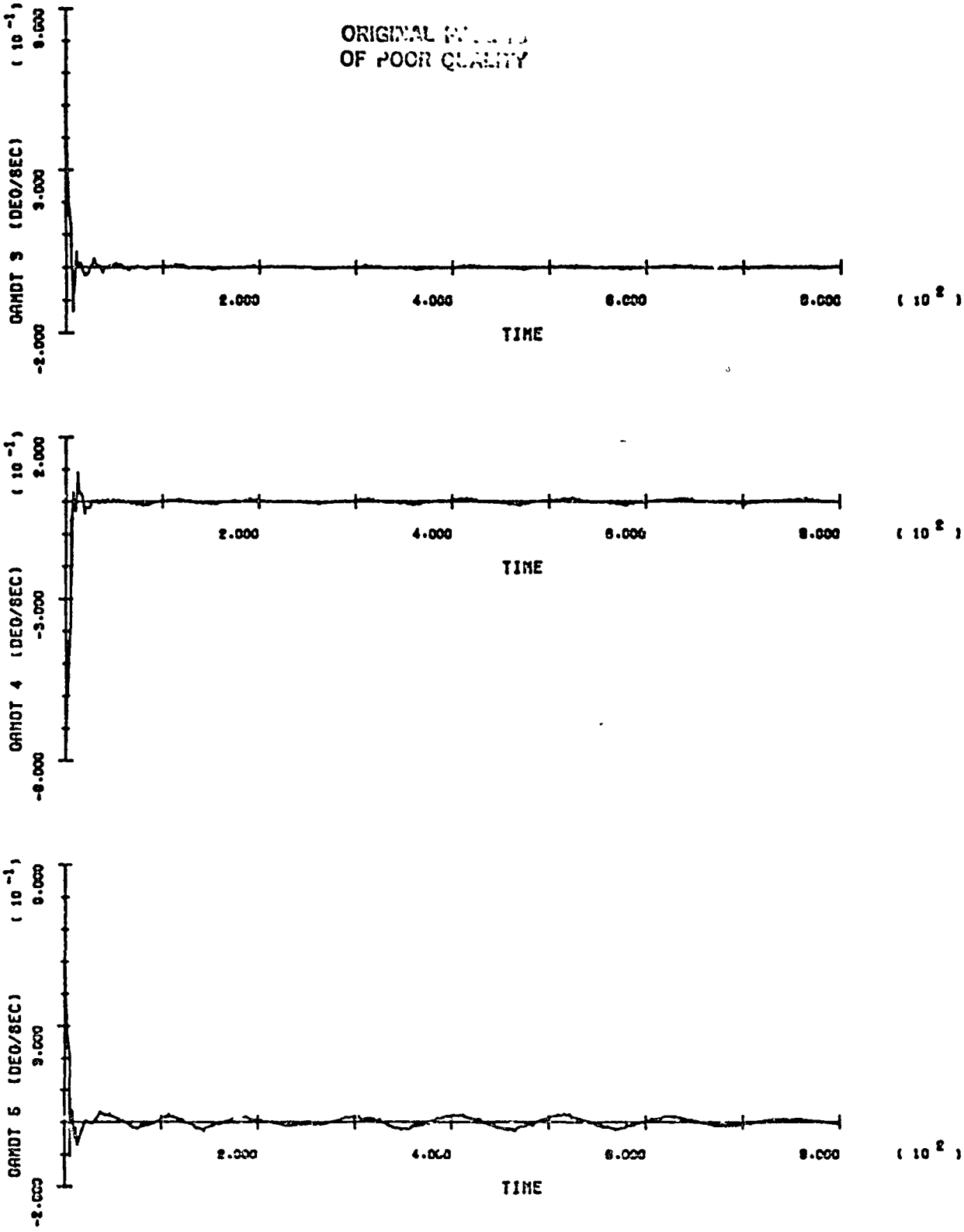


SOC/ORBITER BERTHING RUN 1

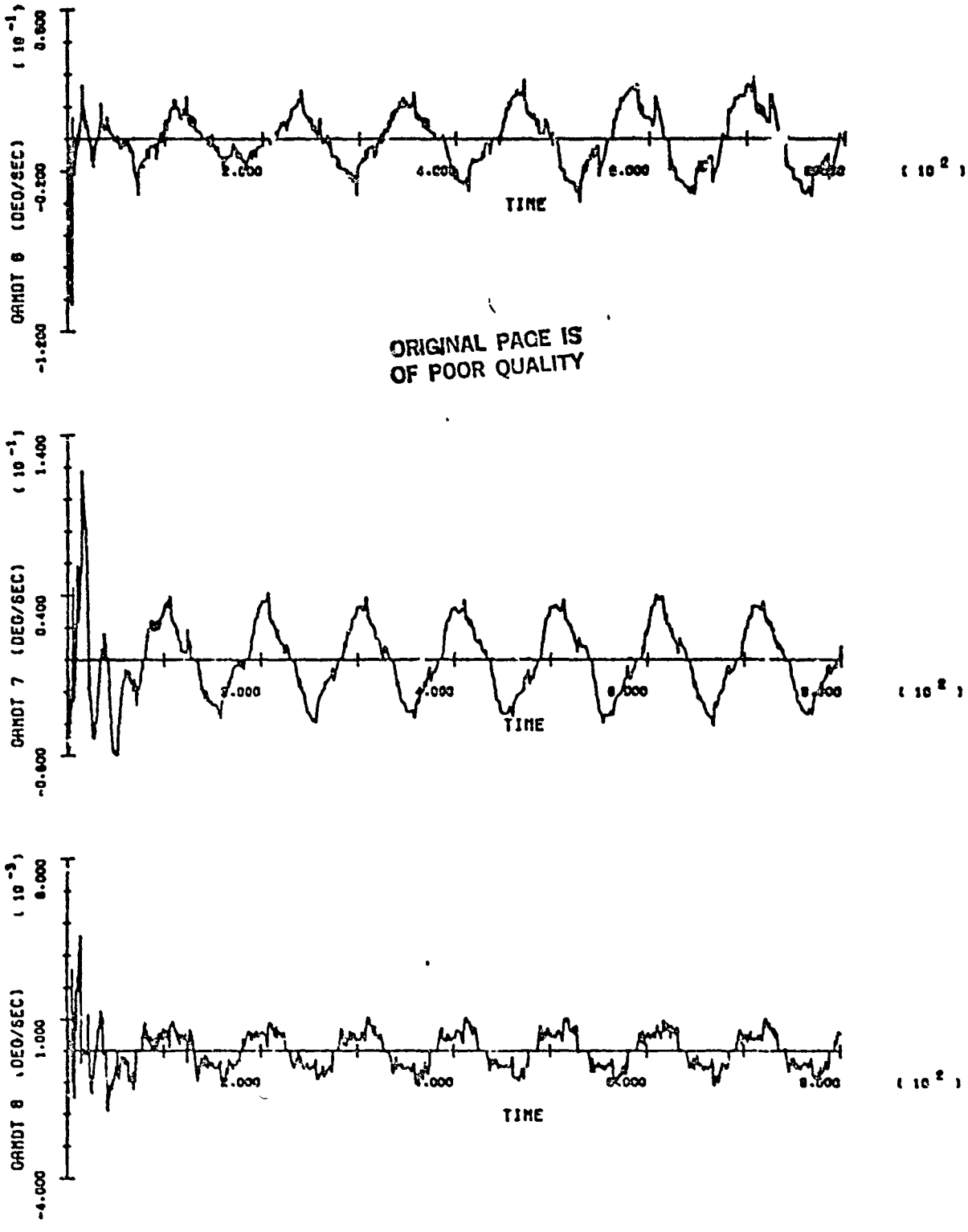


ORIGINAL PAGE IS
OF POOR QUALITY

SOC/ORBITER BERTHING RUN 1

ORIGINAL PAGE IS
OF POOR QUALITY

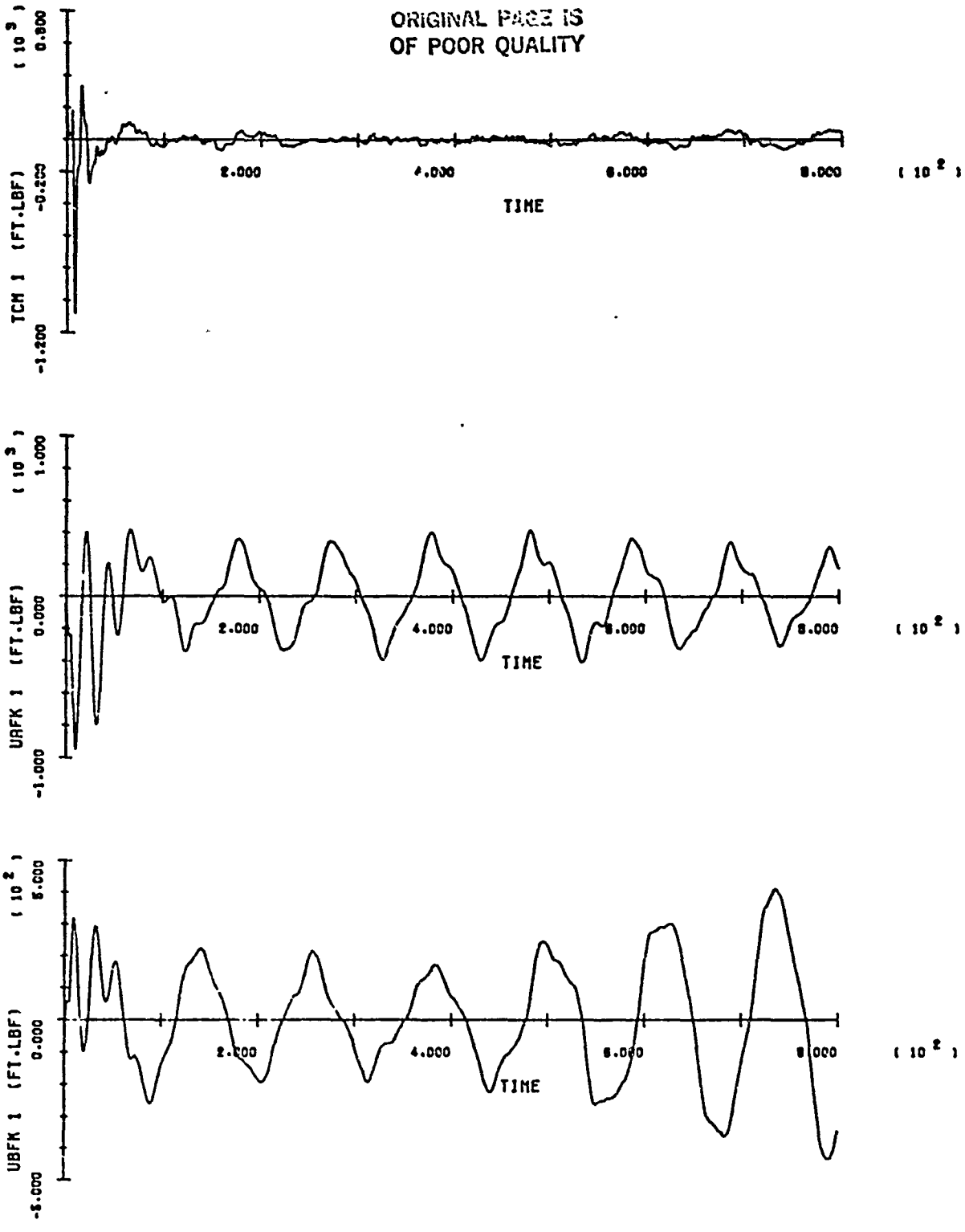


SOC/ORBITER BERTHING RUN 1

ORIGINAL PAGE IS
OF POOR QUALITY

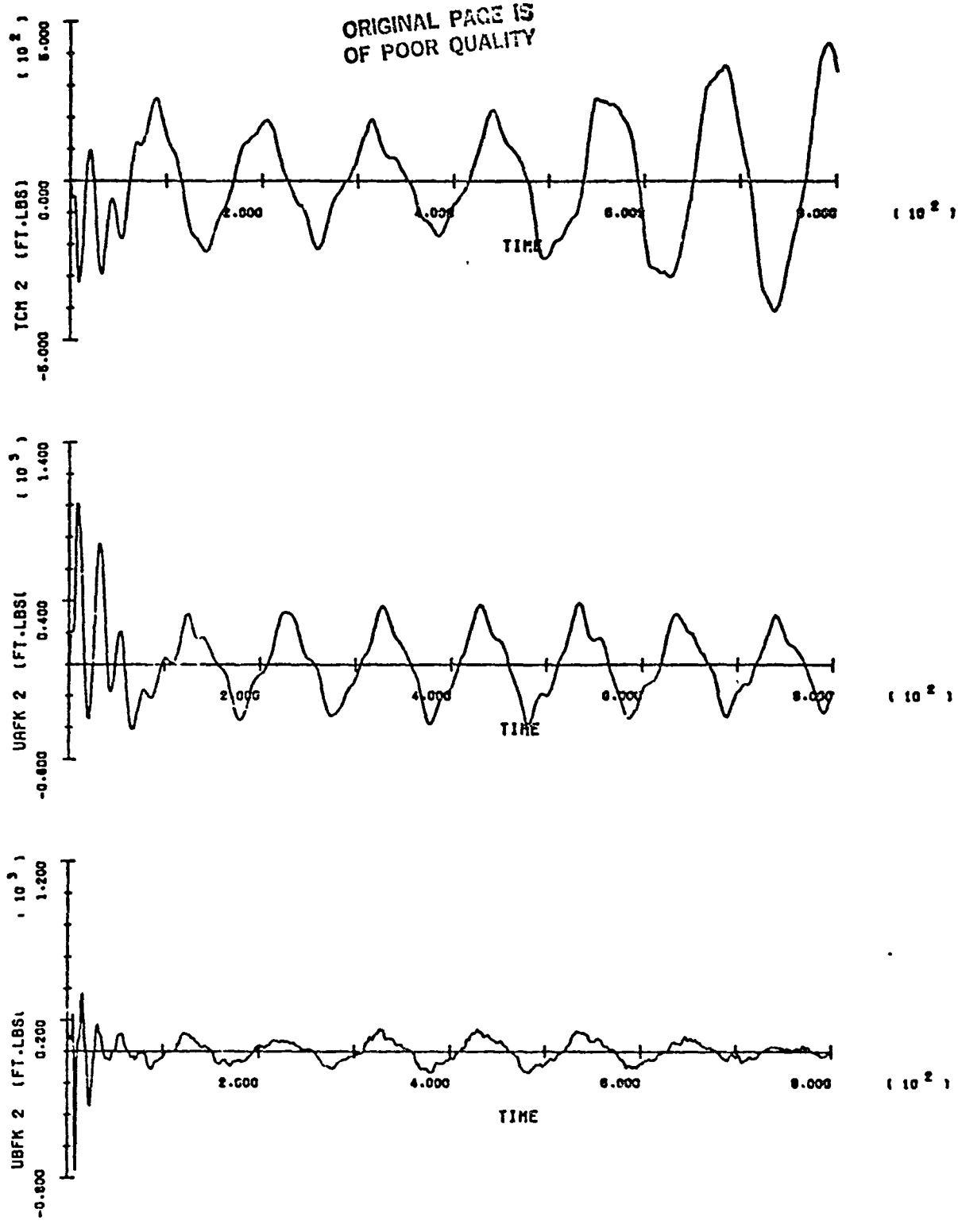


SOC/ORBITER BERTHING RUN 1

ORIGINAL PAGE IS
OF POOR QUALITY

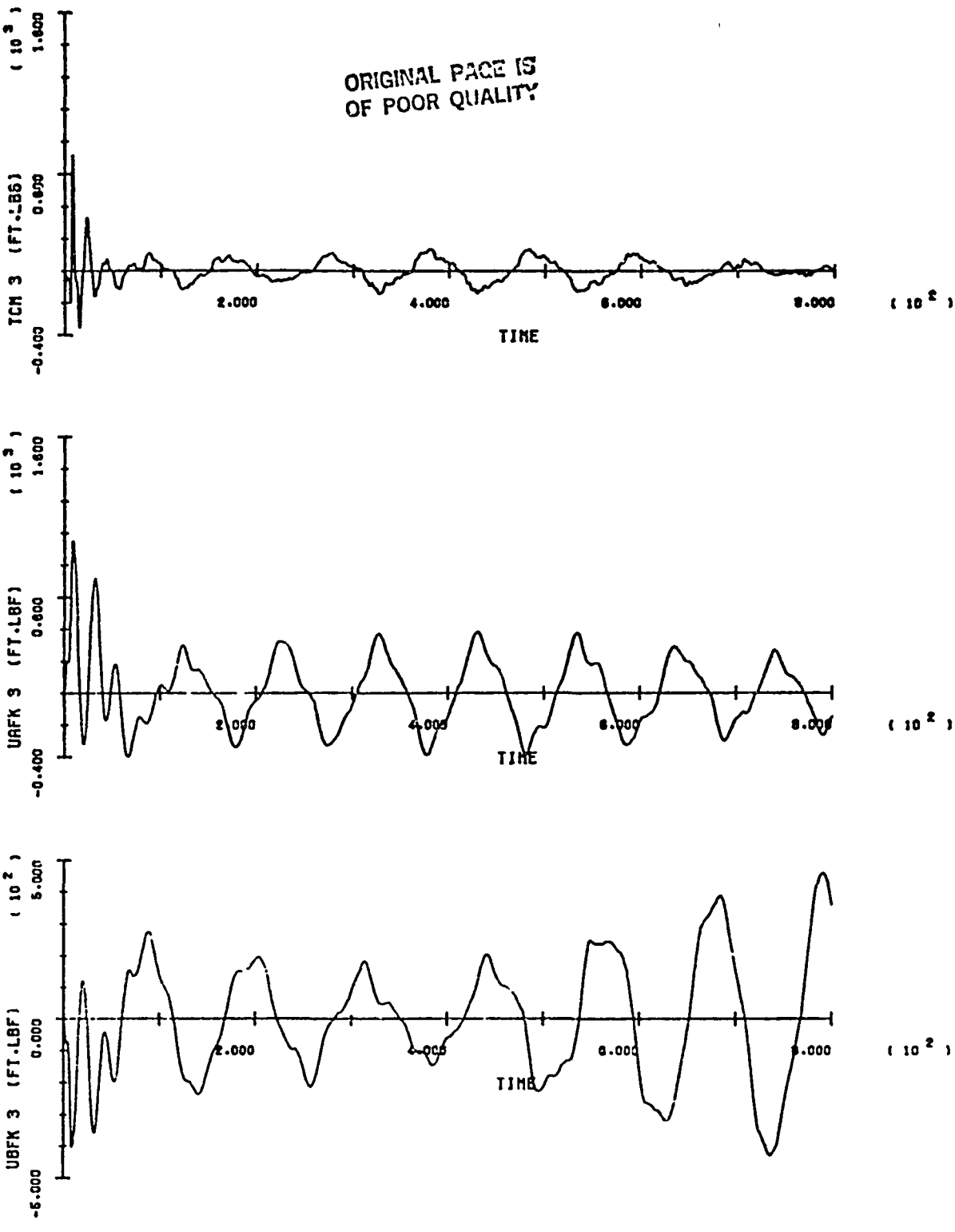


SOC/ORBITER BERTHING RUN 1

ORIGINAL PAGE IS
OF POOR QUALITY

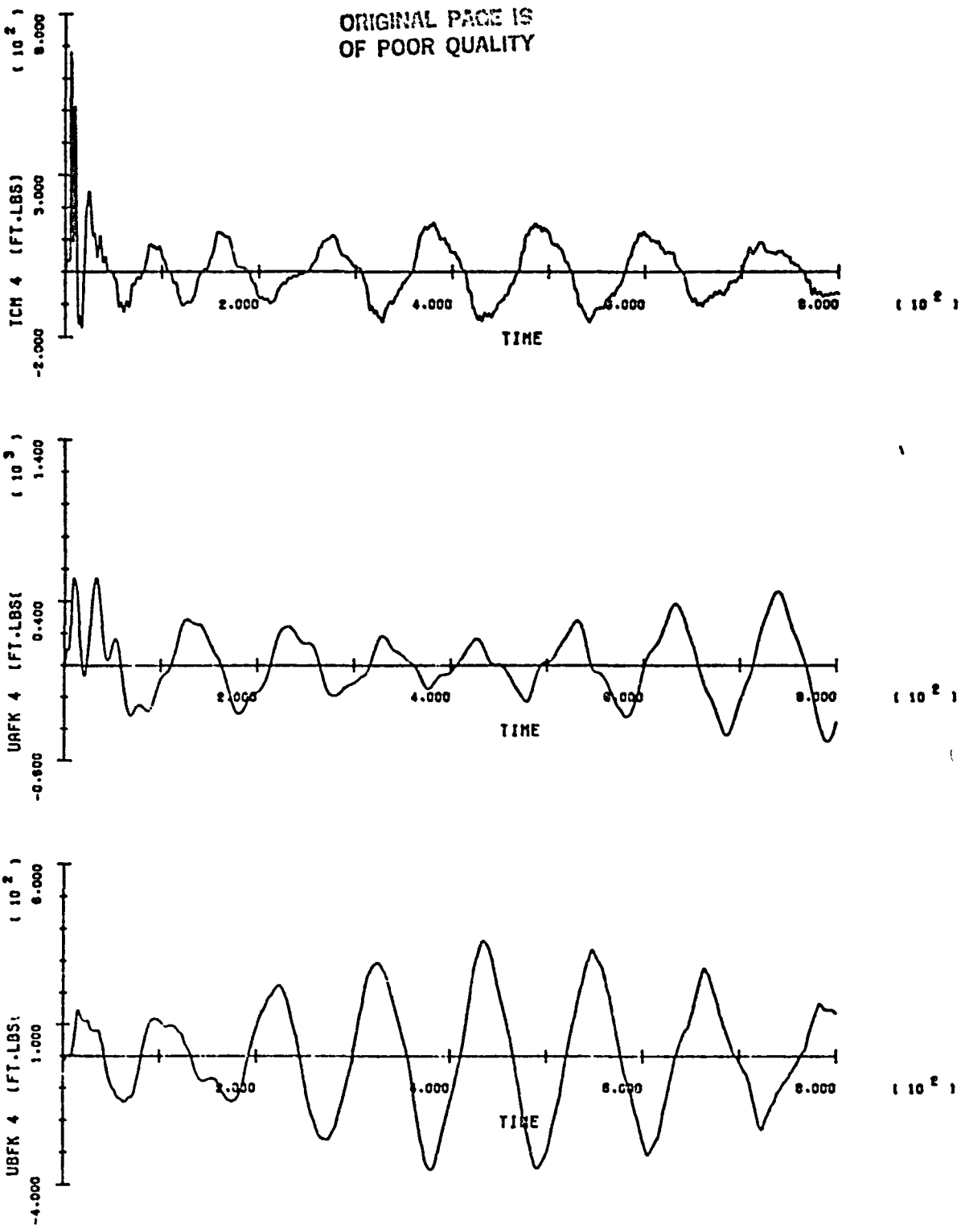


SOC/ORBITER BERTHING RUN 1

ORIGINAL PAGE IS
OF POOR QUALITY

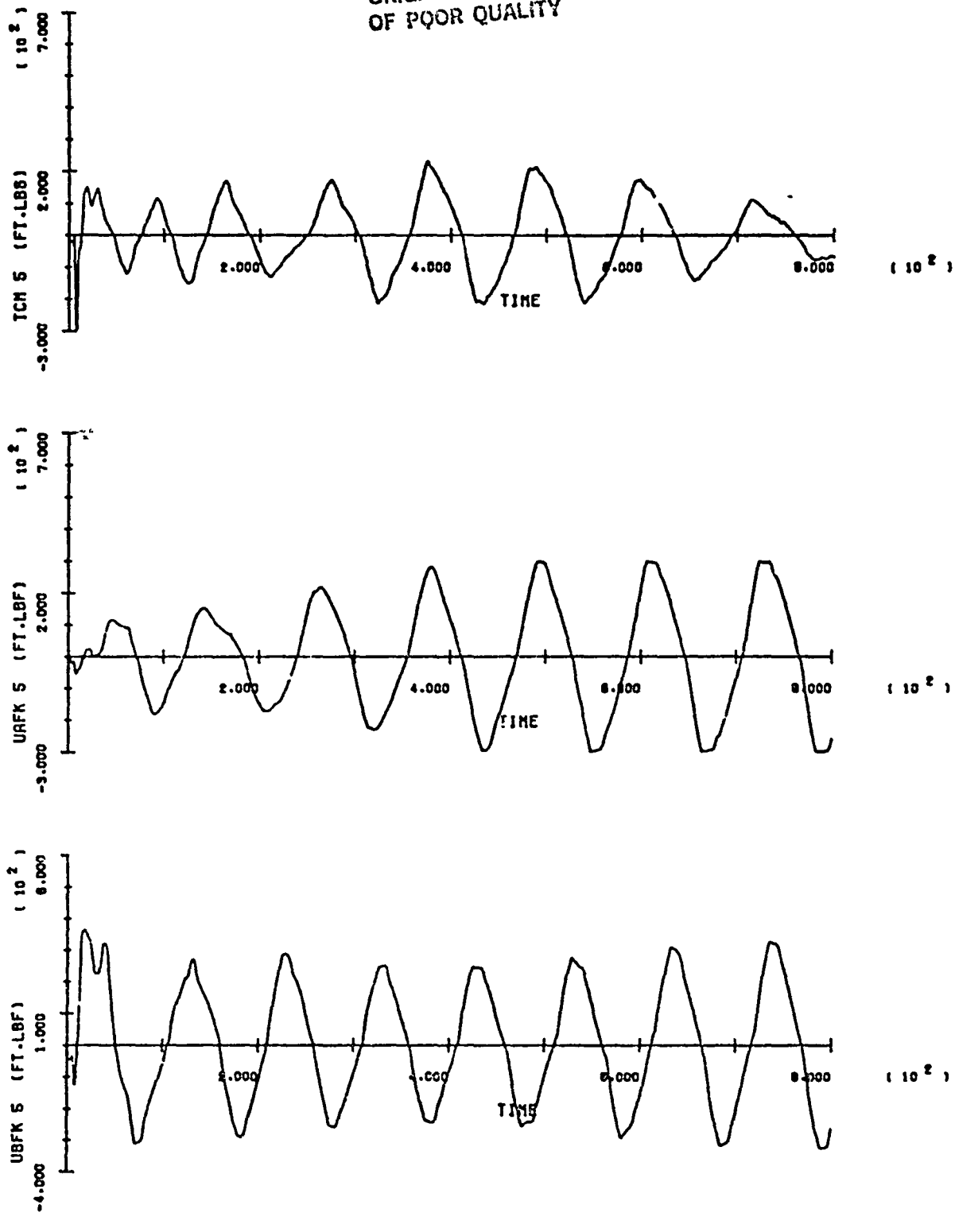


SOC/ORBITER BERTHING RUN 1

ORIGINAL PAGE IS
OF POOR QUALITY

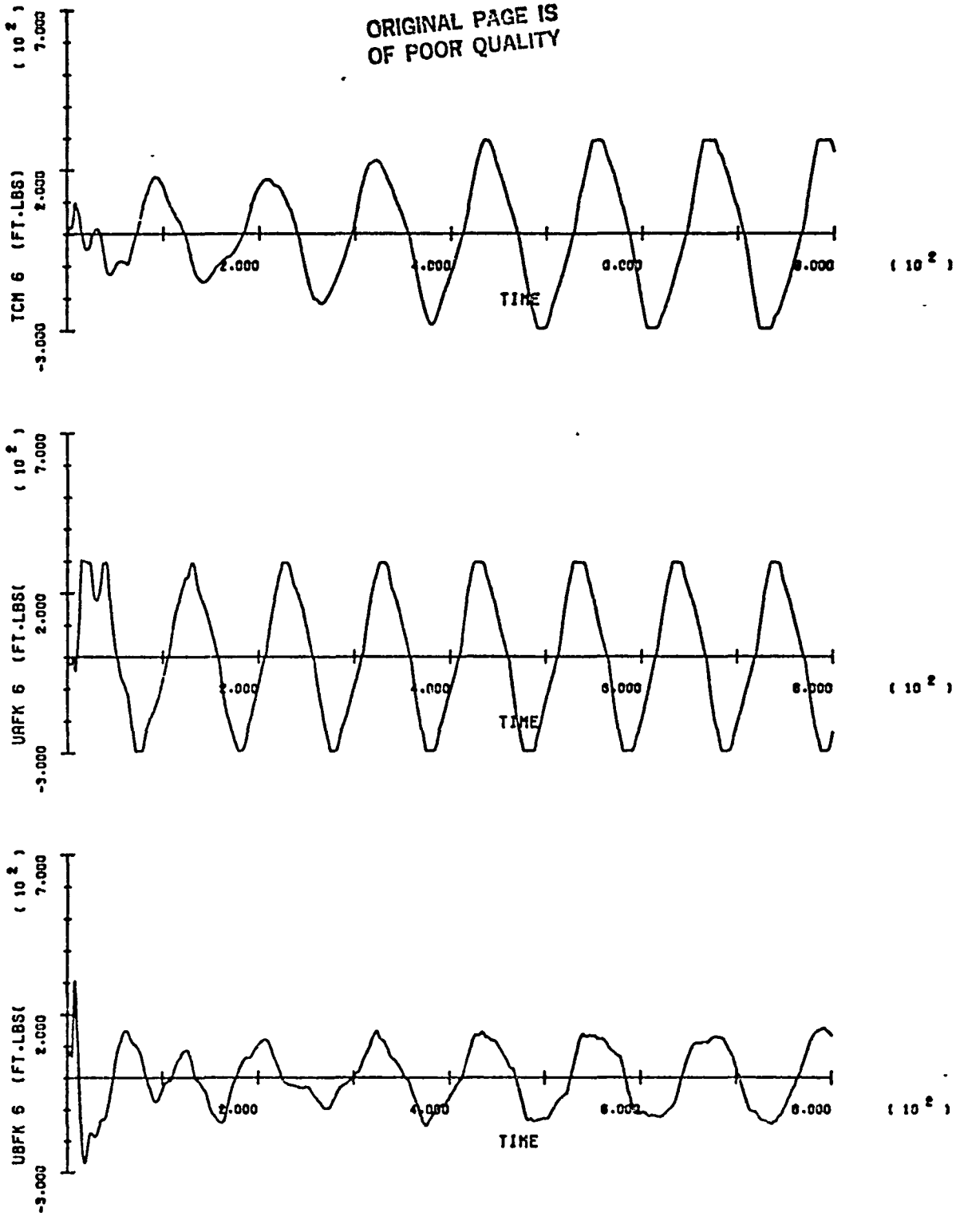


SOC/ORBITER BERTHING RUN 1

ORIGINAL PAGE IS
OF POOR QUALITY

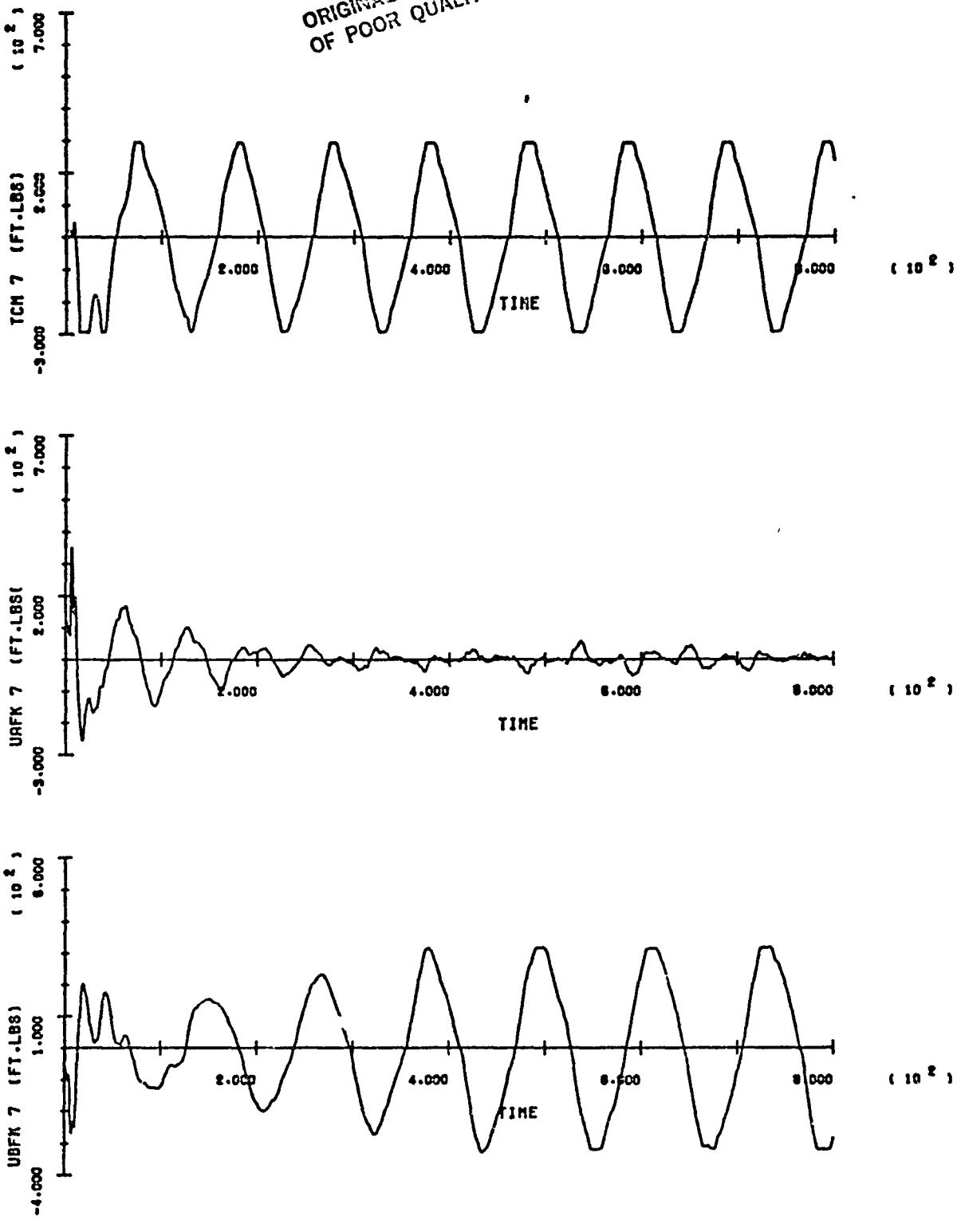


SOC/ORBITER BERTHING RUN 1

ORIGINAL PAGE IS
OF POOR QUALITY

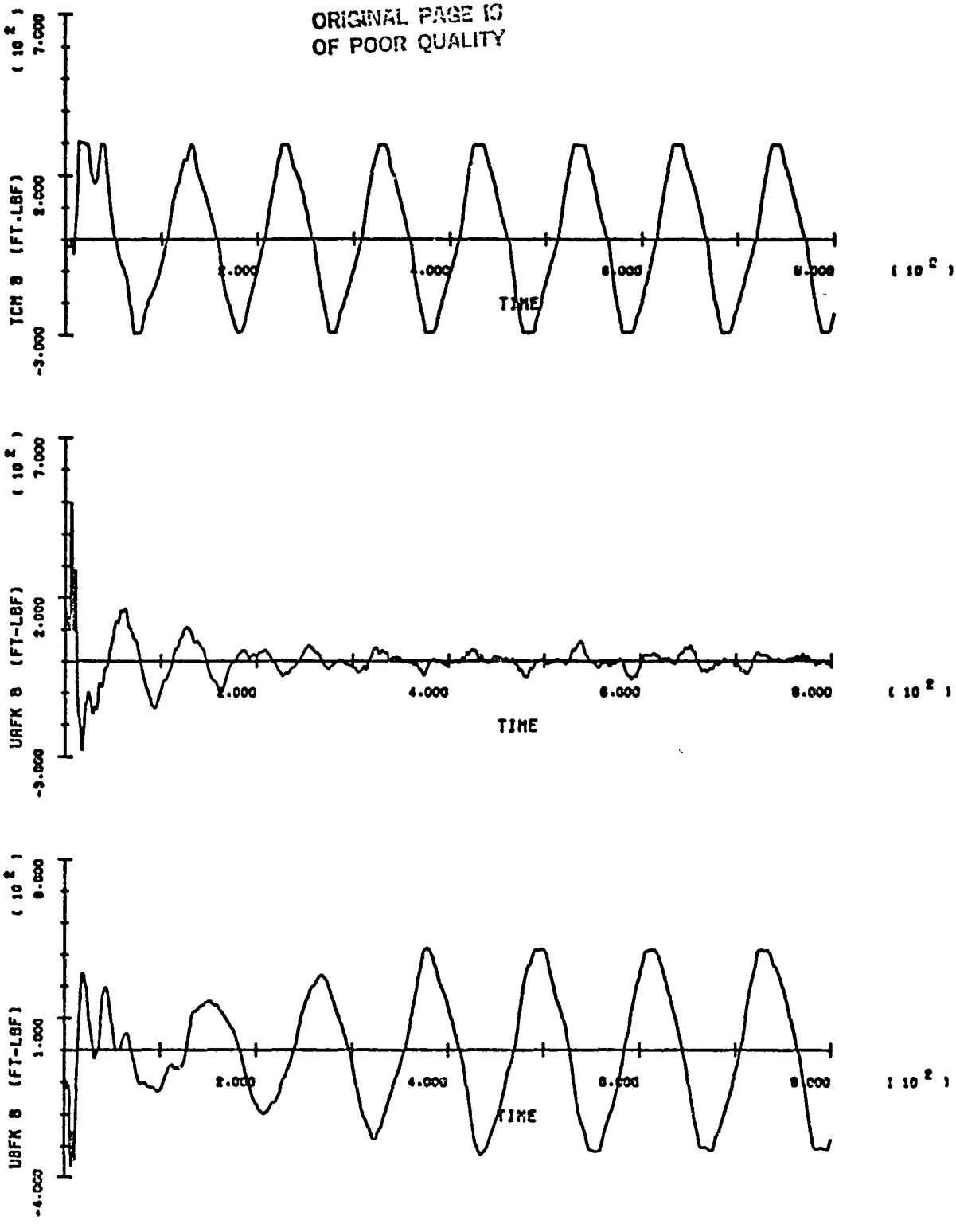


SOC/ORBITER BERTHING RUN 1

ORIGINAL PAGE IS
OF POOR QUALITY

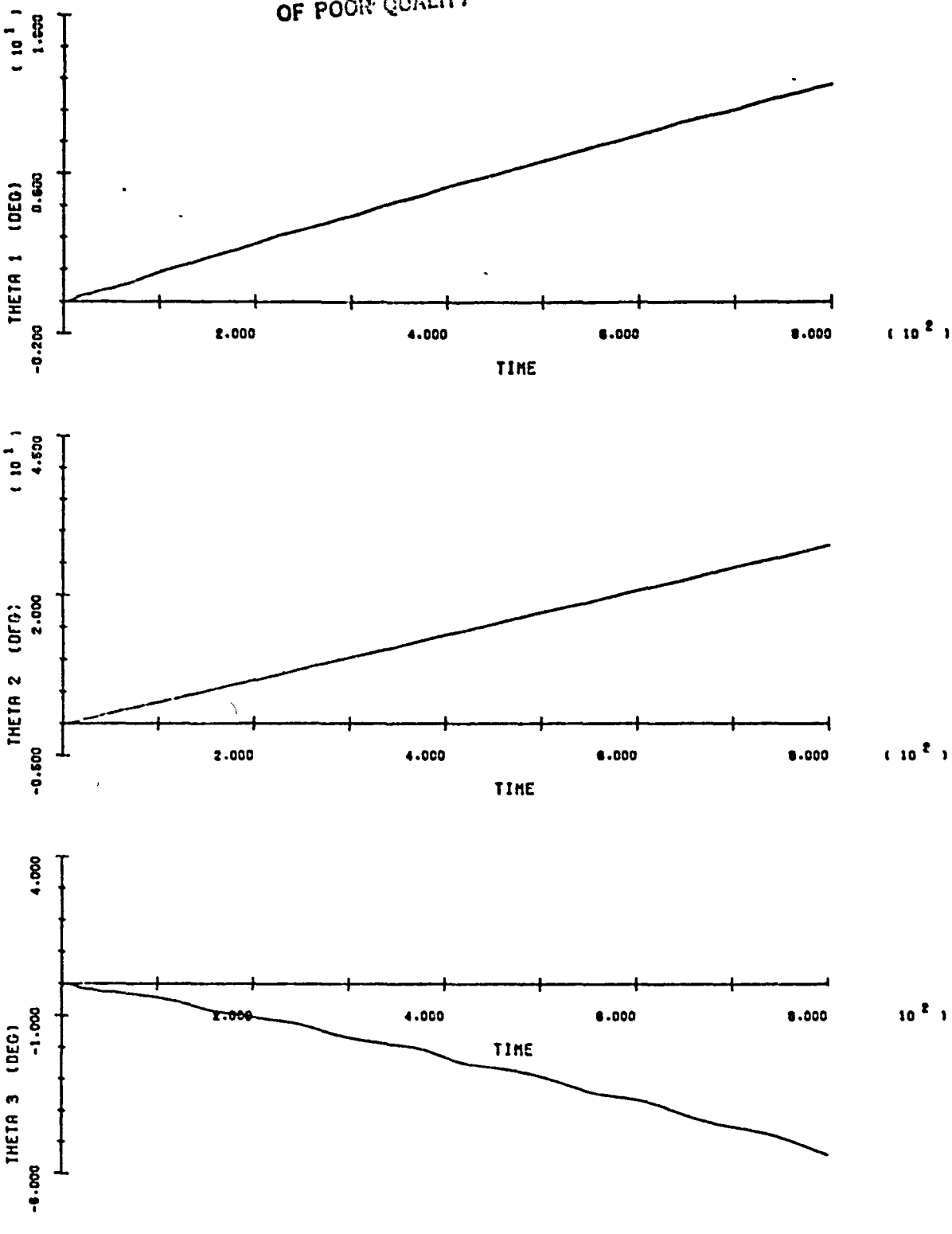


SOC/ORBITER BERTHING RUN 2

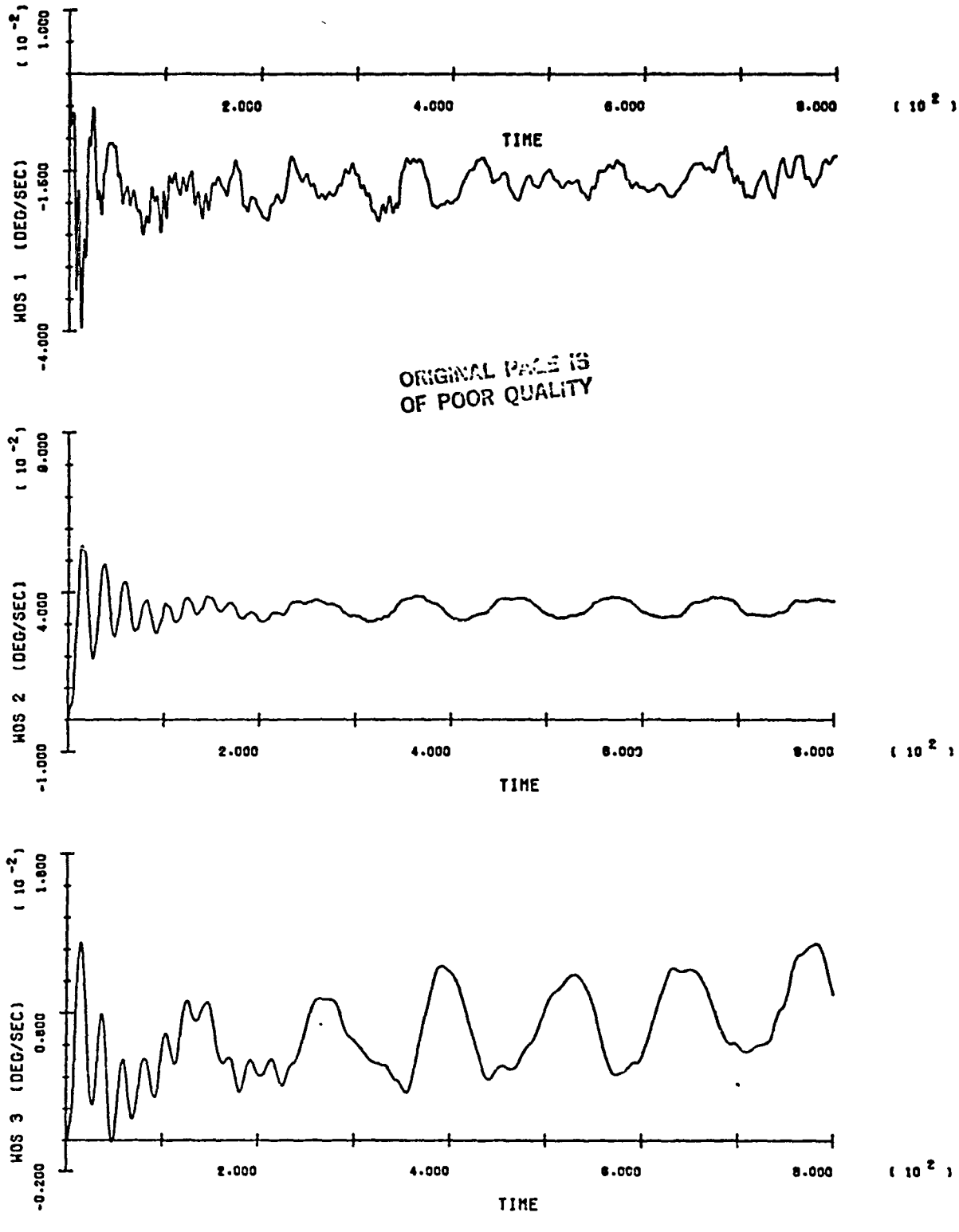


ORIGINAL PAGE IS
OF POOR QUALITY

SOC/ORBITER BERTHING RUN 2

ORIGINAL PAGE IS
OF POOR QUALITY

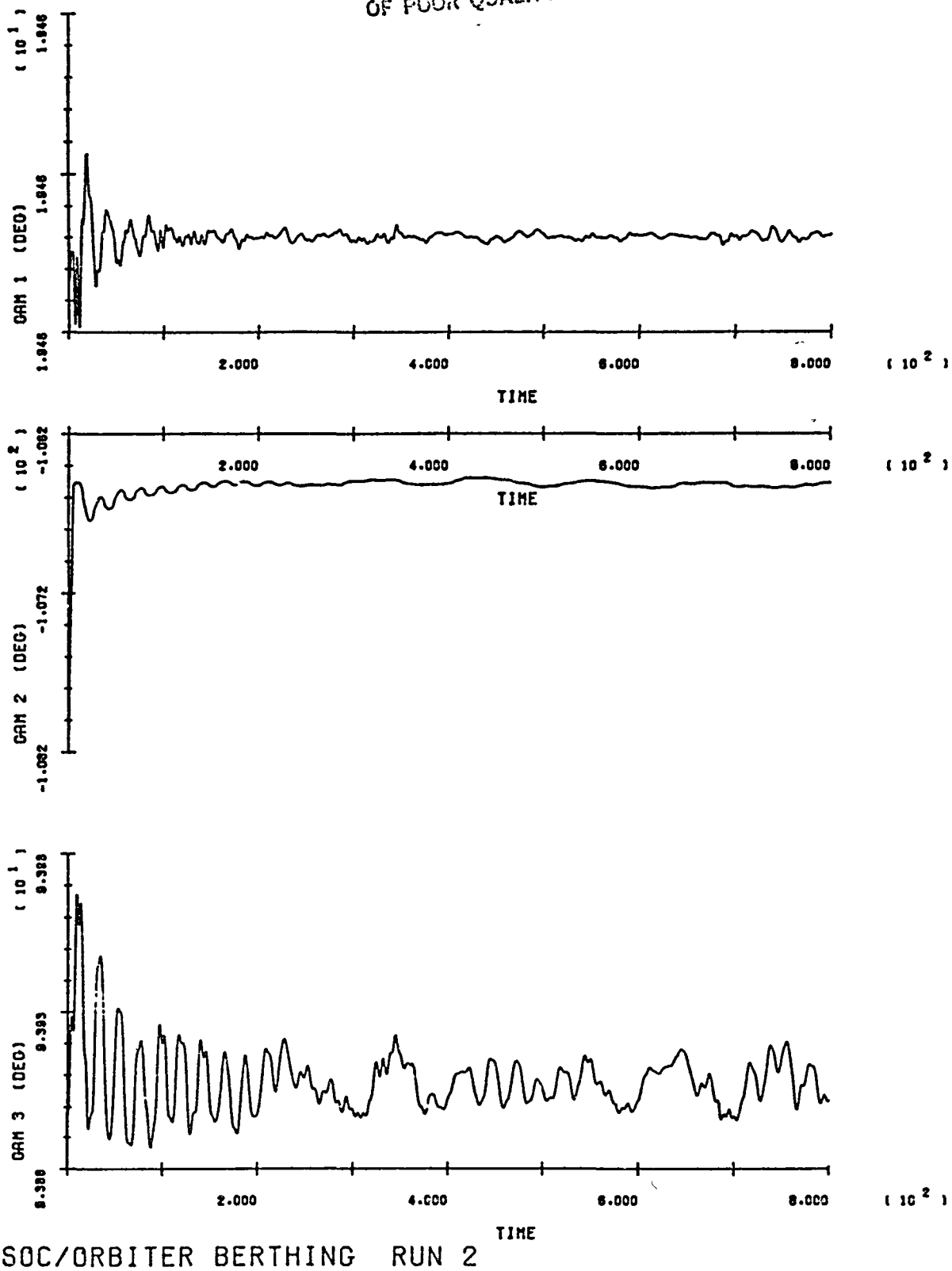


SOC/ORBITER BERTHING RUN 2

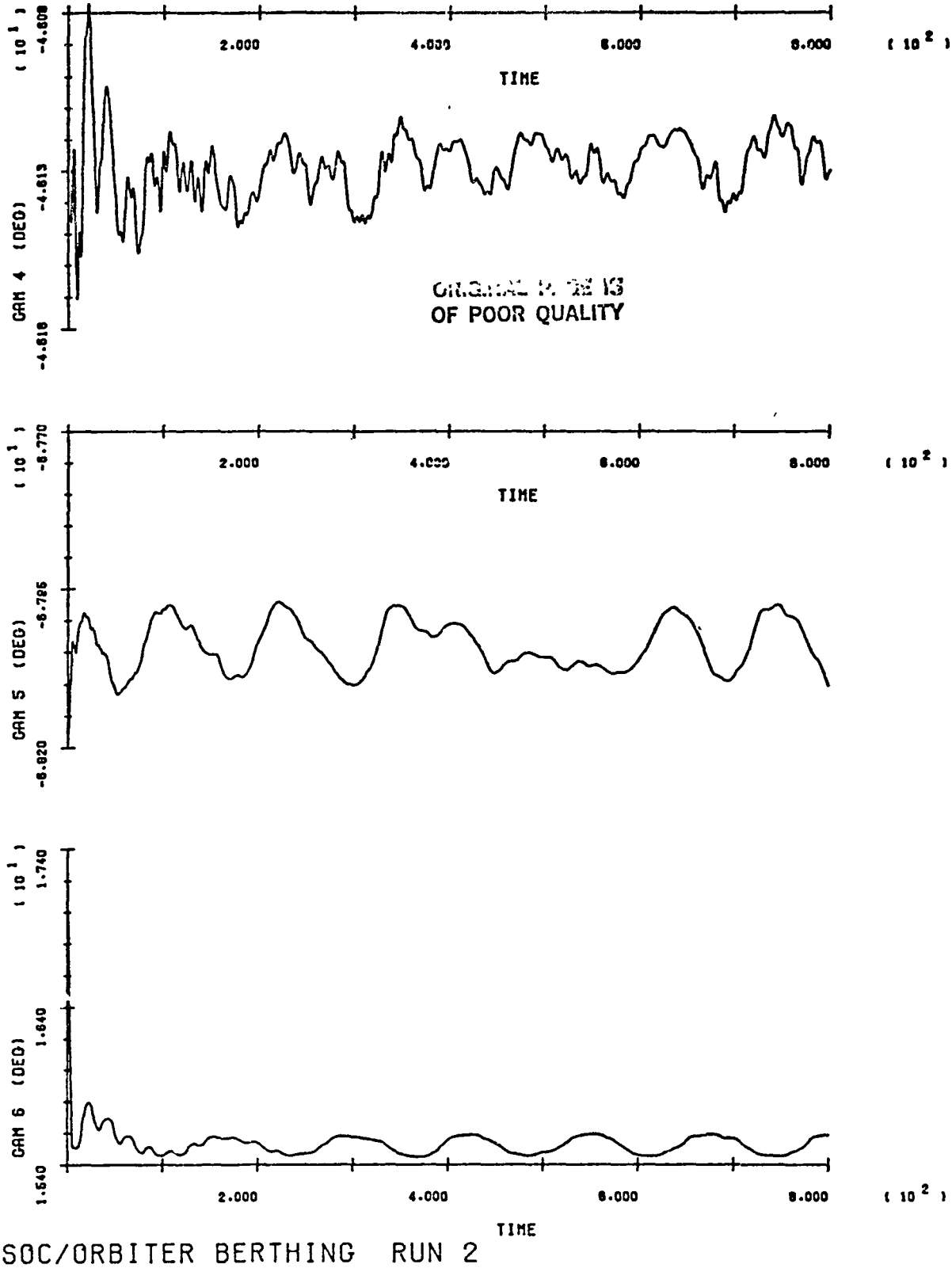


SOC/ORBITER BERTHING RUN 2

ORIGINAL PAGE IS
OF POOR QUALITY

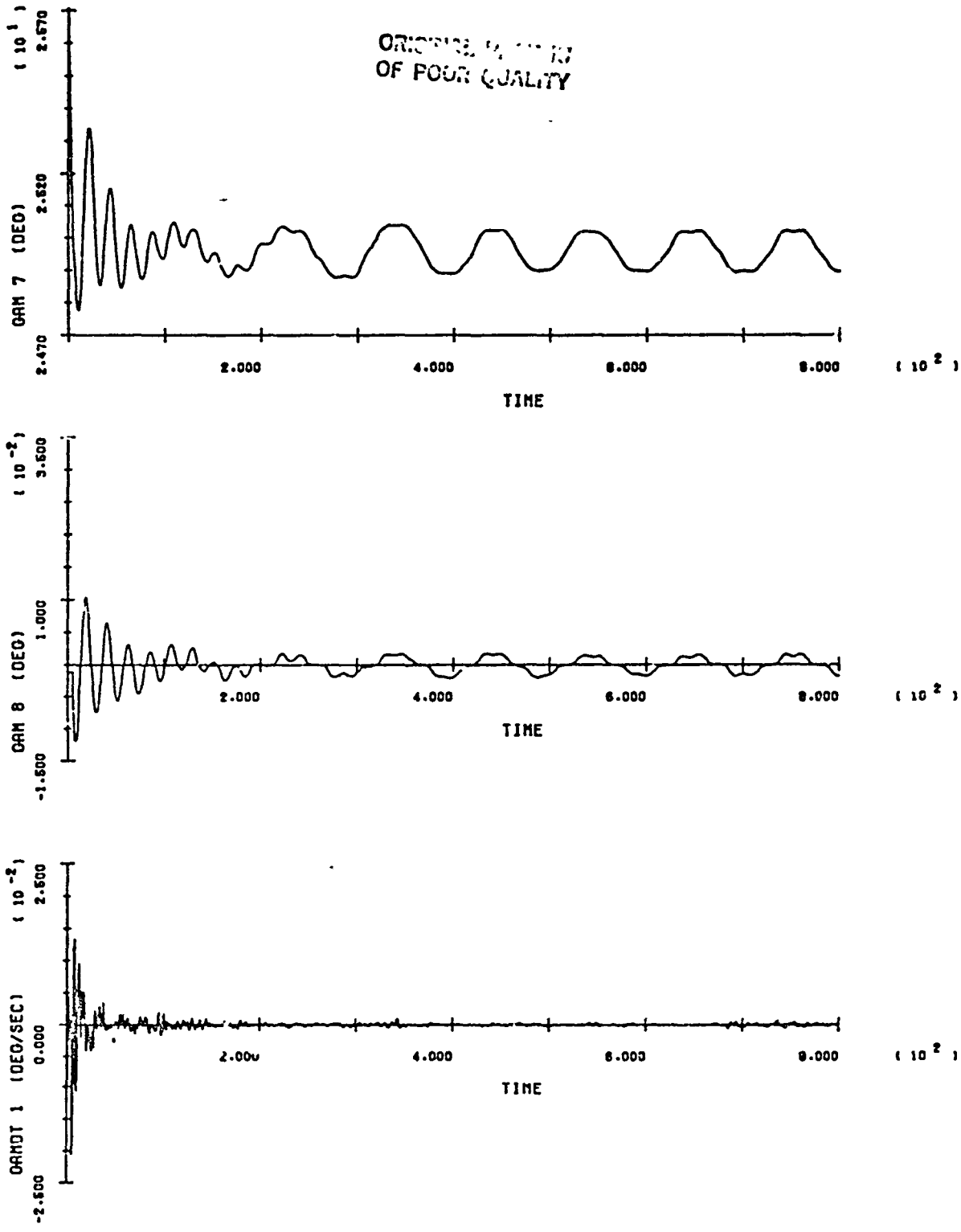


SOC/ORBITER BERTHING RUN 2

ORIGINAL PAGE IS
OF POOR QUALITY

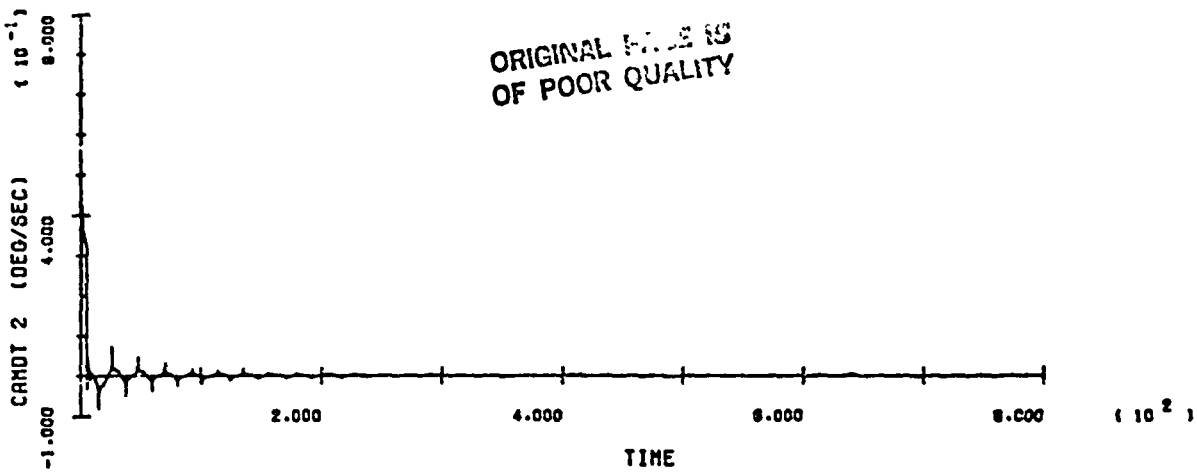


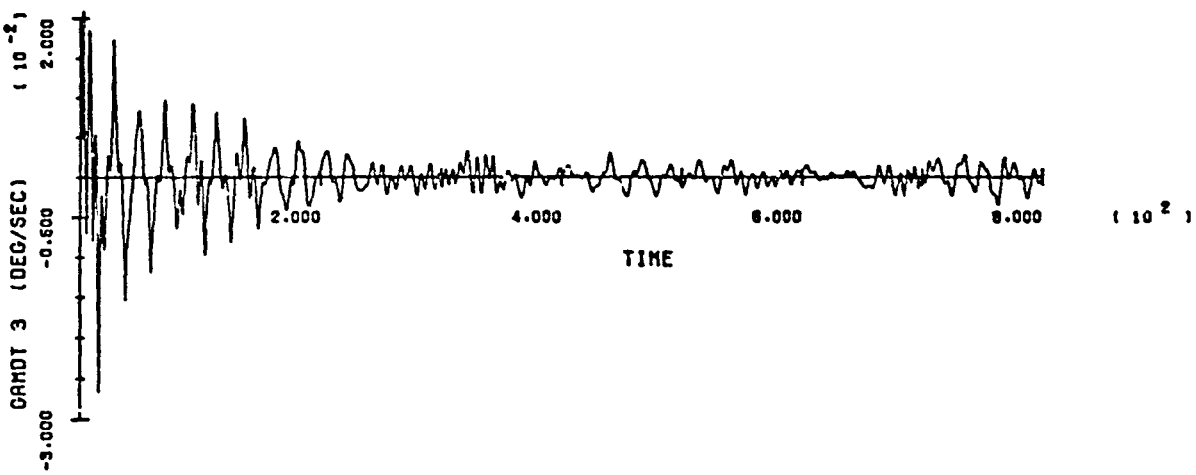


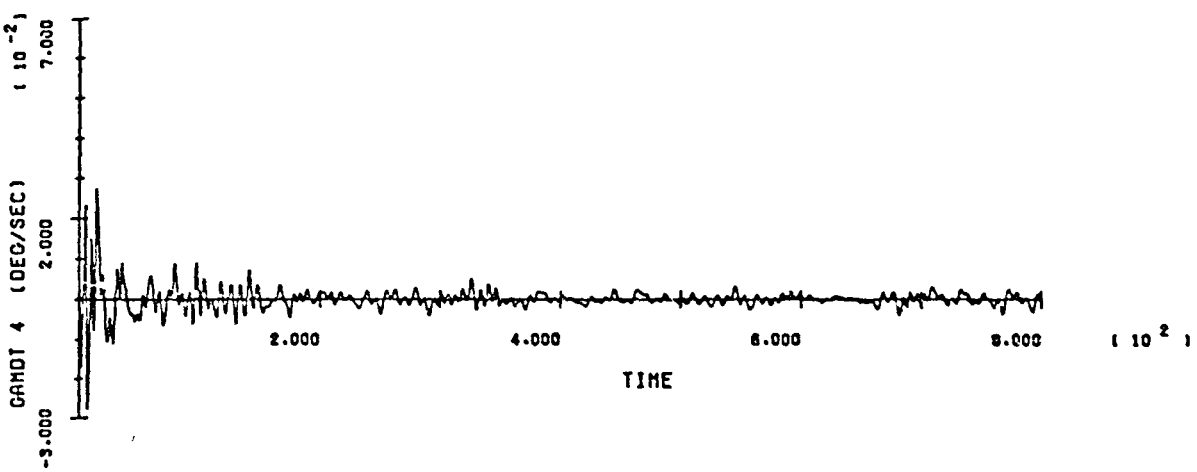


SOC/ORBITER BERTHING RUN 2

ORIGINAL PAGE IS
OF POOR QUALITY

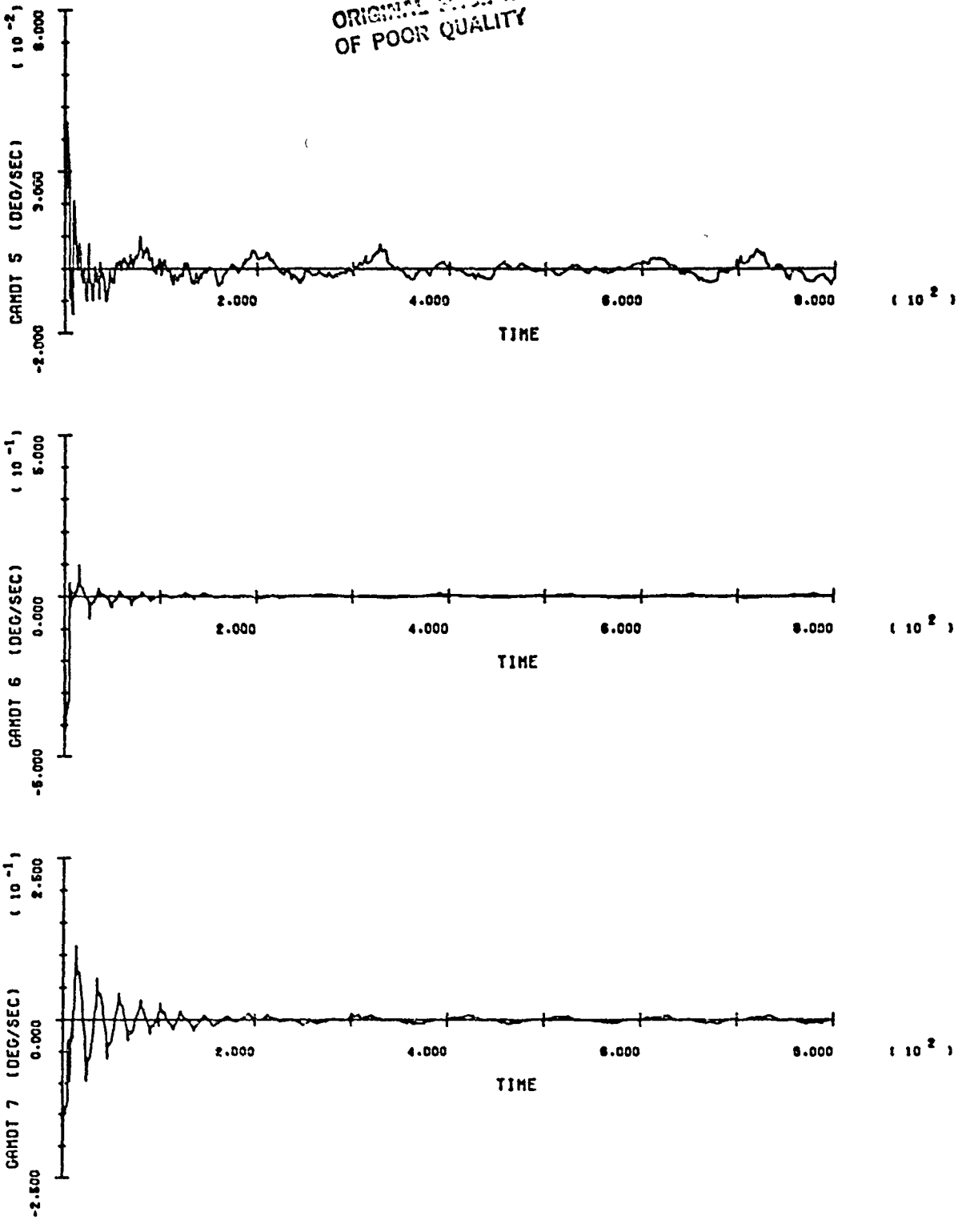


SOC/ORBITER BERTHING RUN 2

ORIGINAL PAGE IS
OF POOR QUALITY

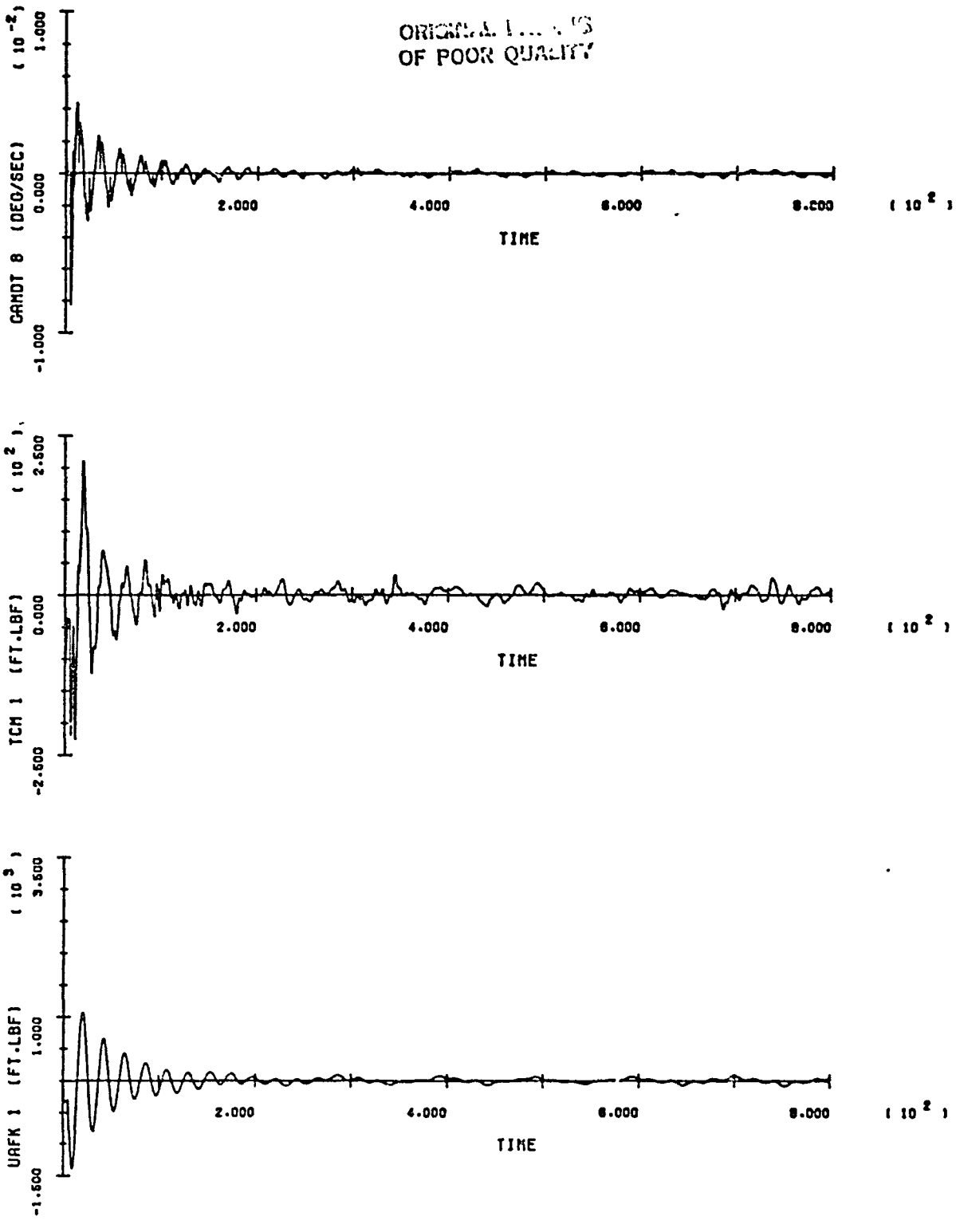


SOC/ORBITER BERTHING RUN 2

ORIGINAL PAGE IS
OF POOR QUALITY

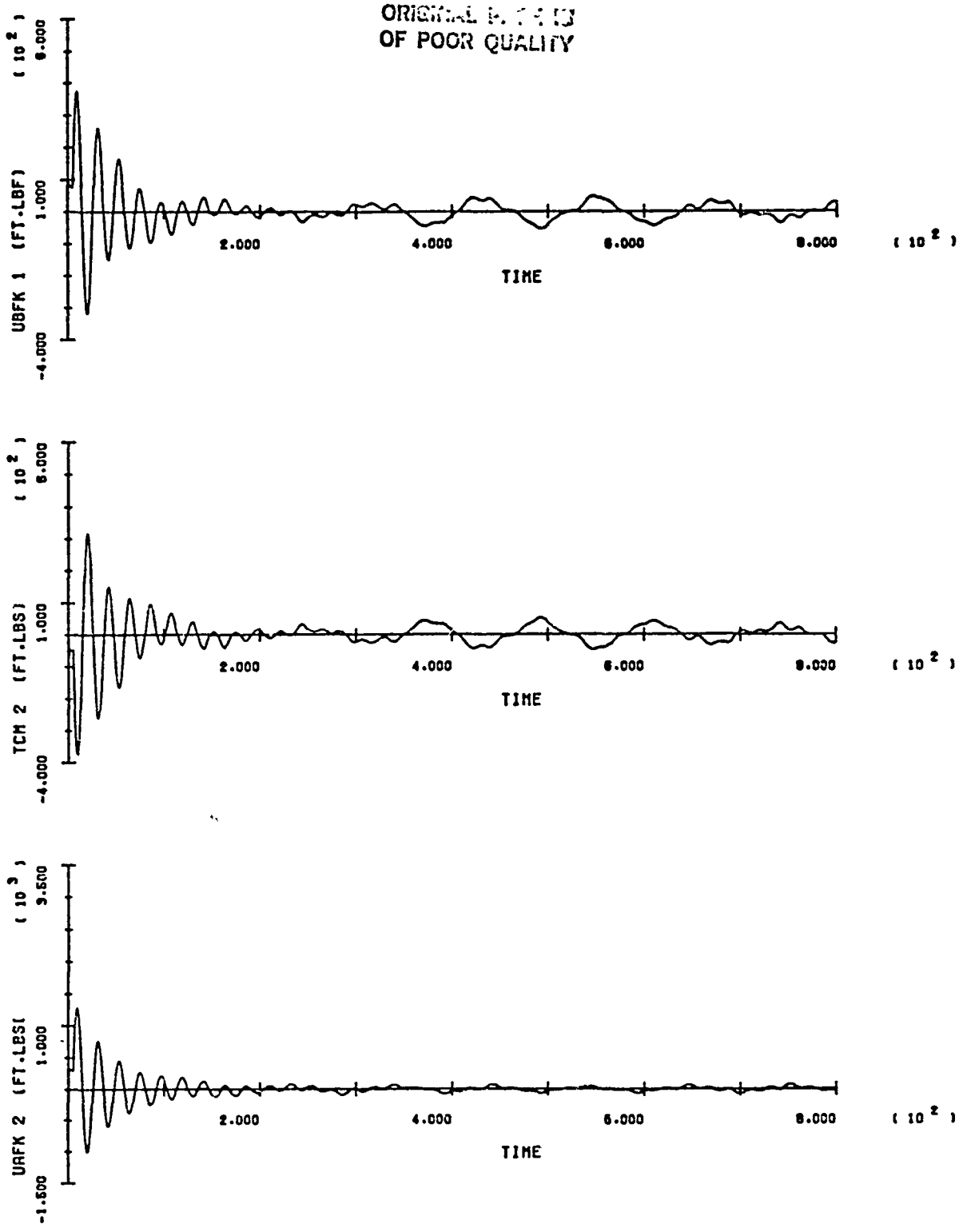


SOC/ORBITER BERTHING RUN 2

ORIGINAL PAGE IS
OF POOR QUALITY

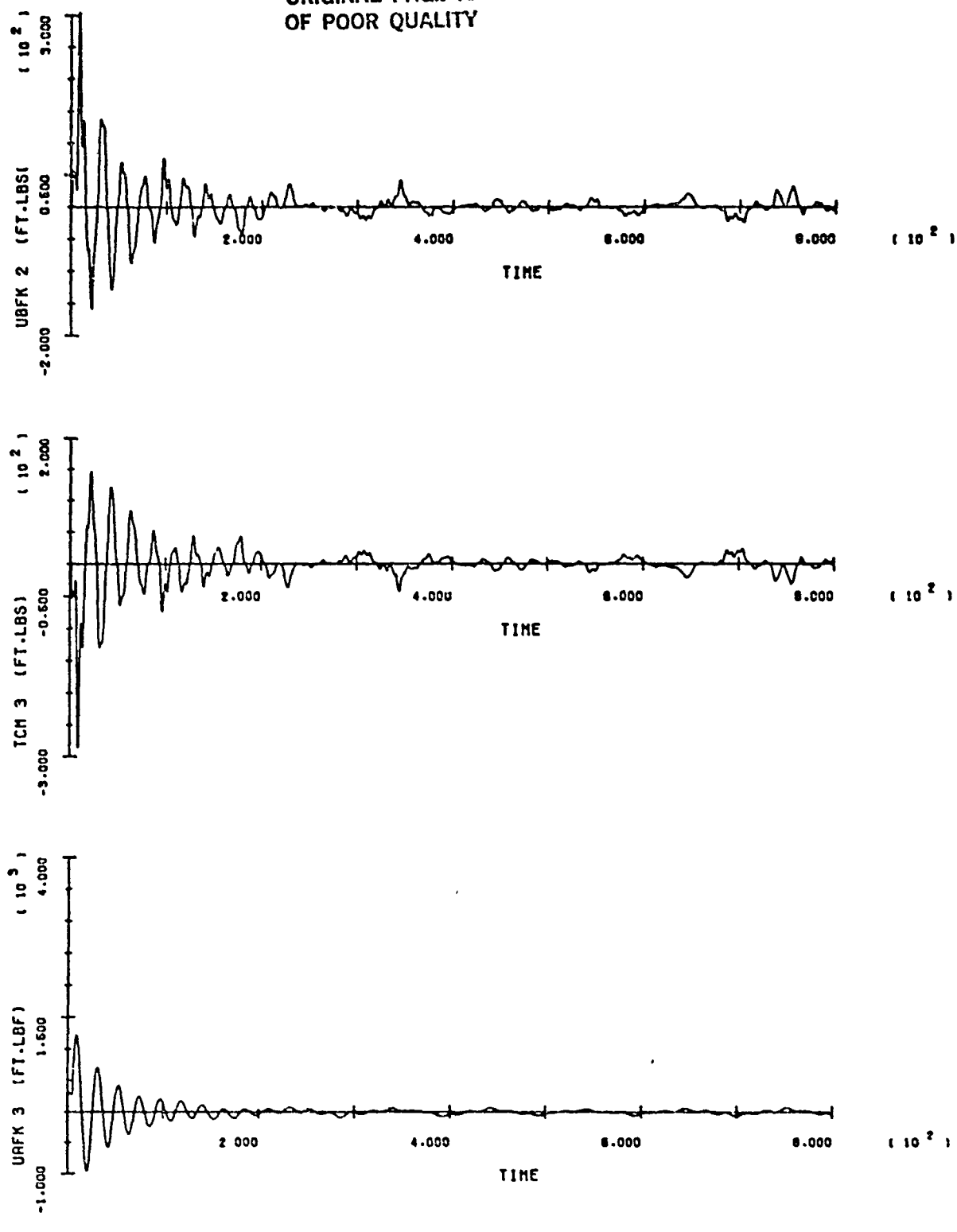


SOC/ORBITER BERTHING RUN 2

ORIGINAL PAGE IS
OF POOR QUALITY

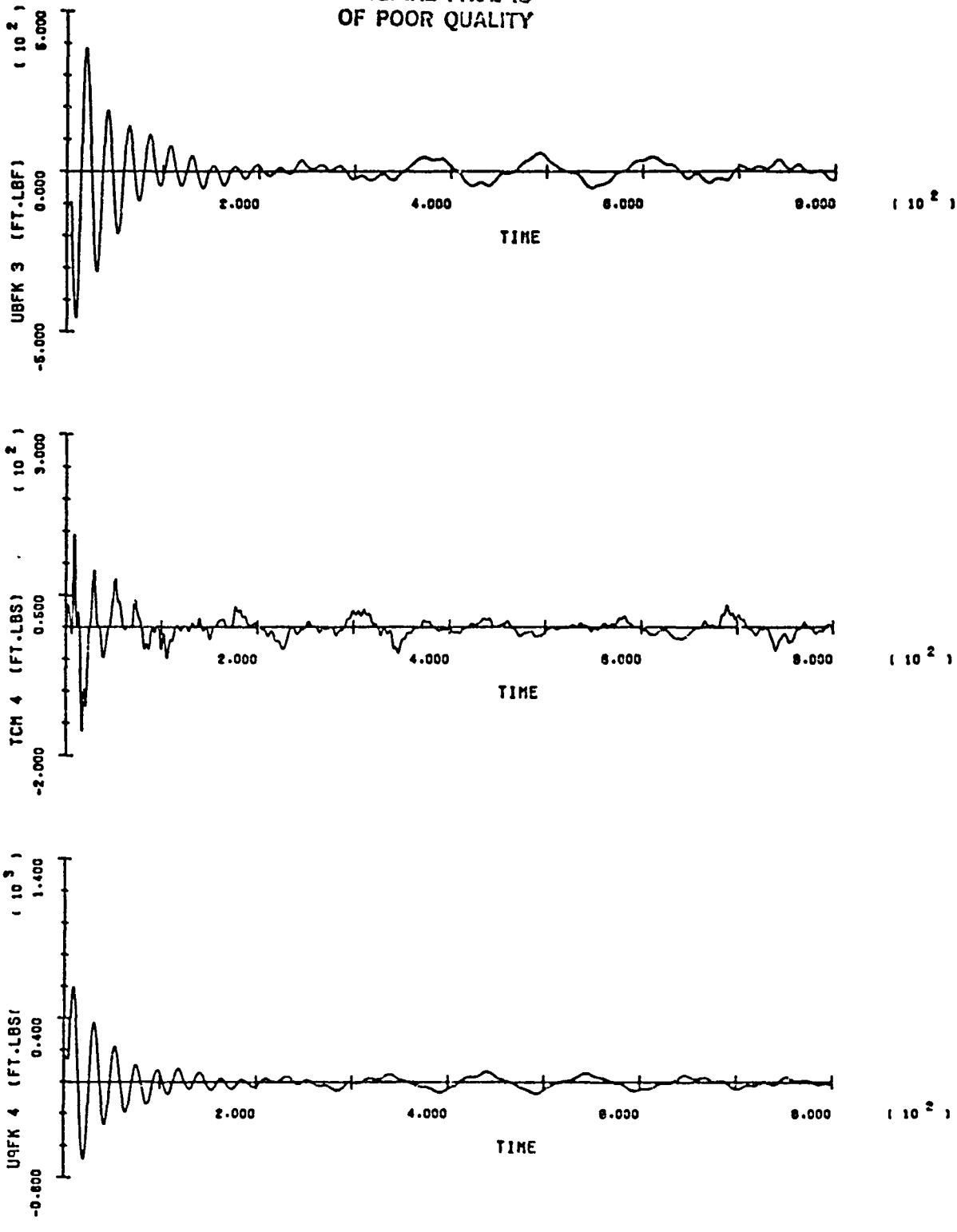


SOC/ORBITER BERTHING RUN 2

ORIGINAL PAGE IS
OF POOR QUALITY

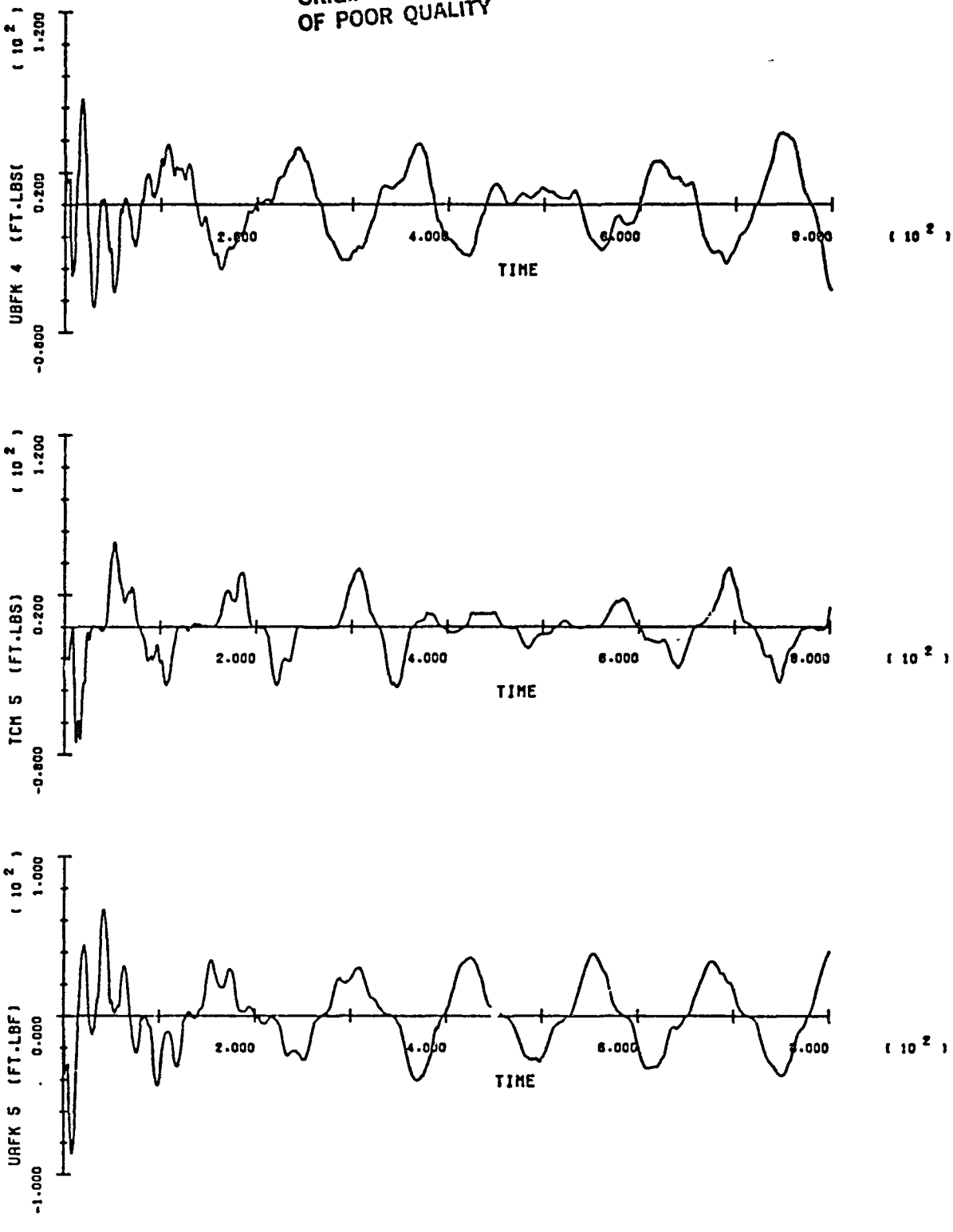


SOC/ORBITER BERTHING RUN 2

ORIGINAL PAGE IS
OF POOR QUALITY

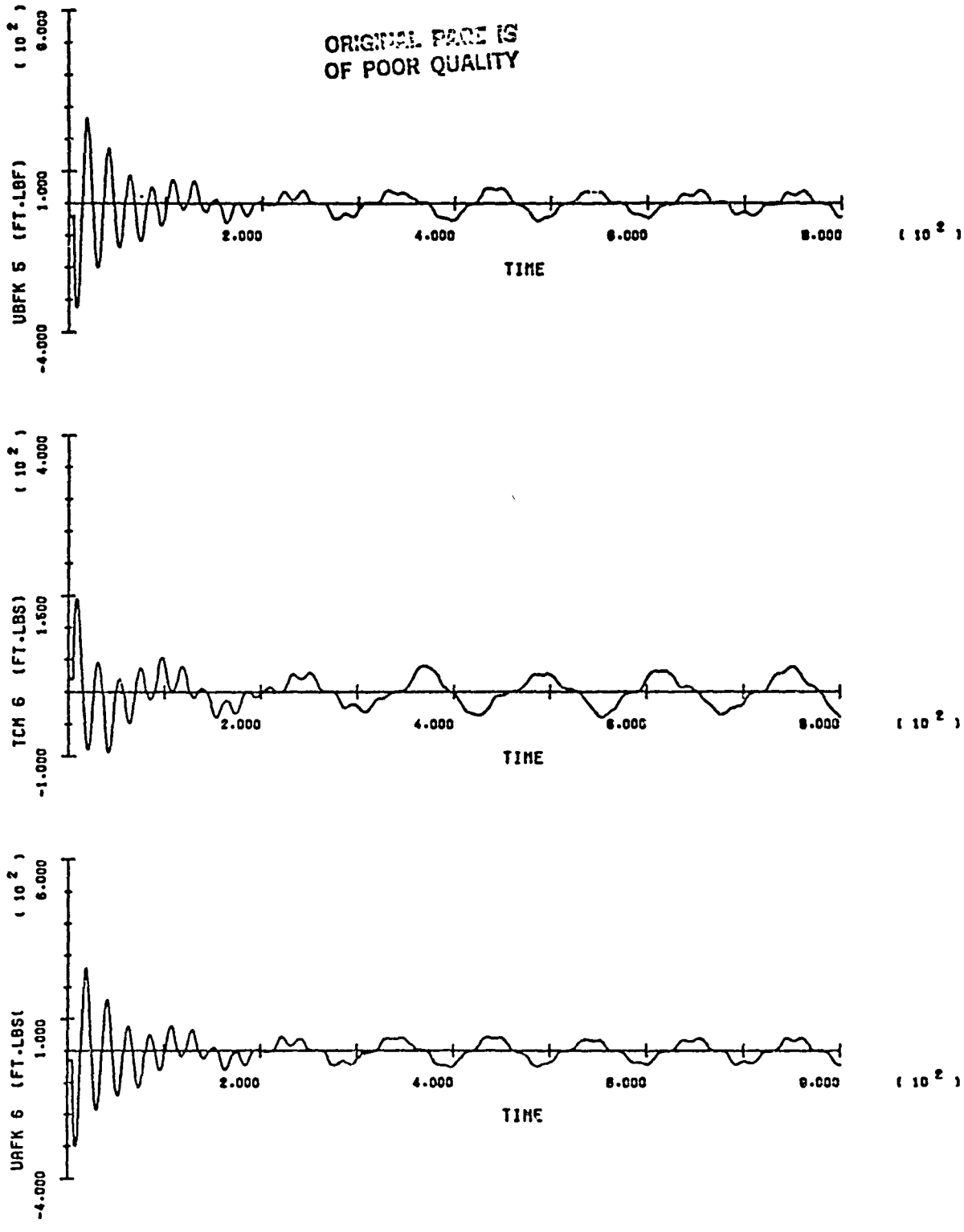


SOC/ORBITER BERTHING RUN 2

ORIGINAL PAGE IS
OF POOR QUALITY

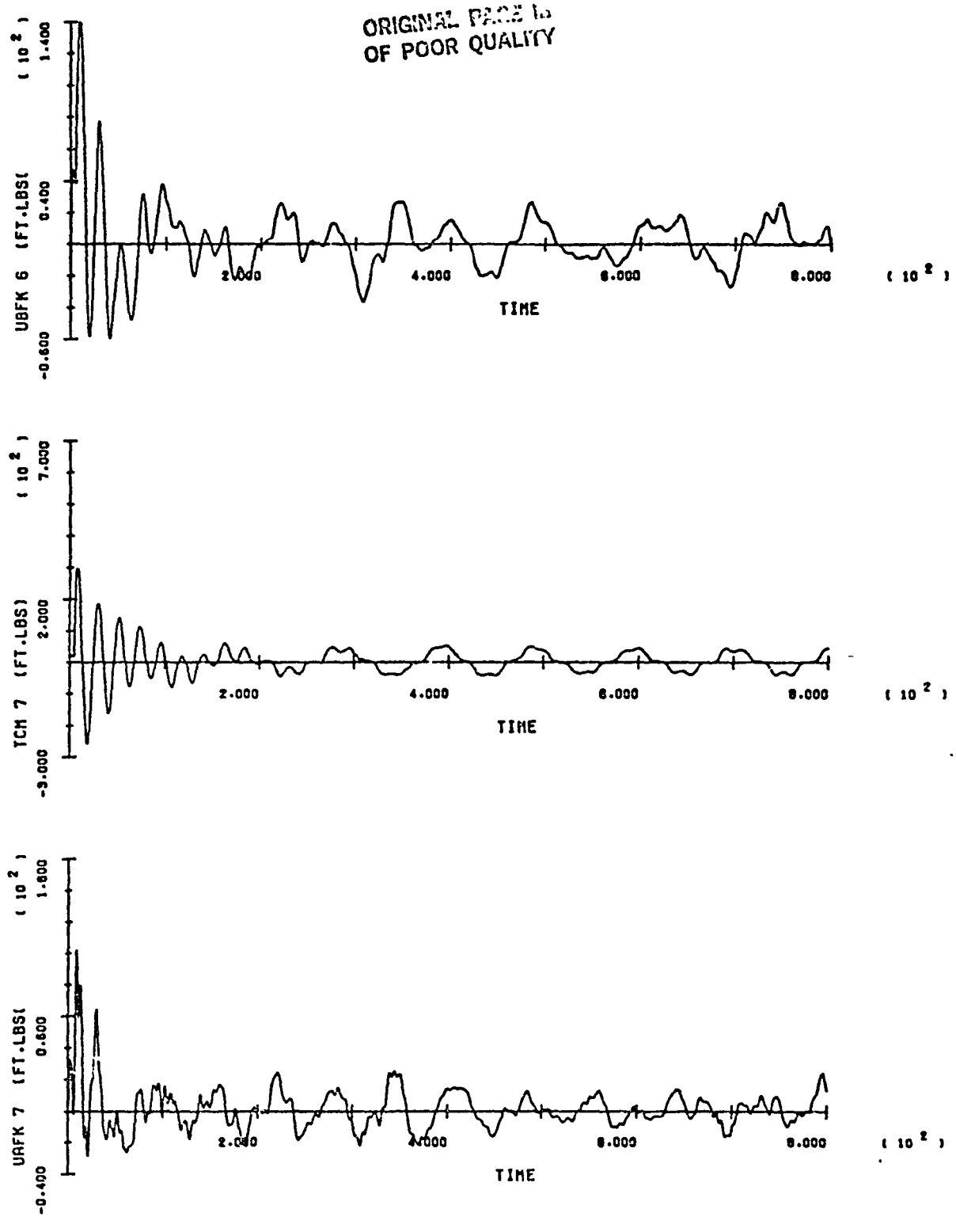


SOC/ORBITER BERTHING RUN 2

ORIGINAL PAGE IS
OF POOR QUALITY

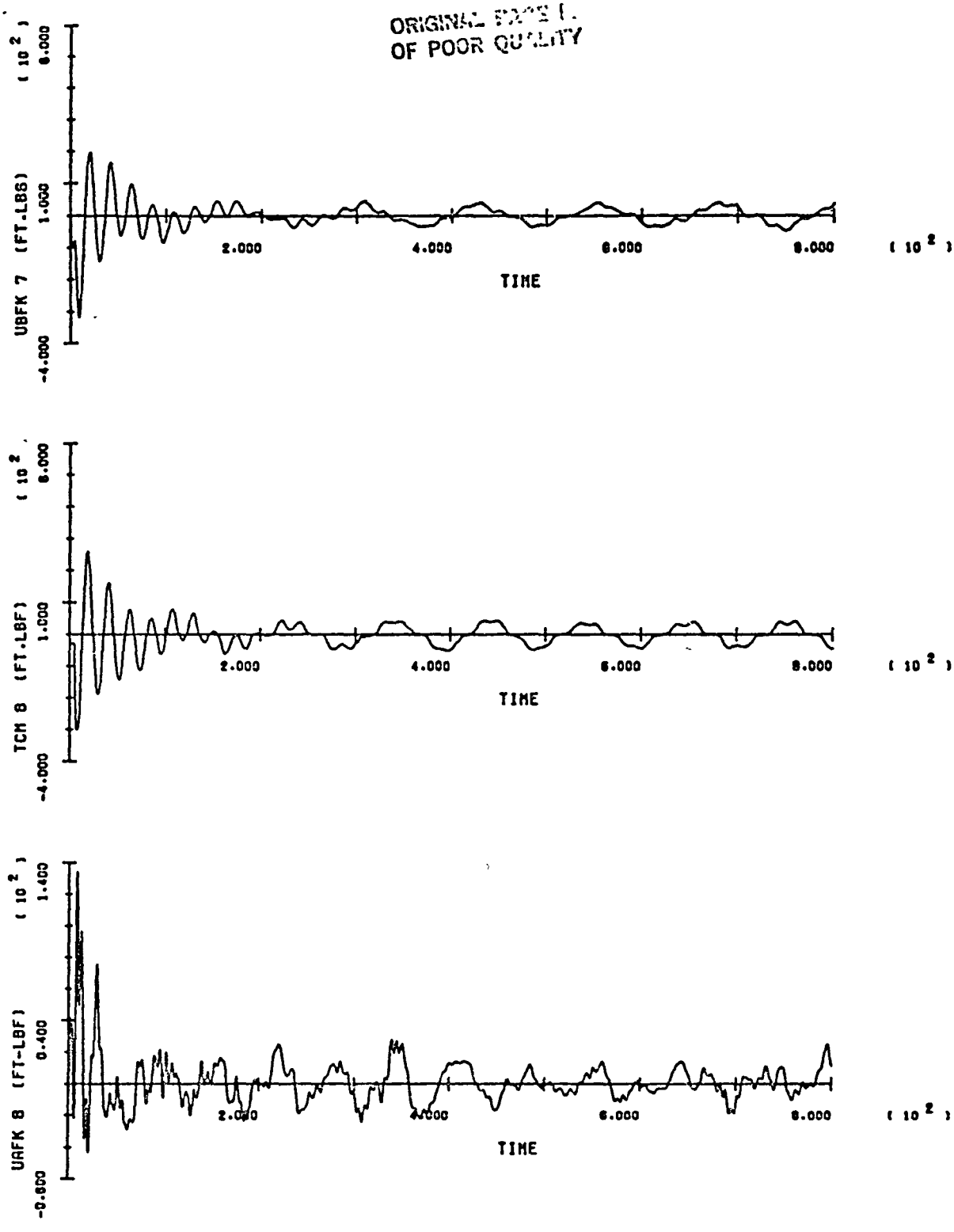


SOC/ORBITER BERTHING RUN 2

ORIGINAL PAGE IS
OF POOR QUALITY

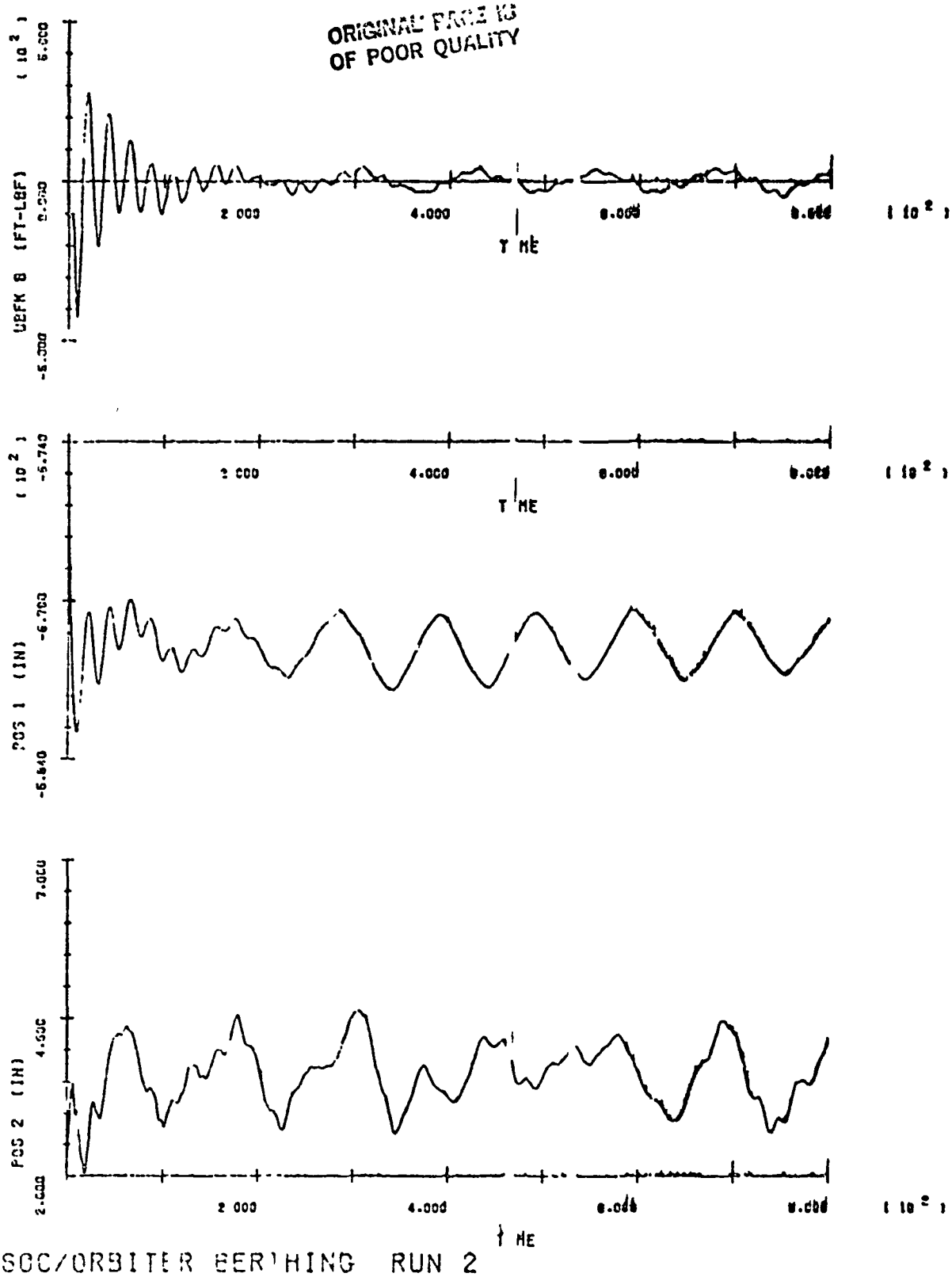


SOC/ORBITER BERTHING RUN 2

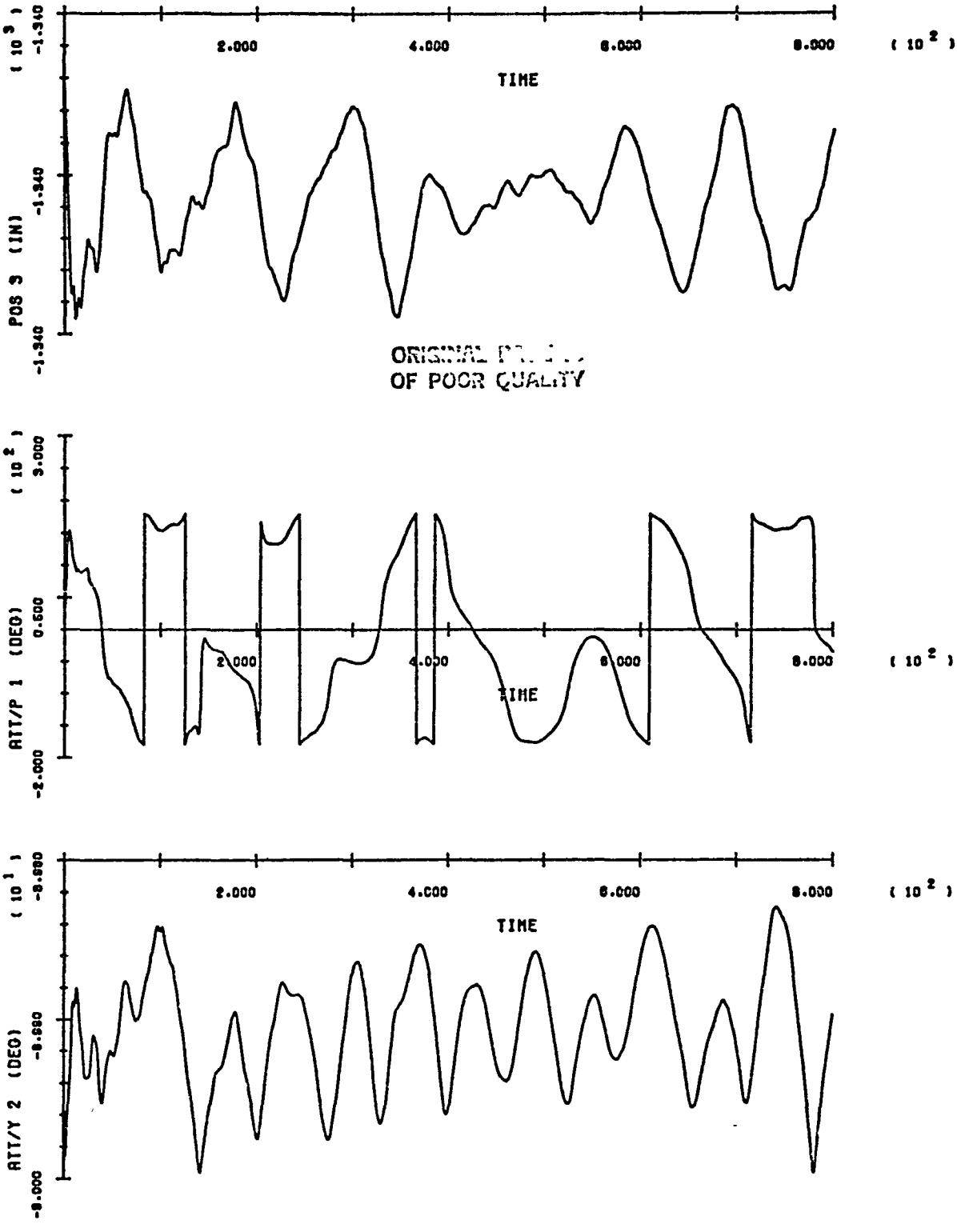


SOC/ORBITER BERTHING RUN 2

ORIGINAL PAGE IS
OF POOR QUALITY

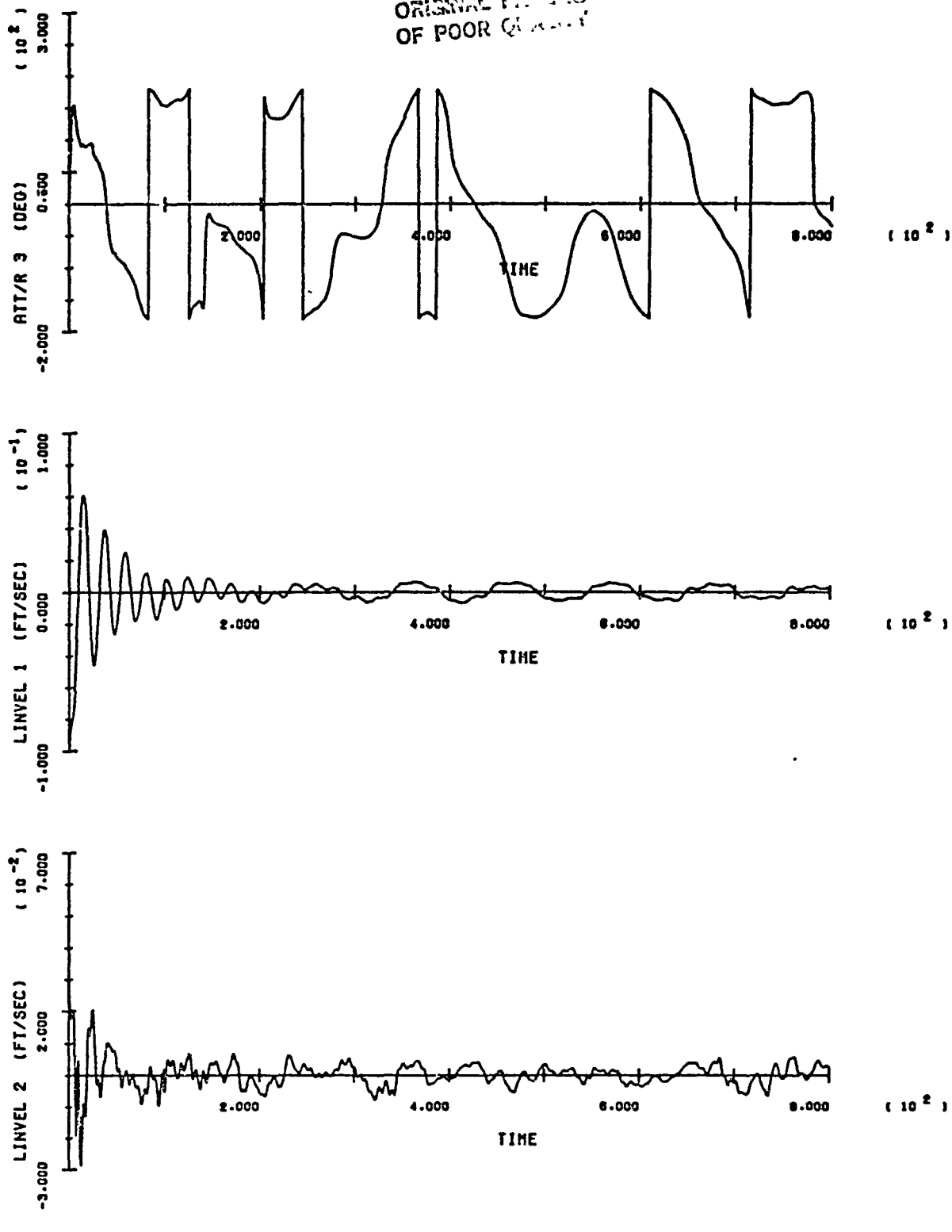


SOC/ORBITER BERTHING RUN 2

ORIGINAL PAGE IS
OF POOR QUALITY

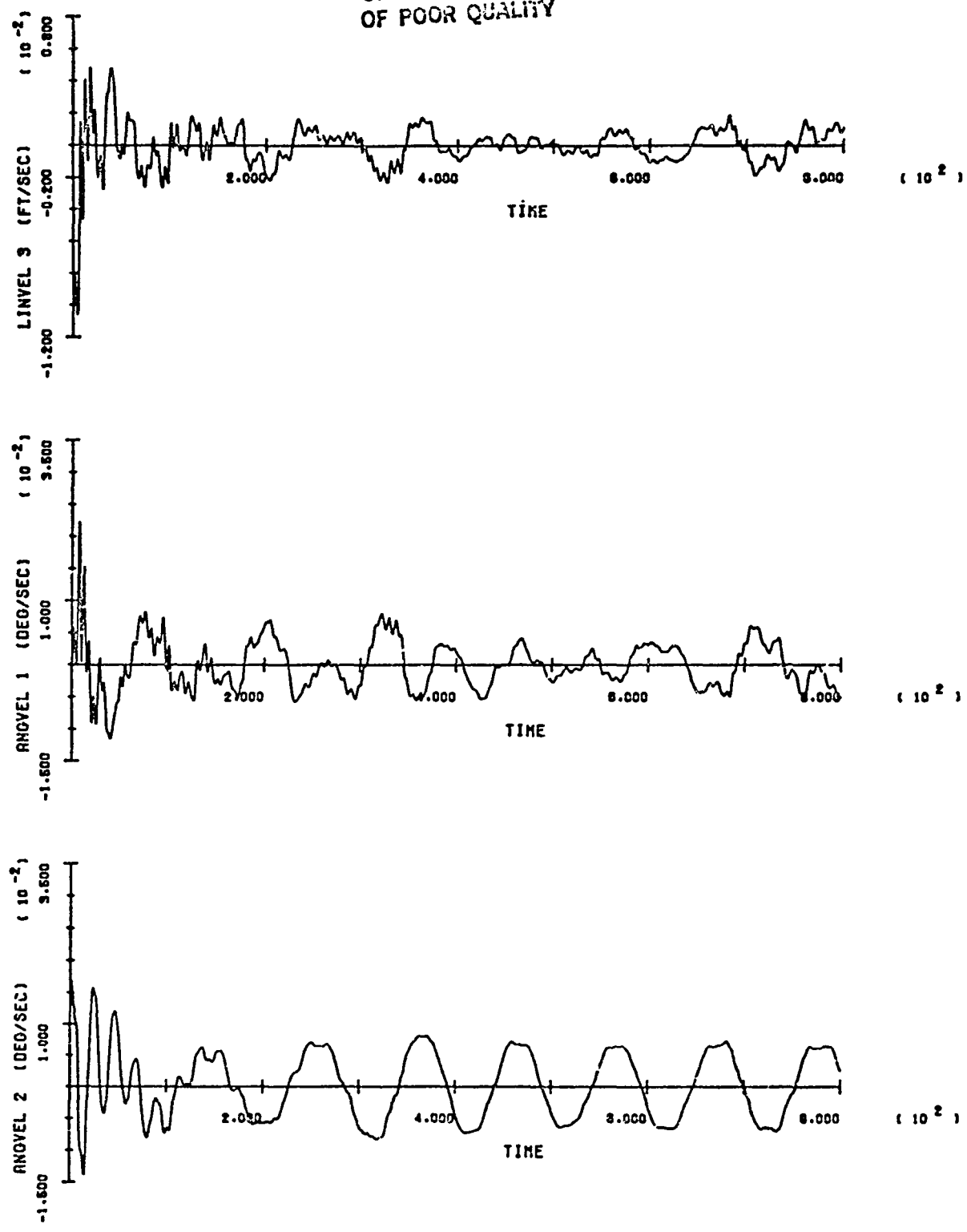


SOC/ORBITER BERTHING RUN 2

ORIGINAL PAGE IS
OF POOR QUALITY

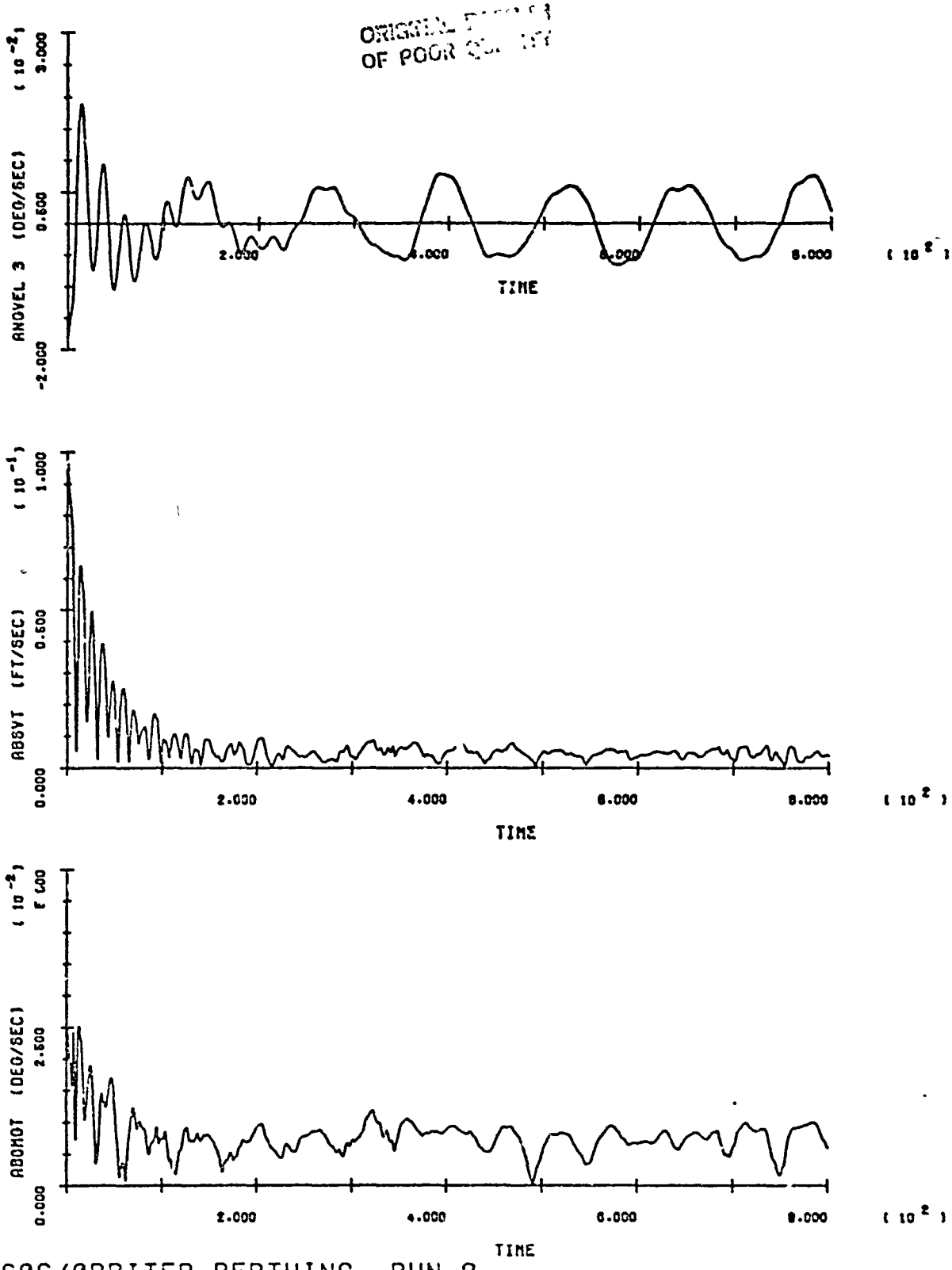


SOC/ORBITER BERTHING RUN 2

ORIGINAL PAGE IS
OF POOR QUALITY

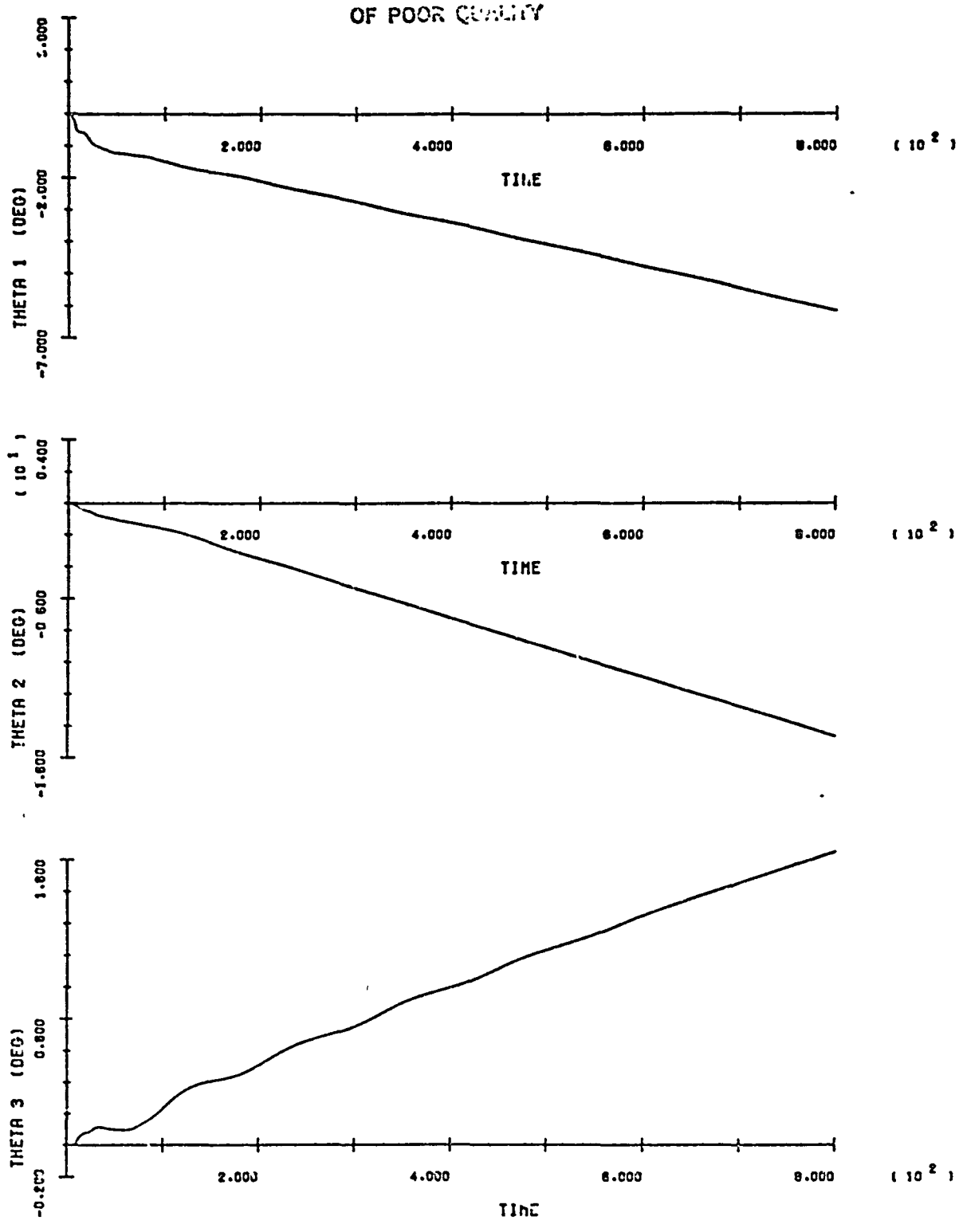


SOC/ORB BERTH RUN 3

ORIGINAL PAGE IS
OF POOR QUALITY

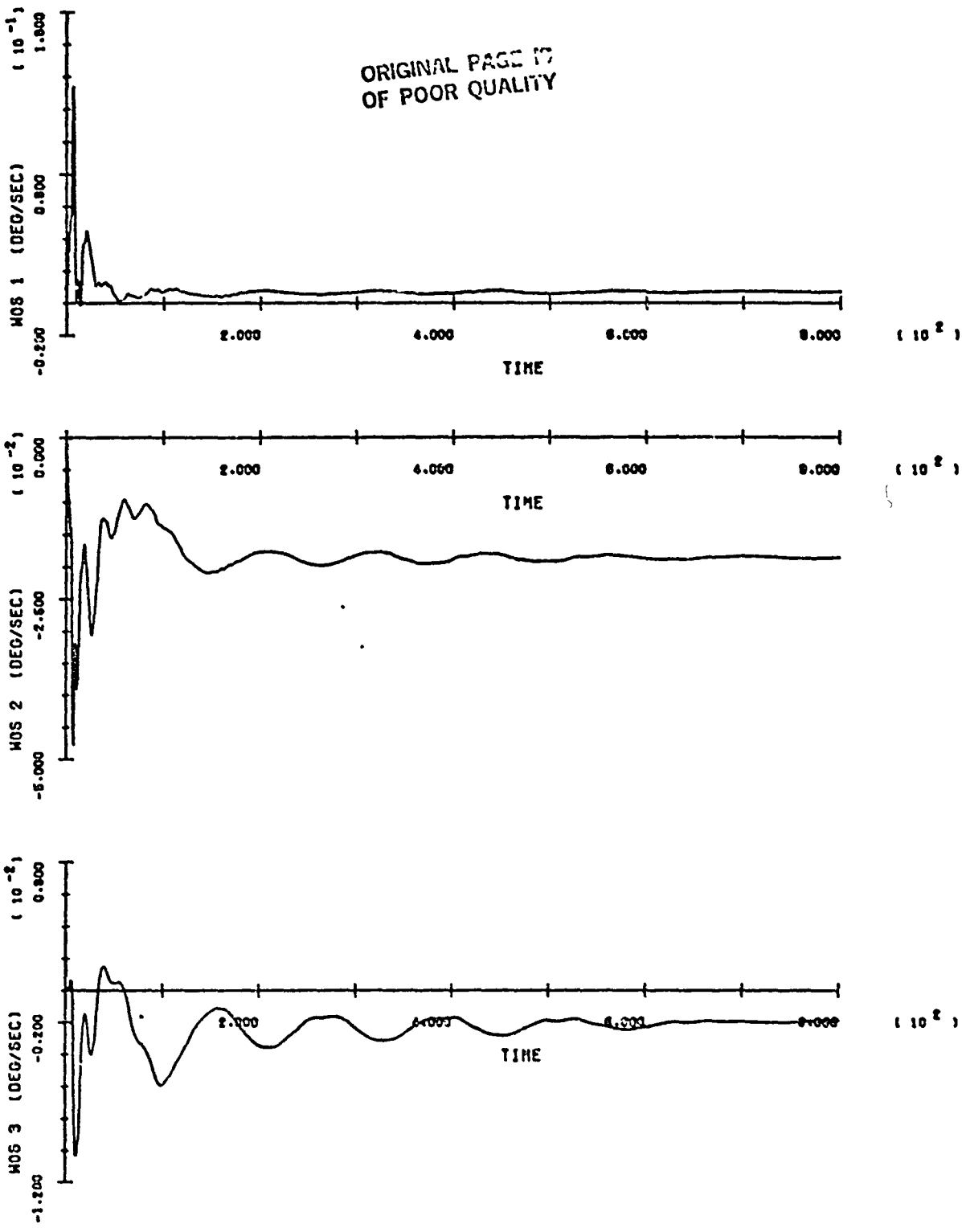


SOC/ORB BERTH RUN 3

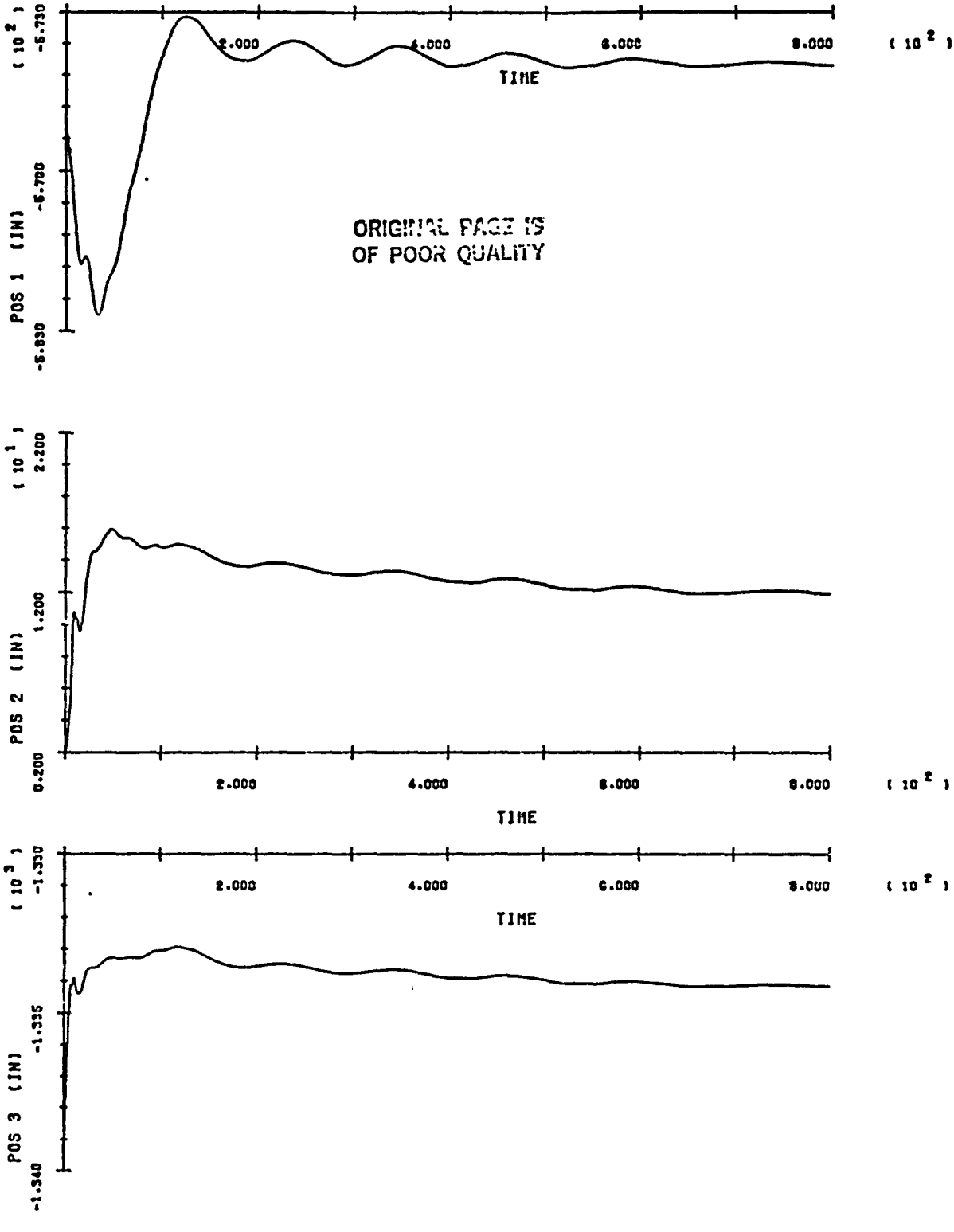


SOC/ORB BERTH RUN 3

ORIGINAL PAGE IS
OF POOR QUALITY

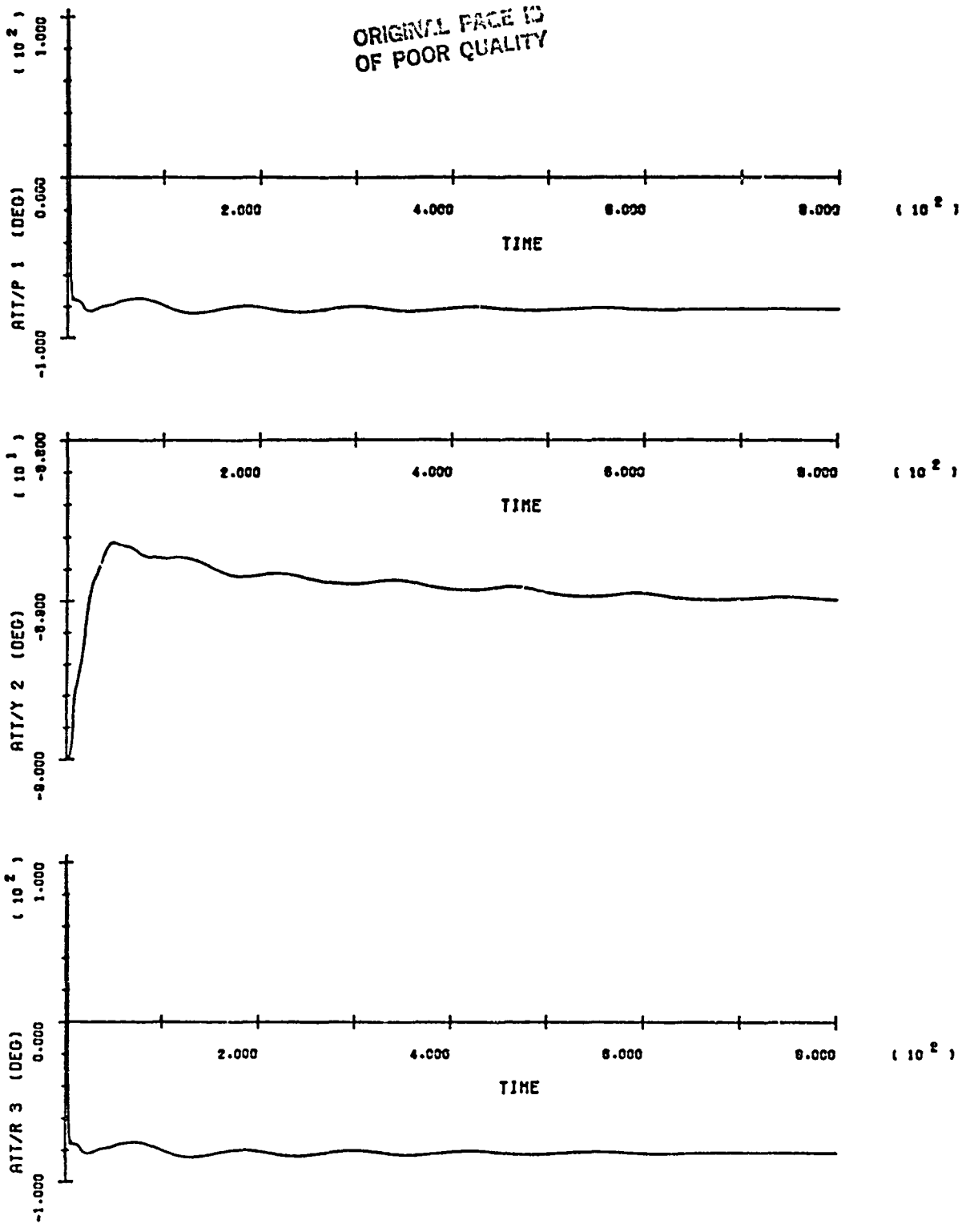


SOC/ORB BERTH RUN 3

ORIGINAL PAGE IS
OF POOR QUALITY

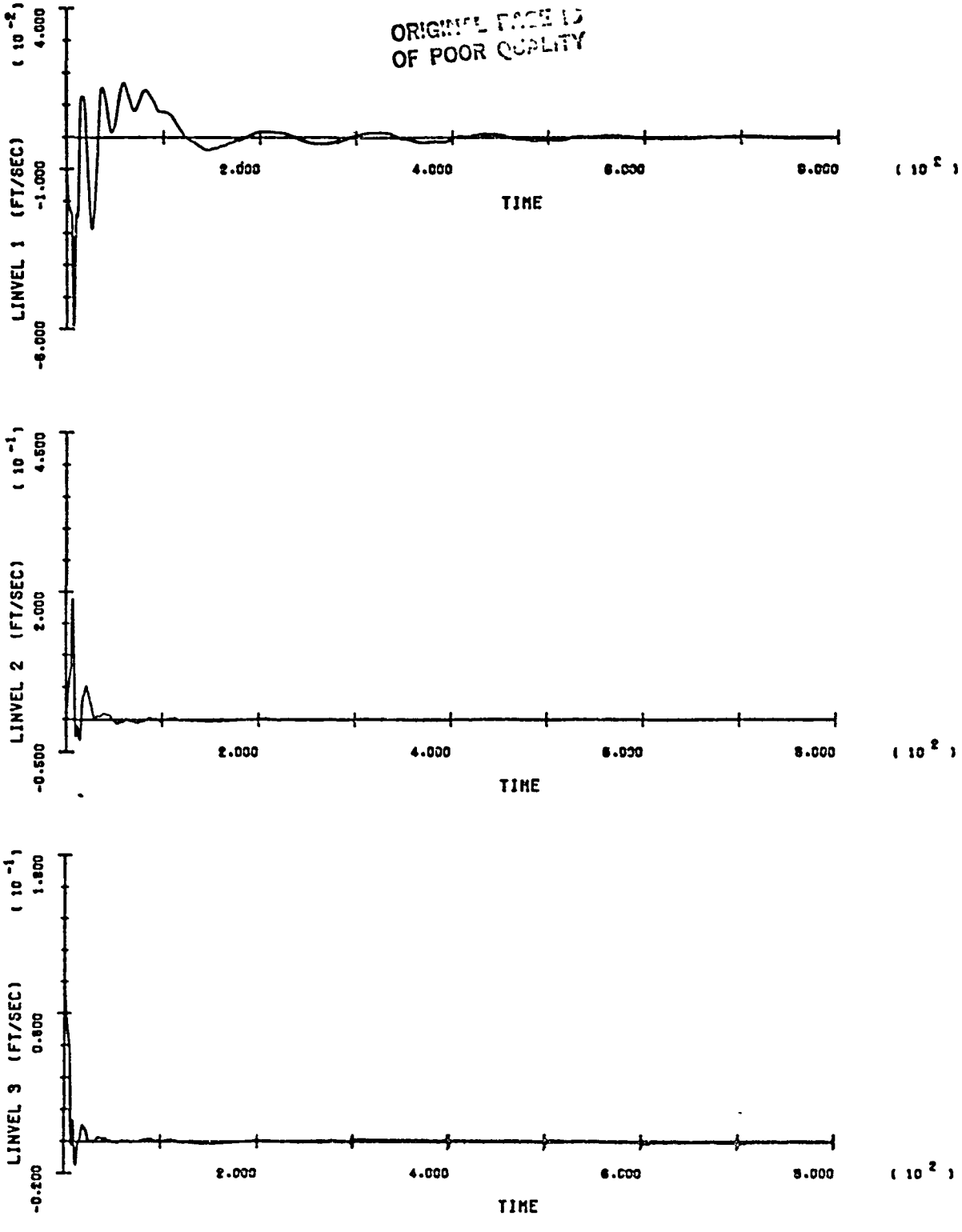


SOC/ORB BERTH RUN 3

ORIGINAL PAGE IS
OF POOR QUALITY

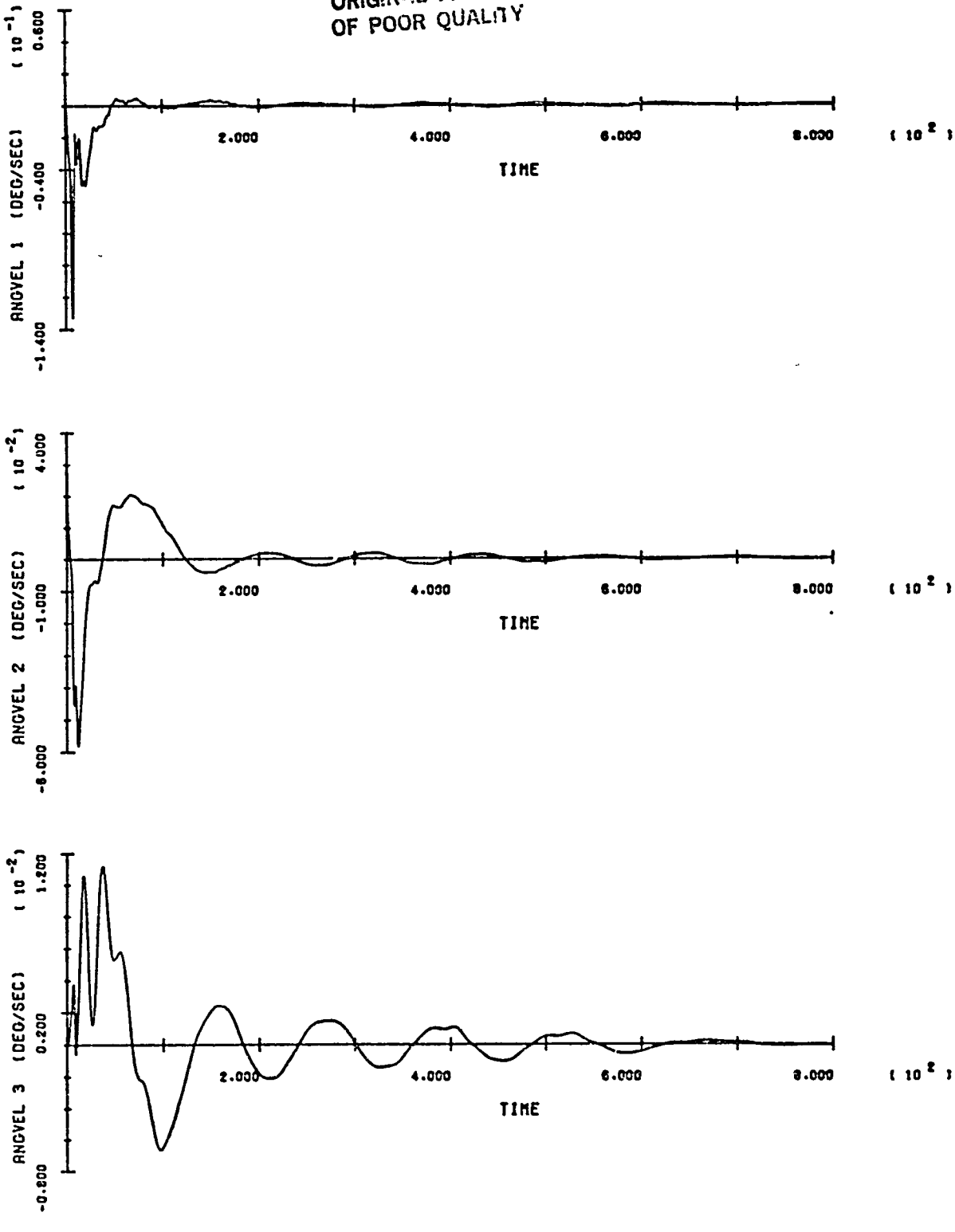


SOC/ORB BERTH RUN 3

ORIGINAL PAGE IS
OF POOR QUALITY

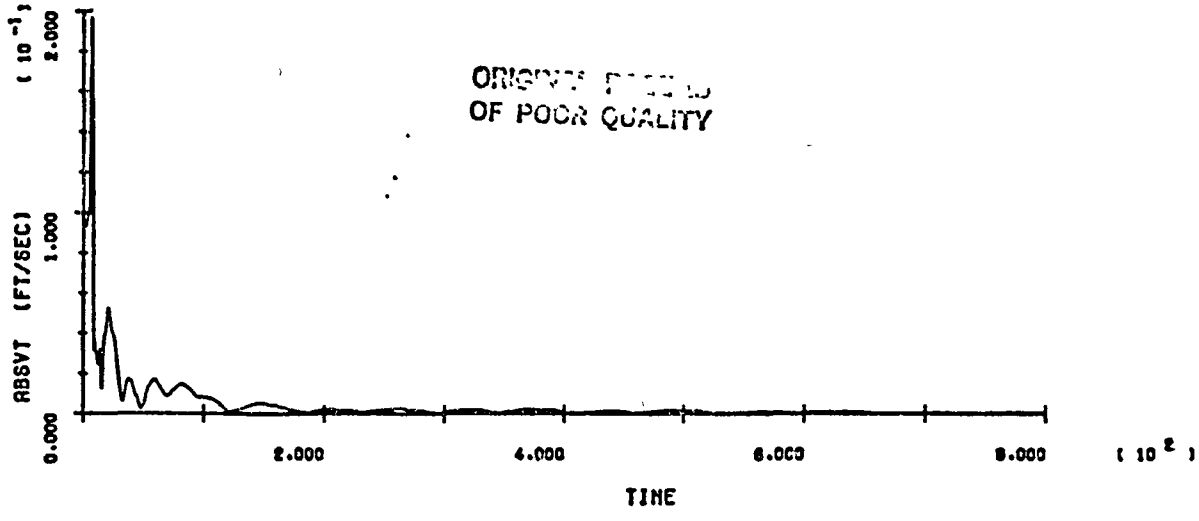


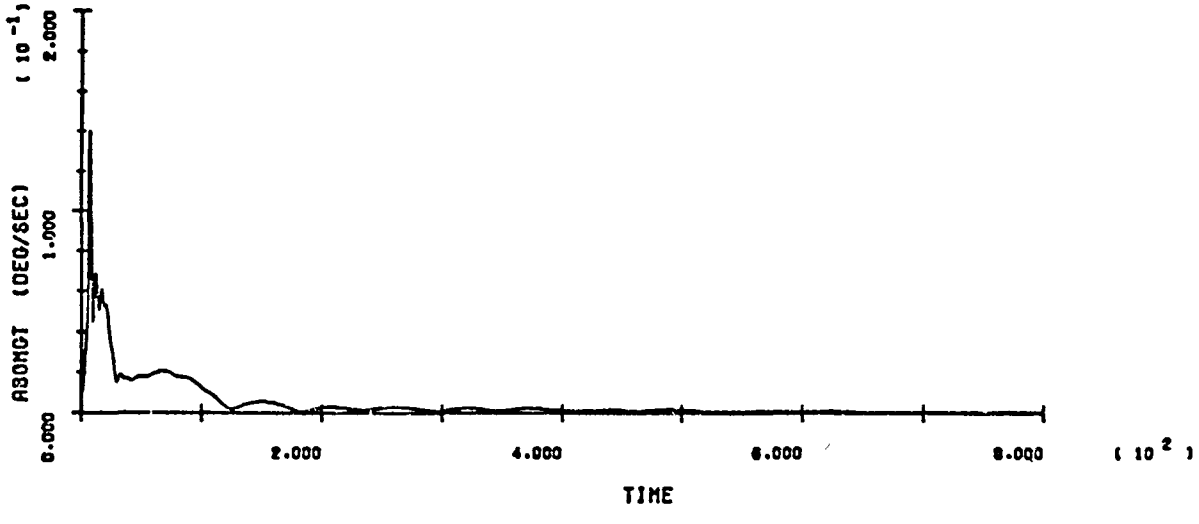


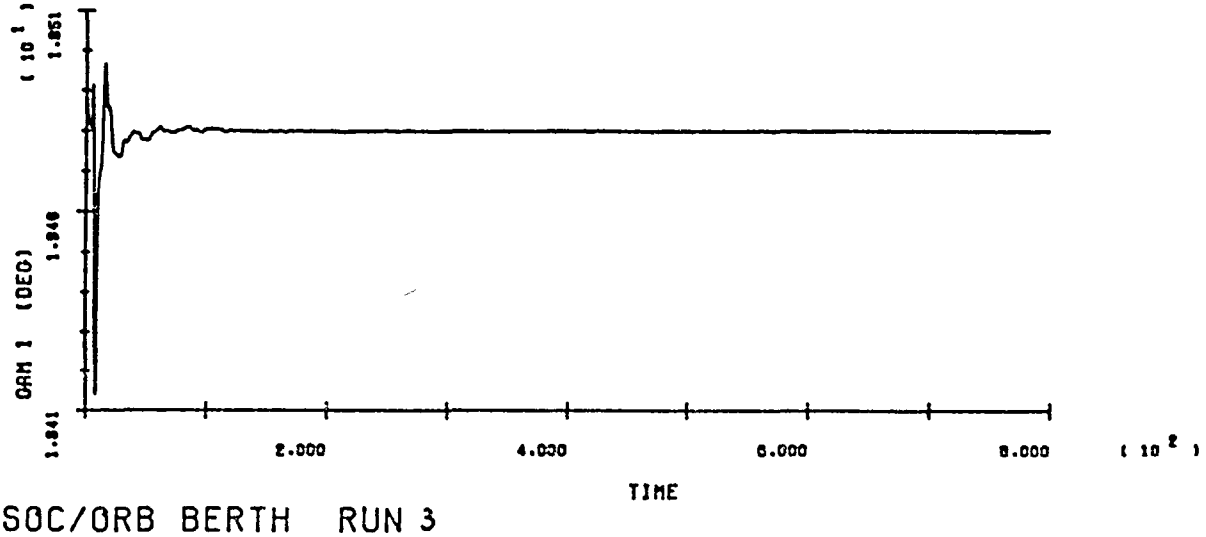


SOC/ORB BERTH RUN 3

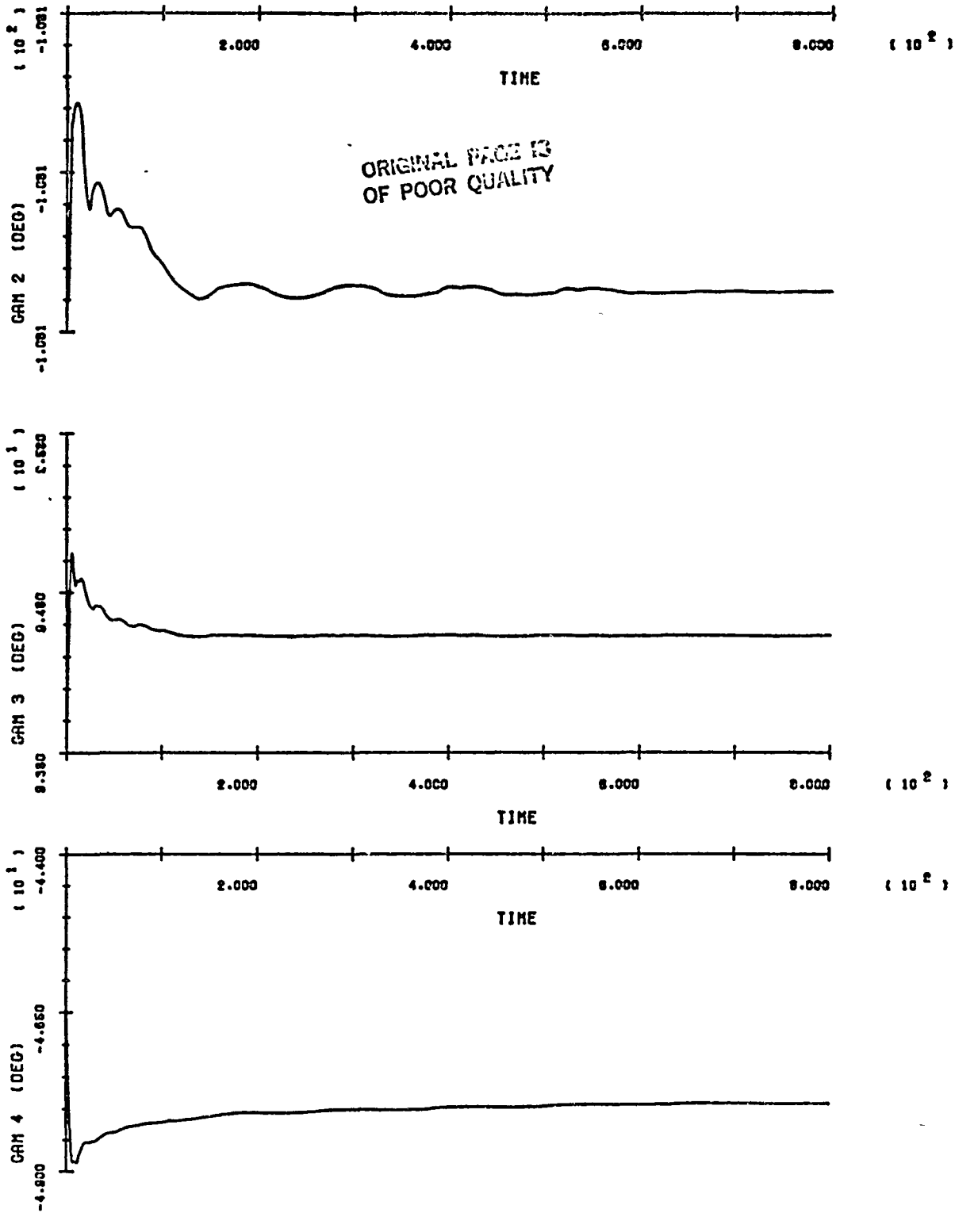


SOC/ORB BERTH RUN 3

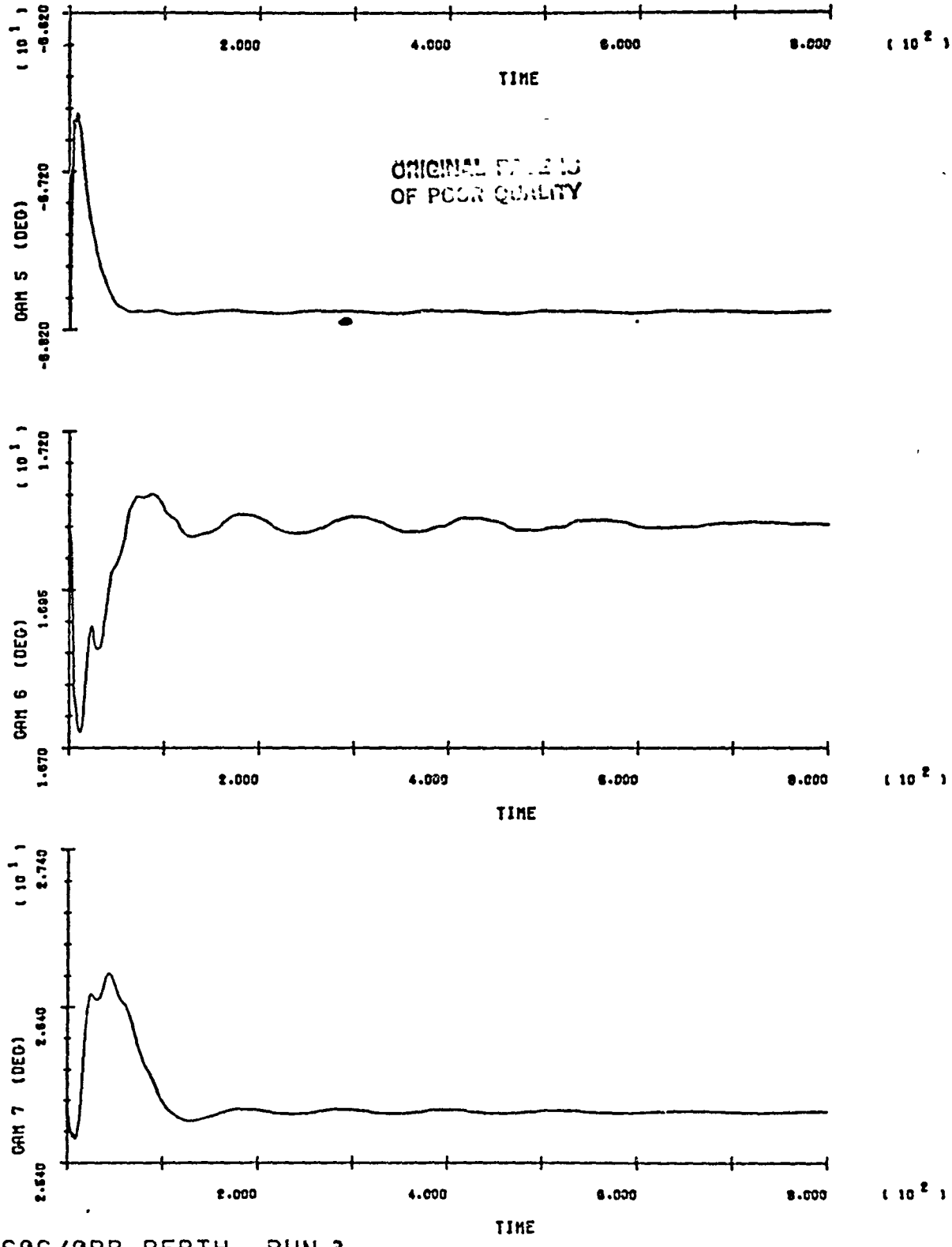


SOC/ORB BERTH RUN 3

ORIGINAL PAGE IS
OF POOR QUALITY

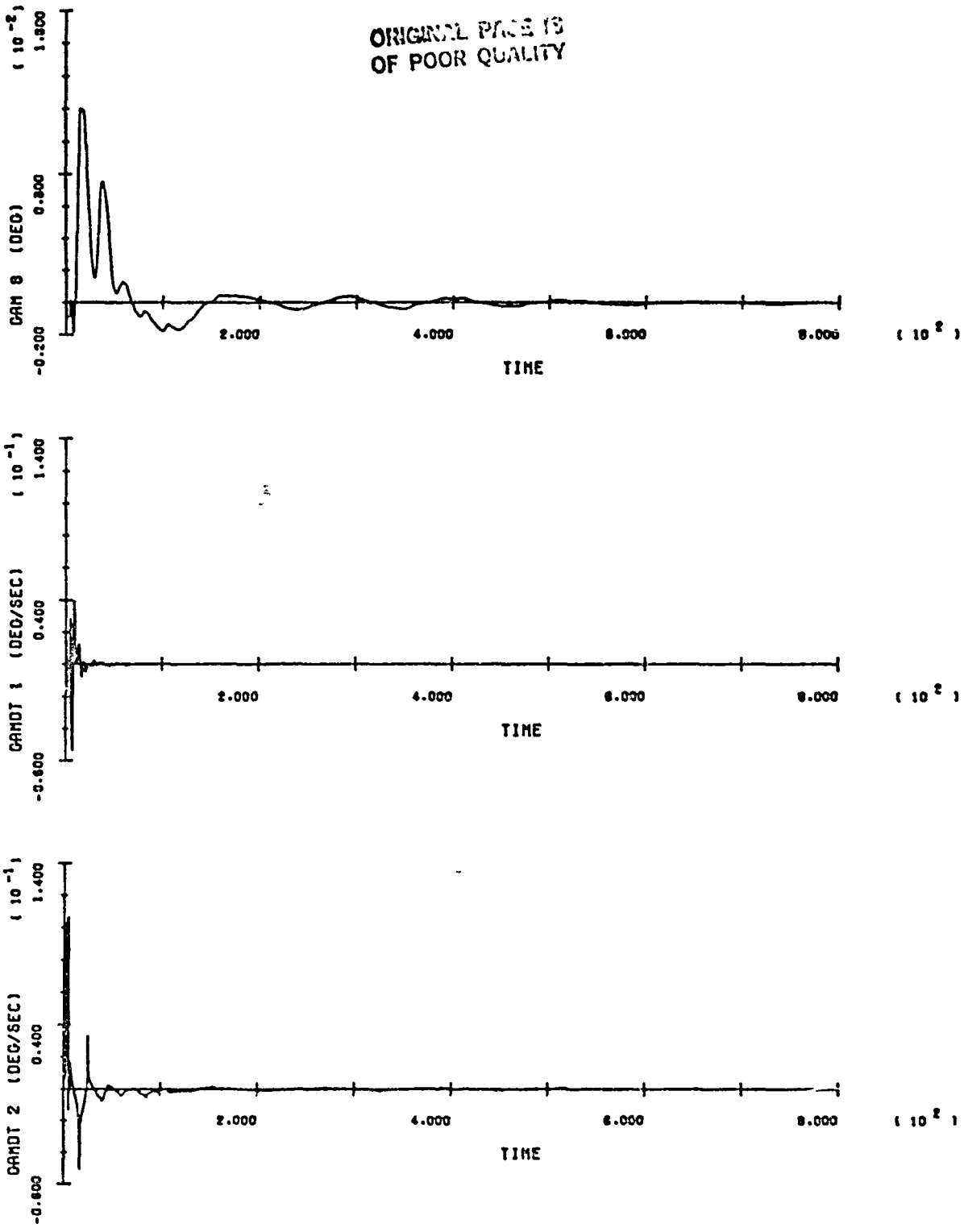


SOC/ORB BERTH RUN 3

ORIGINAL PAGE IS
OF POOR QUALITY

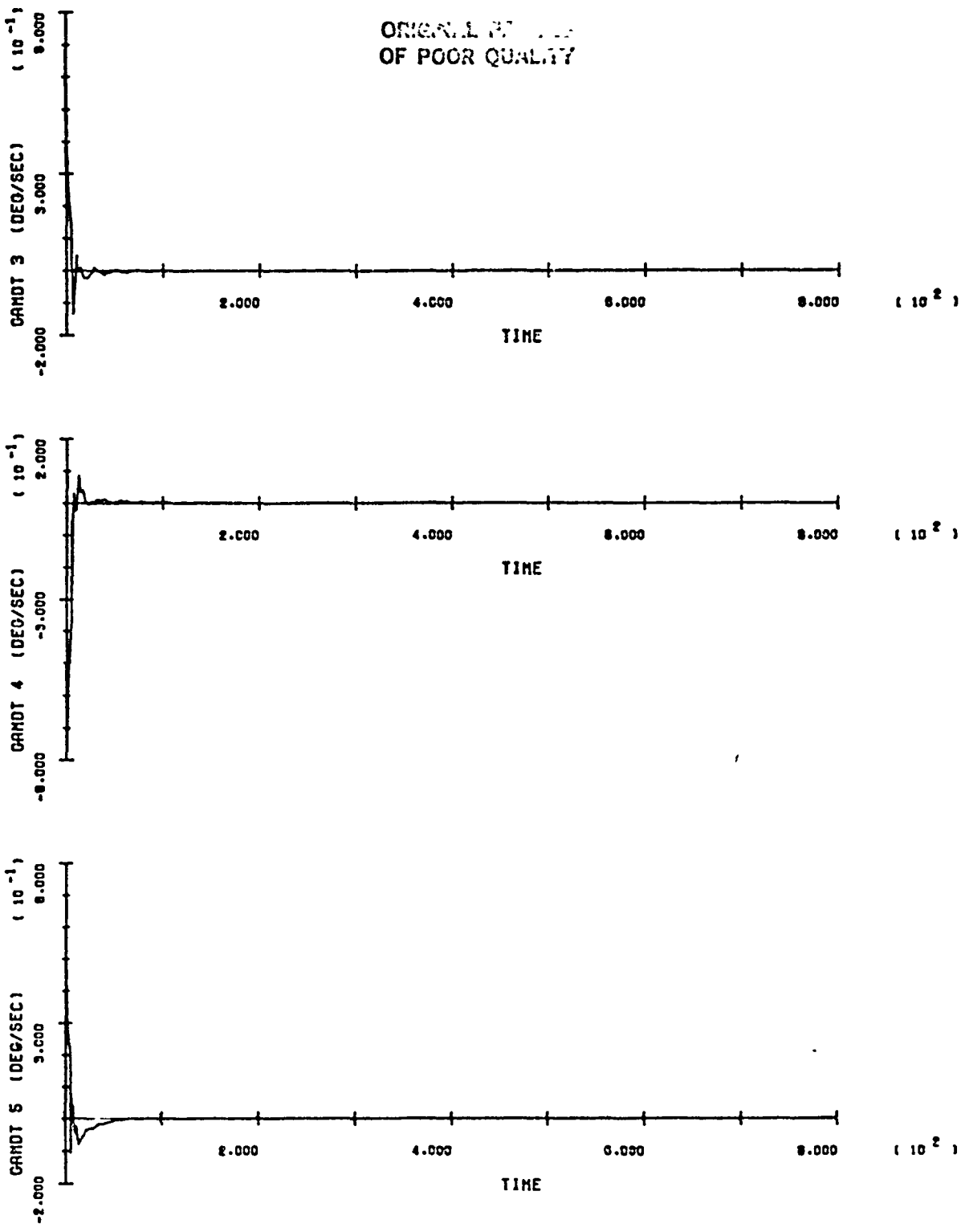


SOC/ORB BERTH RUN 3

ORIGINAL PAGE IS
OF POOR QUALITY

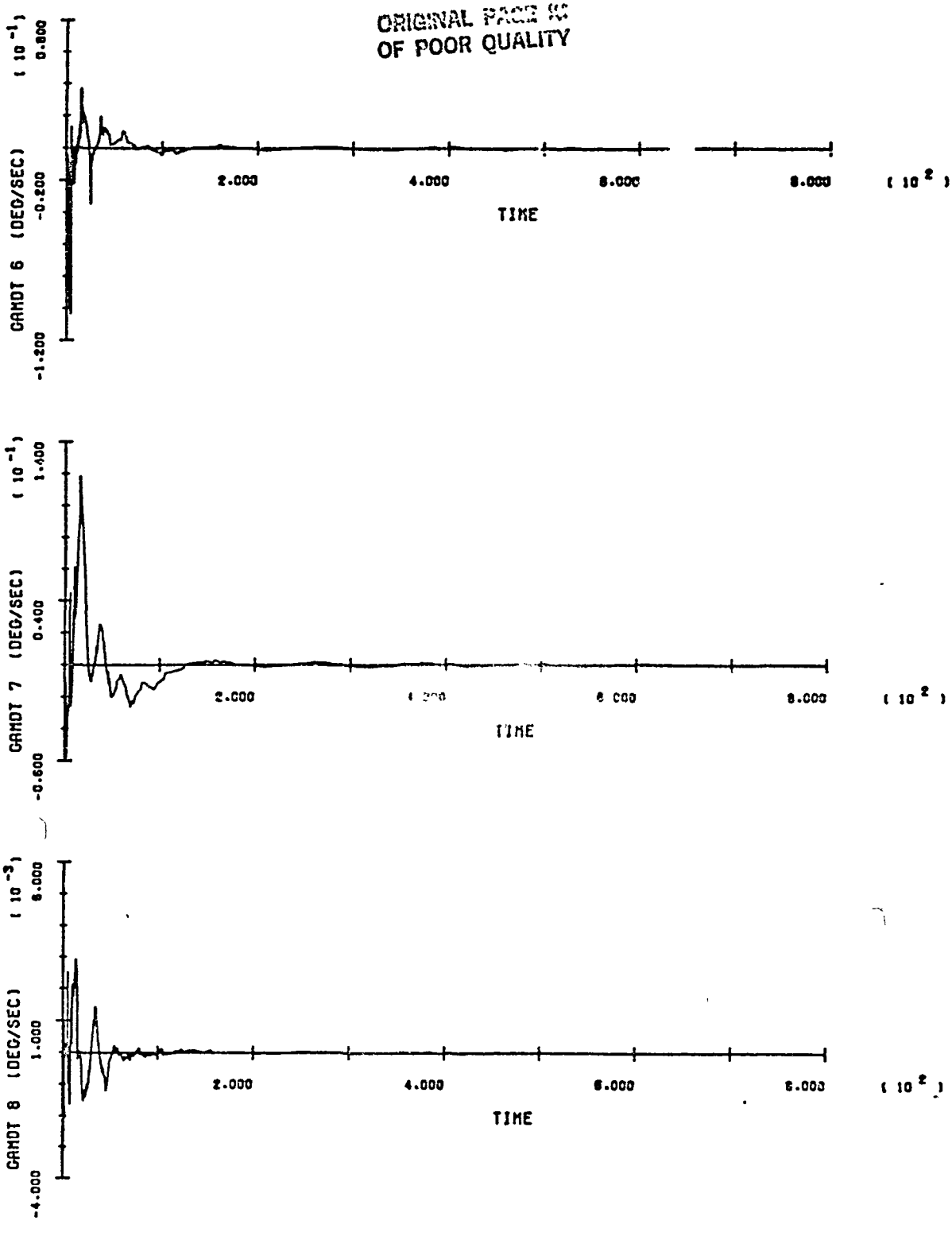


SOC/ORB BERTH RUN 3

ORIGINAL PAGE IS
OF POOR QUALITY

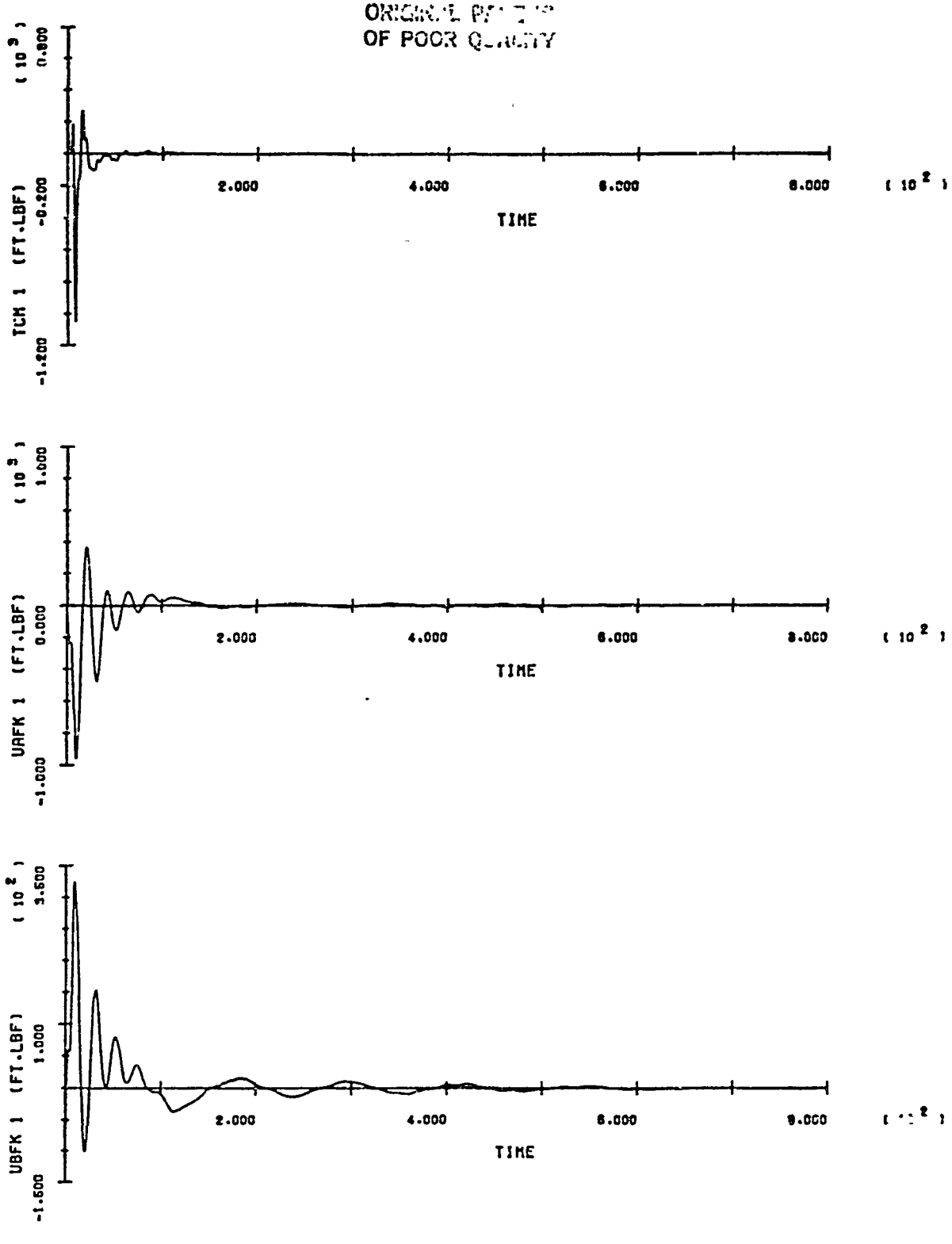


SOC/ORB BERTH RUN

ORIGINAL PAGE IS
OF POOR QUALITY

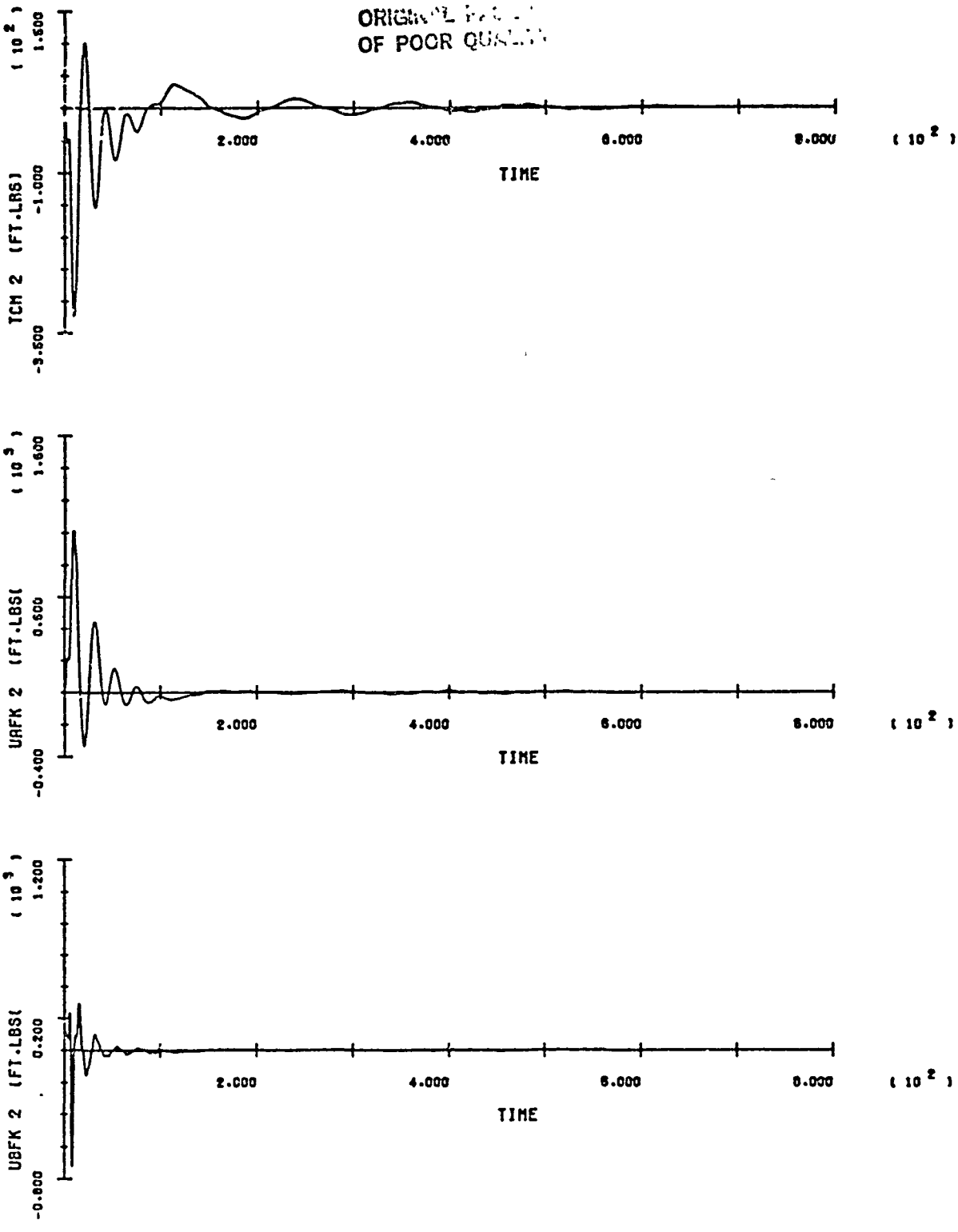


SOC/ORB BERTH RUN

ORIGINAL PAGE IS
OF POOR QUALITY

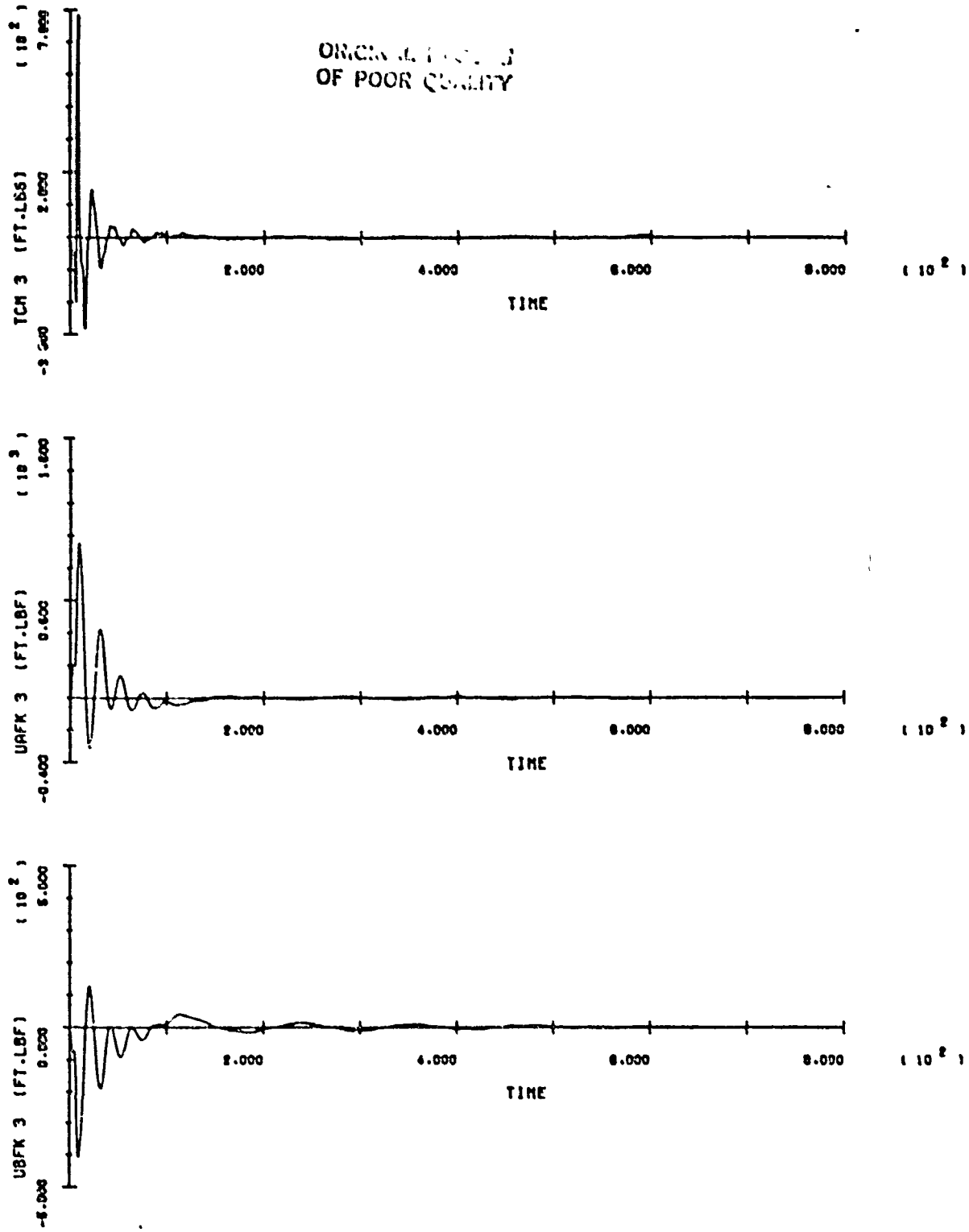


SOC/ORB BERTH RUN 3

ORIGINAL PAGE IS
OF POOR QUALITY

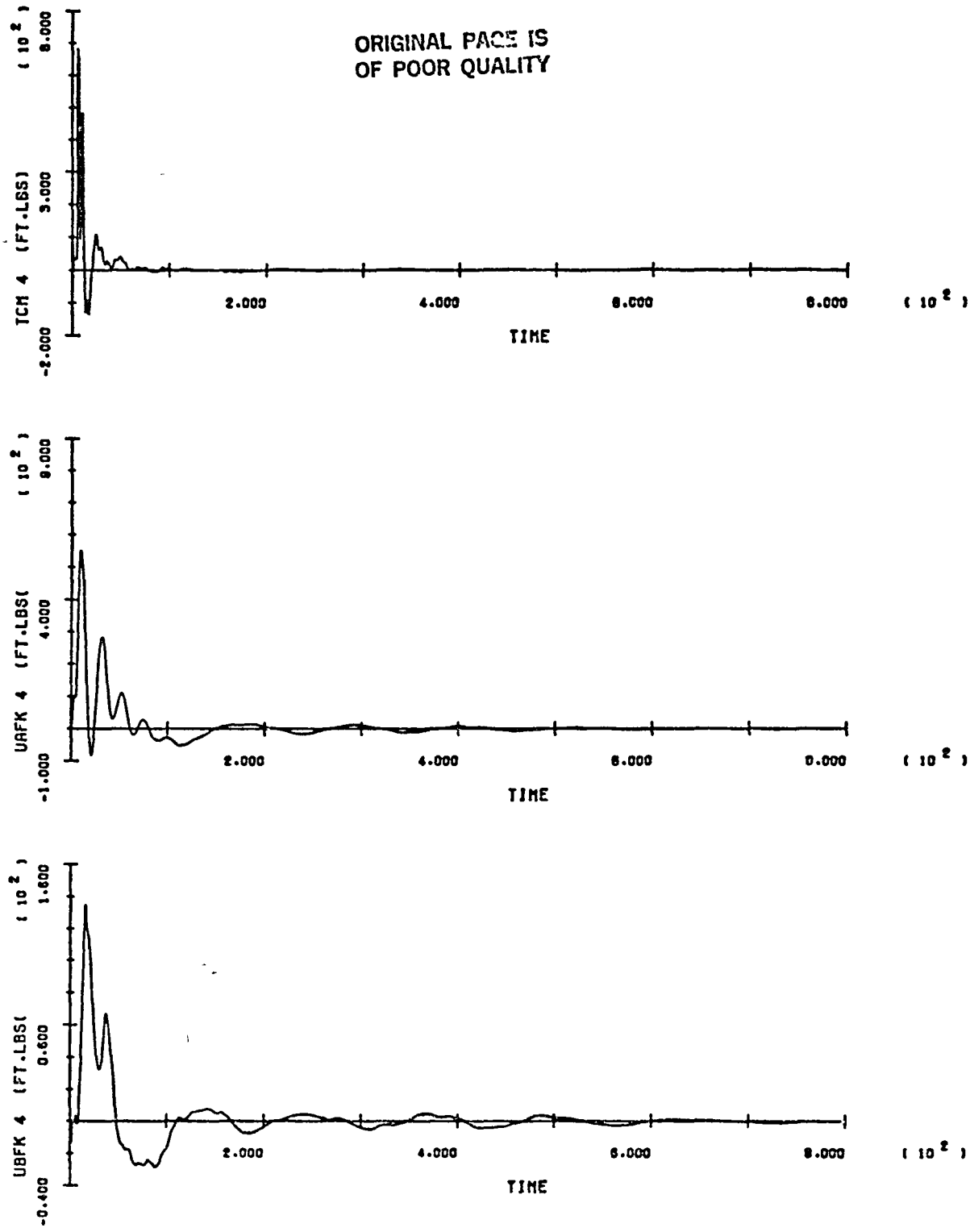


SOC/ORB BERTH RUN 3

ORIGINAL PAGE IS
OF POOR QUALITY

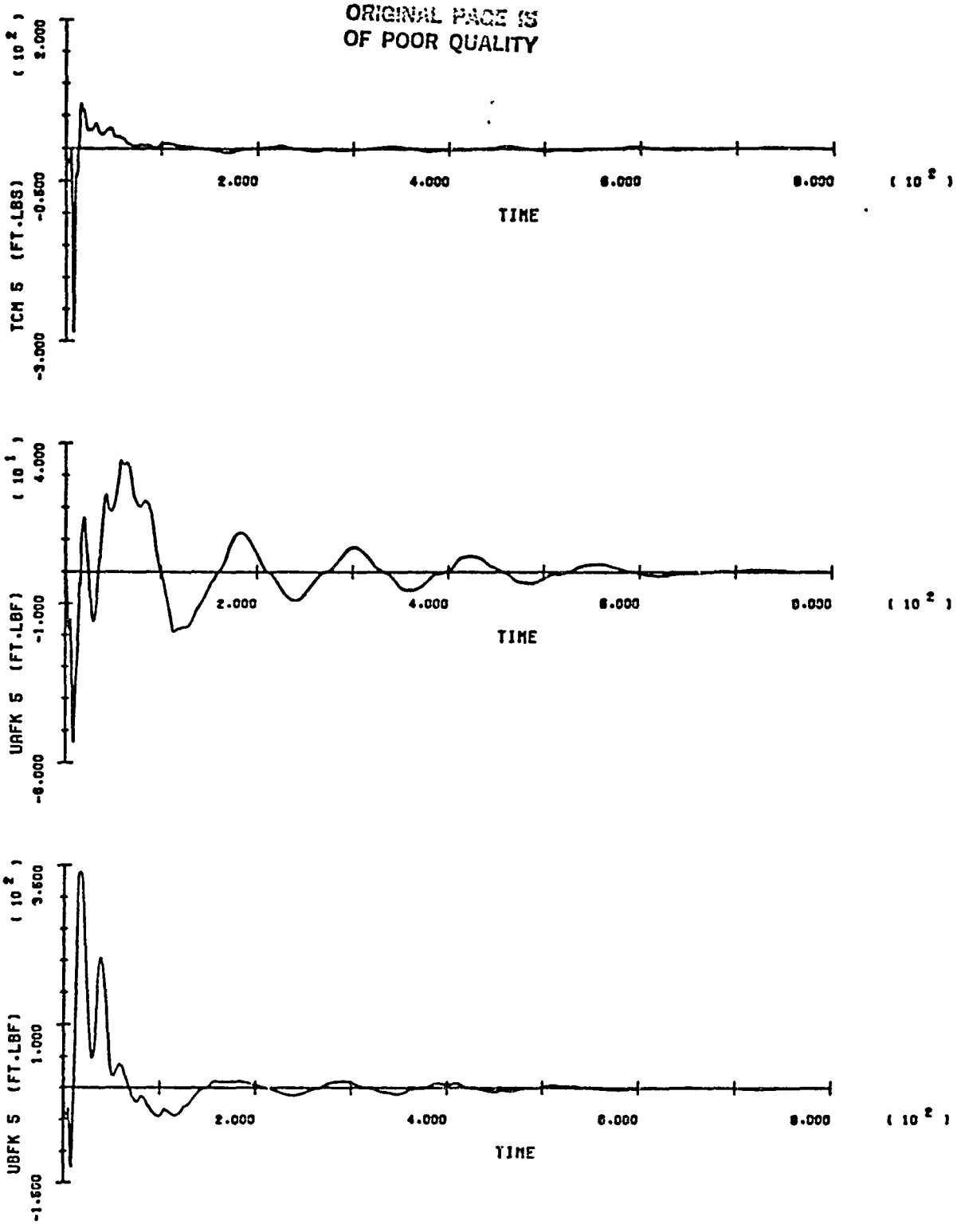


SOC/ORB BERTH RUN 3

ORIGINAL PAGE IS
OF POOR QUALITY

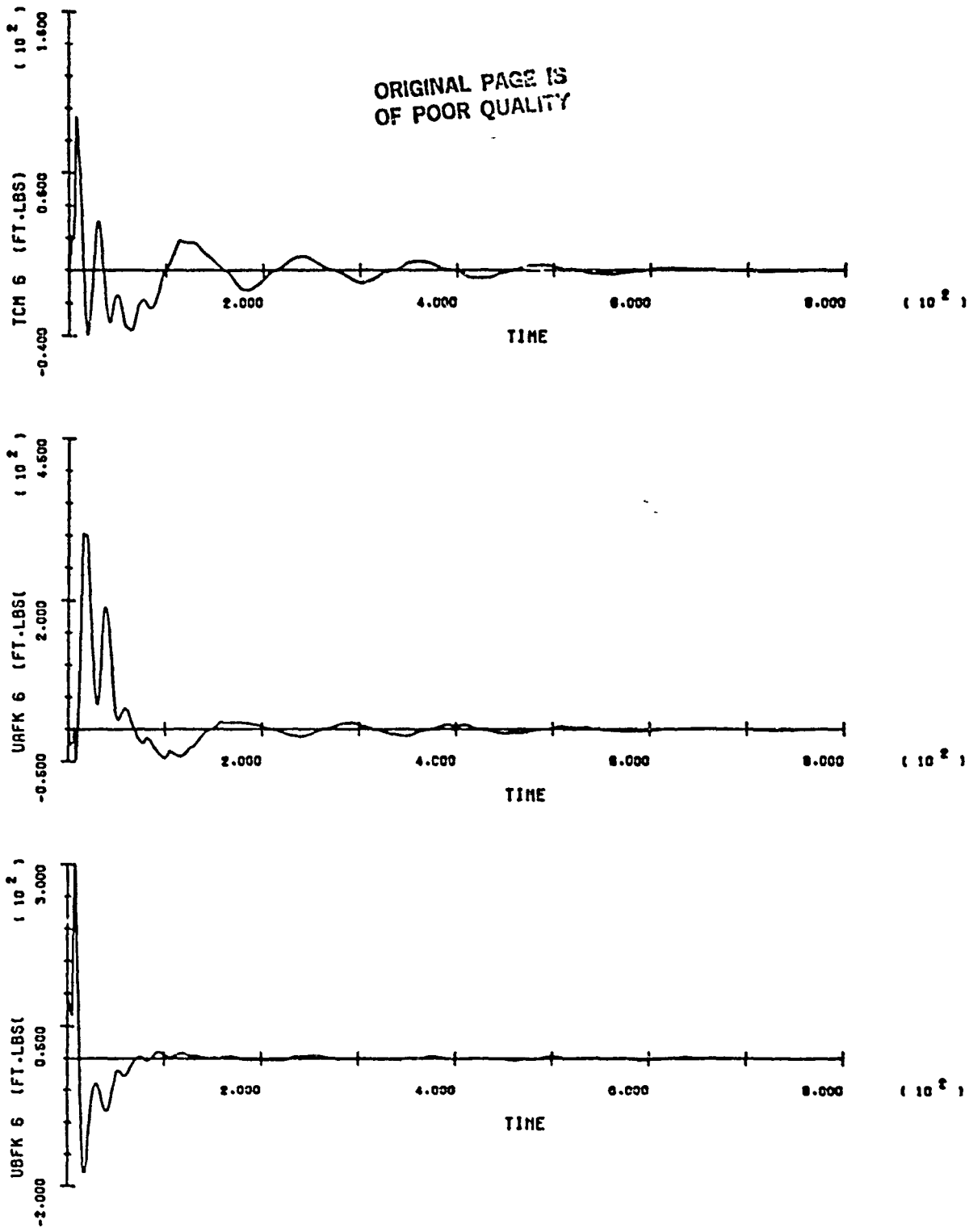


SOC/ORB BERTH RUN 3

ORIGINAL PAGE IS
OF POOR QUALITY

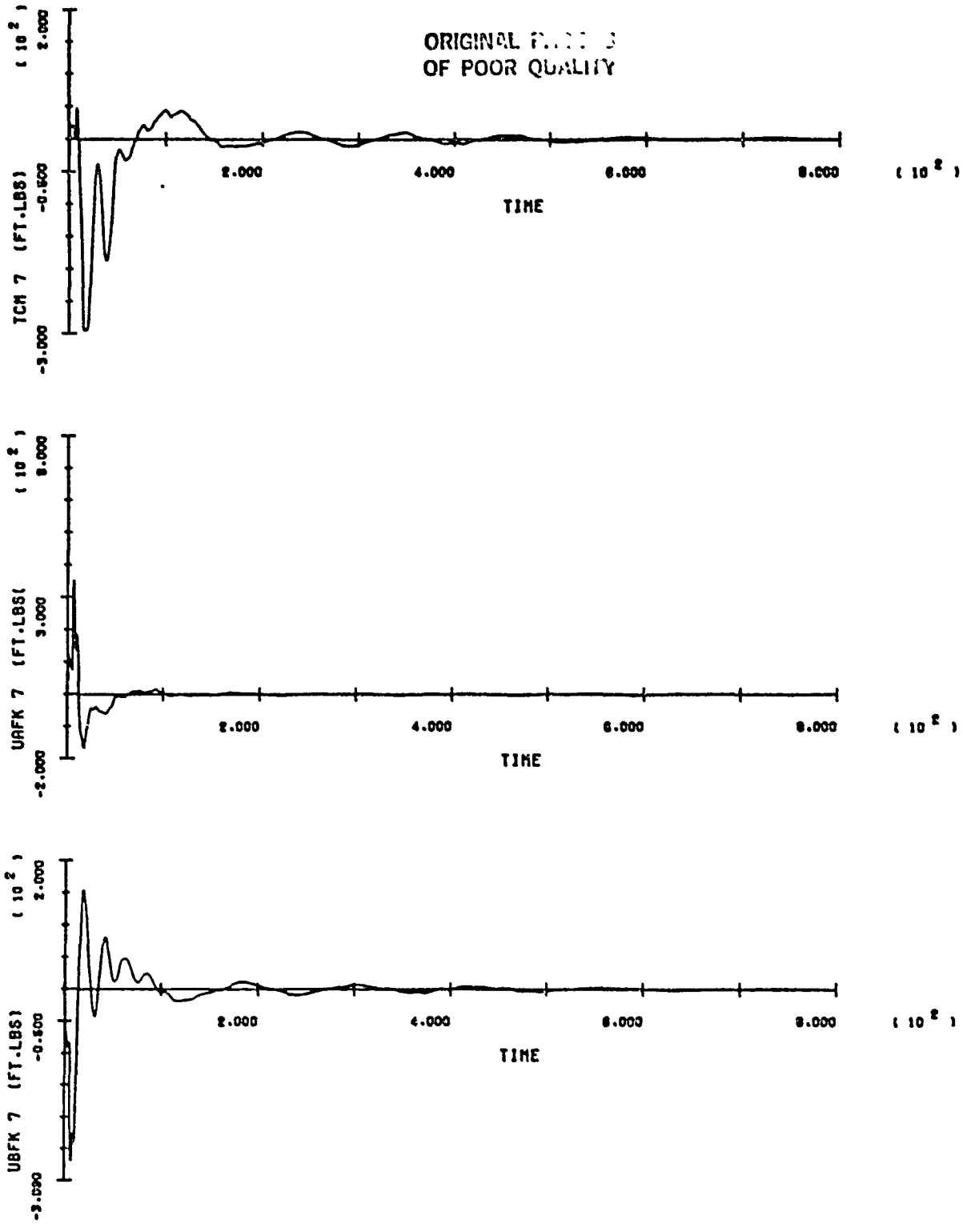


SOC/ORB BERTH RUN 3

ORIGINAL PAGE IS
OF POOR QUALITY

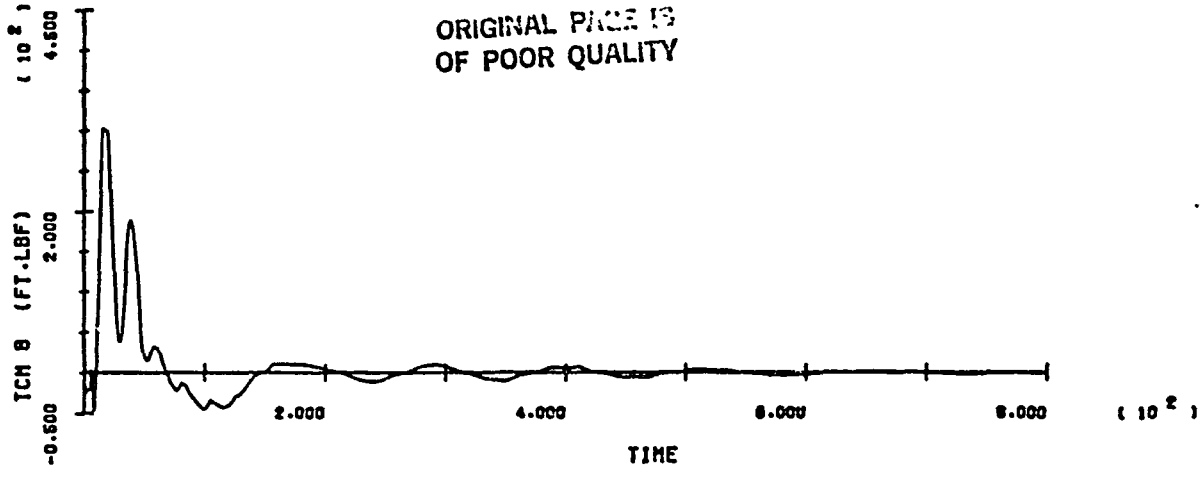


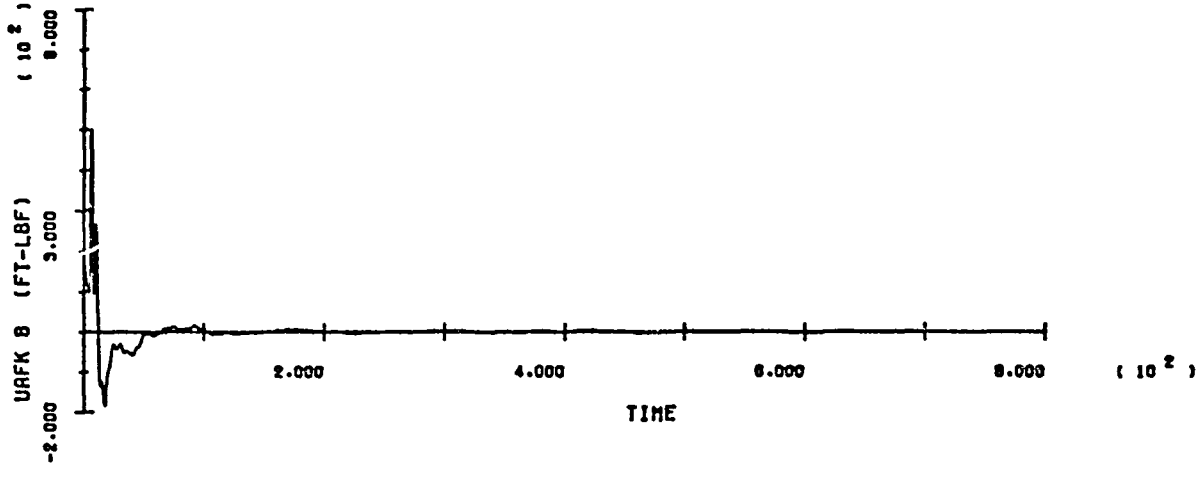


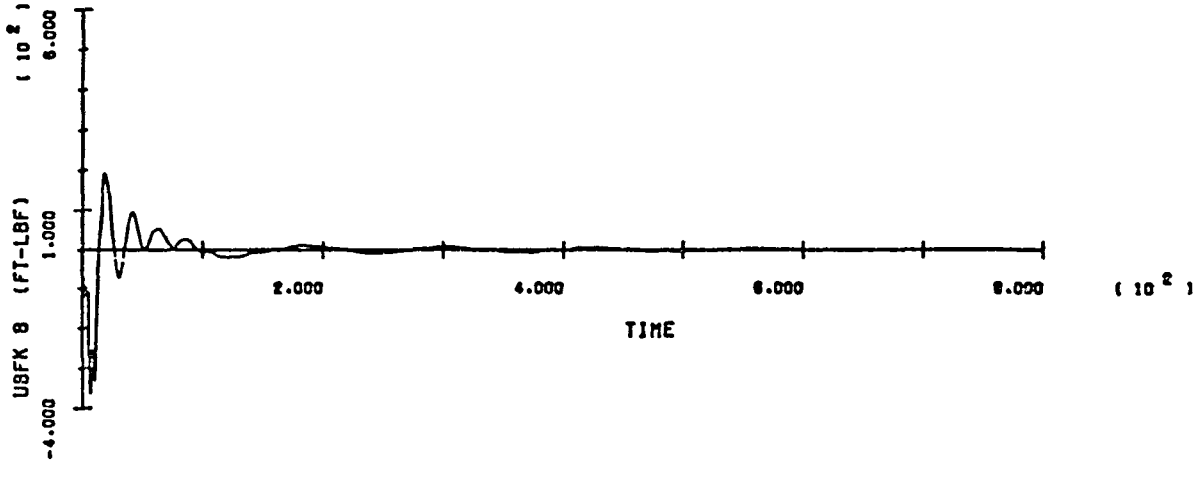


SOC/ORB BERTH RUN 3

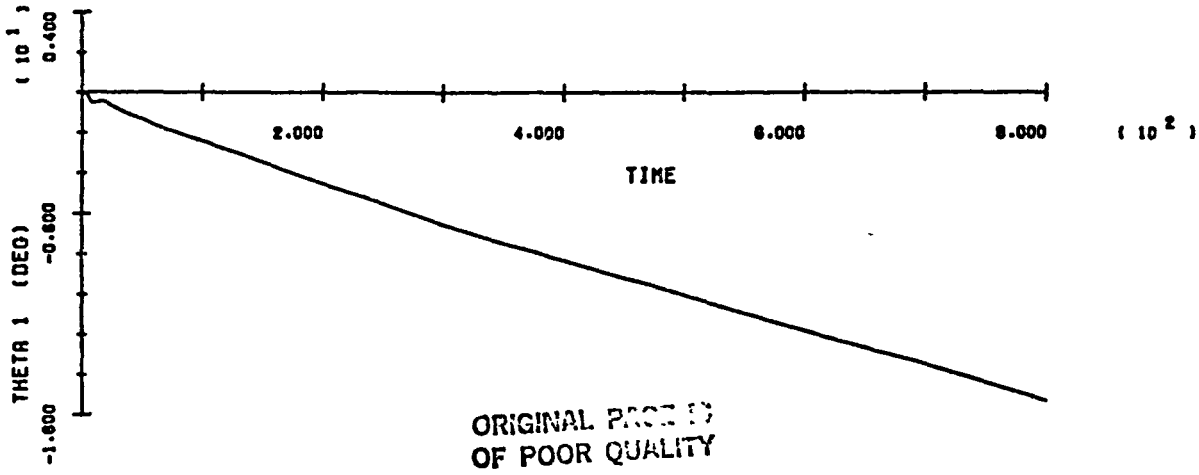


ORIGINAL PAGE IS
OF POOR QUALITY

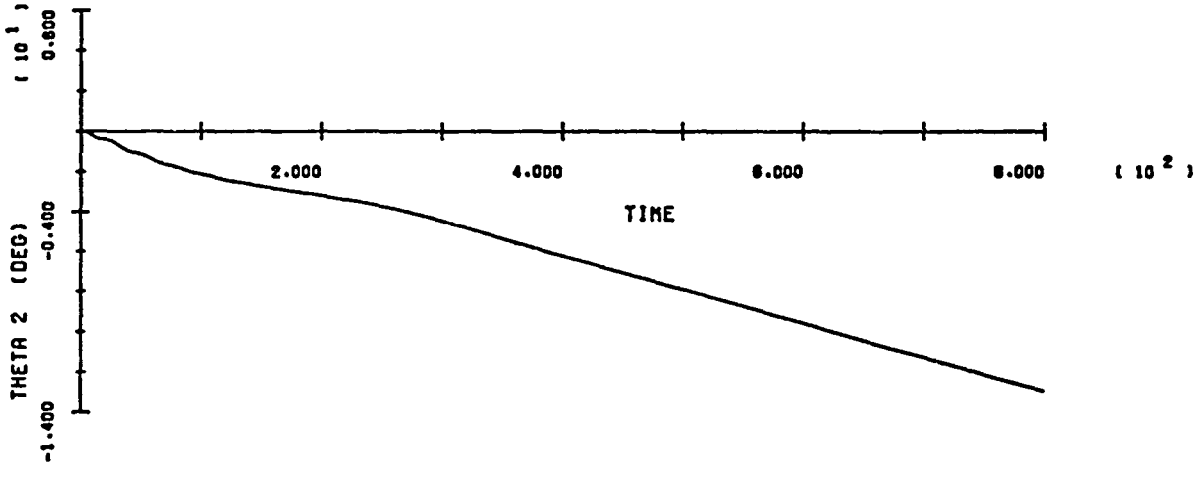


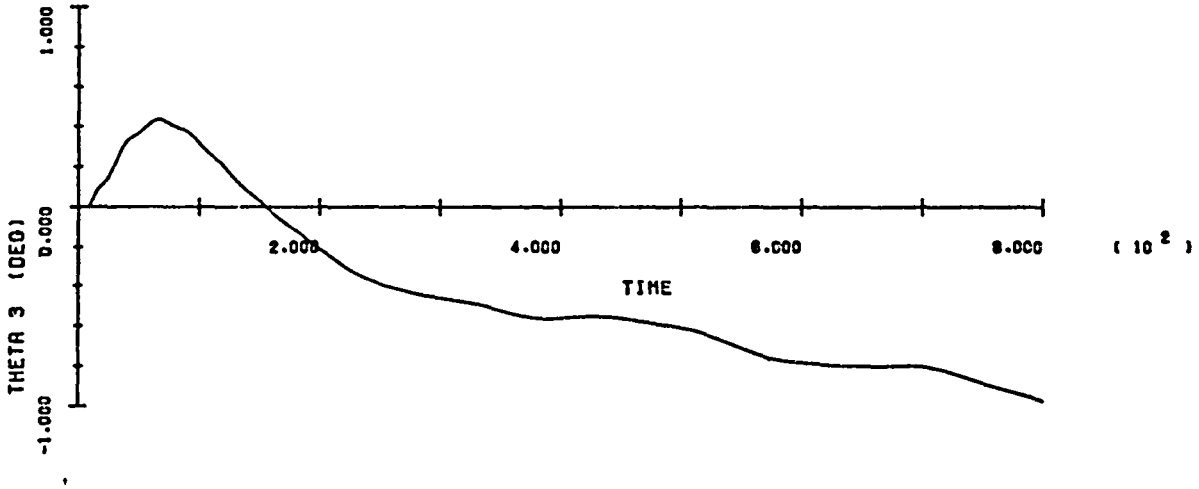


SOC/ORB BERTH - RUN 4

ORIGINAL PAGE IS
OF POOR QUALITY

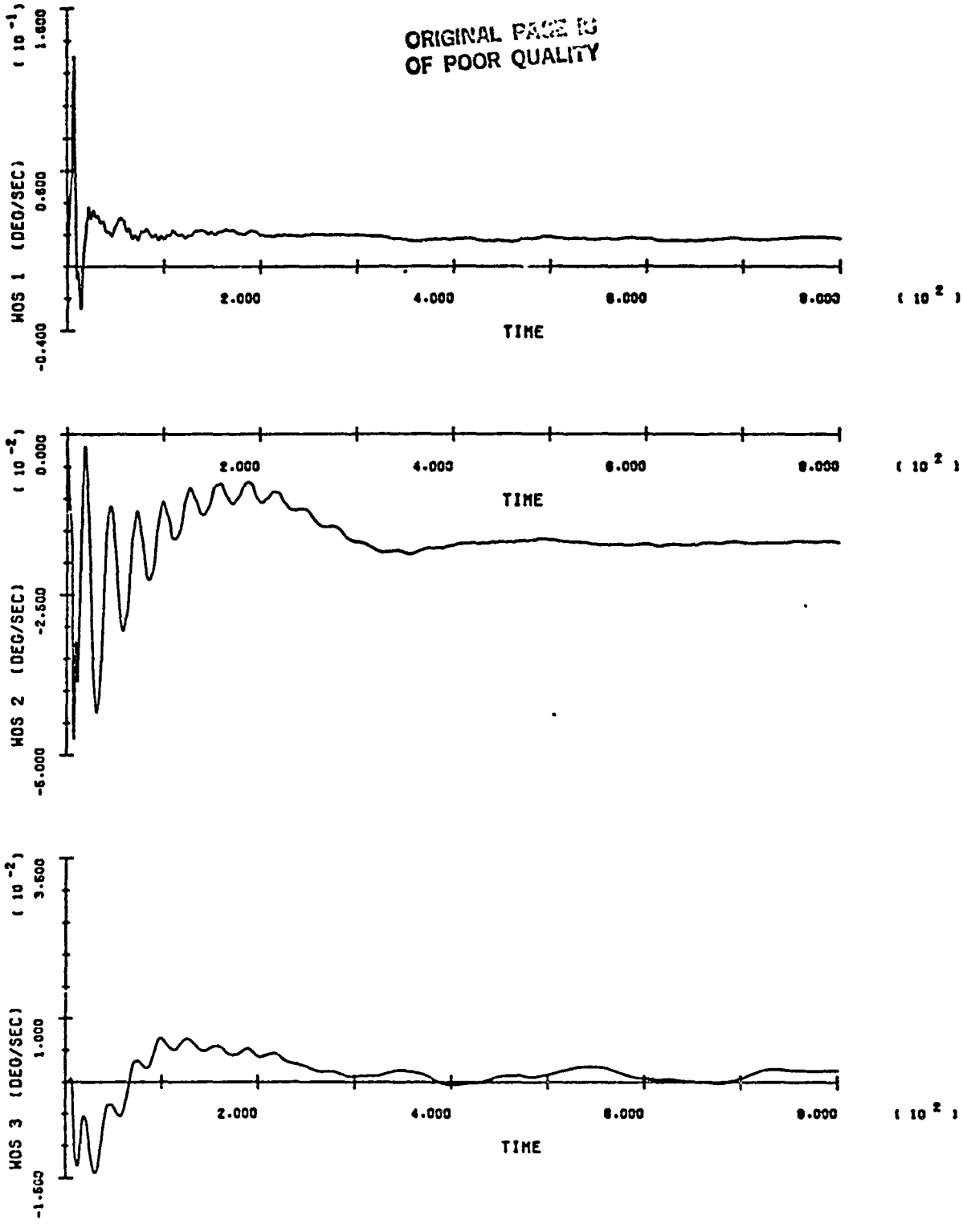


SOC/ORB BERTH - RUN 4

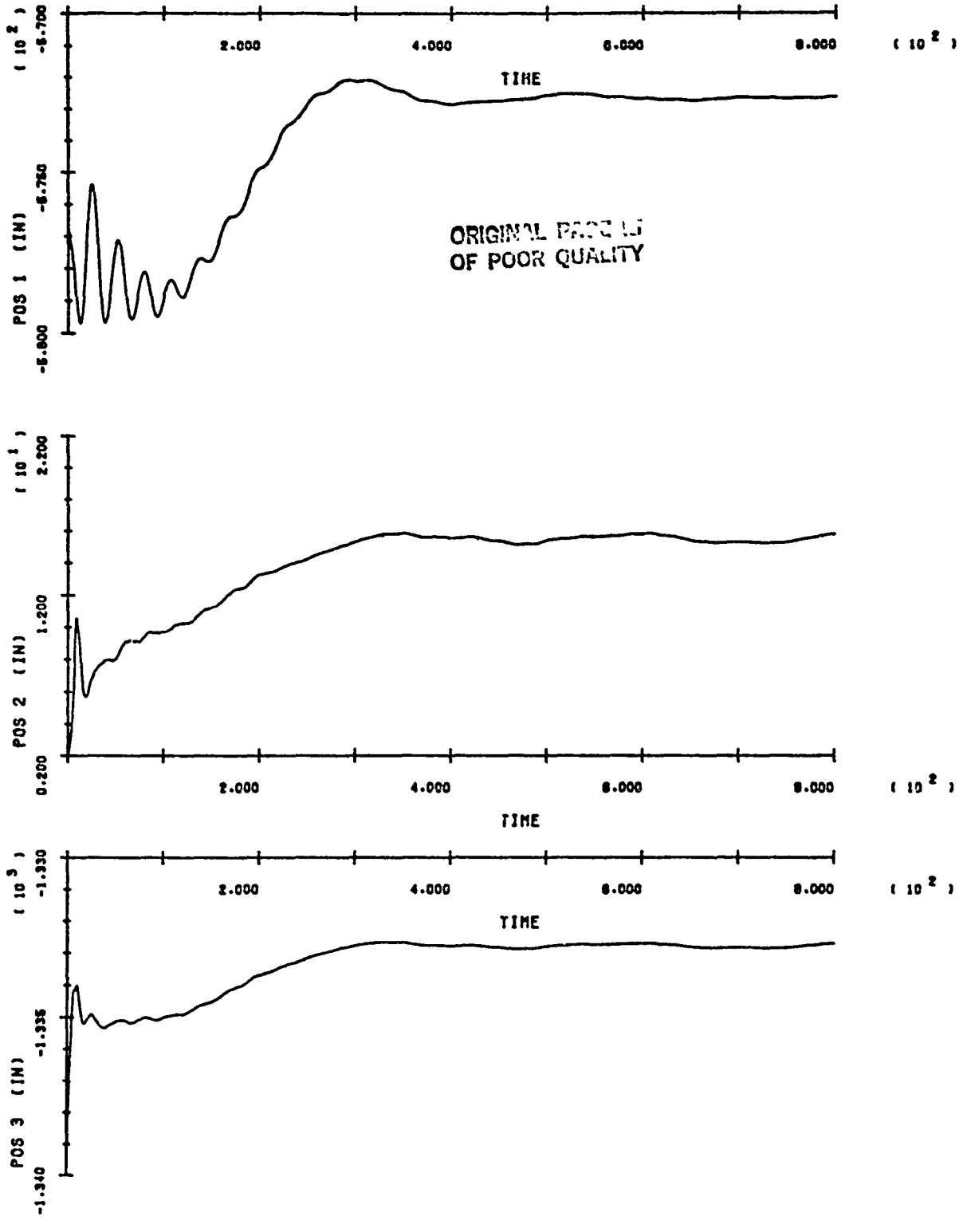


SOC/ORB BERTH - RUN 4

ORIGINAL PAGE IS
OF POOR QUALITY

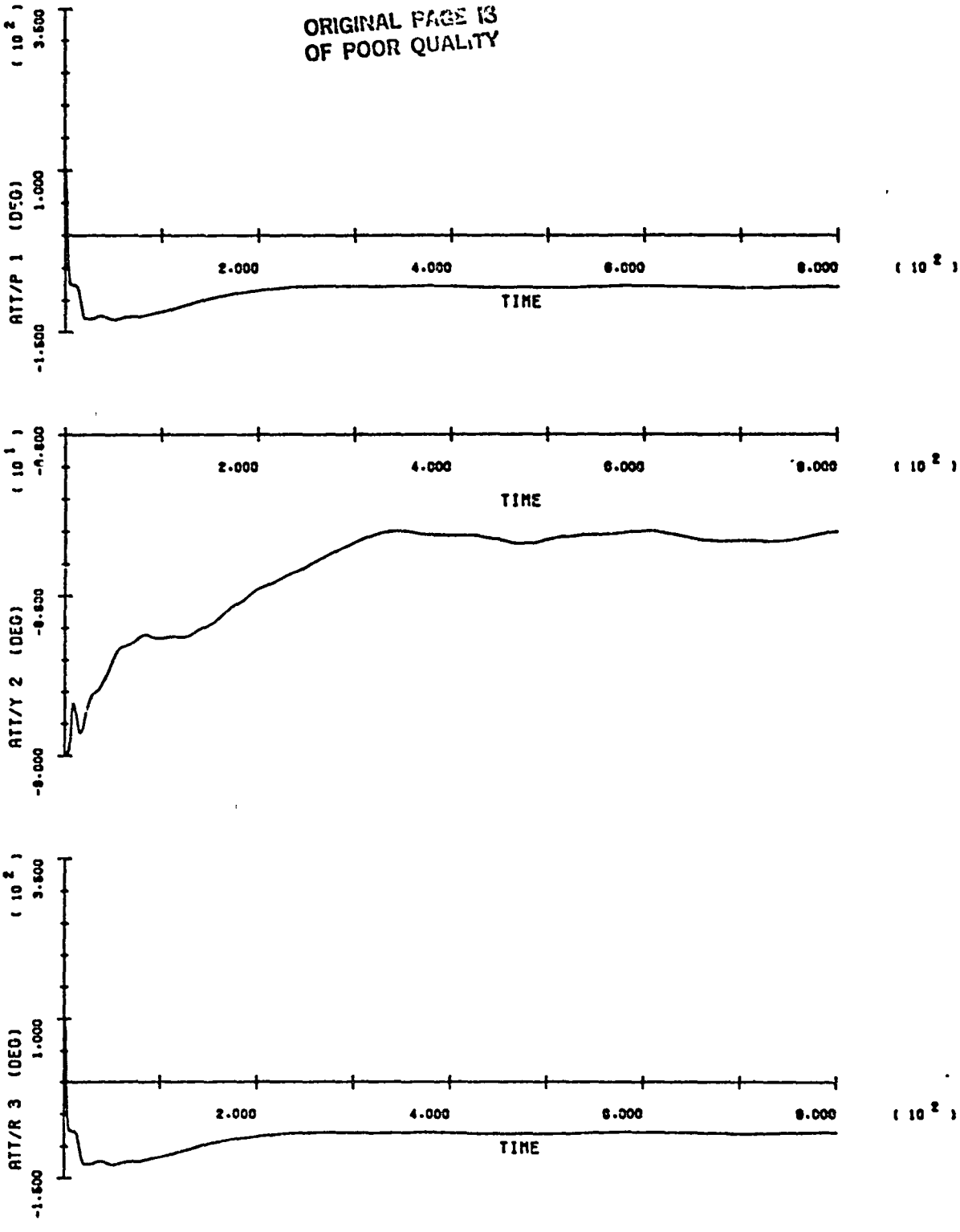


SOC/ORB BERTH - RUN 4

ORIGINAL PAGE IS
OF POOR QUALITY

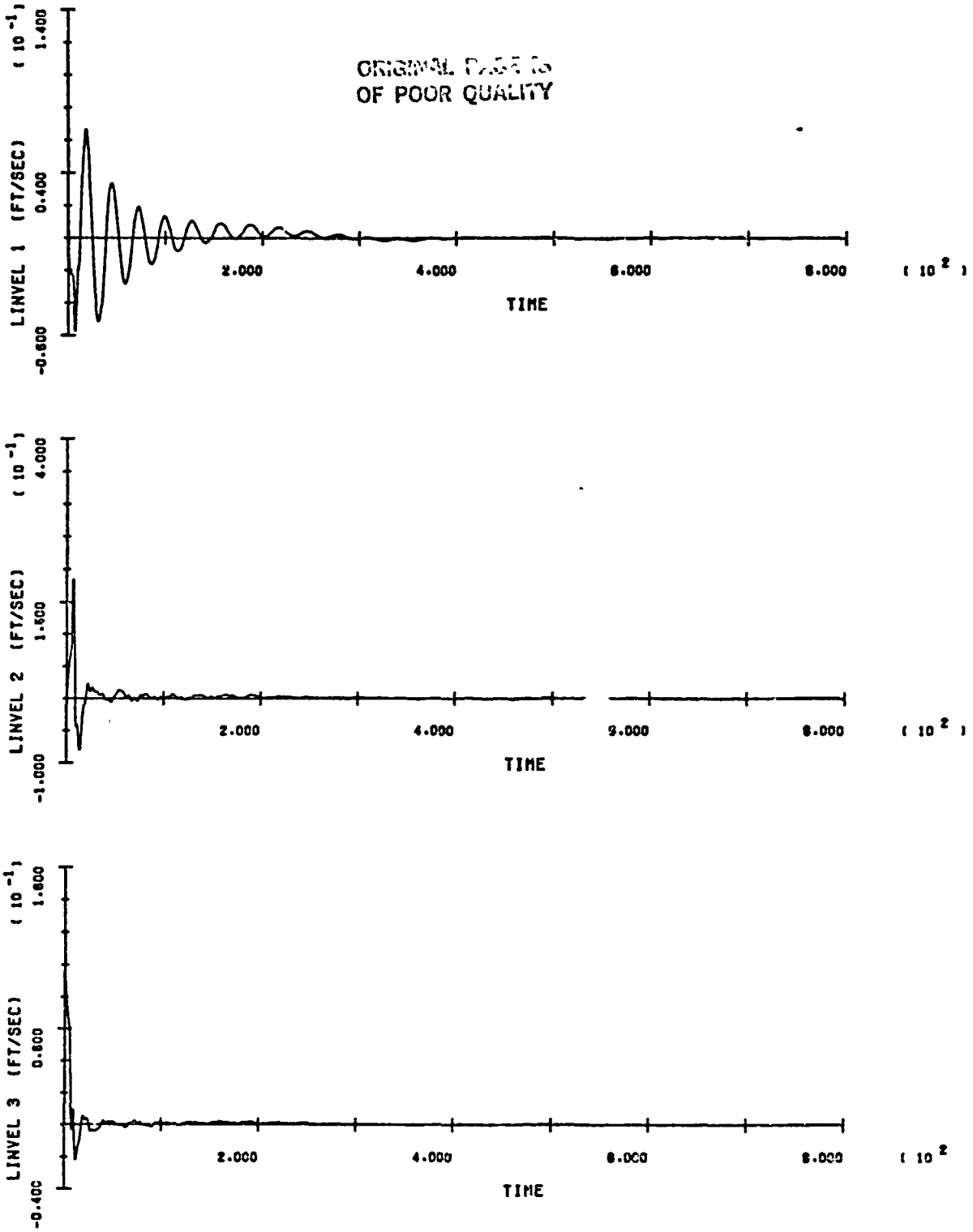


SOC/ORB BERTH - RUN 4

ORIGINAL PAGE IS
OF POOR QUALITY

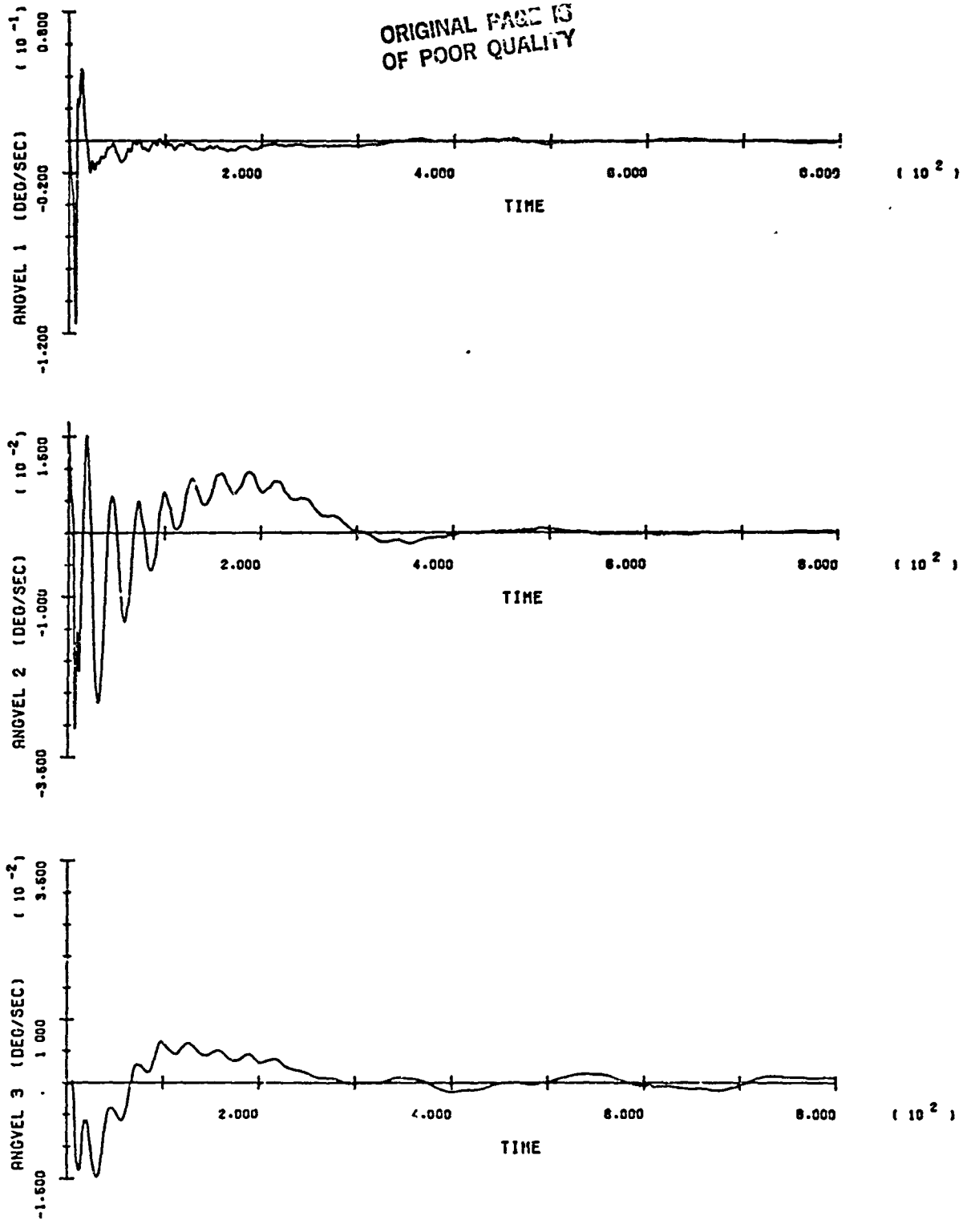


SOC/ORB BERTH - RUN 4

ORIGINAL PAGE IS
OF POOR QUALITY

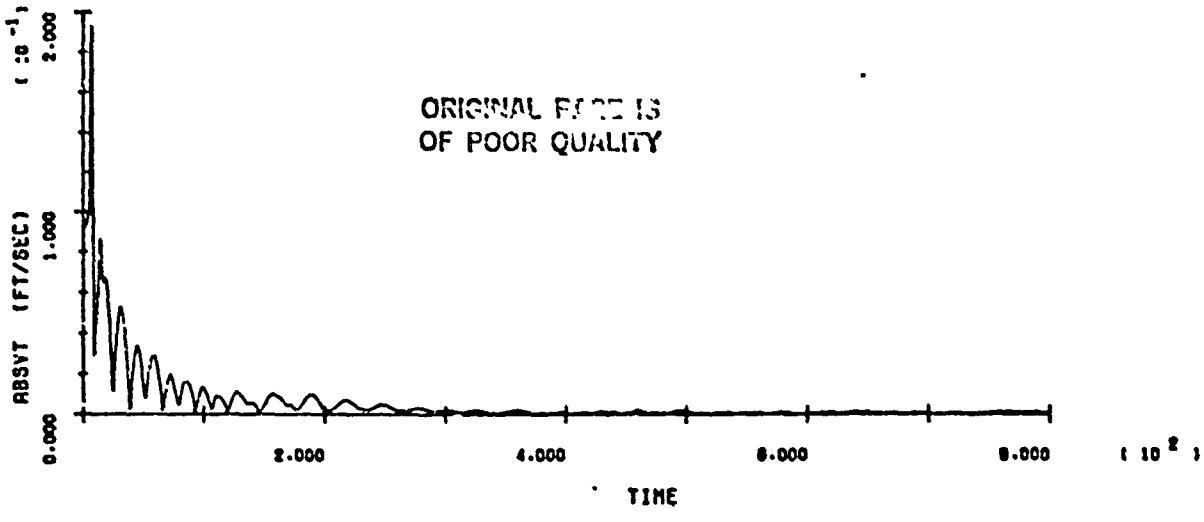


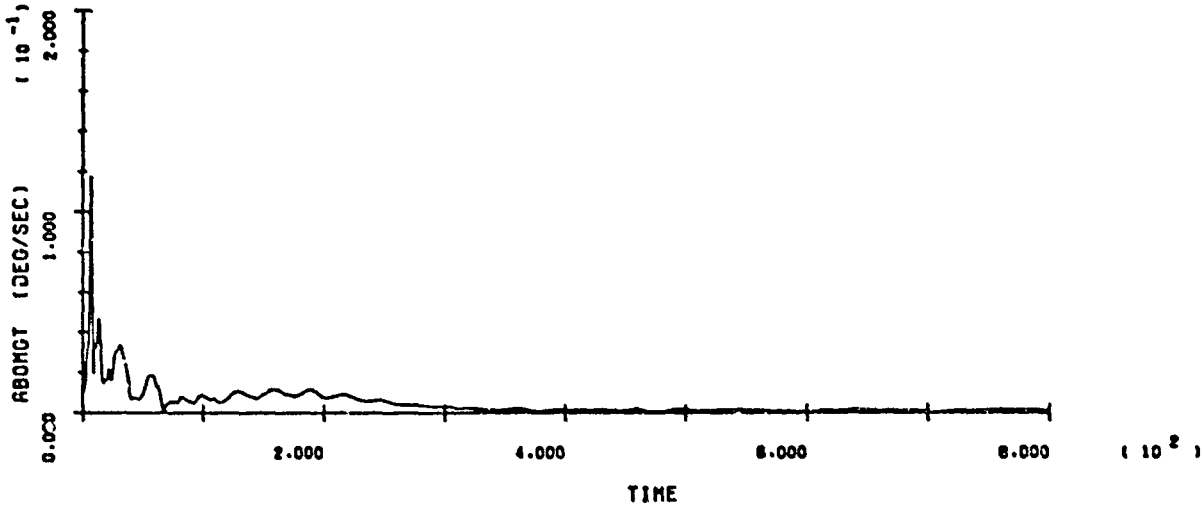


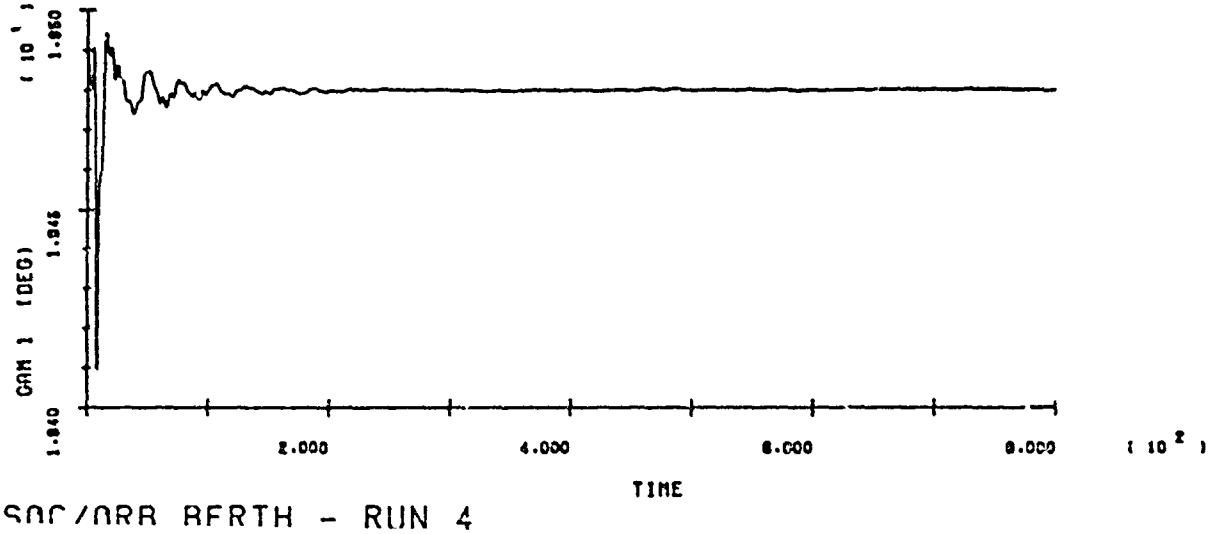


SOC/ORB BERTH - RUN 4

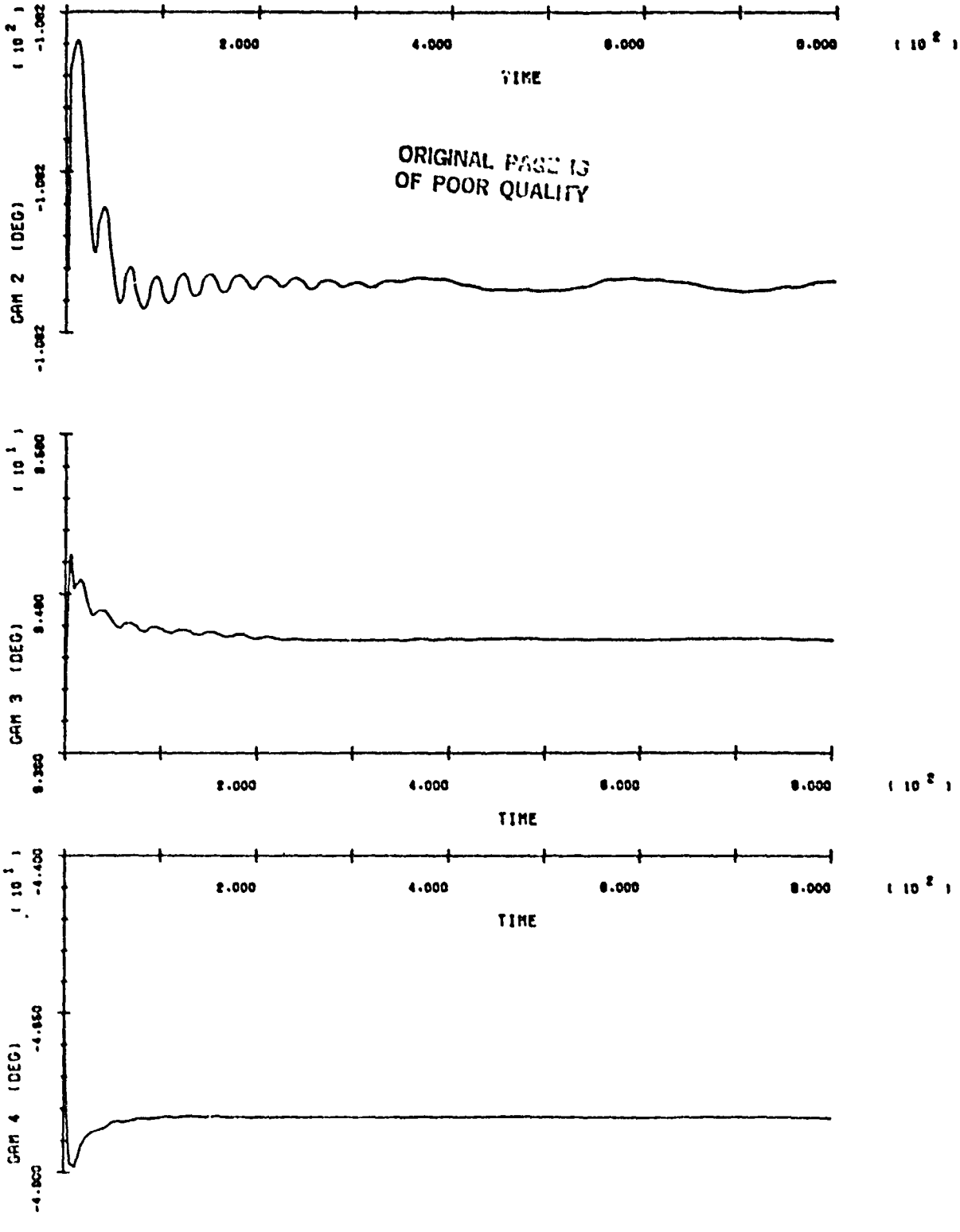


SOC/ORB BERTH - RUN 4

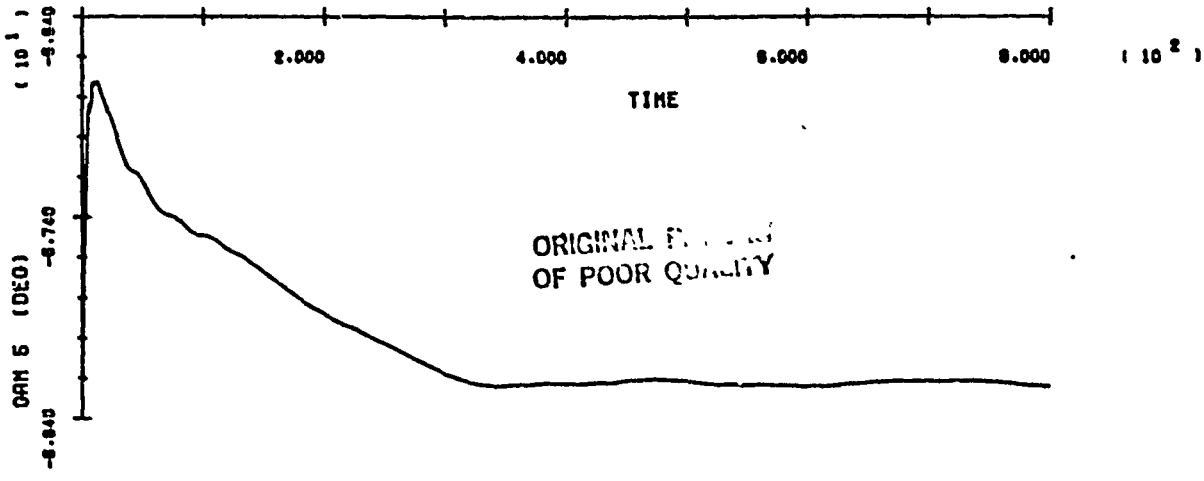


ORIGINAL PAGE IS
OF POOR QUALITY

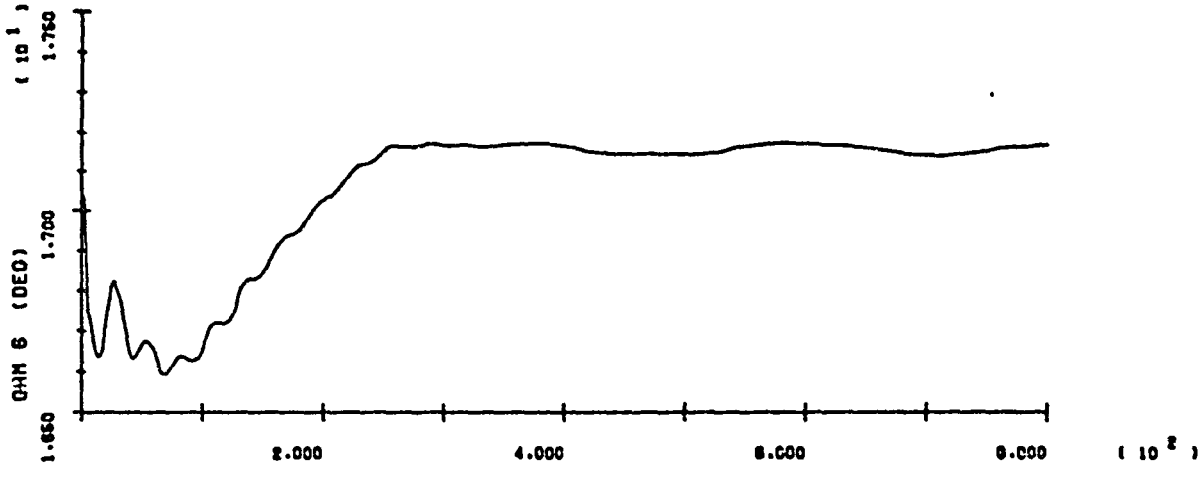


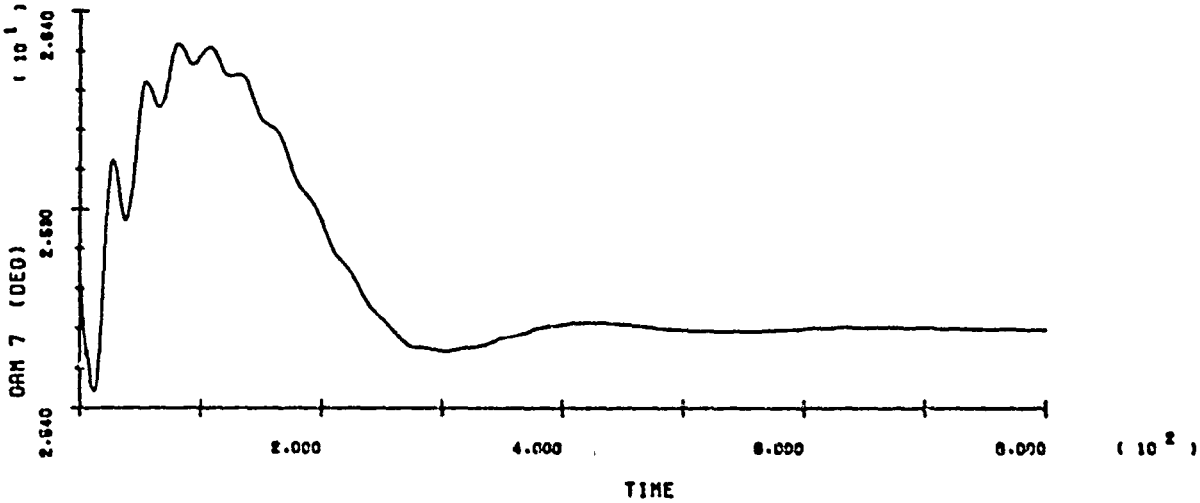


SOC/ORB BERTH - RUN 4

ORIGINAL PAGE IS
OF POOR QUALITY

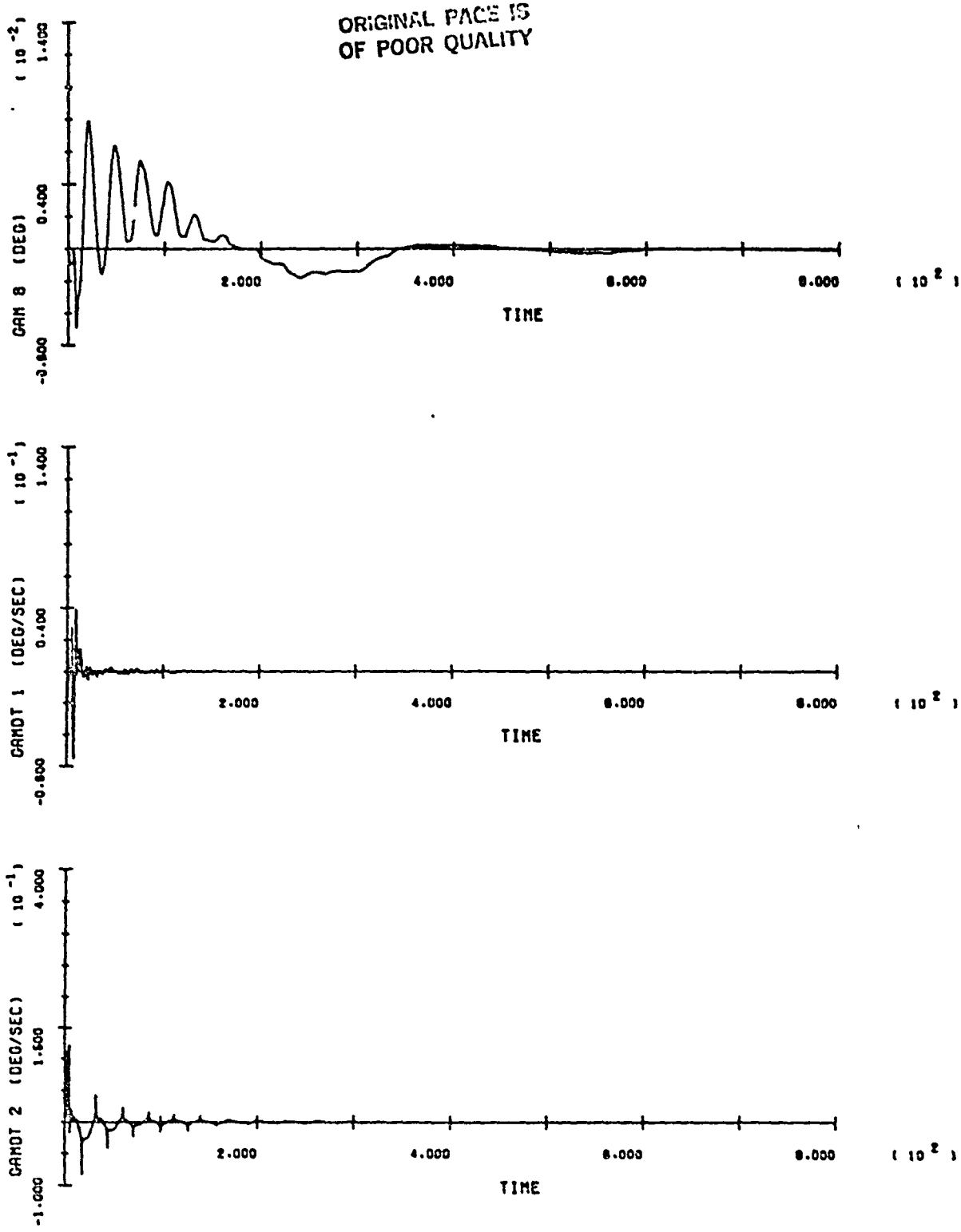


SOC/ORB BERTH - RUN 4

ORIGINAL PAGE IS
OF POOR QUALITY

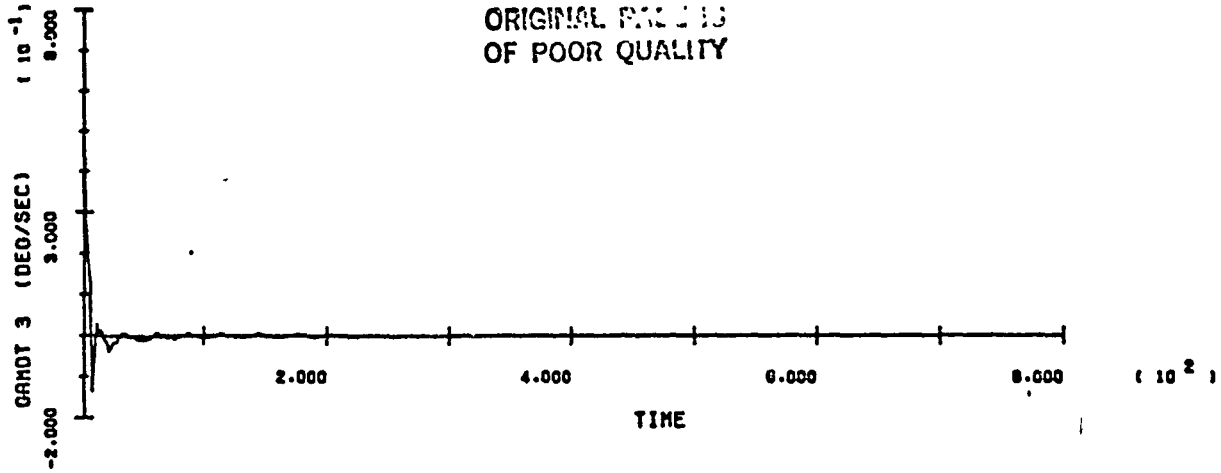


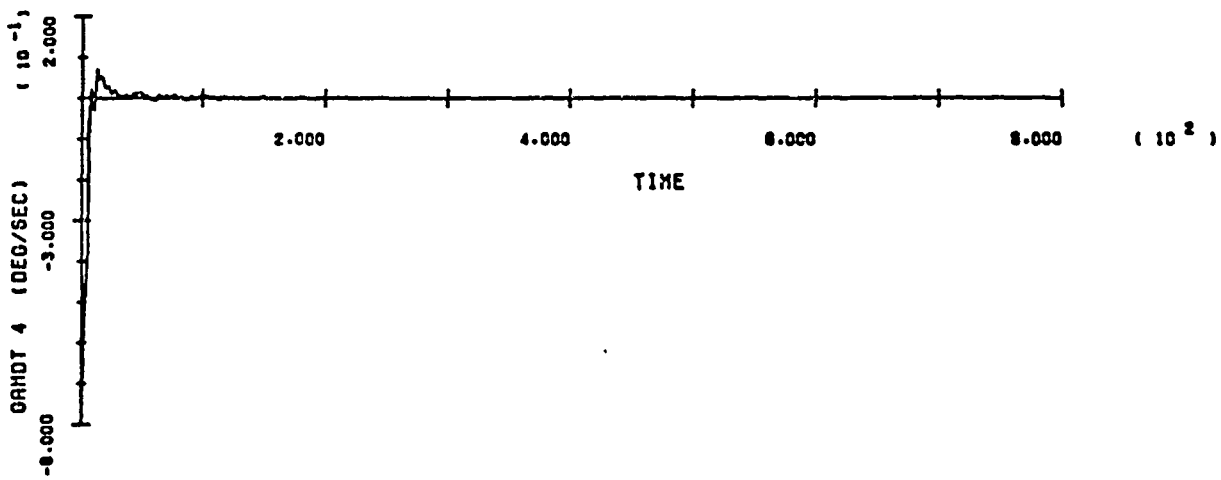


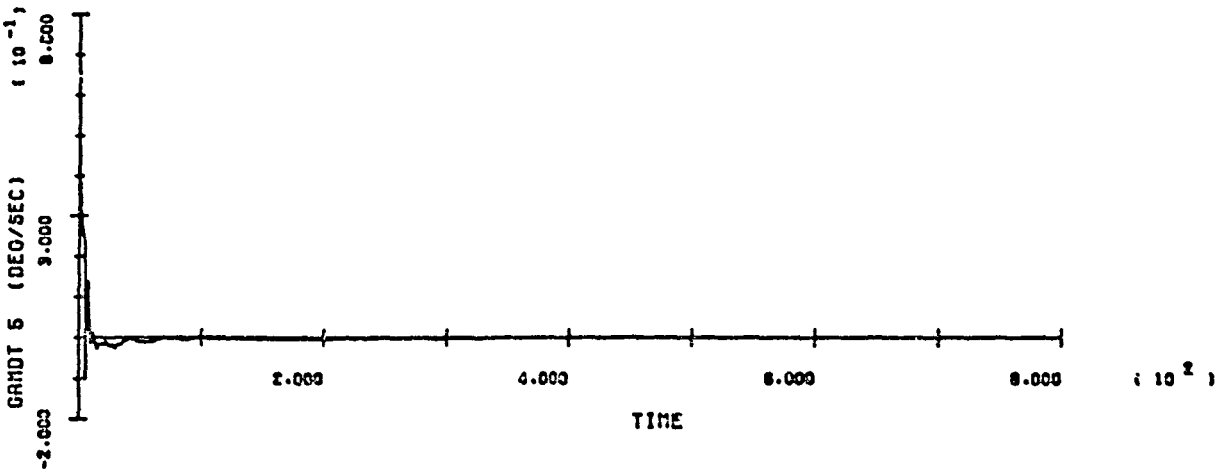

ORIGINAL PAGE IS
OF POOR QUALITY

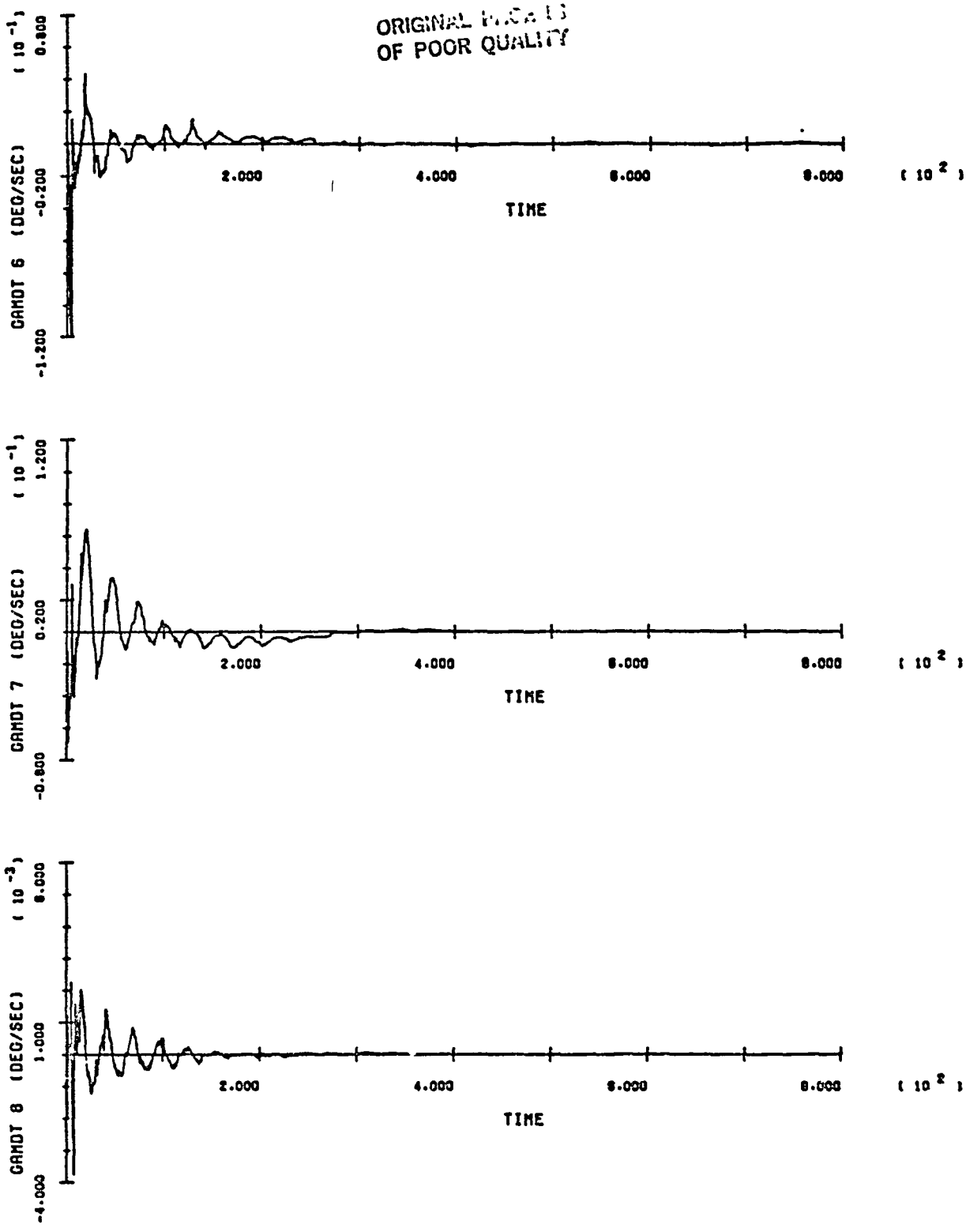


SOC/ORB BERTH - RUN 4

ORIGINAL PAGE IS
OF POOR QUALITY

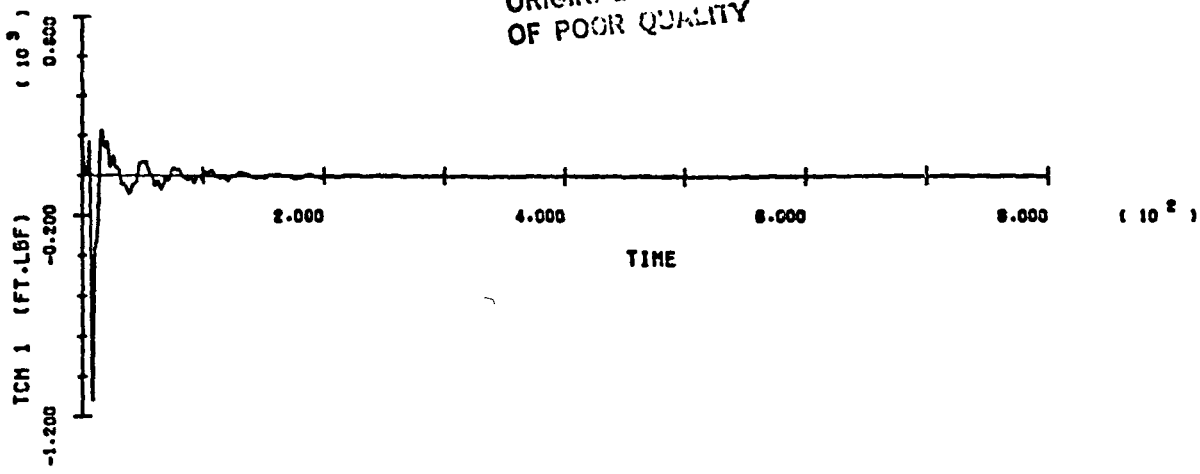


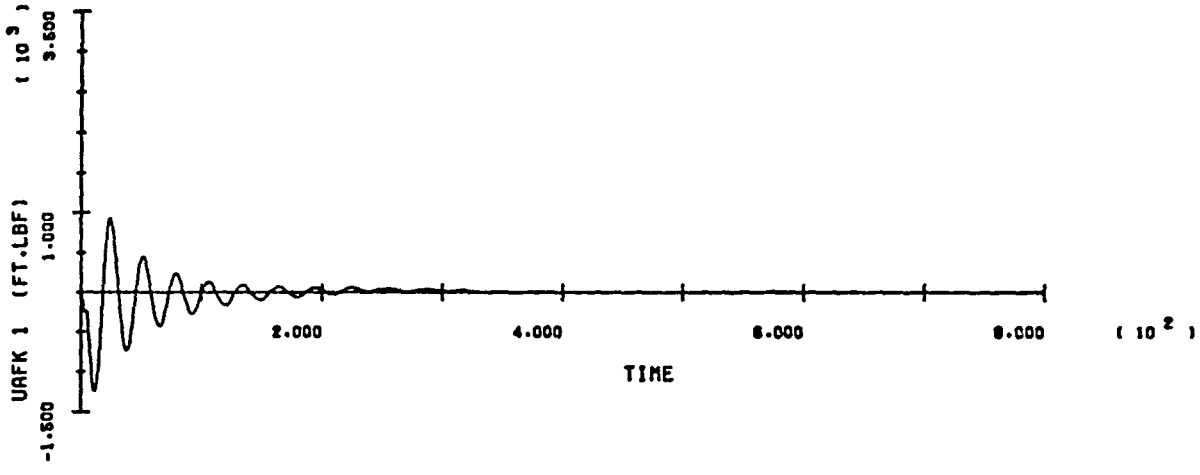


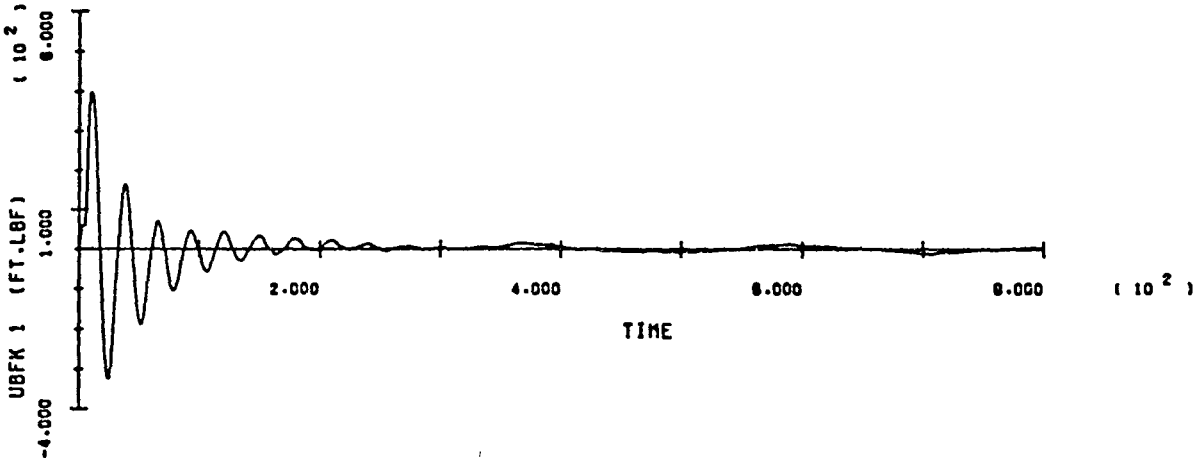


SOC/ORB BERTH - RUN 4

ORIGINAL PAGE IS
OF POOR QUALITY

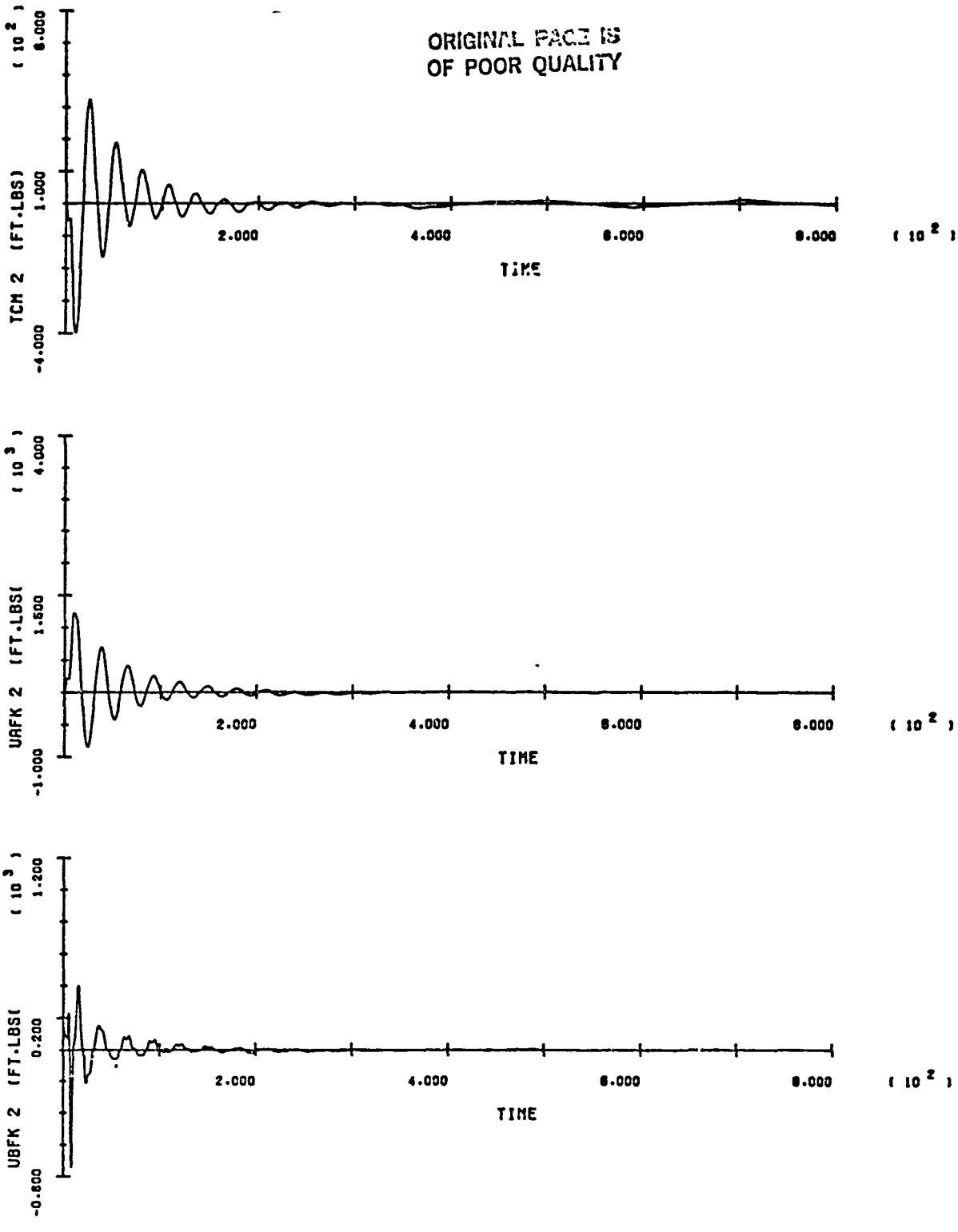


SOC/ORB BERTH - RUN 4

ORIGINAL PAGE IS
OF POOR QUALITY

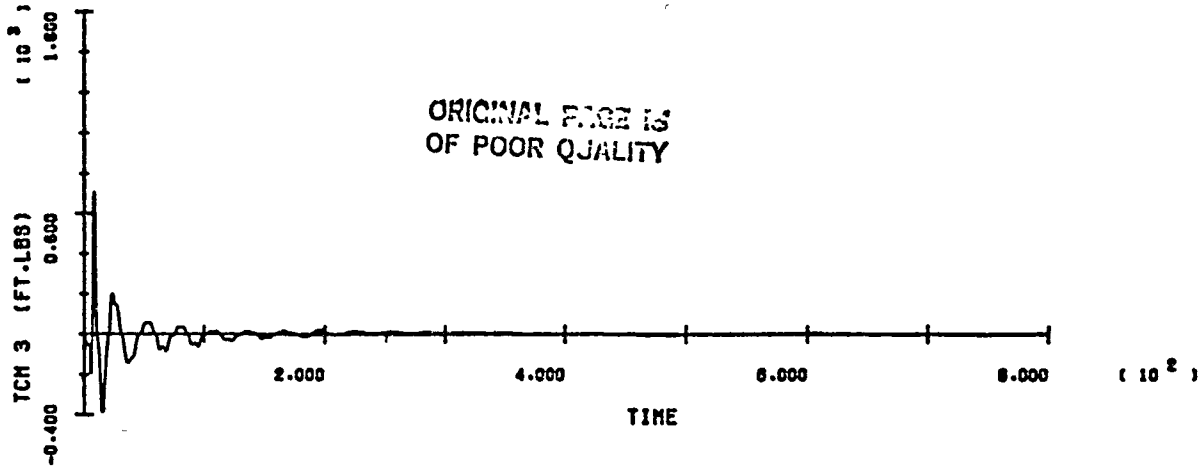


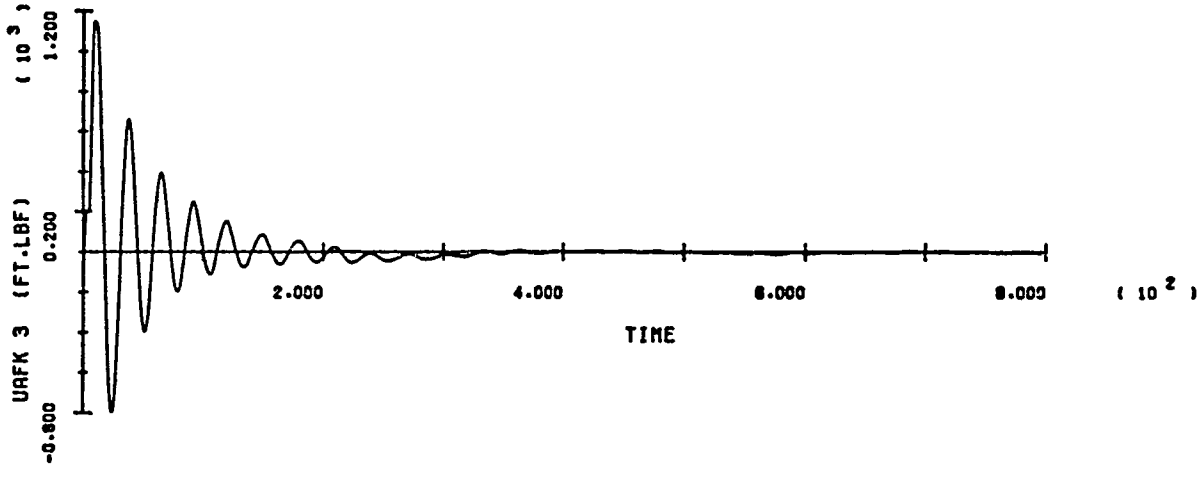


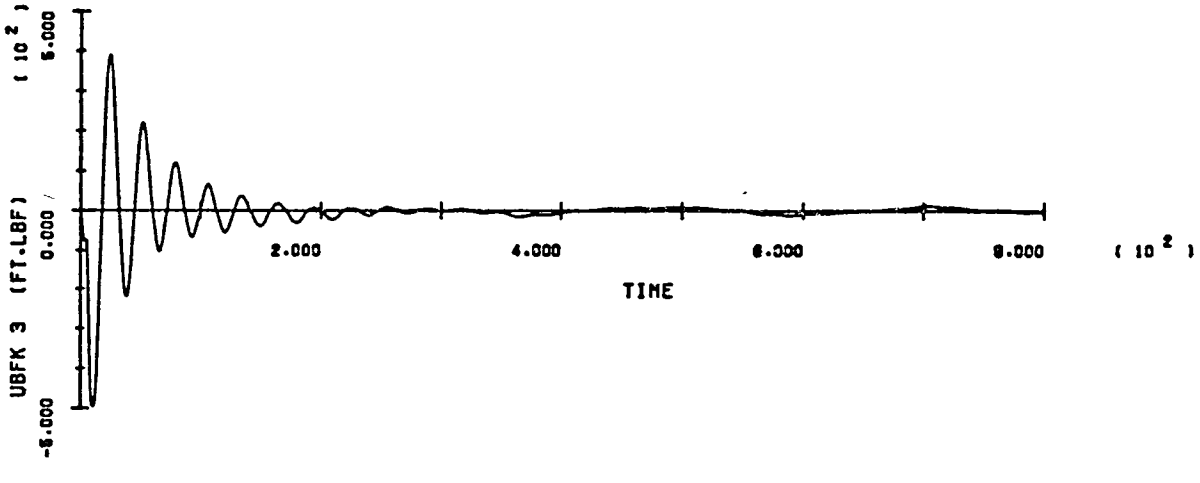


SOC/ORB BERTH - RUN 4

ORIGINAL PAGE IS
OF POOR QUALITY

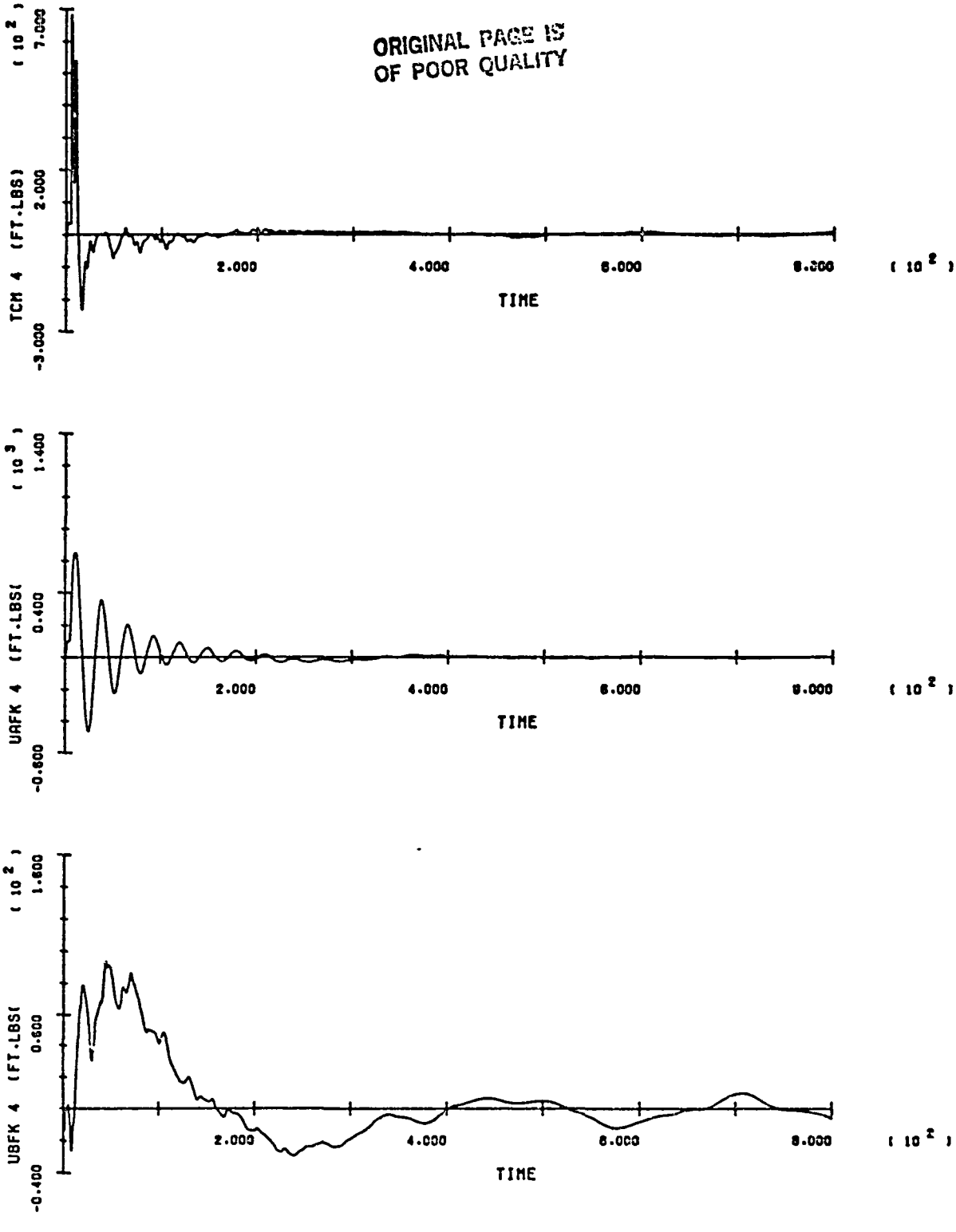


SOC/ORB BERTH - RUN 4

ORIGINAL PAGE IS
OF POOR QUALITY

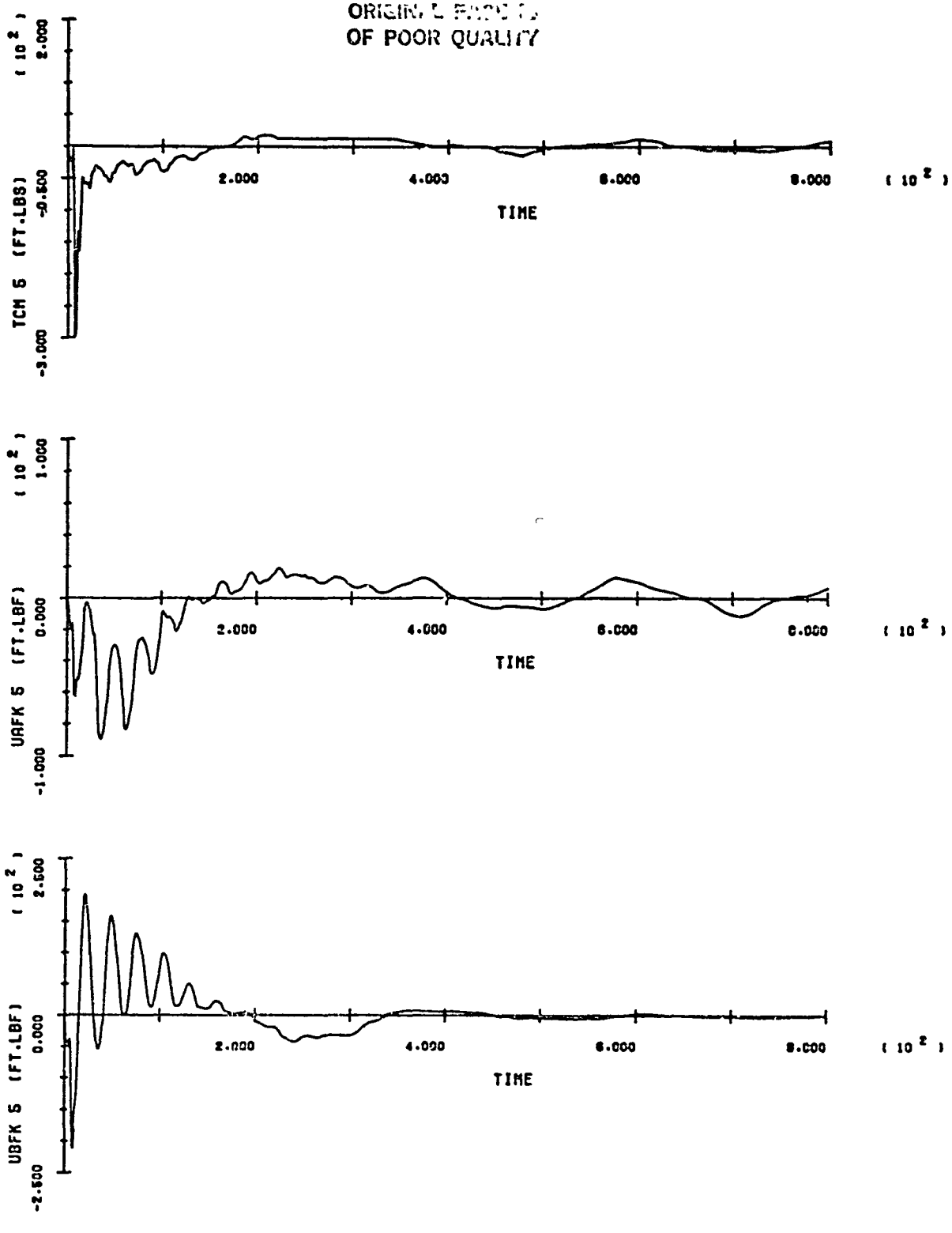


SOC/ORB BERTH - RUN 4

ORIGINAL PAGE IS
OF POOR QUALITY

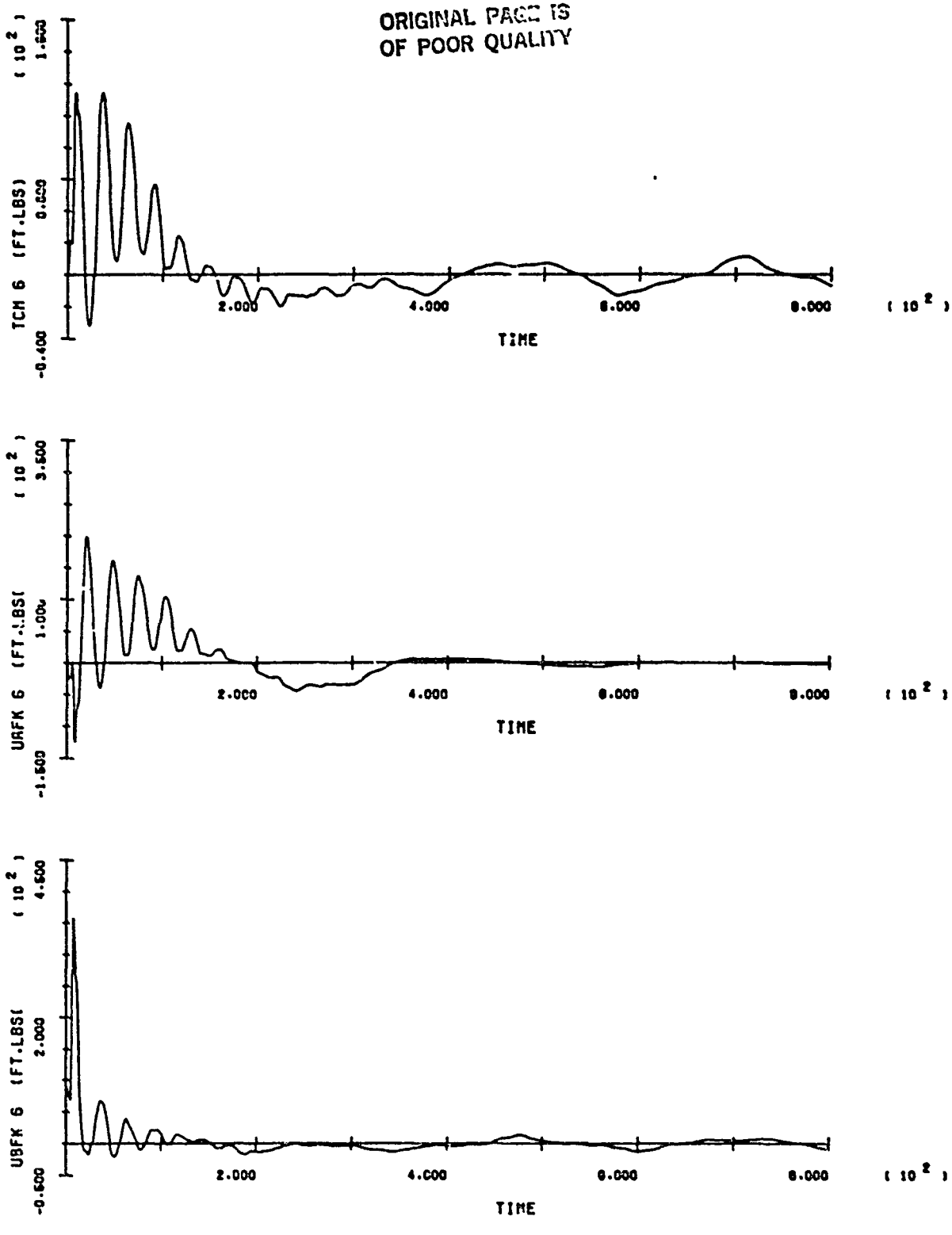


SOC/ORB BERTH - RUN 4

ORIGINAL PAGE IS
OF POOR QUALITY

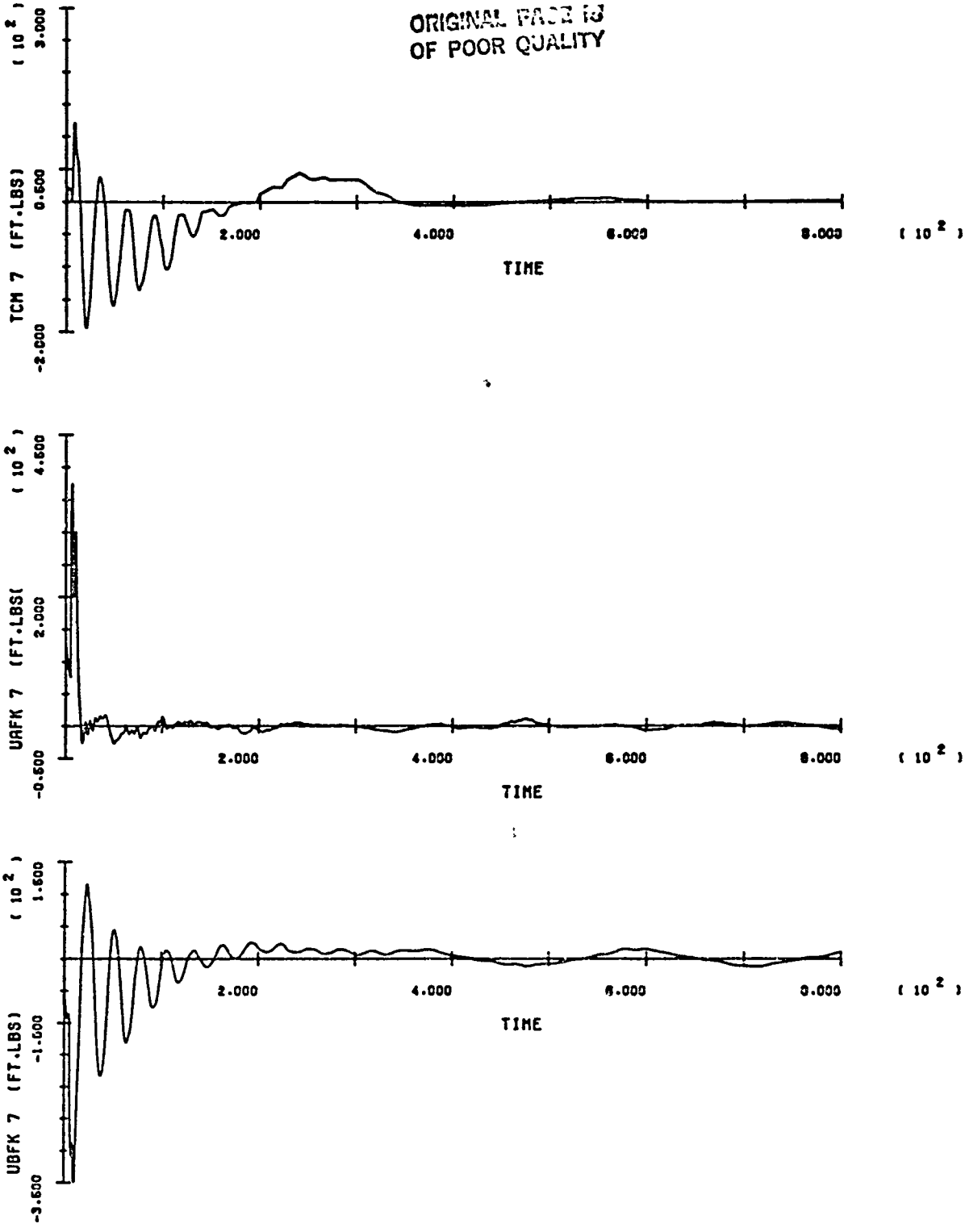


SOC/ORB BERTH - RUN 4

ORIGINAL PAGE IS
OF POOR QUALITY

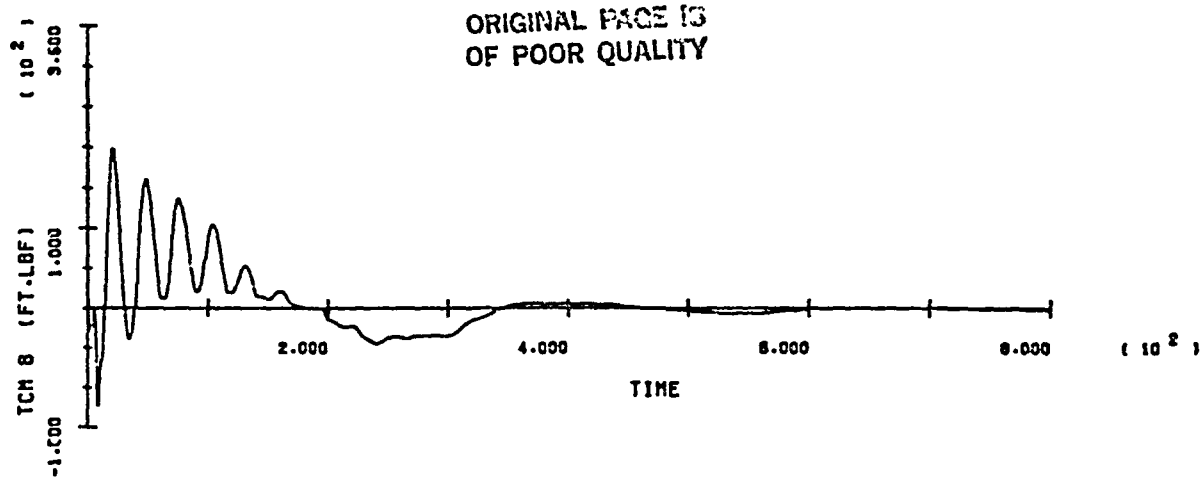


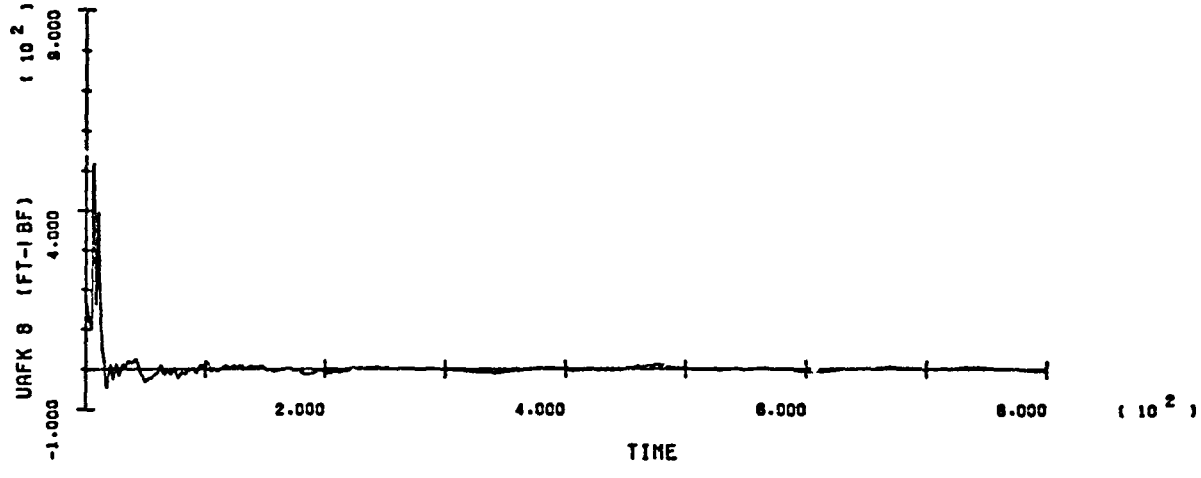


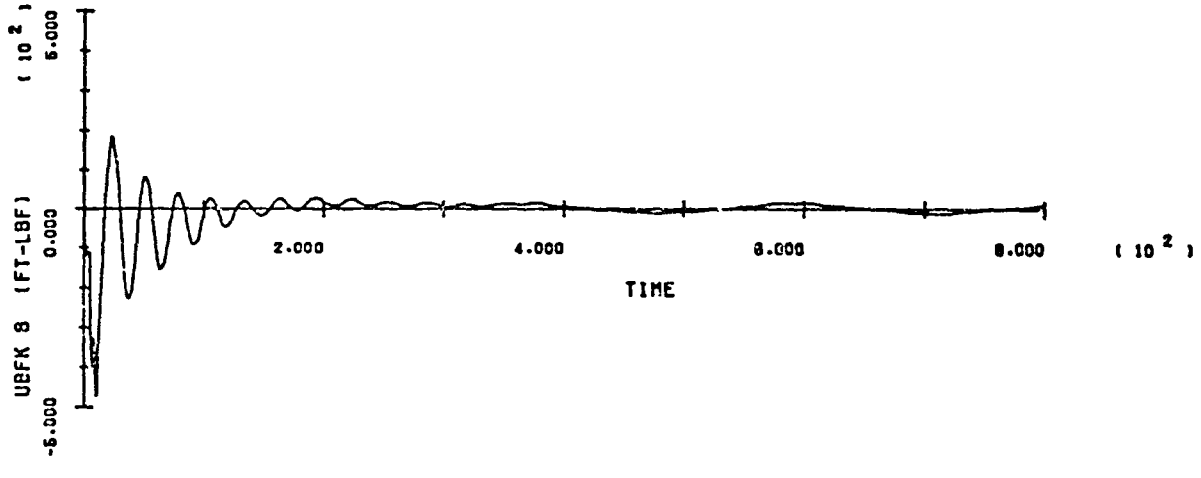


SOC/ORB BERTH - RUN 4

ORIGINAL PAGE IS
OF POOR QUALITY

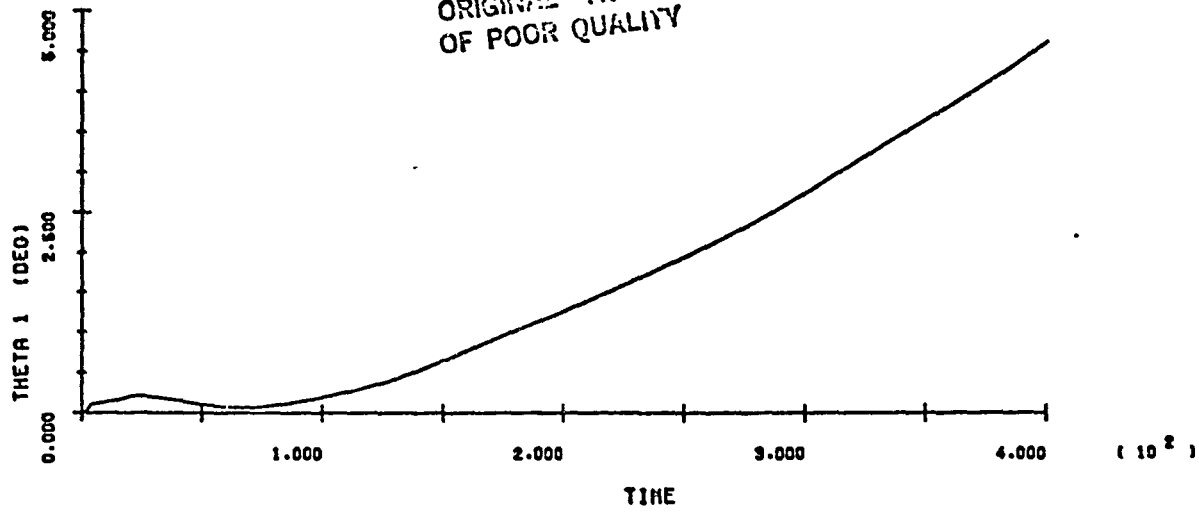


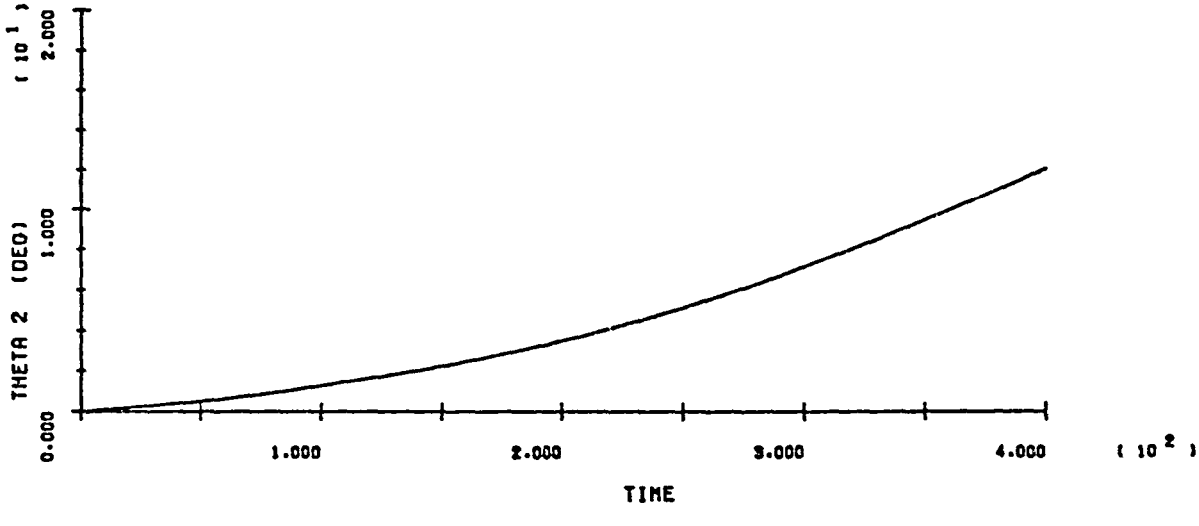


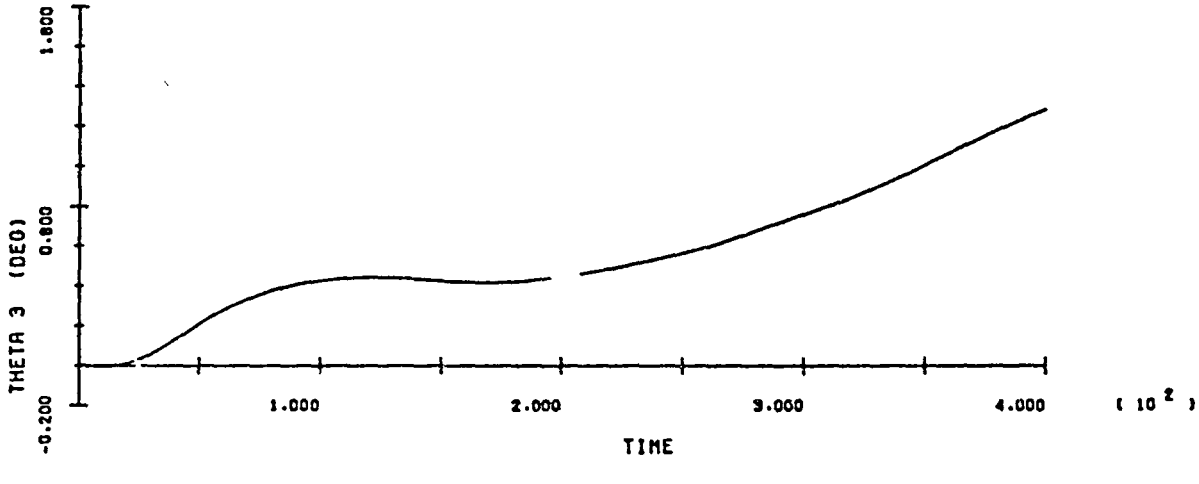


SOC/ORB BERTH - RUN 5

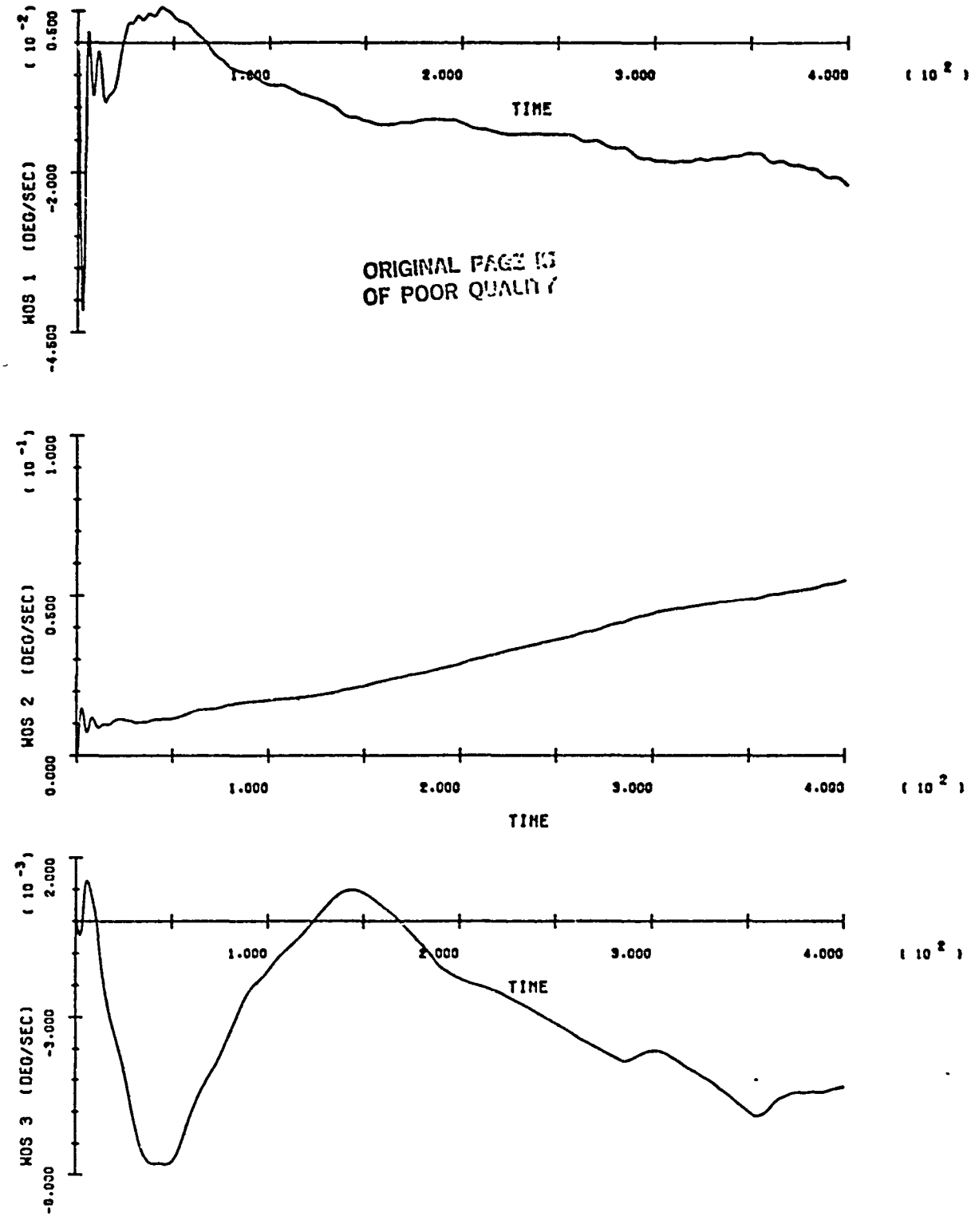


ORIGINAL PAGE IS
OF POOR QUALITY

SOC/ORB BERTH - RUN 5

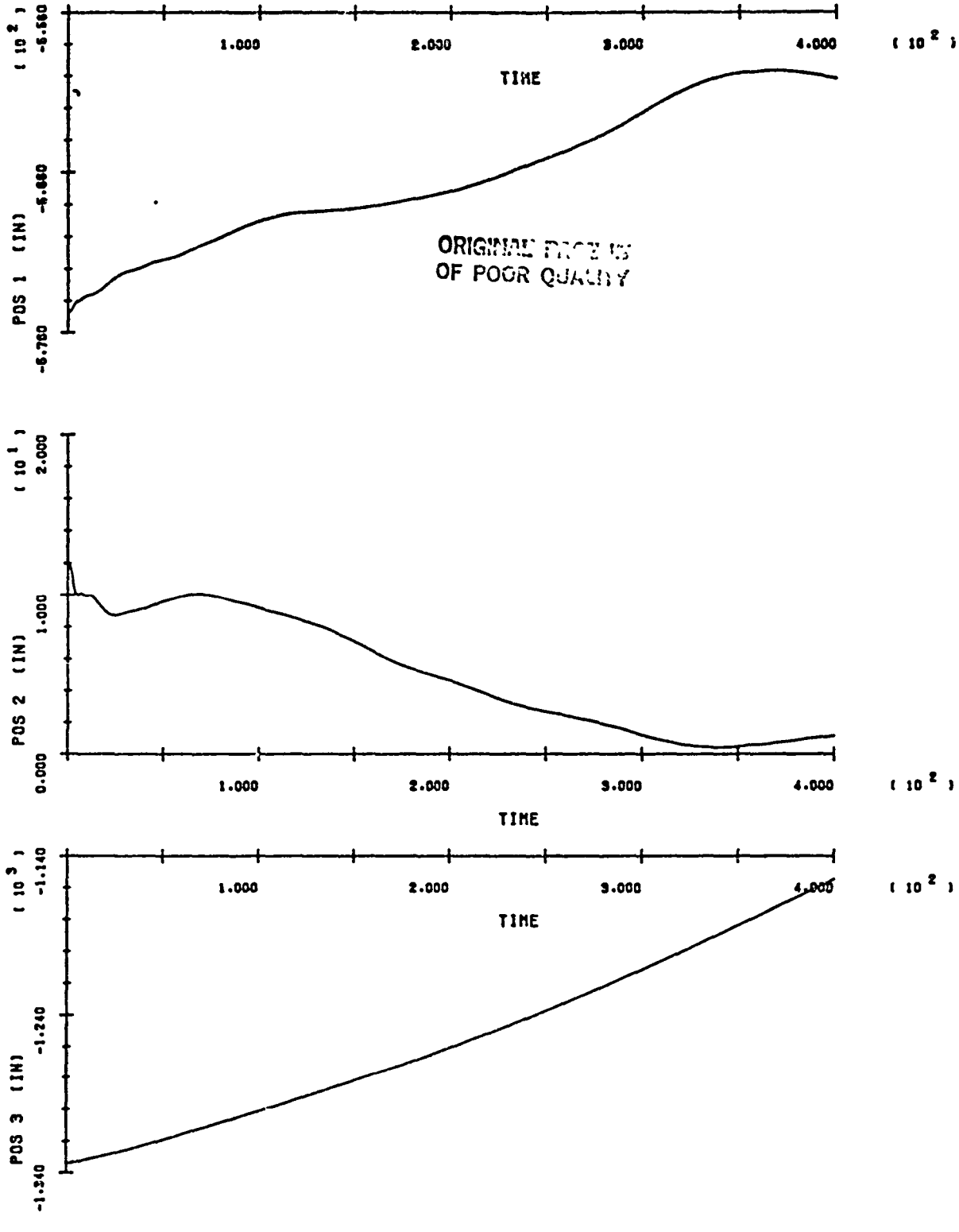


ORIGINAL PAGE IS
OF POOR QUALITY

SOC/ORB BERTH - RUN 5

ORIGINAL PAGE IS
OF POOR QUALITY

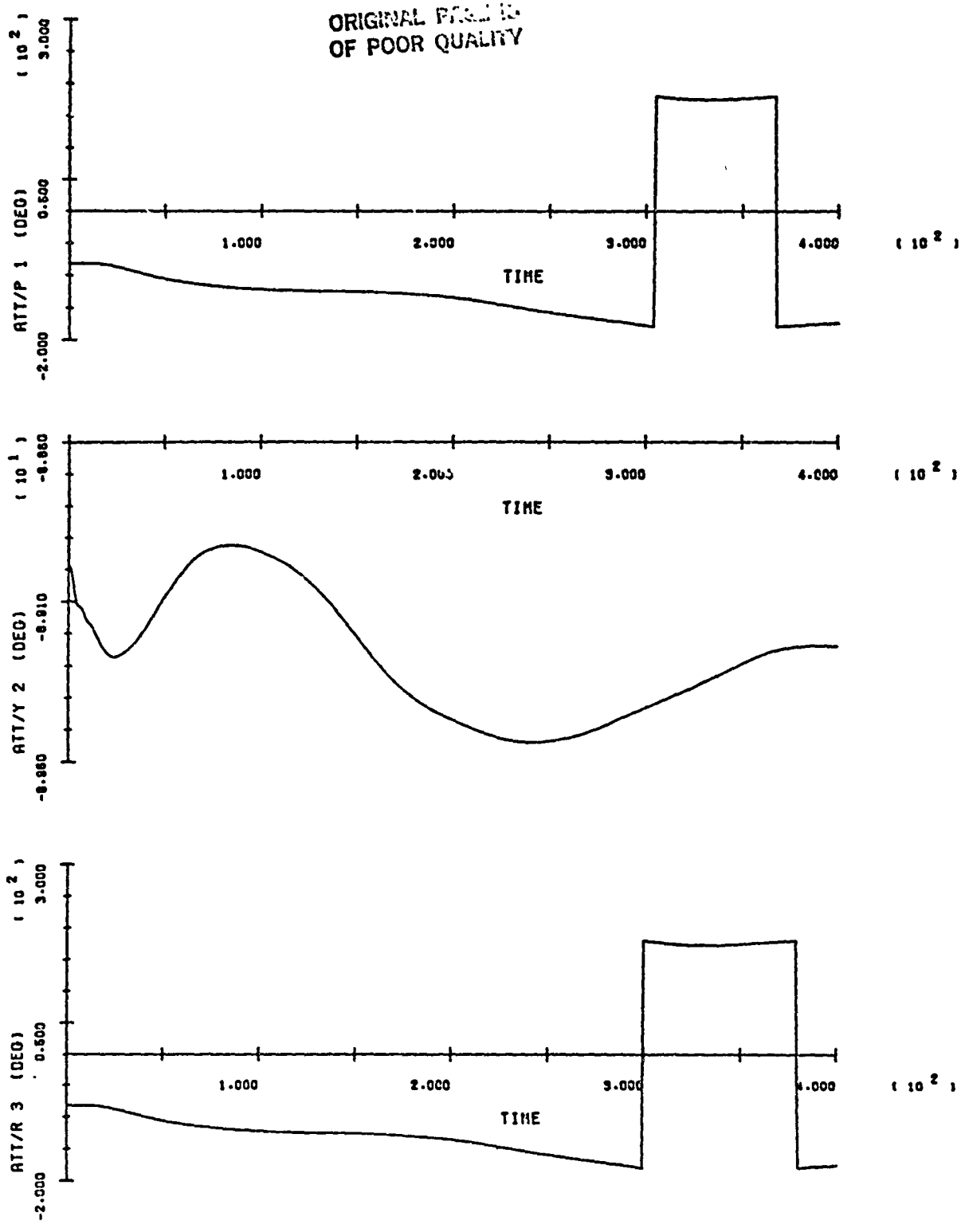


SOC/ORB BERTH - RUN 5

ORIGINAL PAGE IS
OF POOR QUALITY

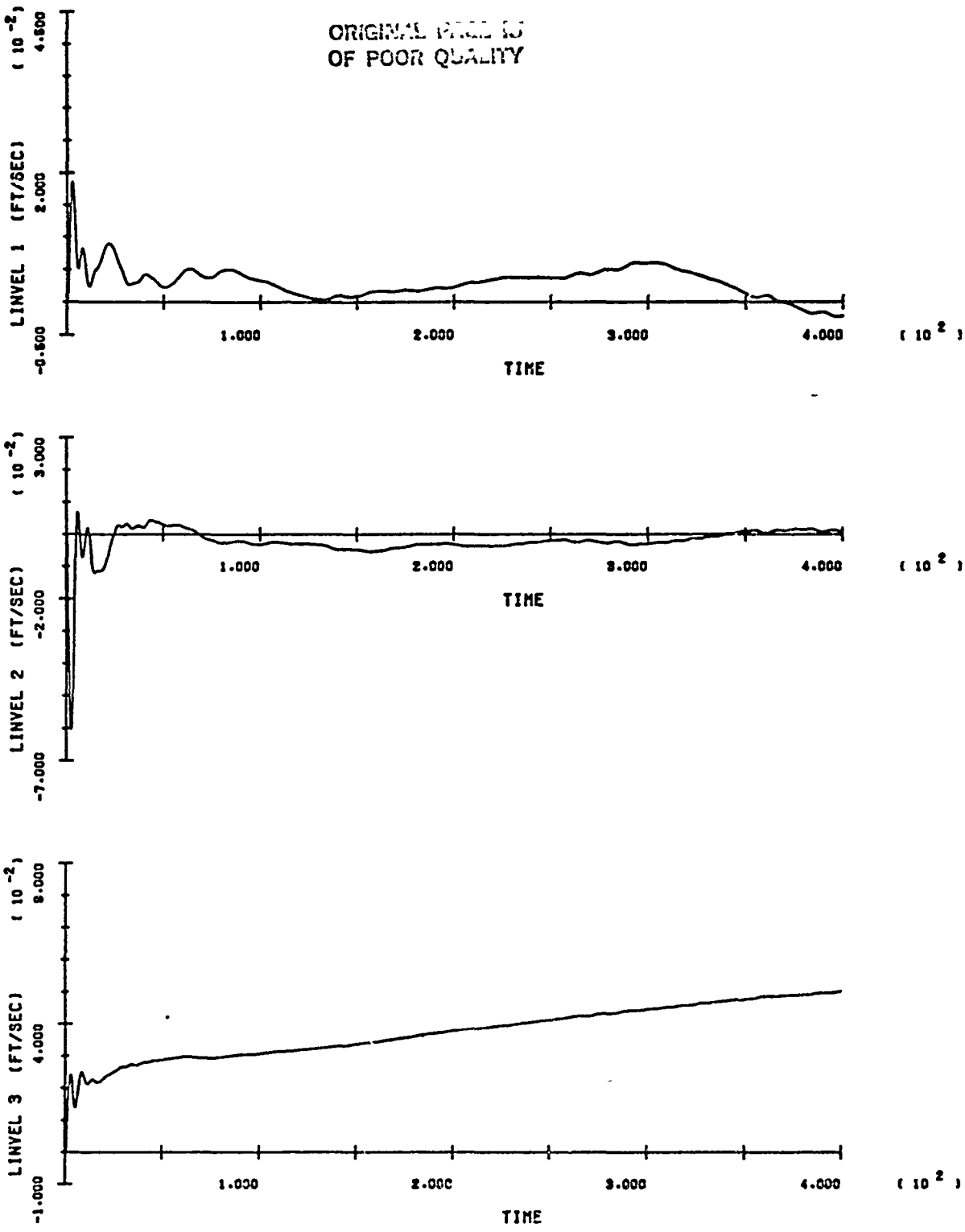


SOC/ORB BERTH - RUN 5

ORIGINAL PAGE IS
OF POOR QUALITY

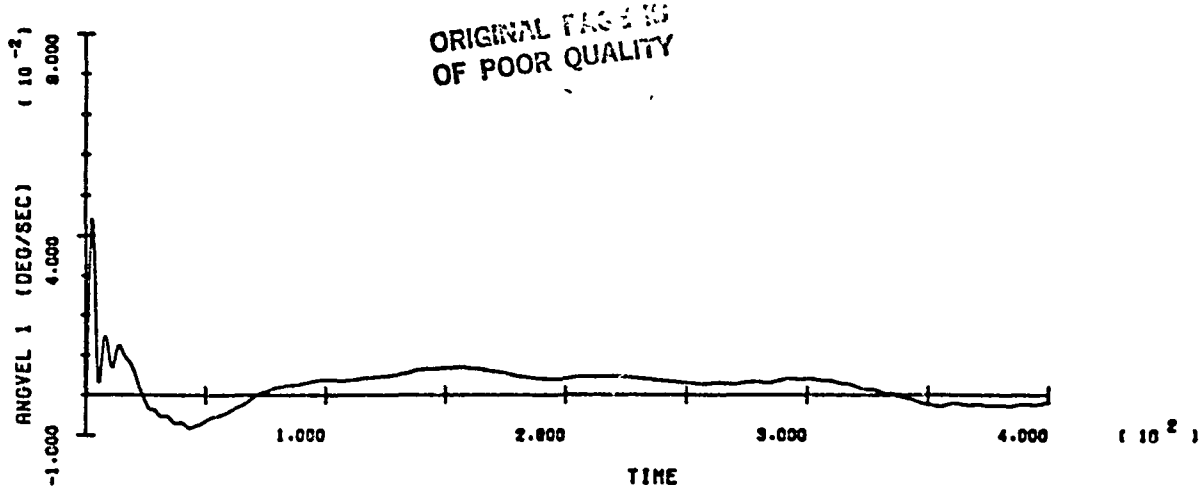


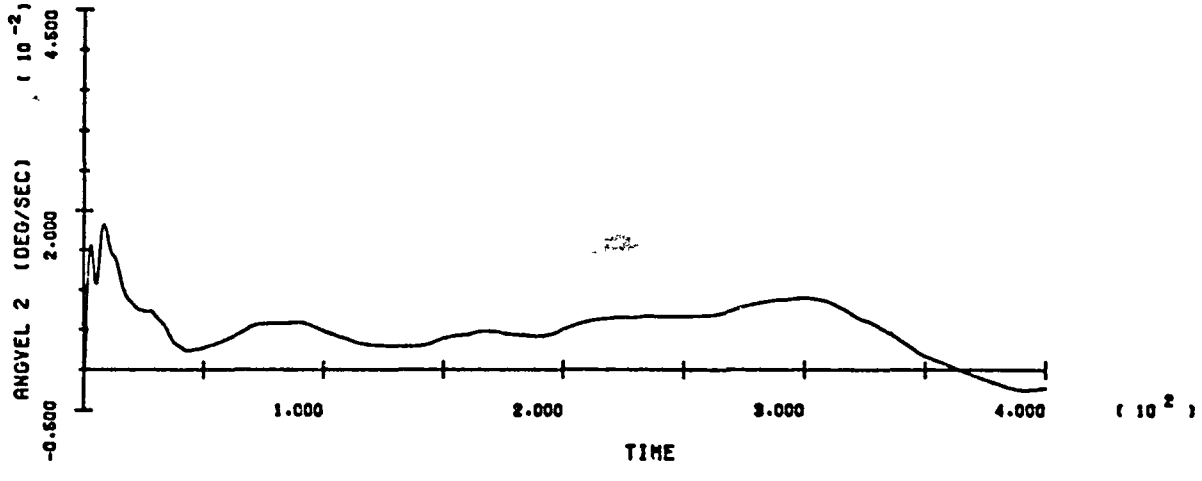


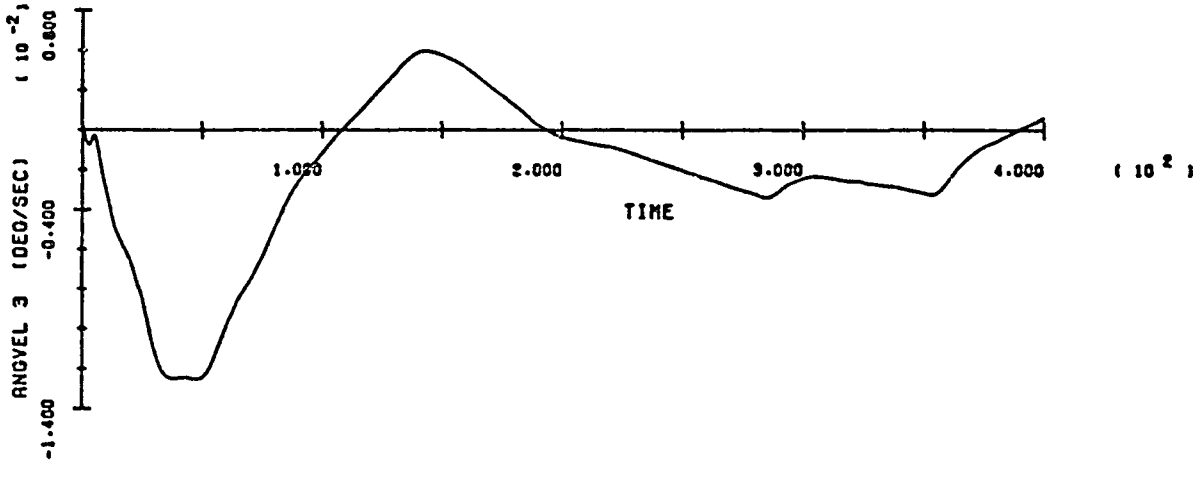


SOC/ORB BERTH - RUN 5

ORIGINAL PAGE IS
OF POOR QUALITY

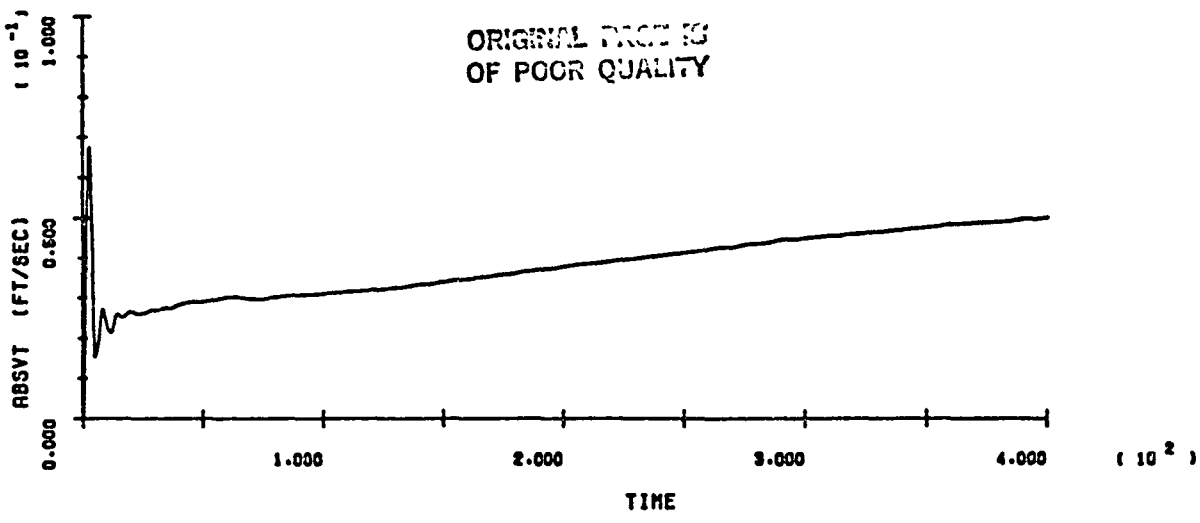


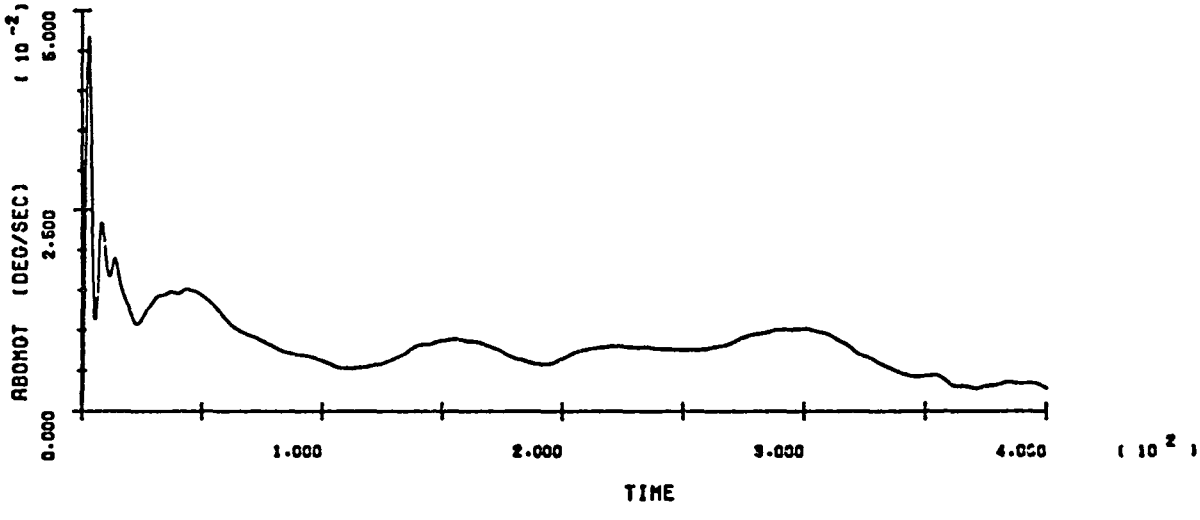


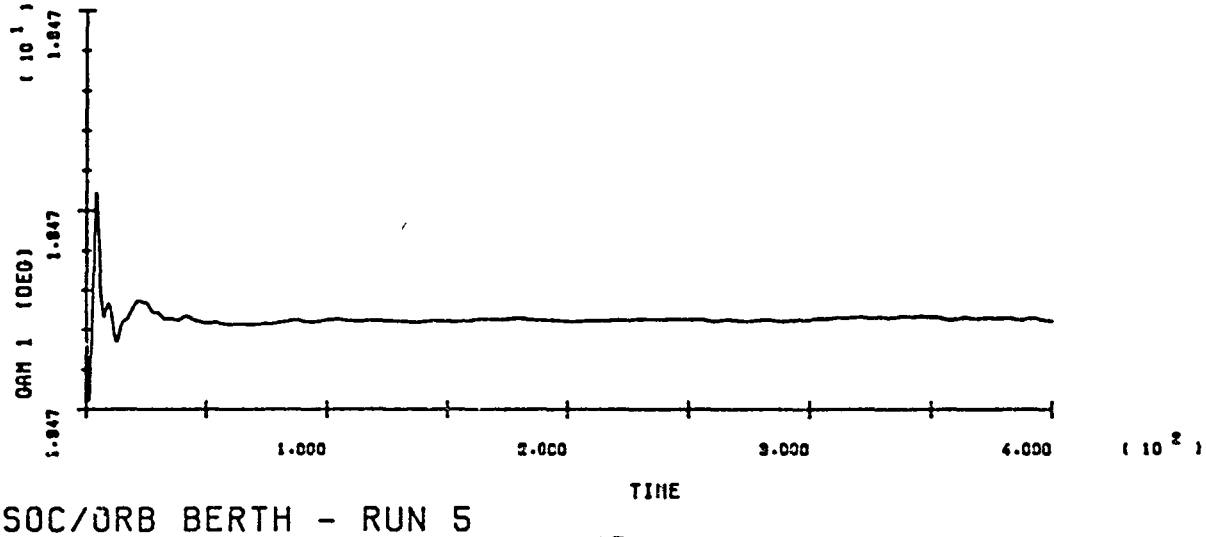


SOC/ORB BERTH - RUN 5

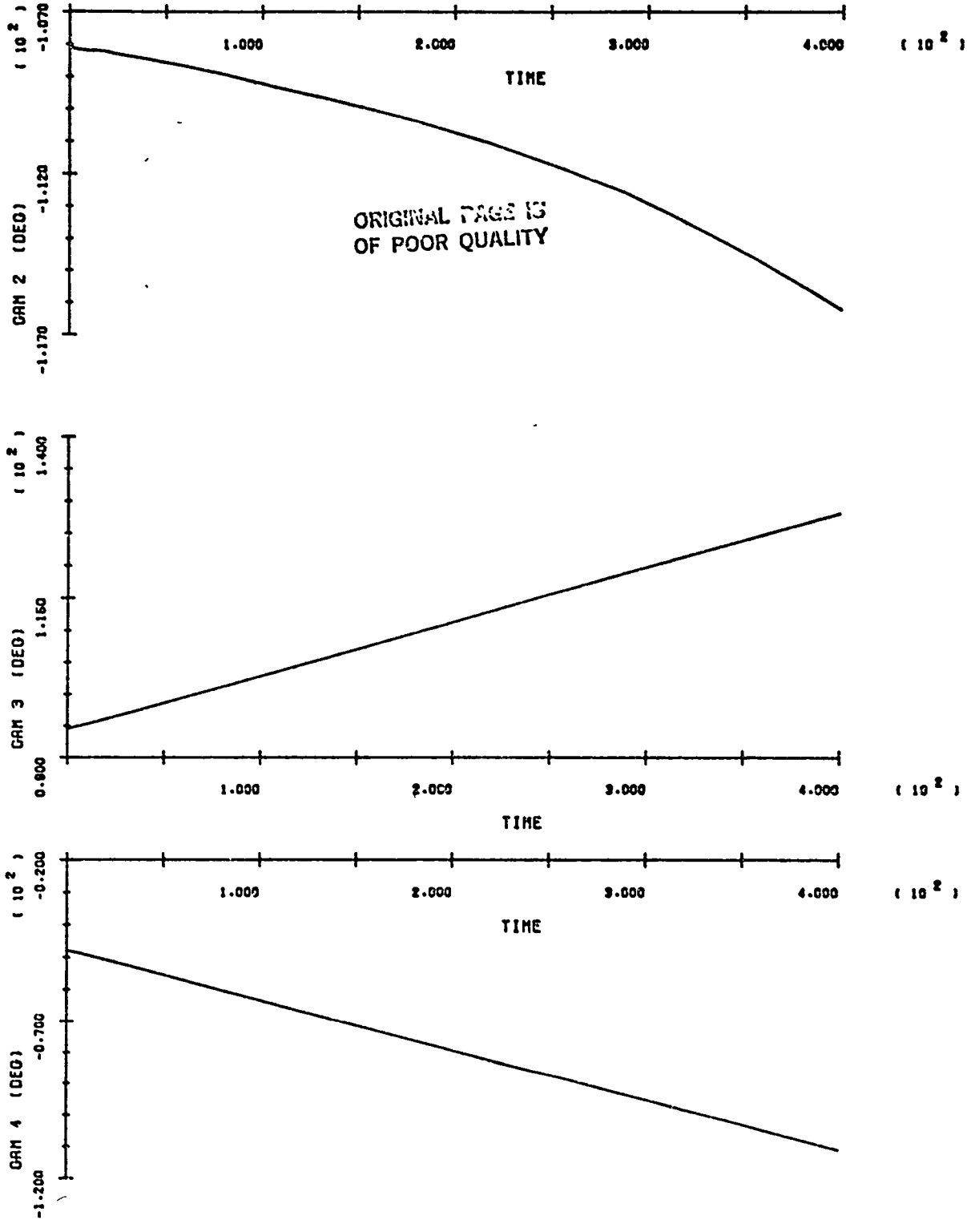


SOC/ORB BERTH - RUN 5

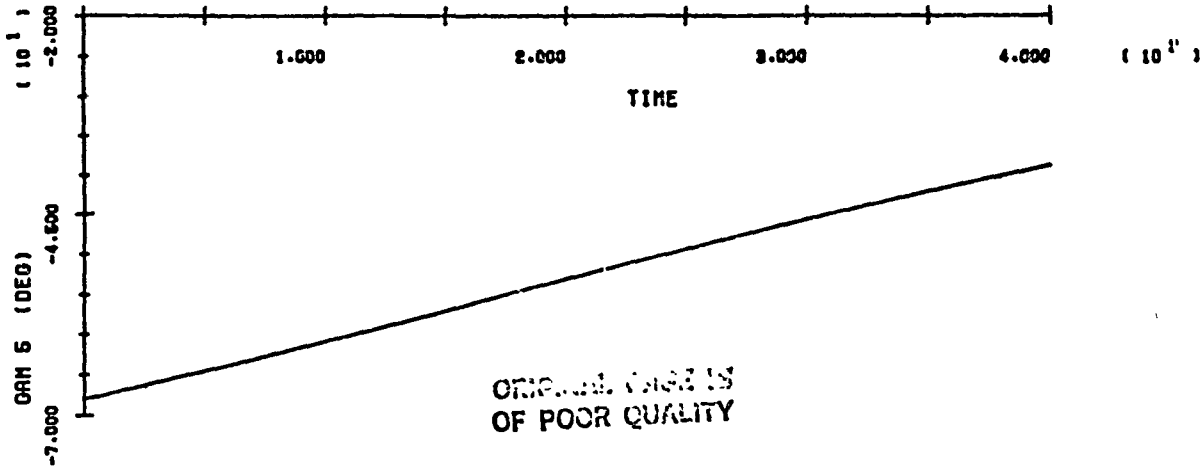


ORIGINAL PAGE IS
OF POOR QUALITY

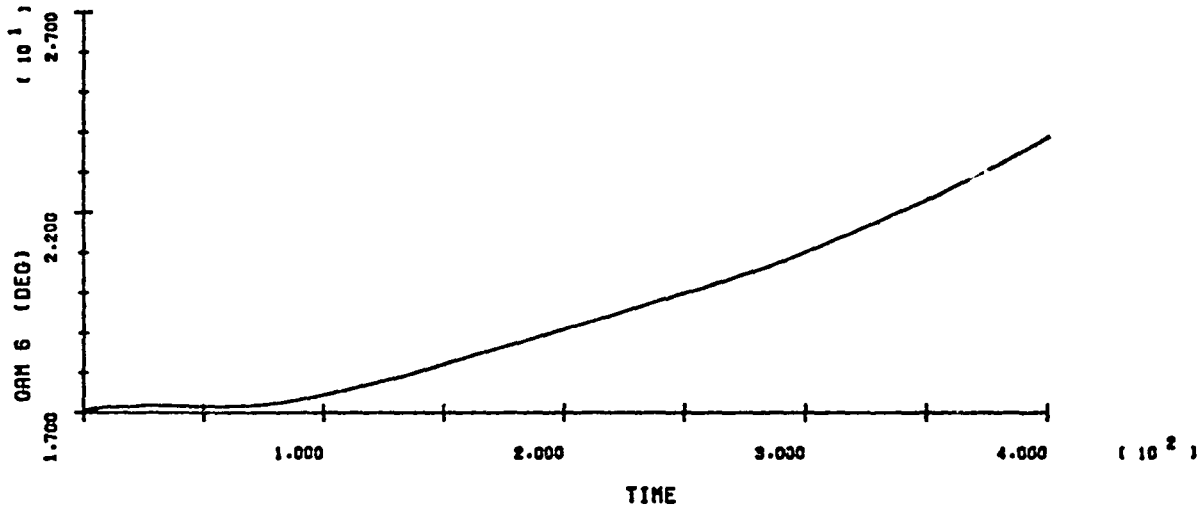


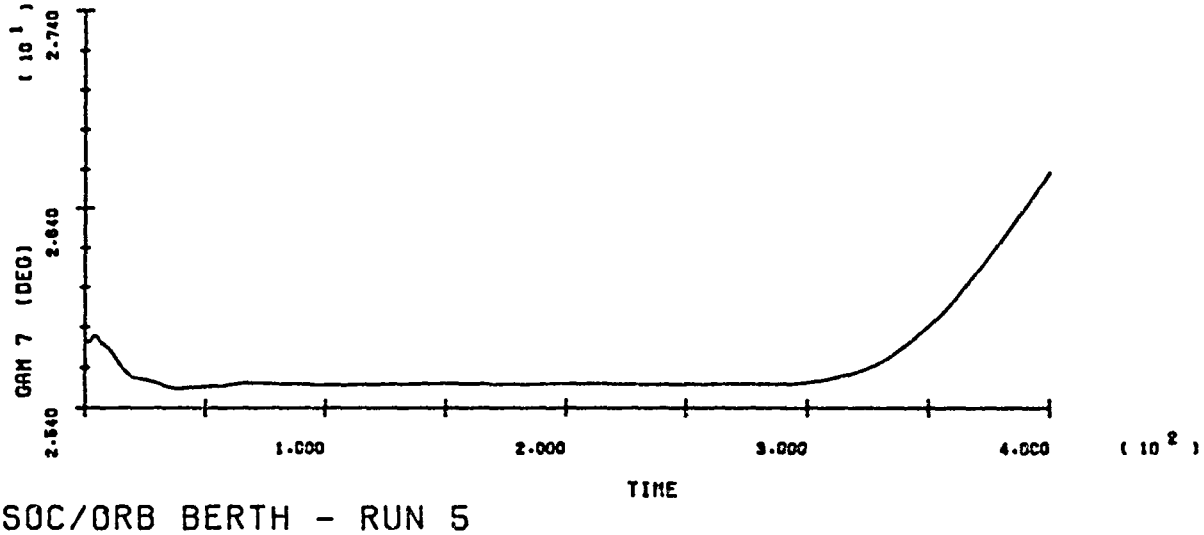


SOC/ORB BERTH - RUN 5

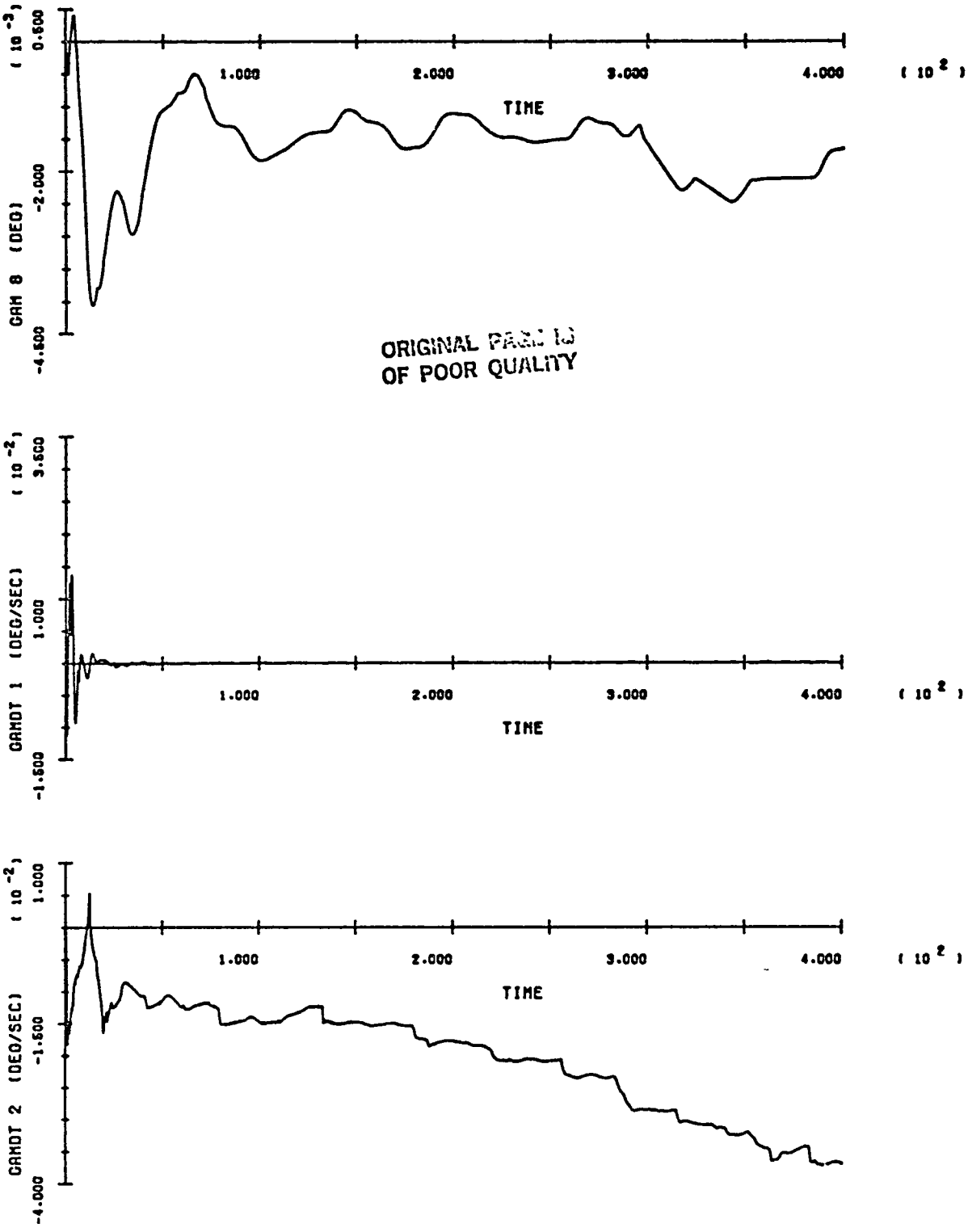


ORIGINAL PAGE IS
OF POOR QUALITY

SOC/ORB BERTH - RUN 5

ORIGINAL PAGE IS
OF POOR QUALITY

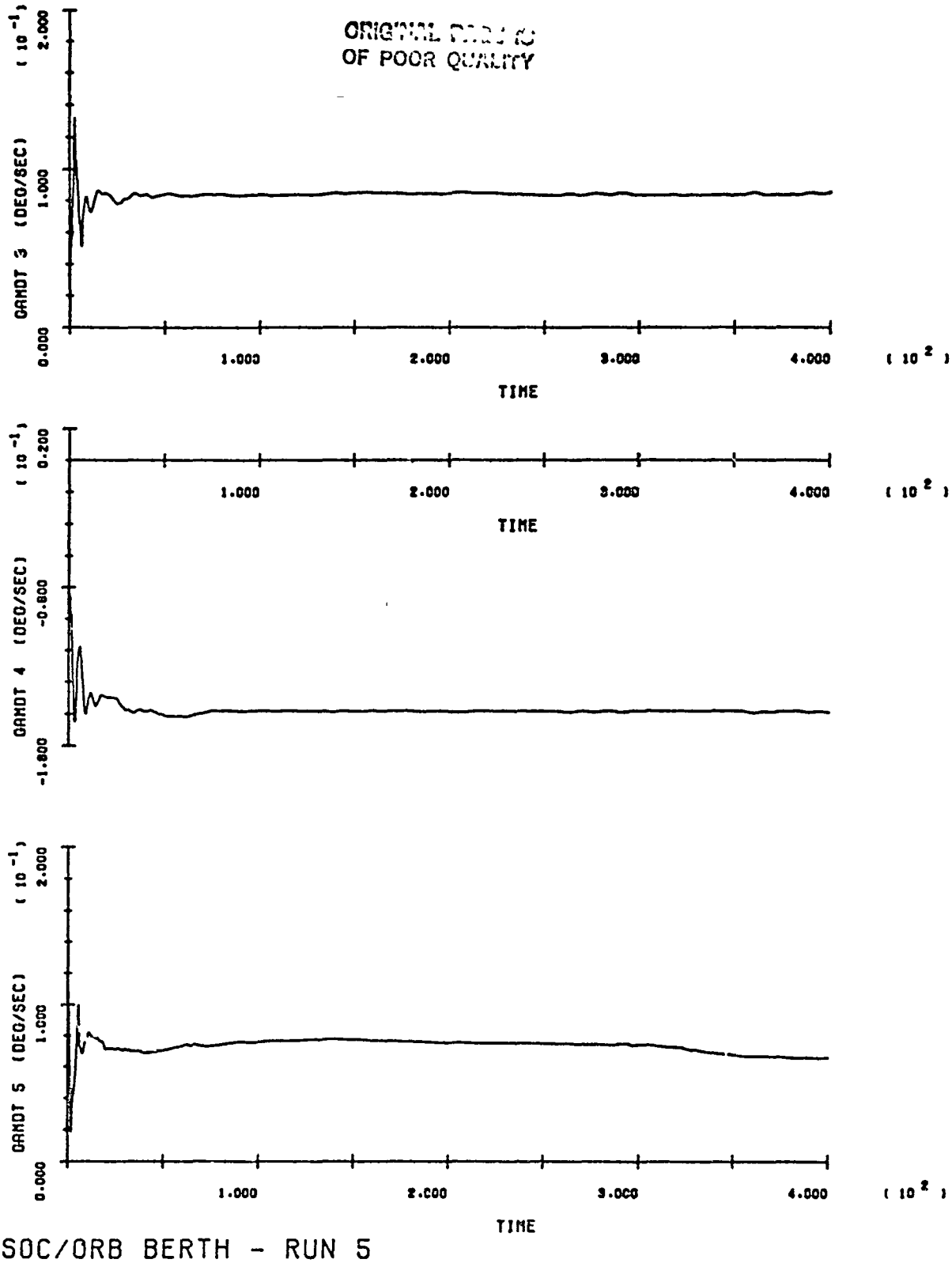


SOC/ORB BERTH - RUN 5

ORIGINAL PAGE IS
OF POOR QUALITY

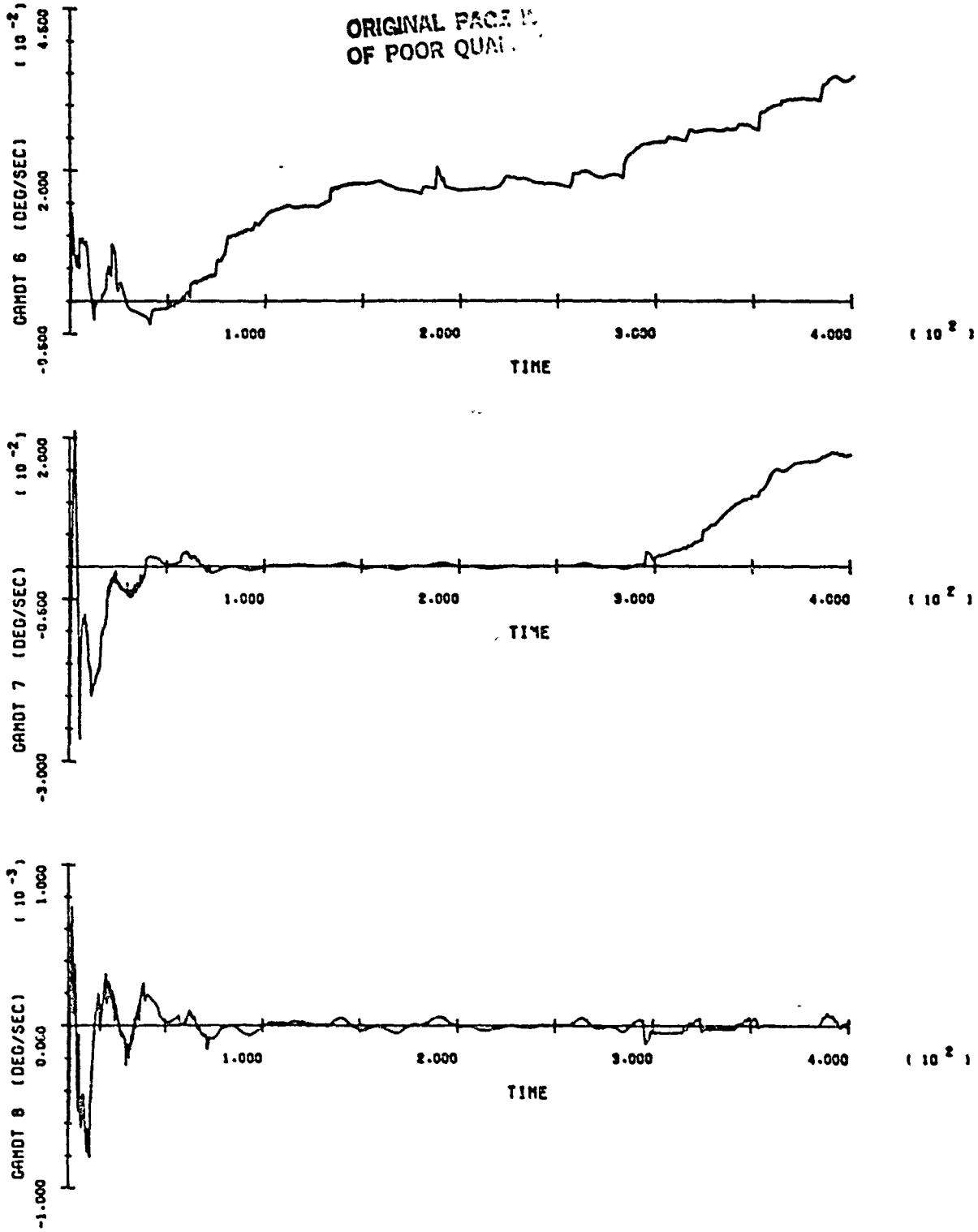


SOC/ORB BERTH - RUN 5

ORIGINAL PAGE IS
OF POOR QUALITY

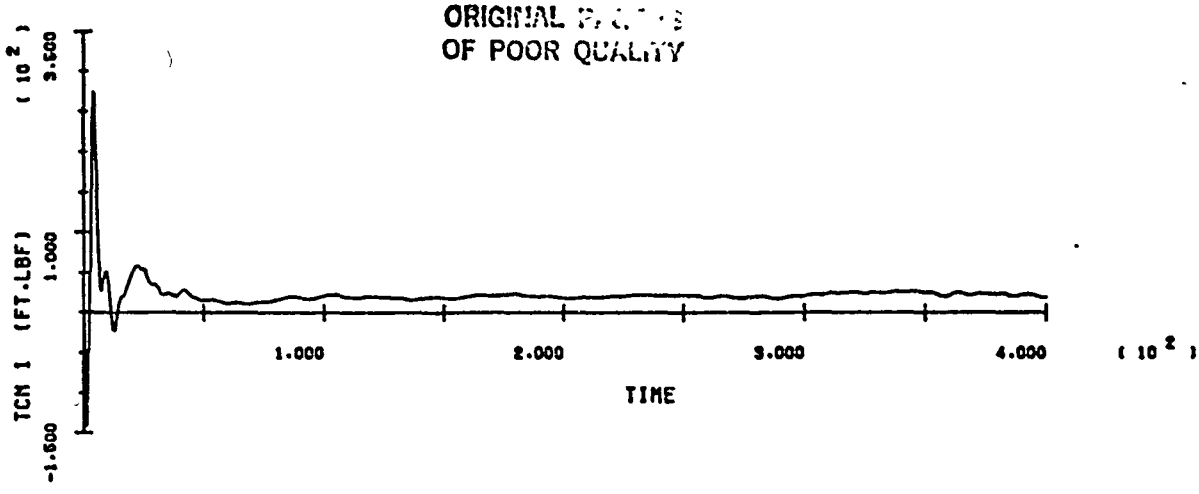


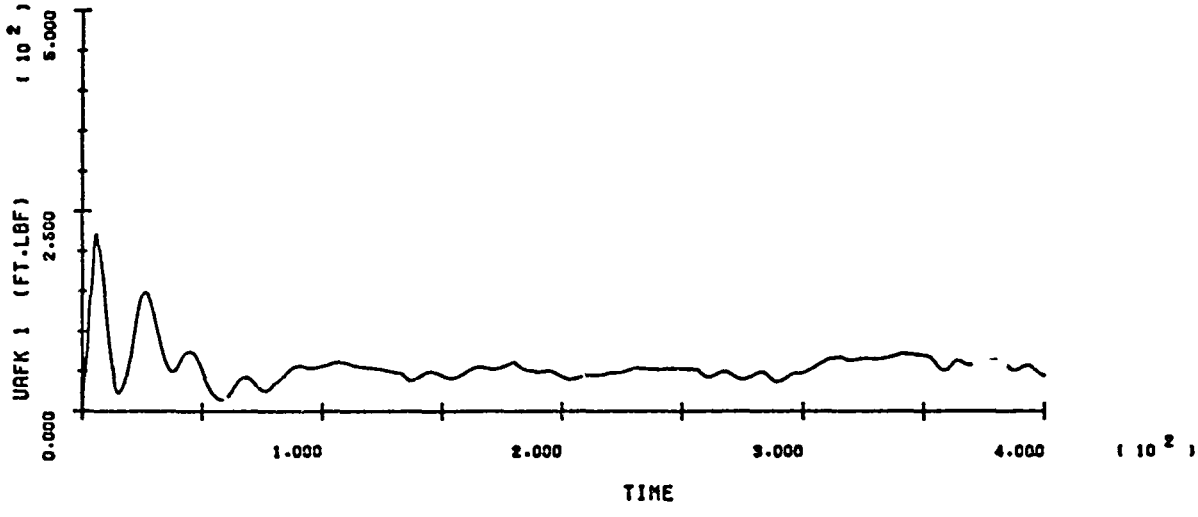


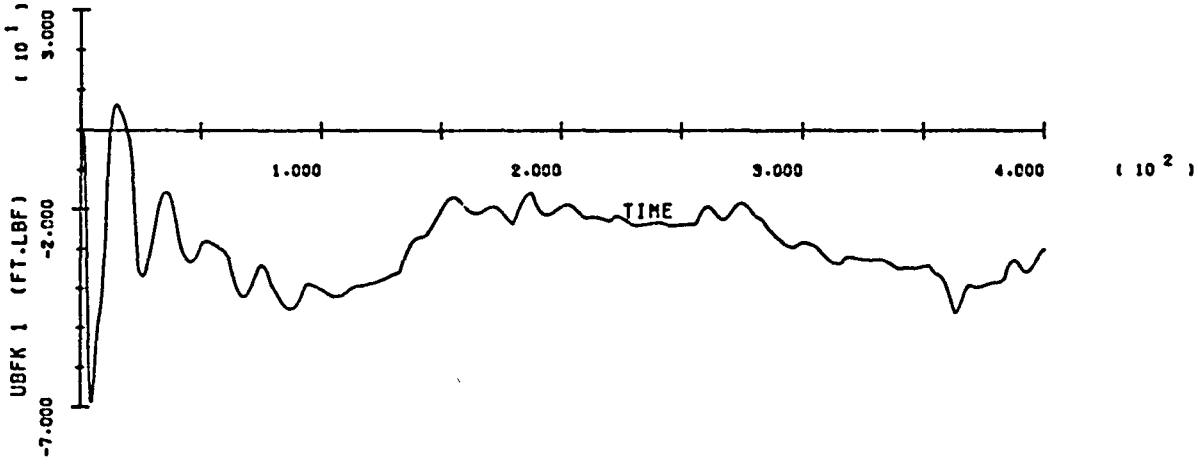


SOC/ORB BERTH - RUN 5

ORIGINAL PAGE IS
OF POOR QUALITY

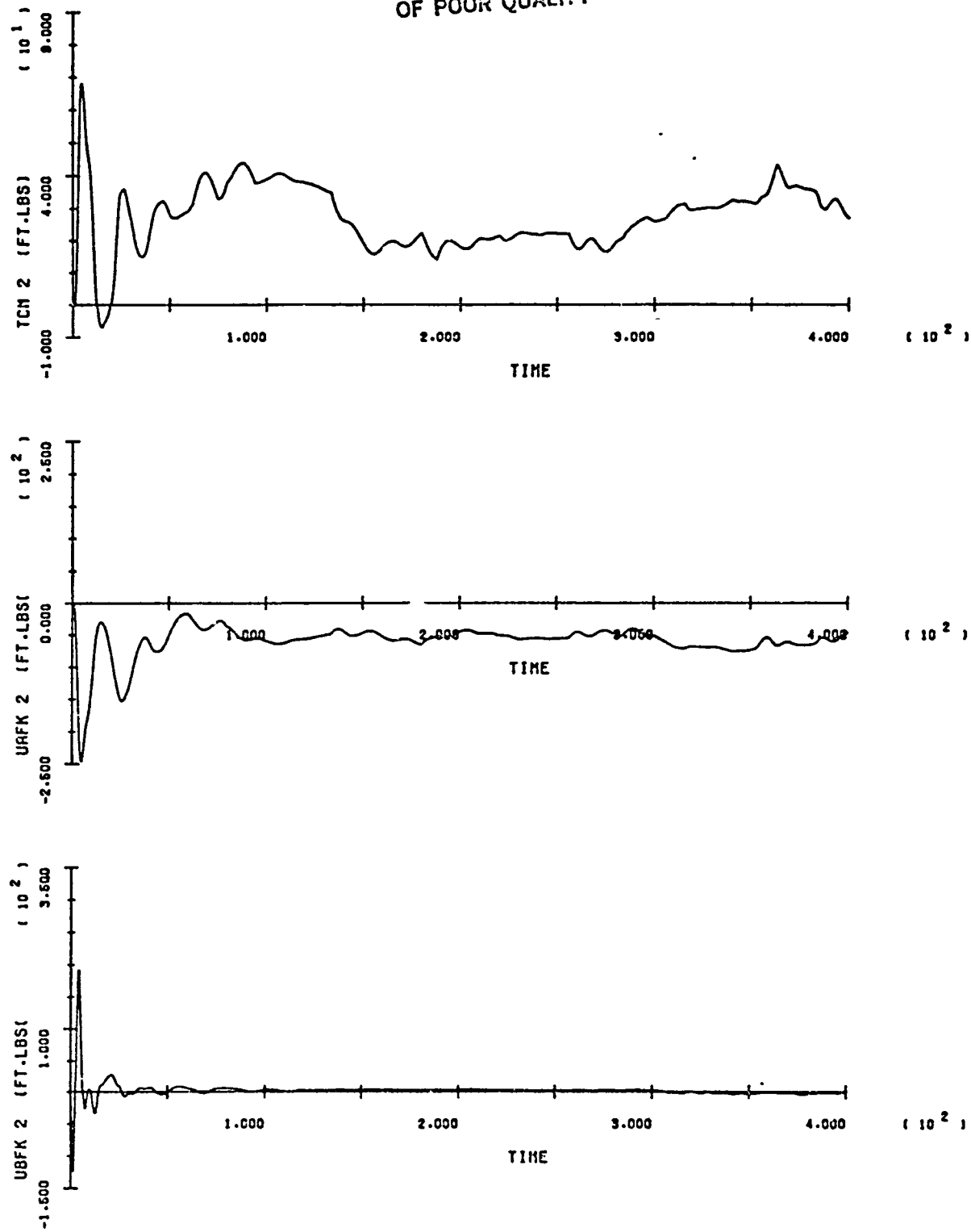


SOC/ORB BERTH - RUN 5

ORIGINAL PAGE IS
OF POOR QUALITY

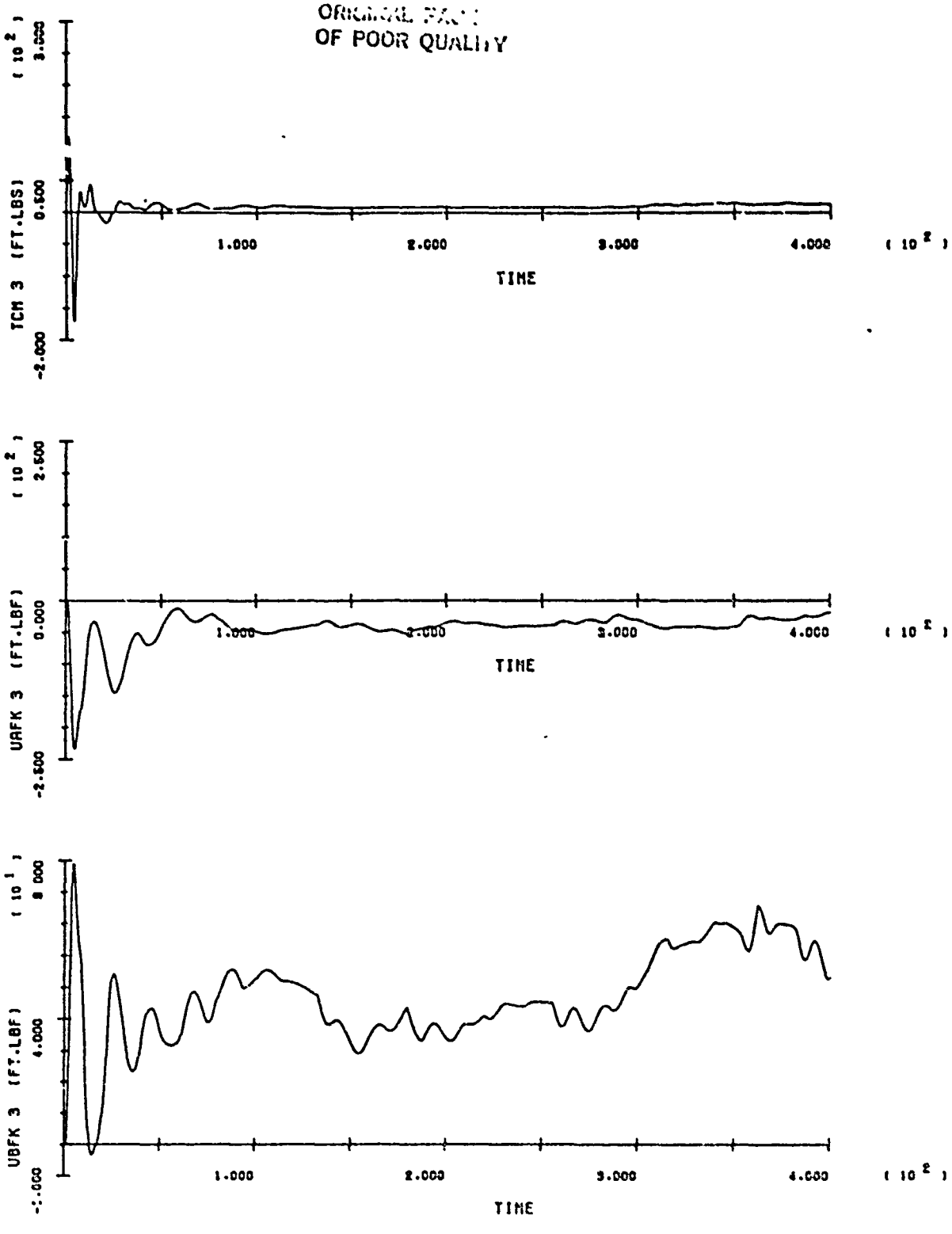


SOC/ORB BERTH - RUN 5

ORIGINAL PAGE IS
OF POOR QUALITY

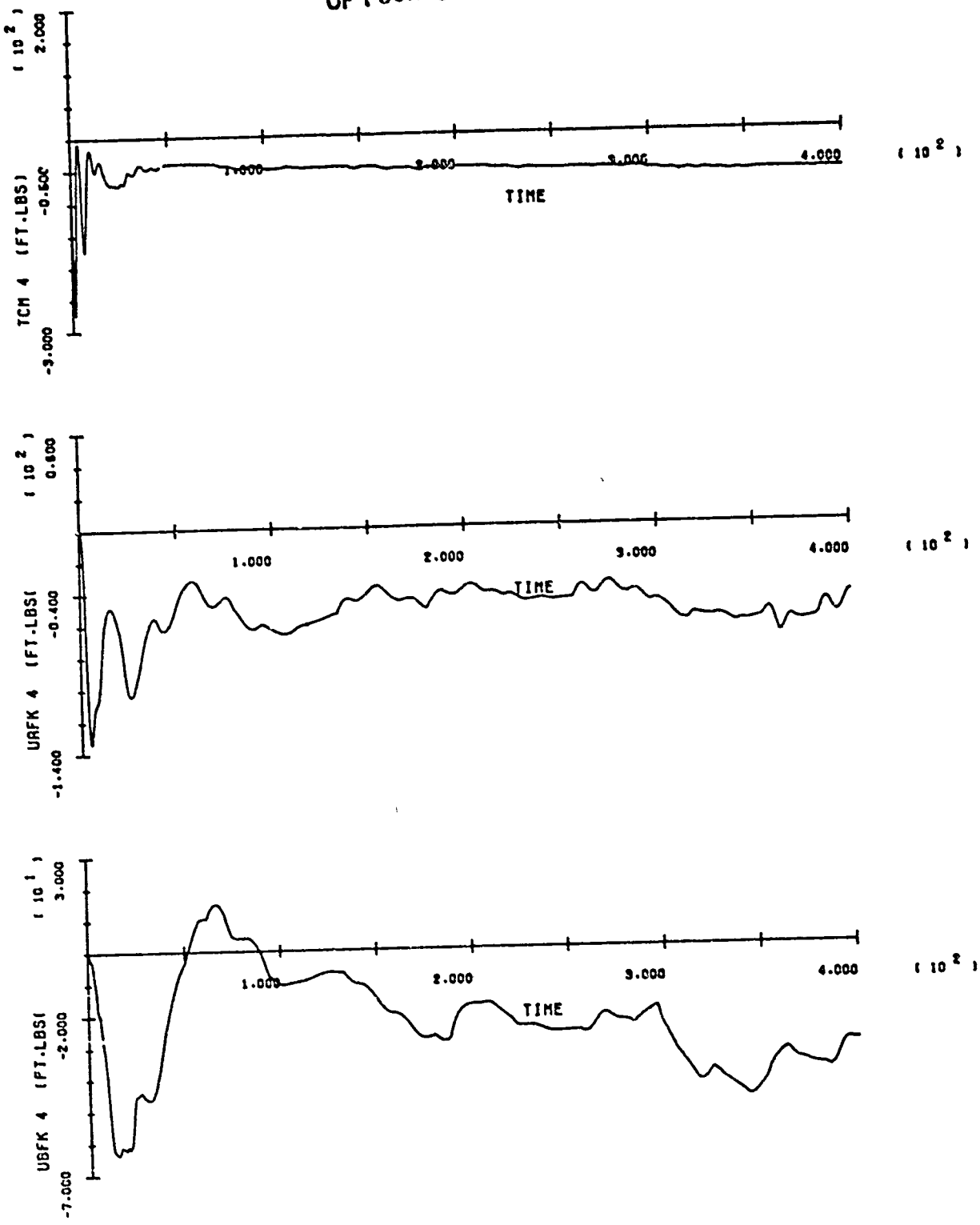


SOC/ORB BERTH - RUN 5

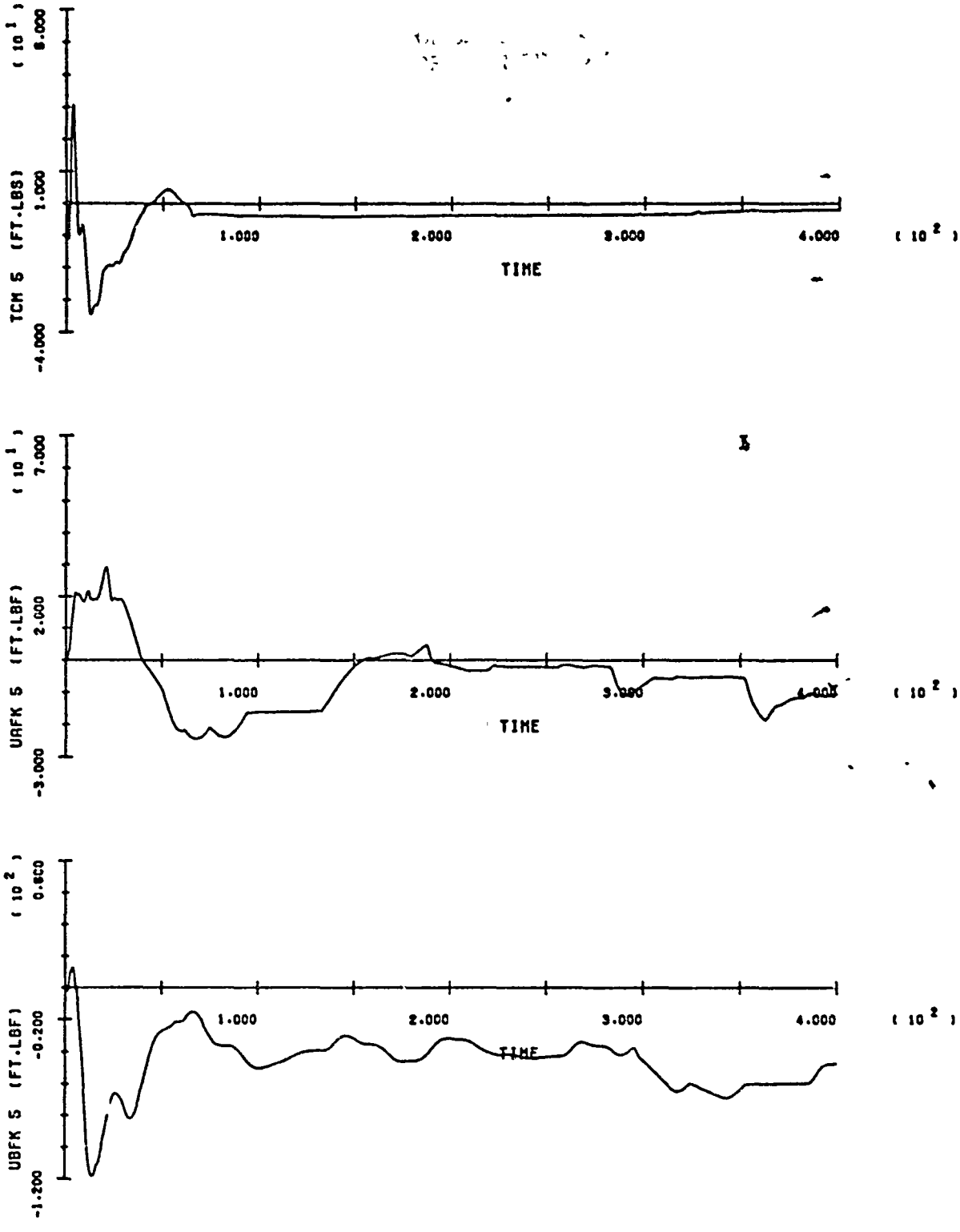


SOC/ORB BERTH - RUN 5

ORIGINAL PAGE IS
OF POOR QUALITY

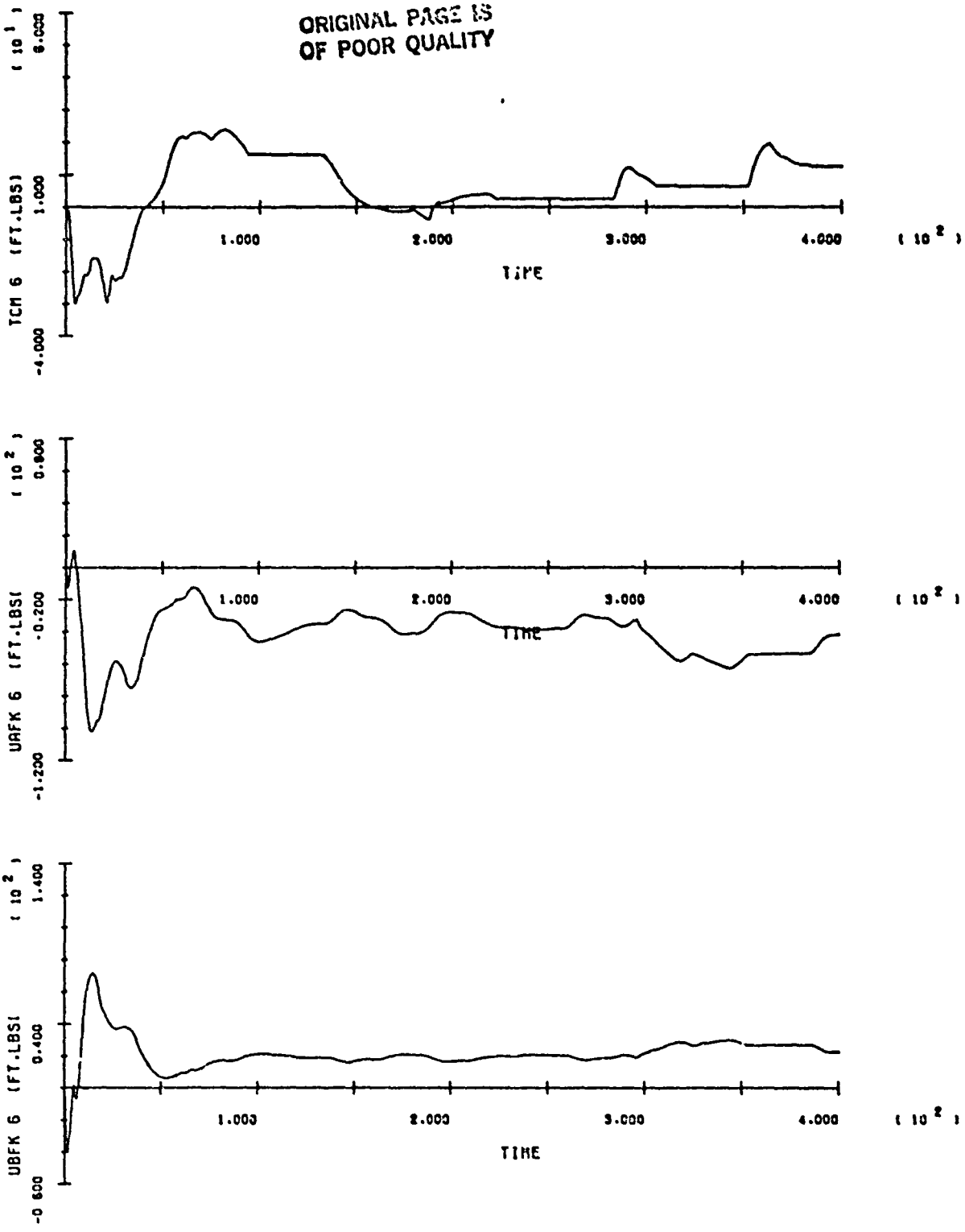


SOC/ORB BERTH - RUN 5

ORIGINAL PAGE IS
OF POOR QUALITY

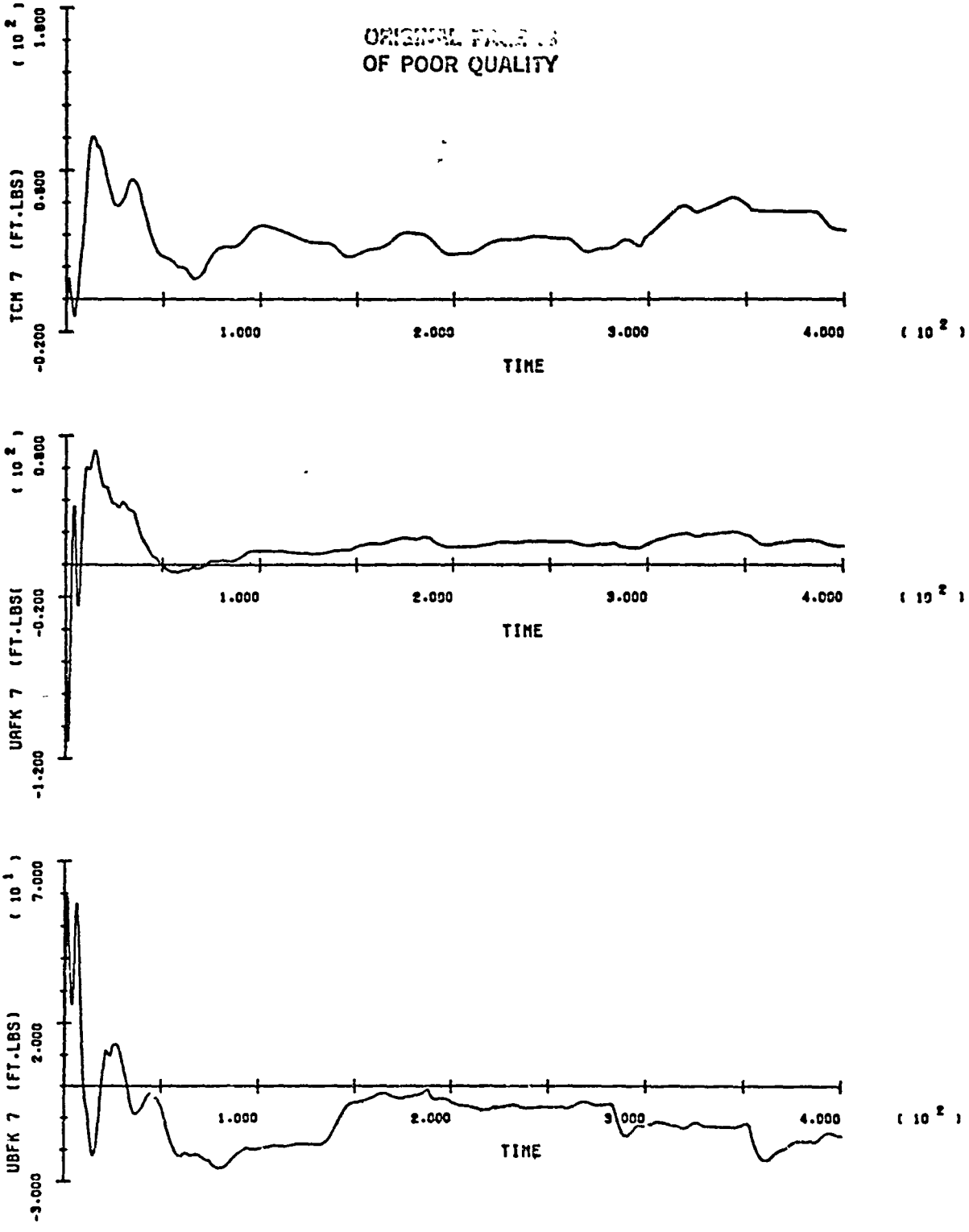


SOC/ORB BERTH - RUN 5

ORIGINAL PAGE IS
OF POOR QUALITY

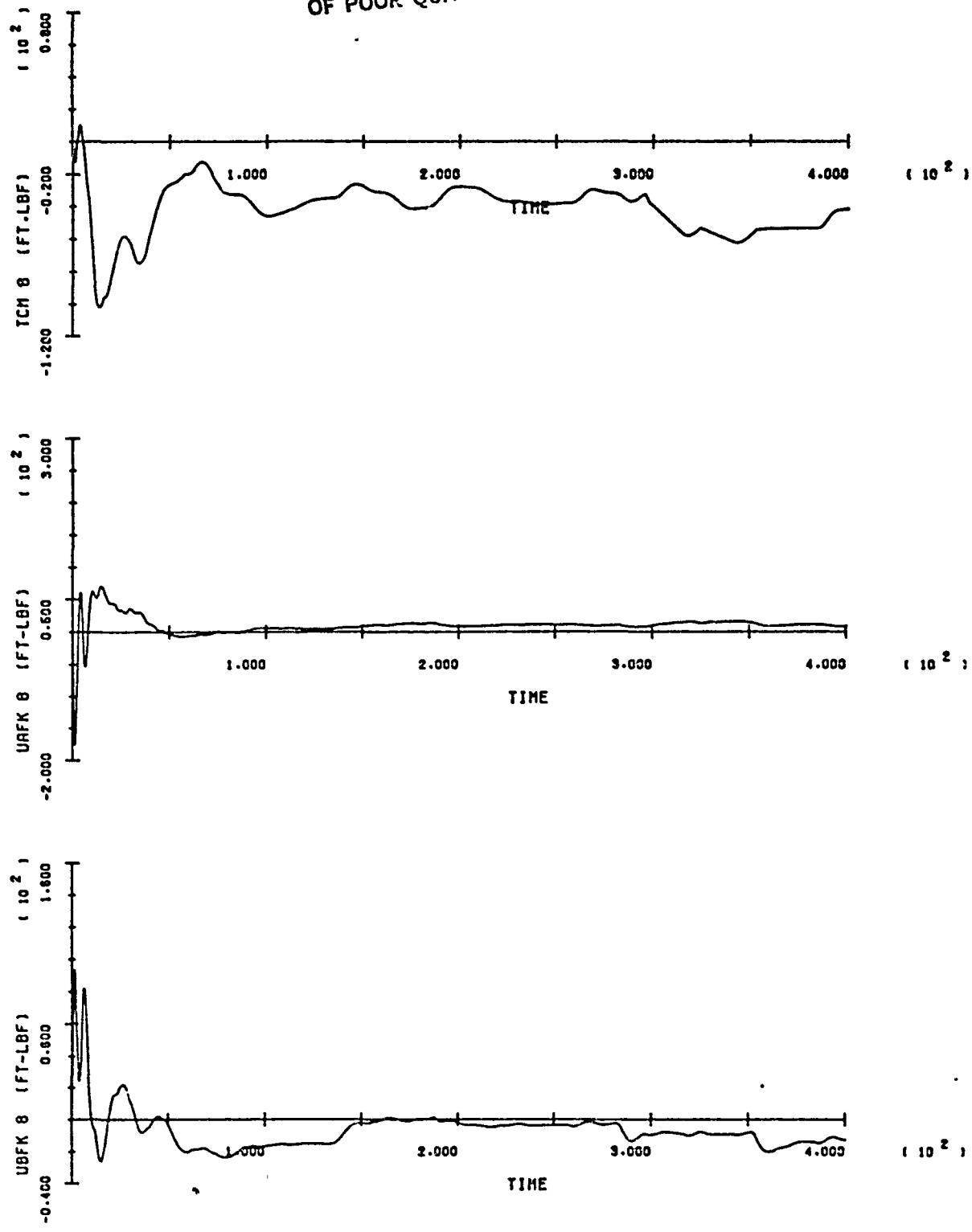


SOC/ORB BERTH - RUN 5

ORIGINAL PAGE IS
OF POOR QUALITY

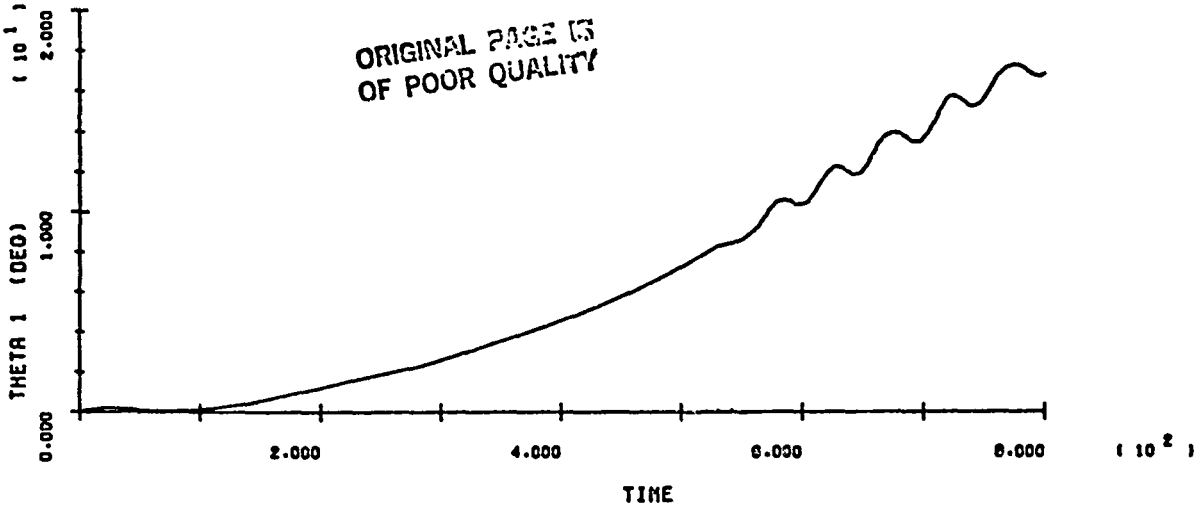


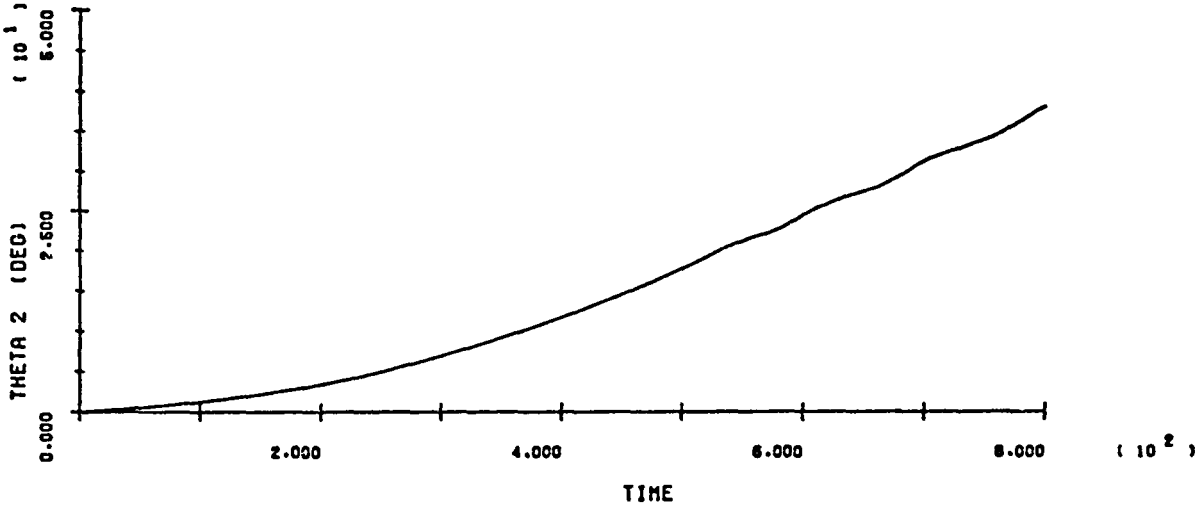


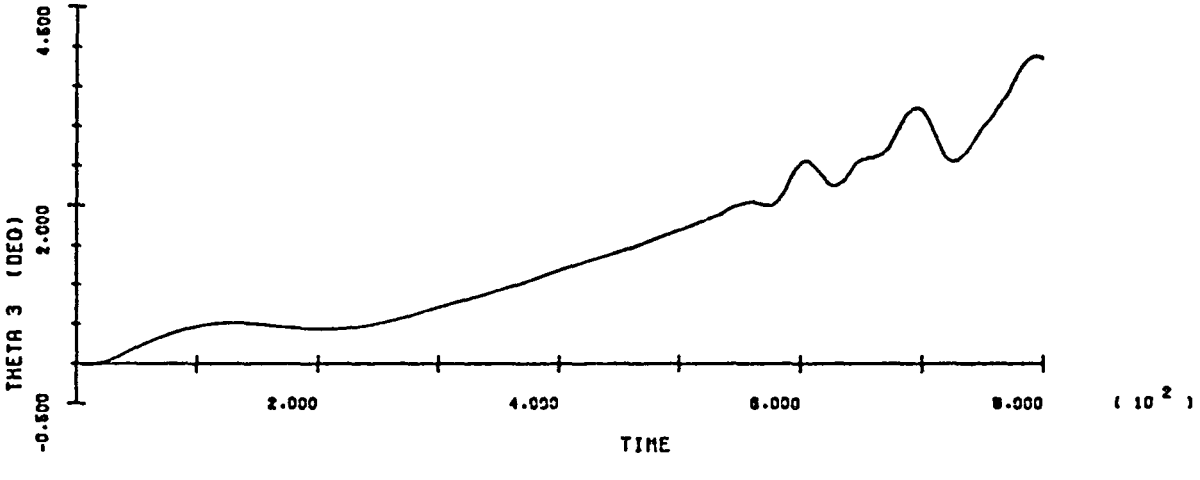


SOC/ORB BERTH - RUN 6

ORIGINAL PAGE IS
OF POOR QUALITY

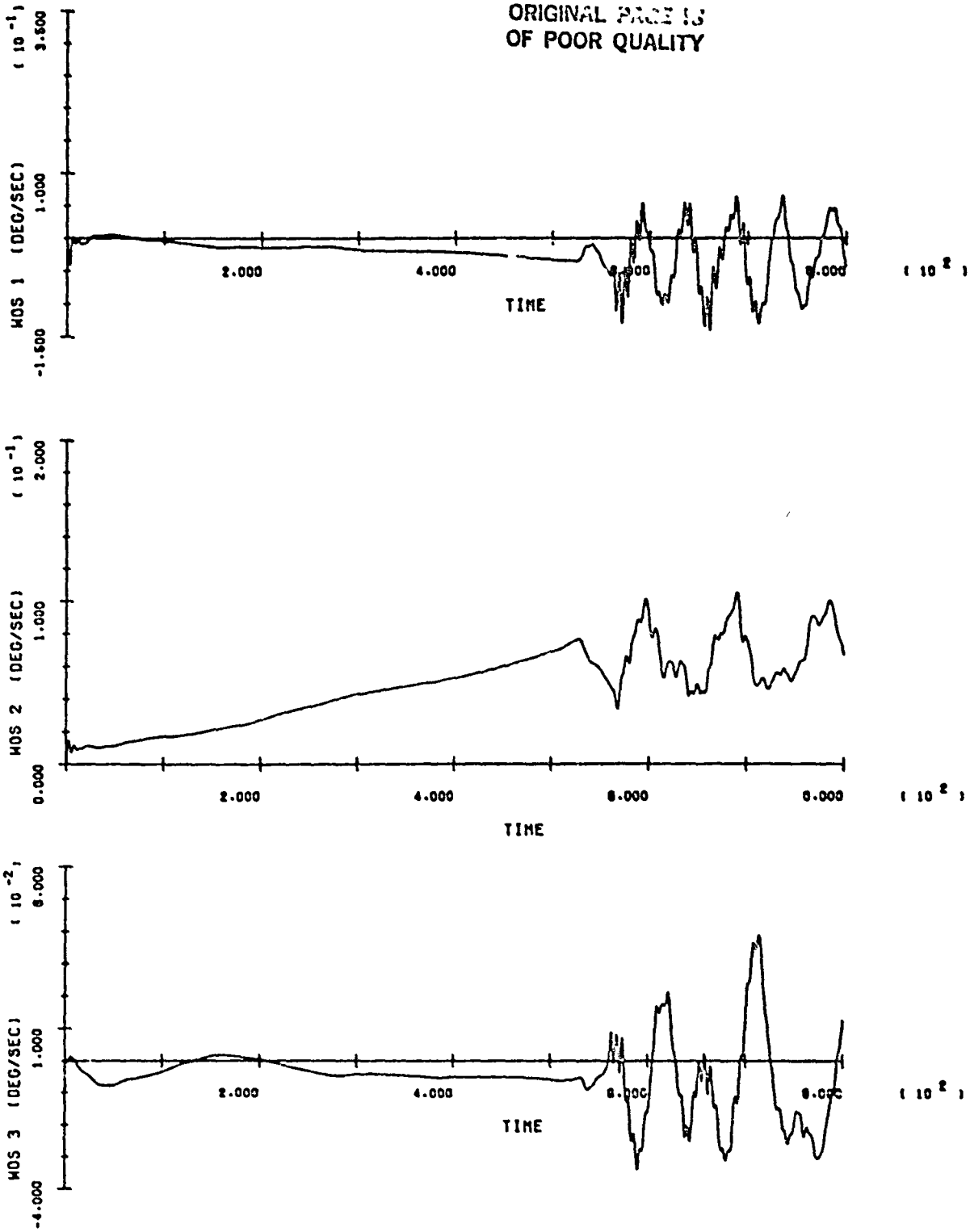


SOC/ORB BERTH - RUN 6

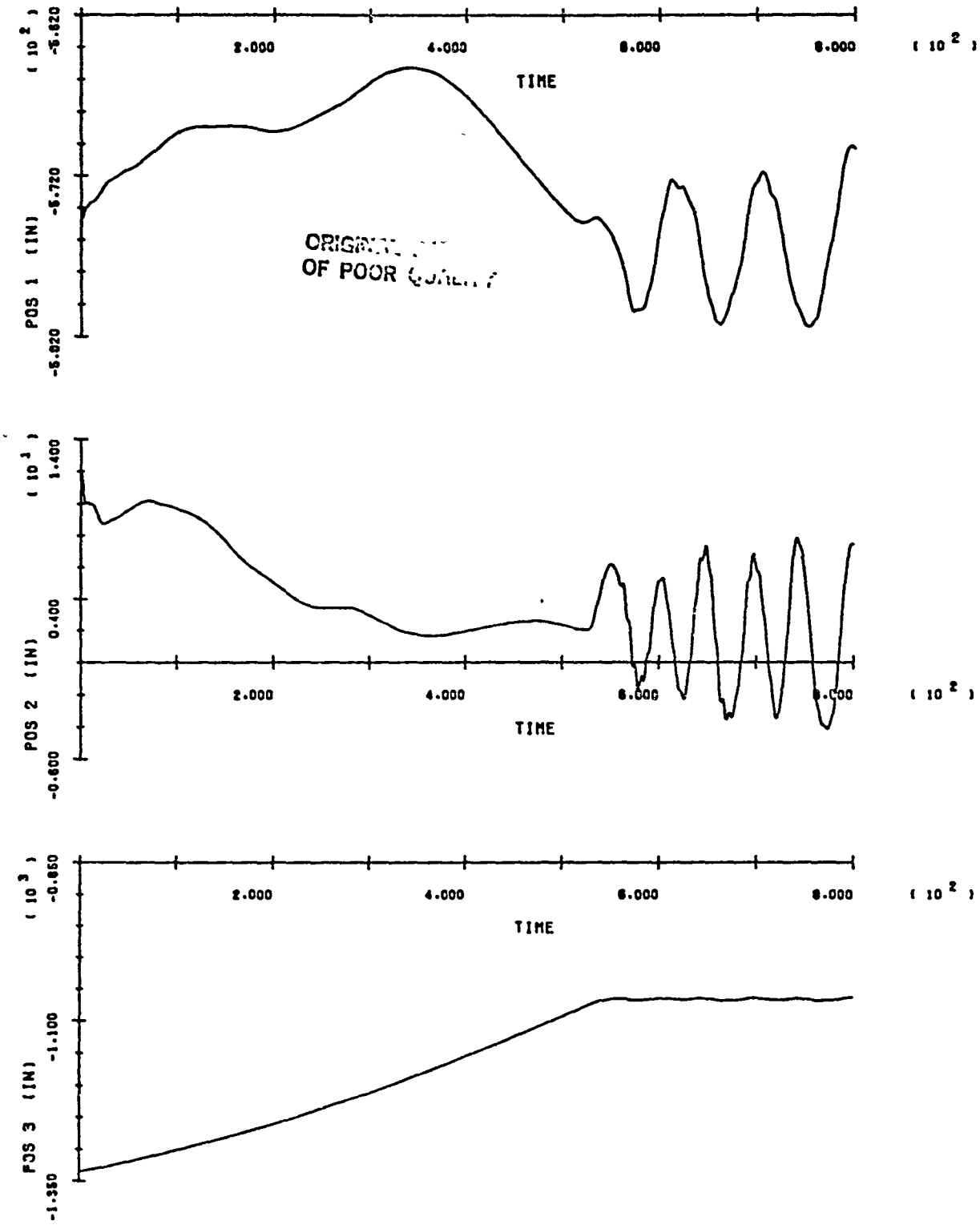


SOC/ORB BERTH - RUN 6

ORIGINAL PAGE IS
OF POOR QUALITY

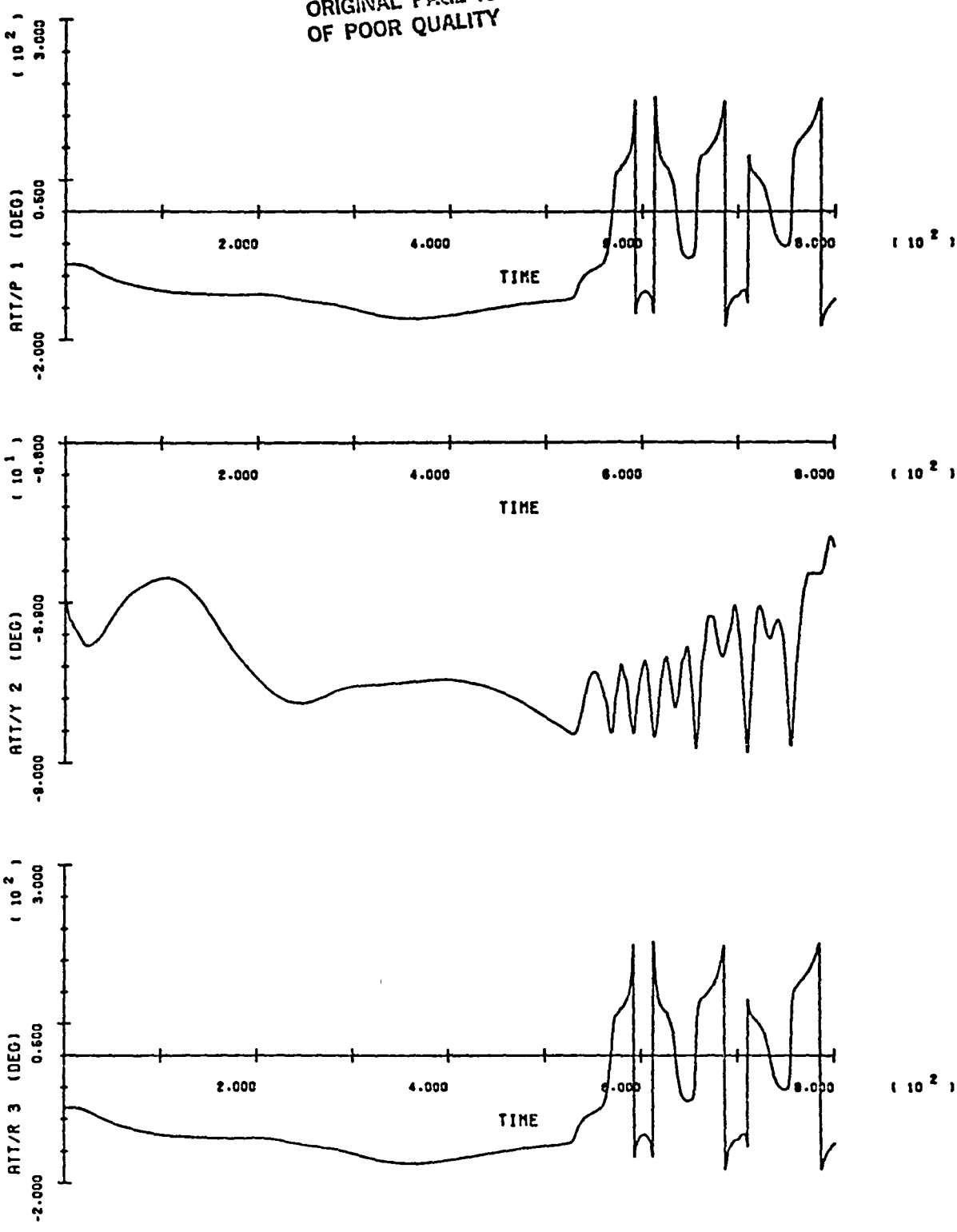


SOC/ORB BERTH - RUN 6

ORIGINAL PAGE IS
OF POOR QUALITY

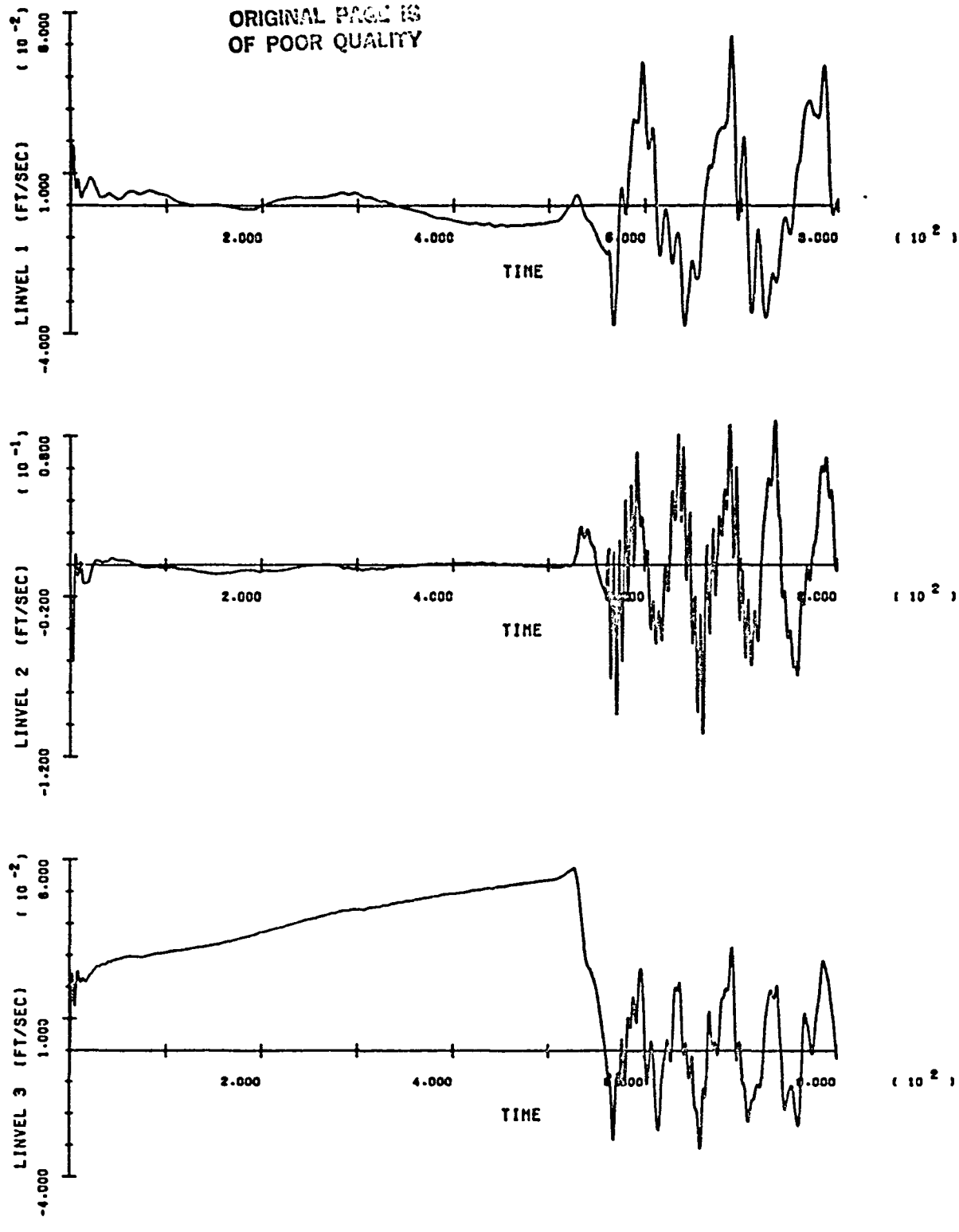


SOC/ORB BERTH - RUN 6

ORIGINAL PAGE IS
OF POOR QUALITY

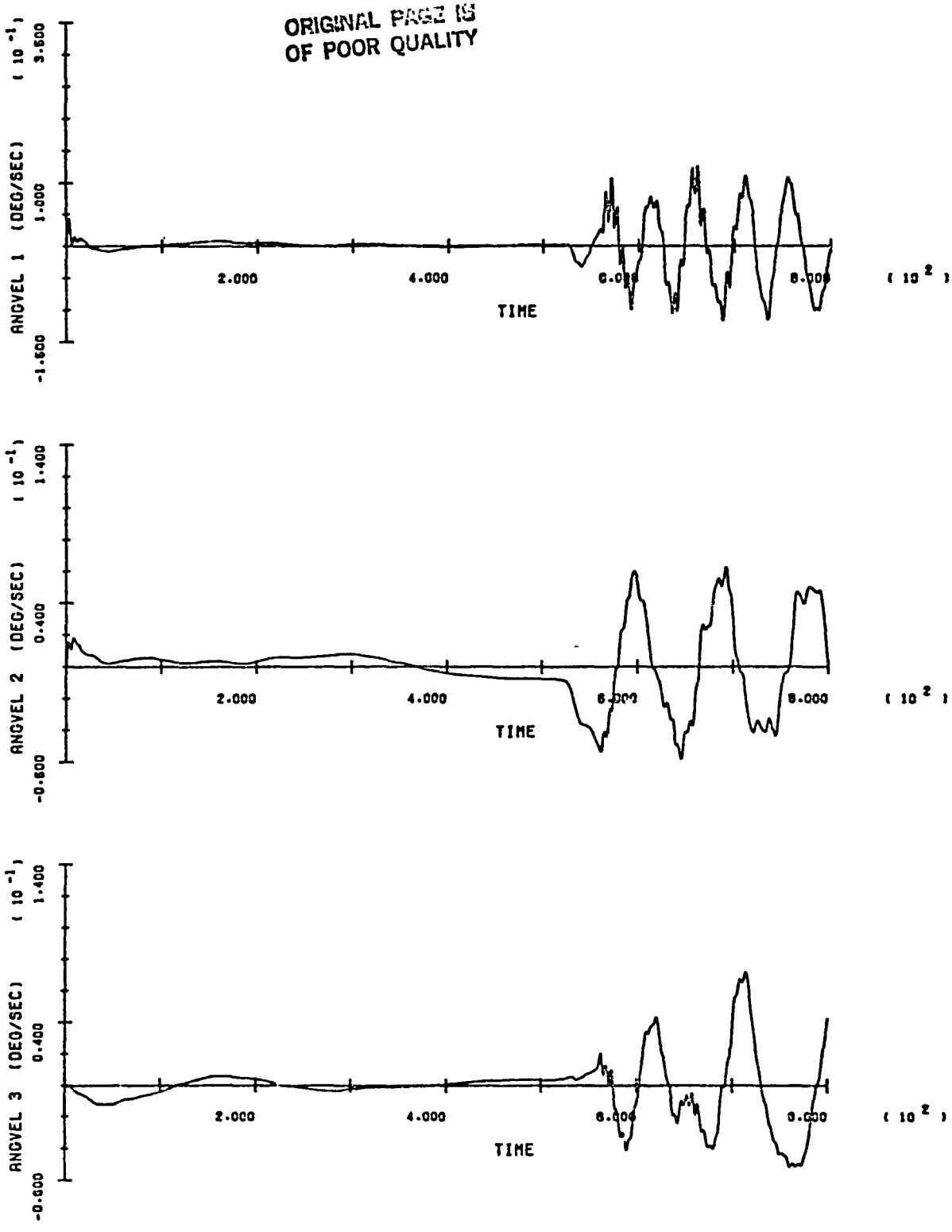


SOC/ORB BERTH - RUN 6

ORIGINAL PAGE IS
OF POOR QUALITY

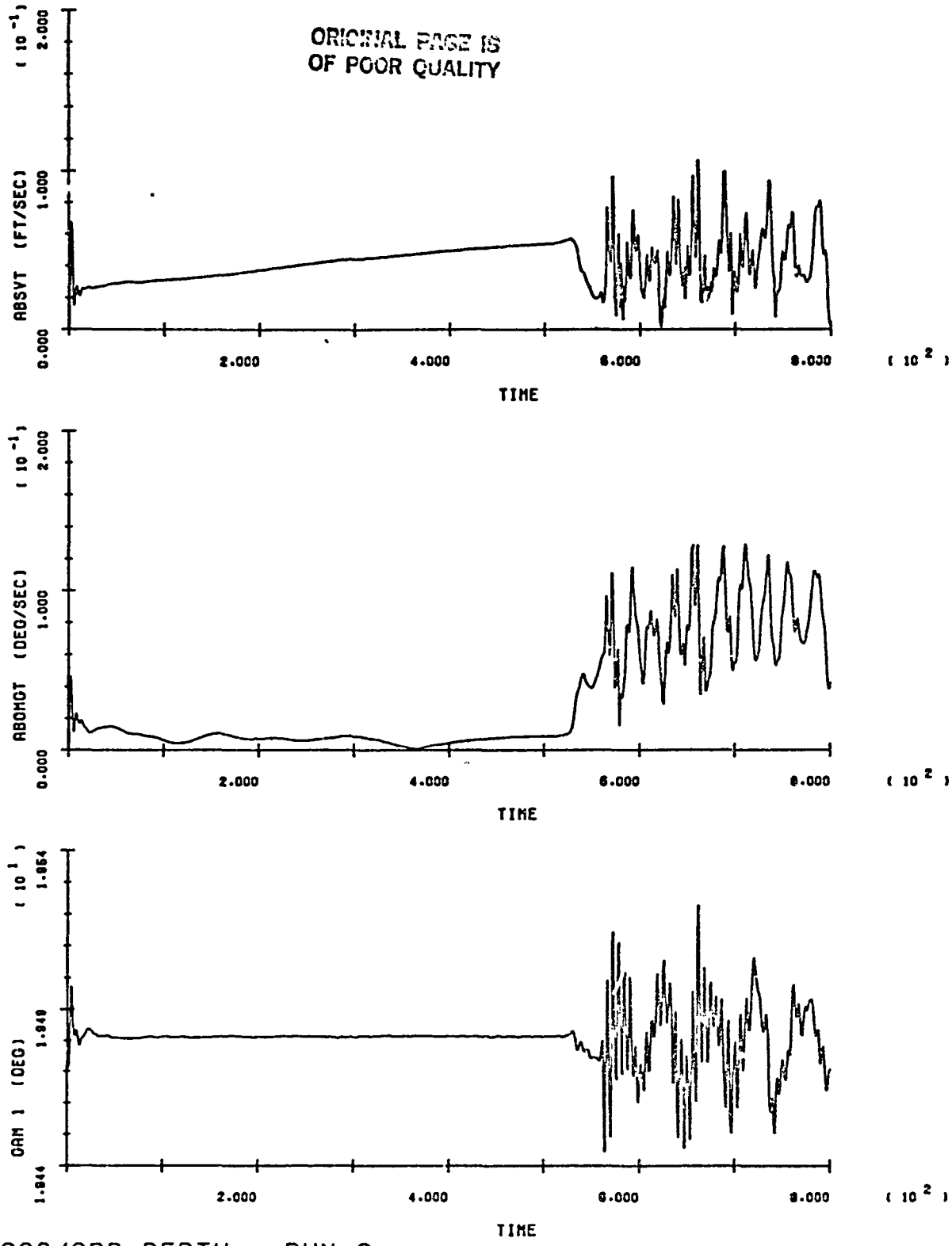


SOC/ORB BERTH - RUN 6

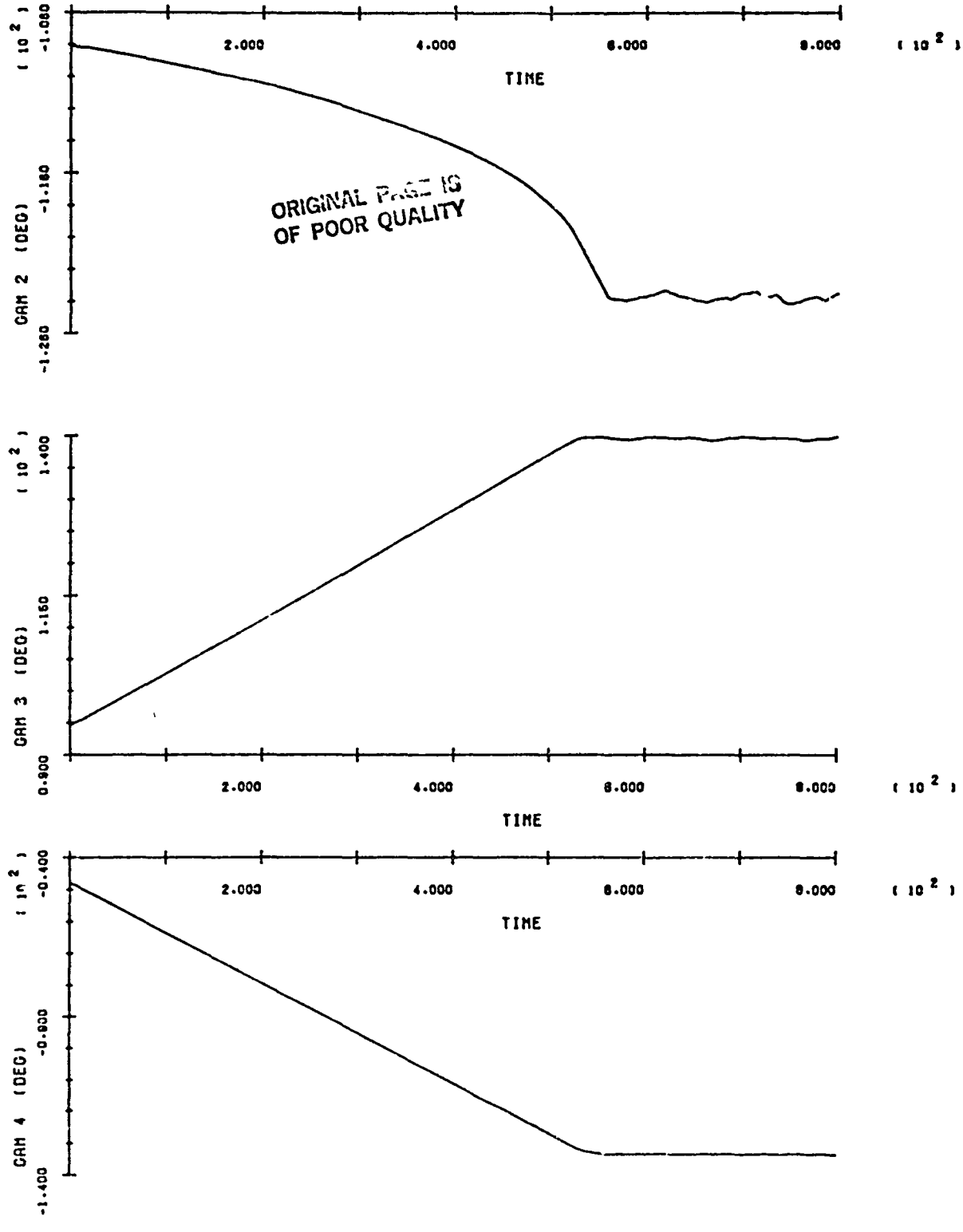


SOC/ORB BERTH - RUN 6

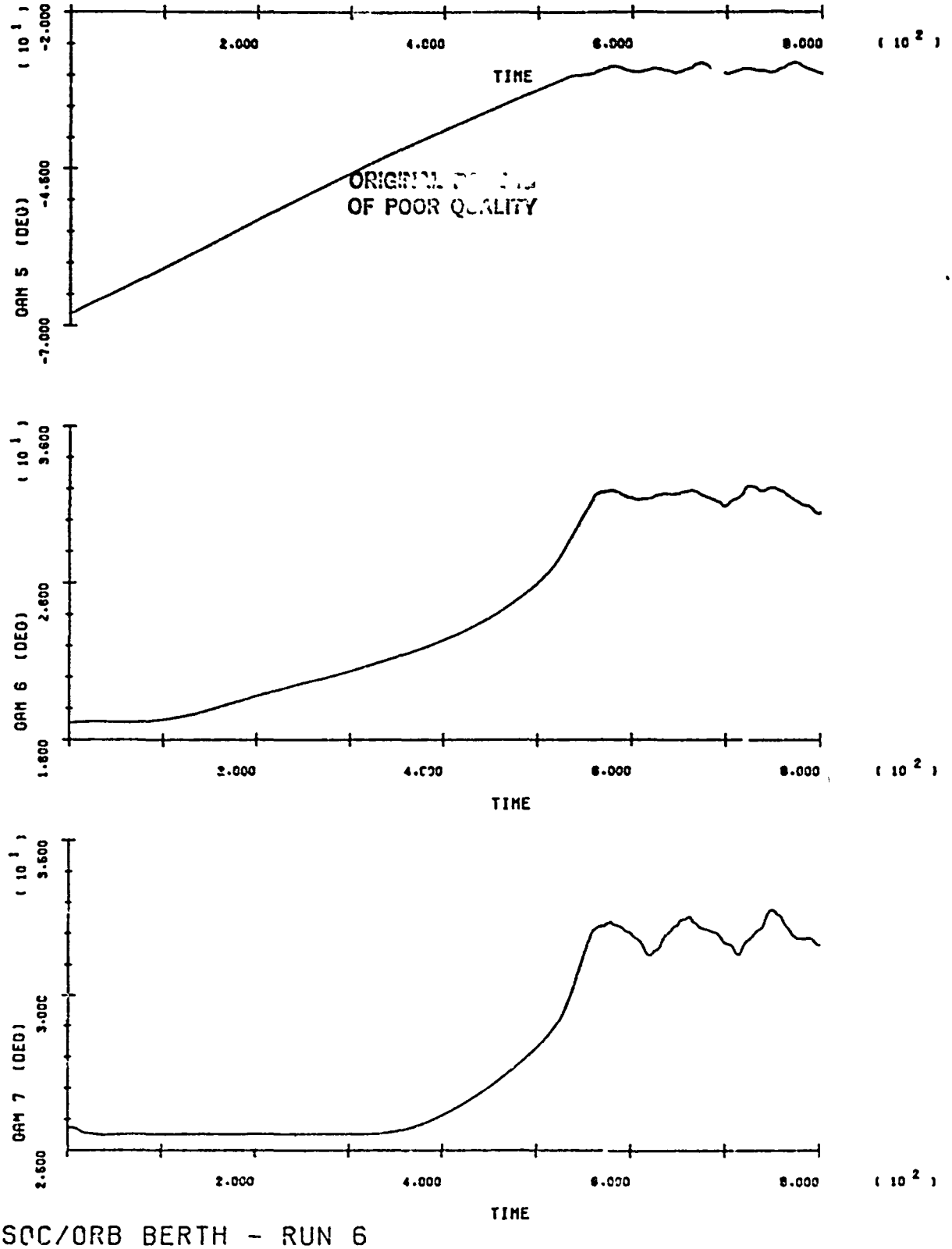


SOC/ORB BERTH - RUN 6

ORIGINAL PAGE IS
OF POOR QUALITY

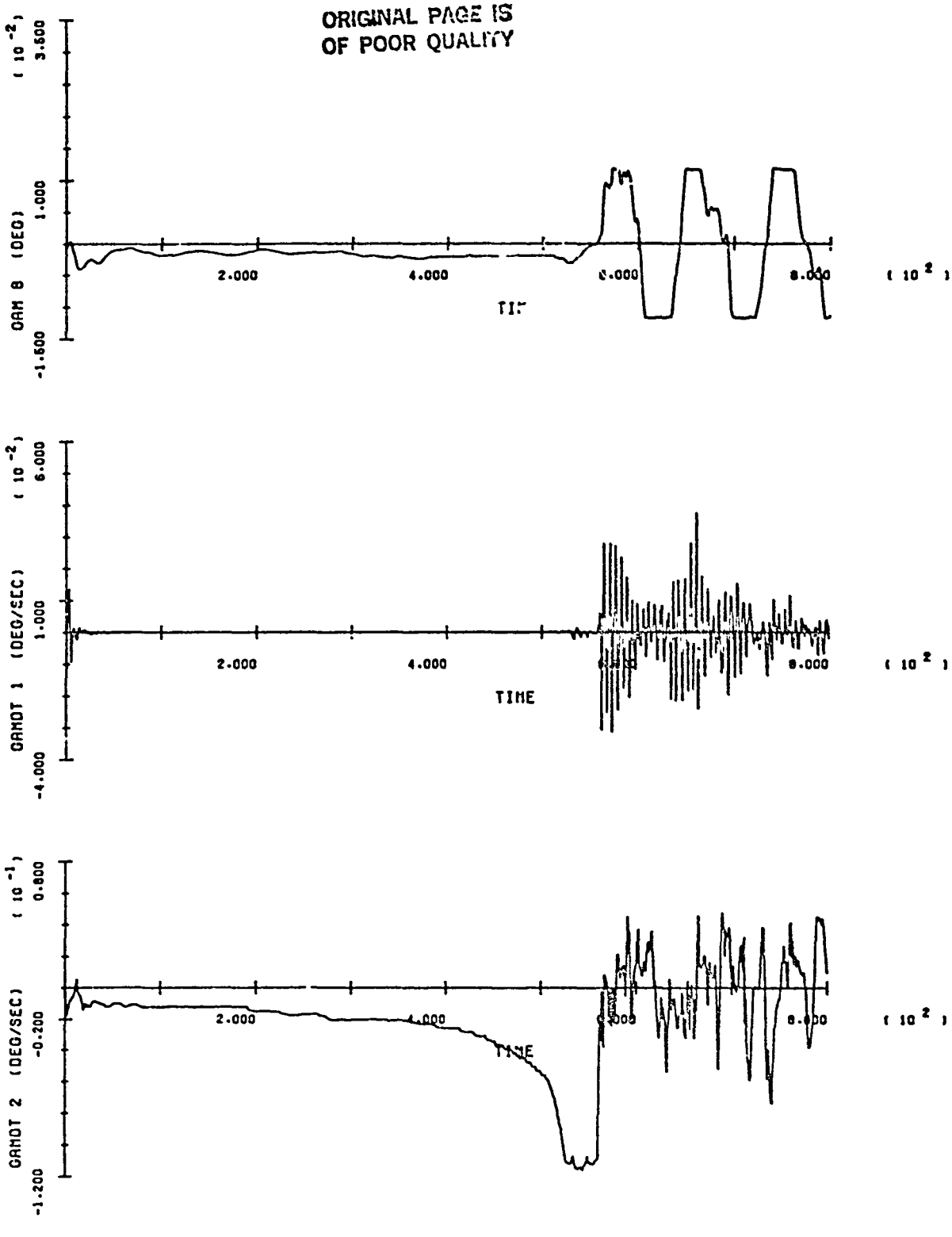


SOC/ORB RERTH - RUN 6

ORIGINAL PAGE IS
OF POOR QUALITY

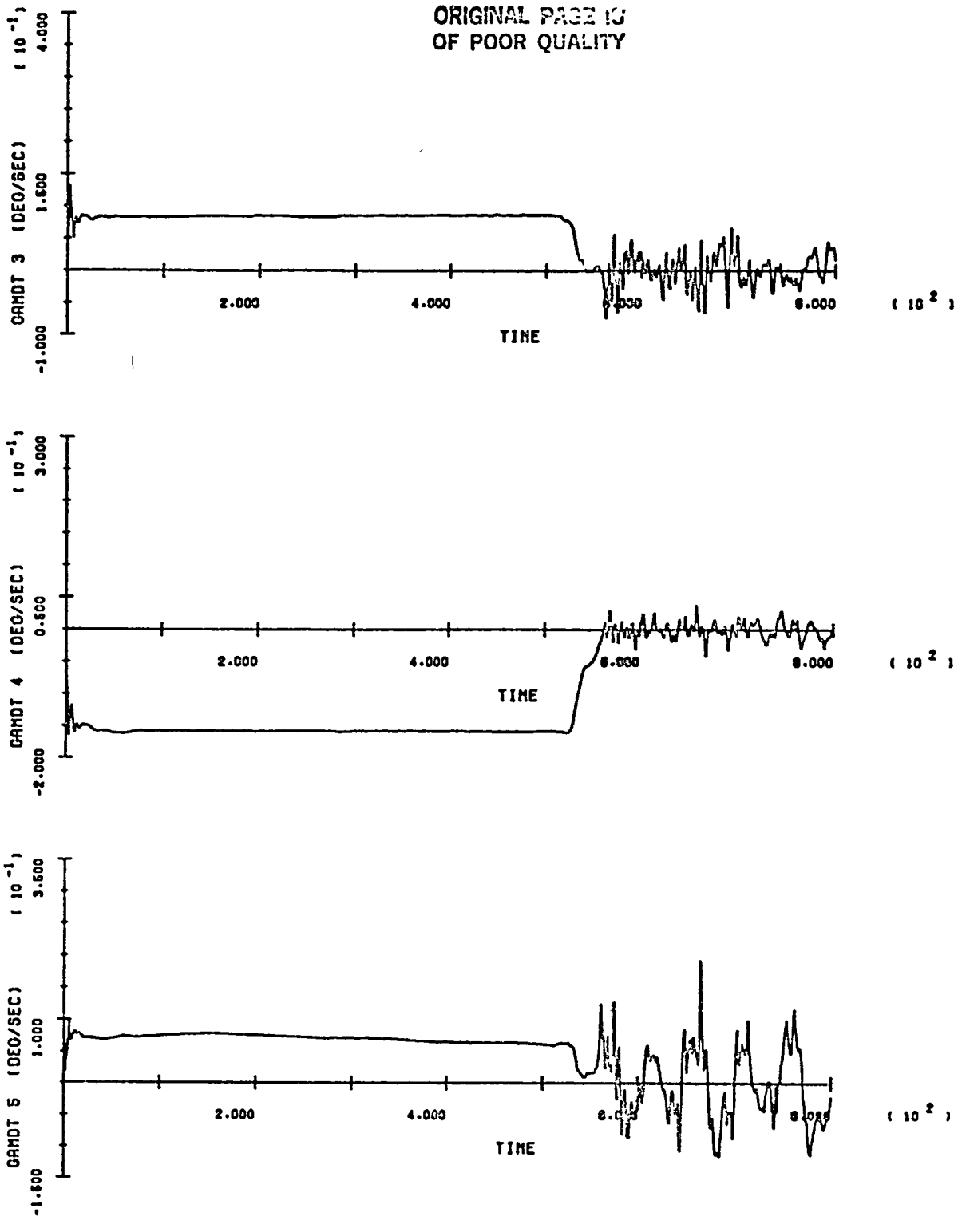


SOC/ORB BERTH - RUN 6

ORIGINAL PAGE IS
OF POOR QUALITY

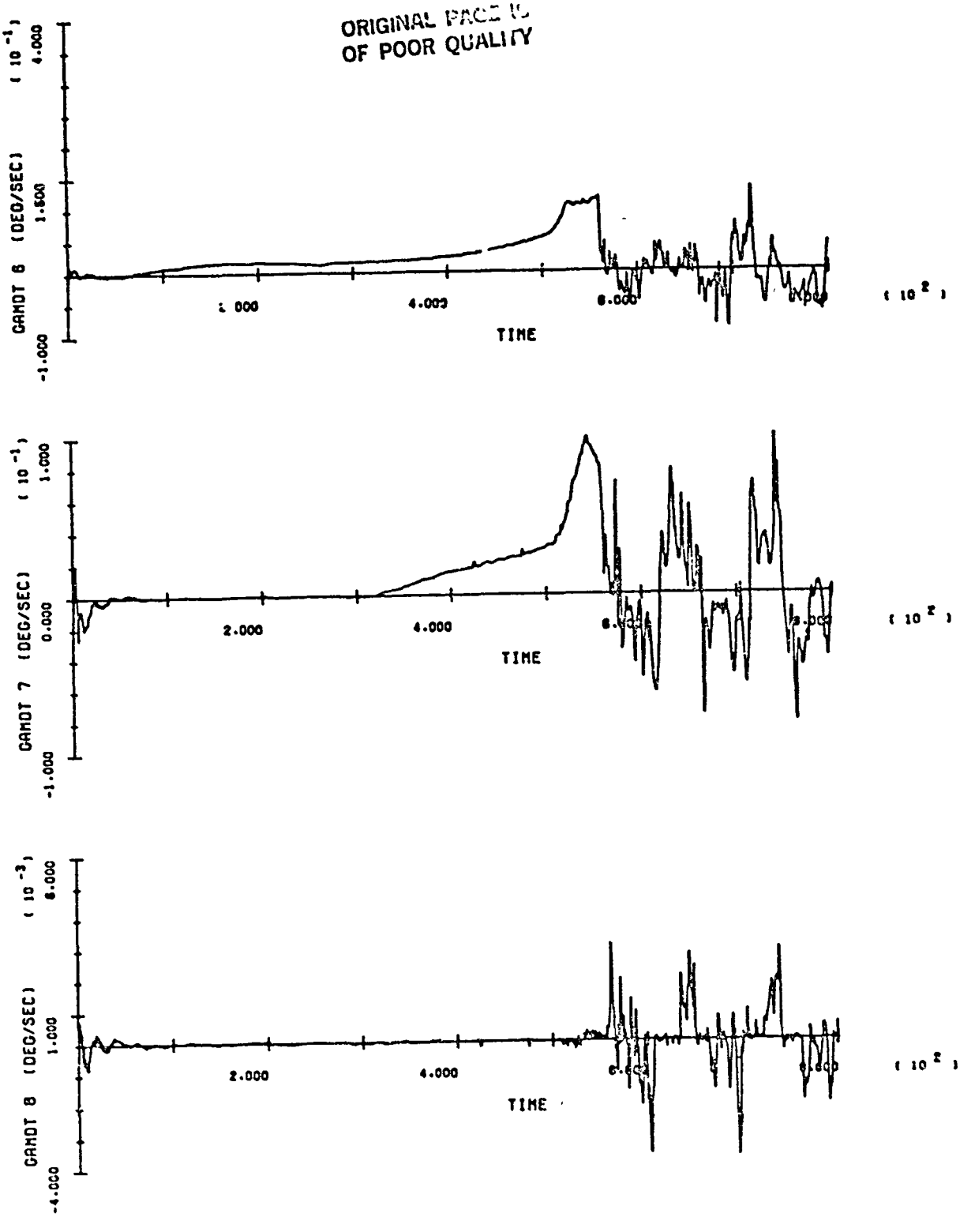


SOC/ORB BERTH - RUN 6

ORIGINAL PAGE IS
OF POOR QUALITY

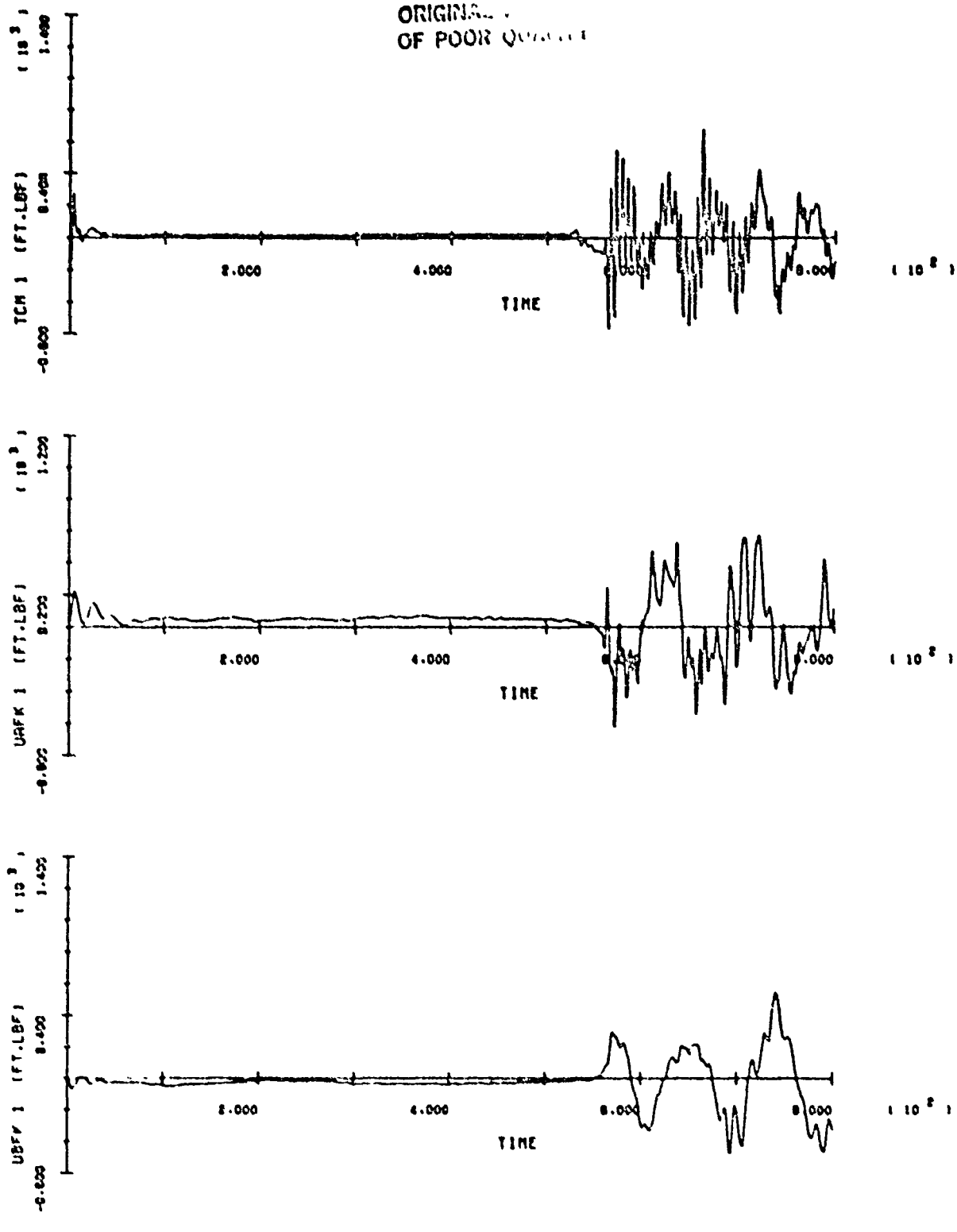


SOC/ORB BERTH - RUN 6

ORIGINAL PAGE IS
OF POOR QUALITY

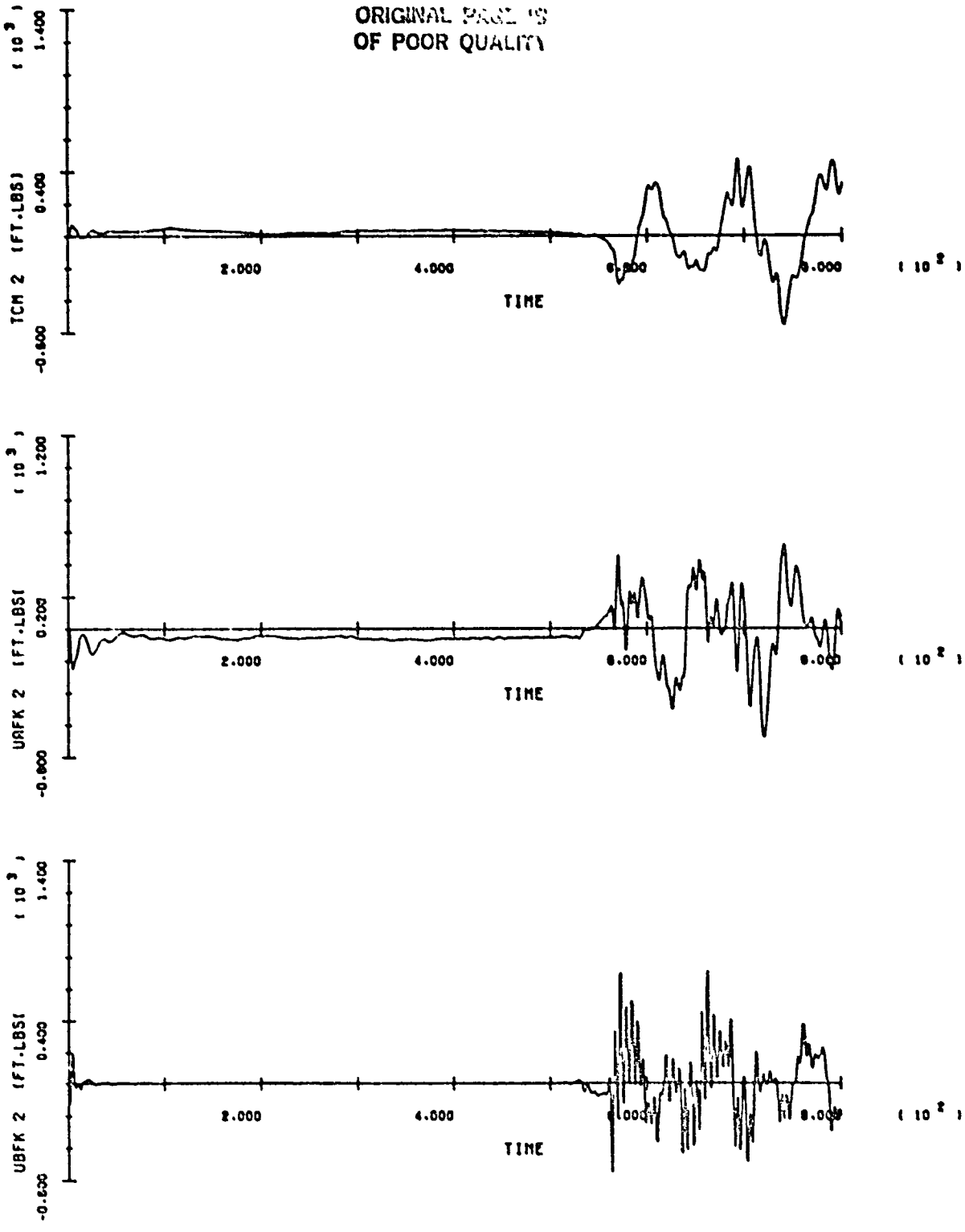


SOC/ORB BERTH - RUN 6

ORIGINAL
OF POOR QUALITY

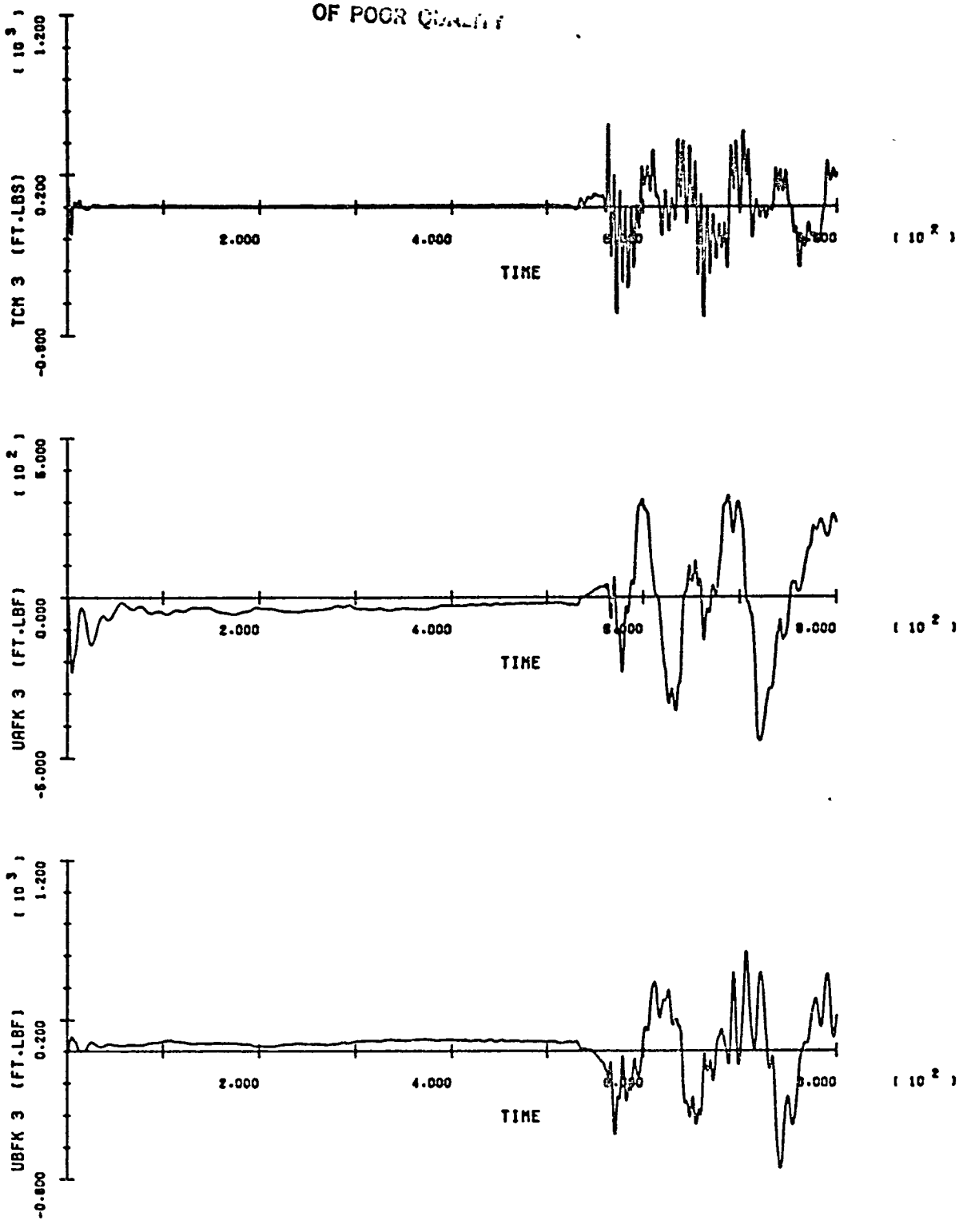


SOC/ORB BERTH - RUN 6

ORIGINAL PAGE IS
OF POOR QUALITY

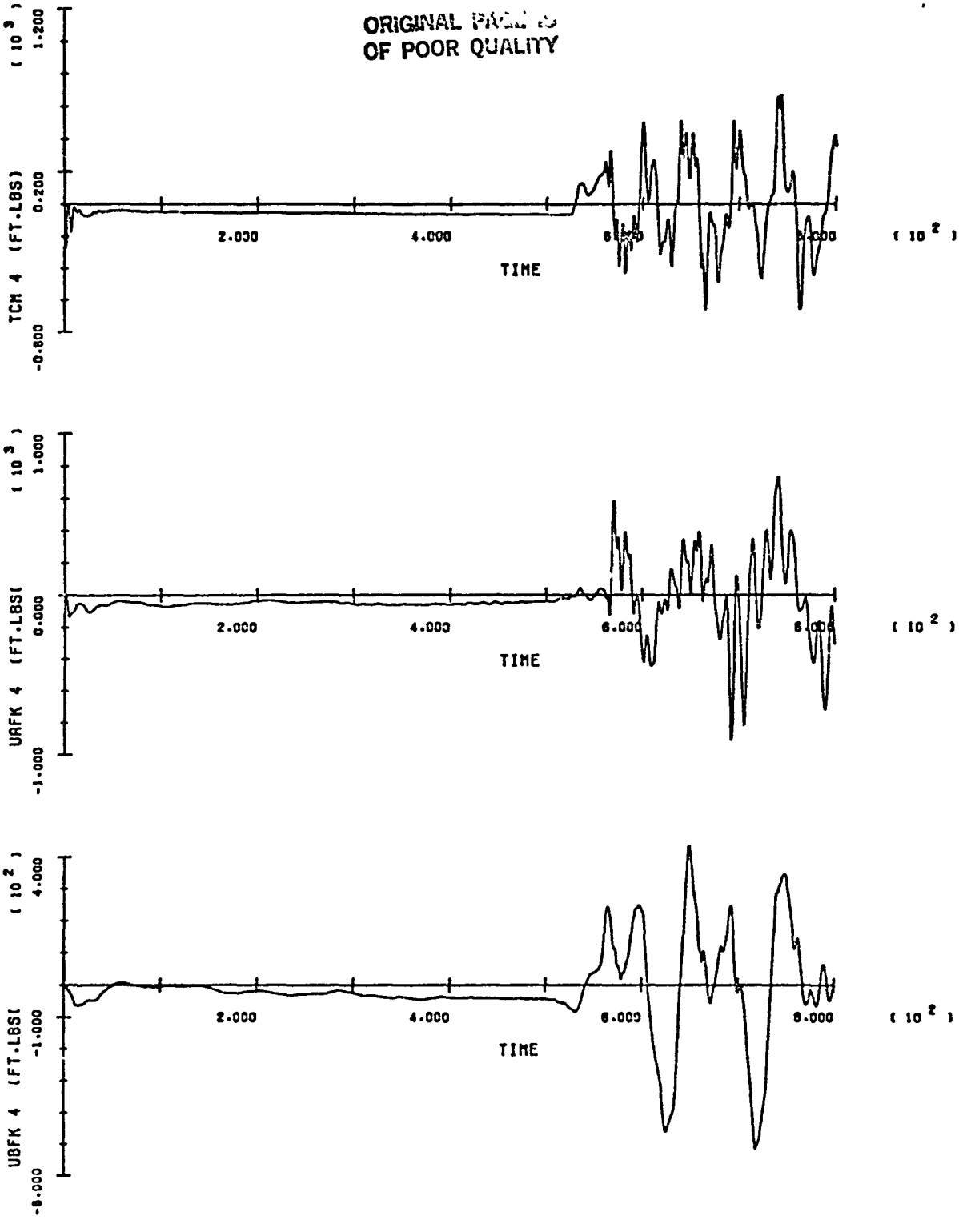


SOC/ORB BERTH - RUN 6

ORIGINAL PAGE IS
OF POOR QUALITY

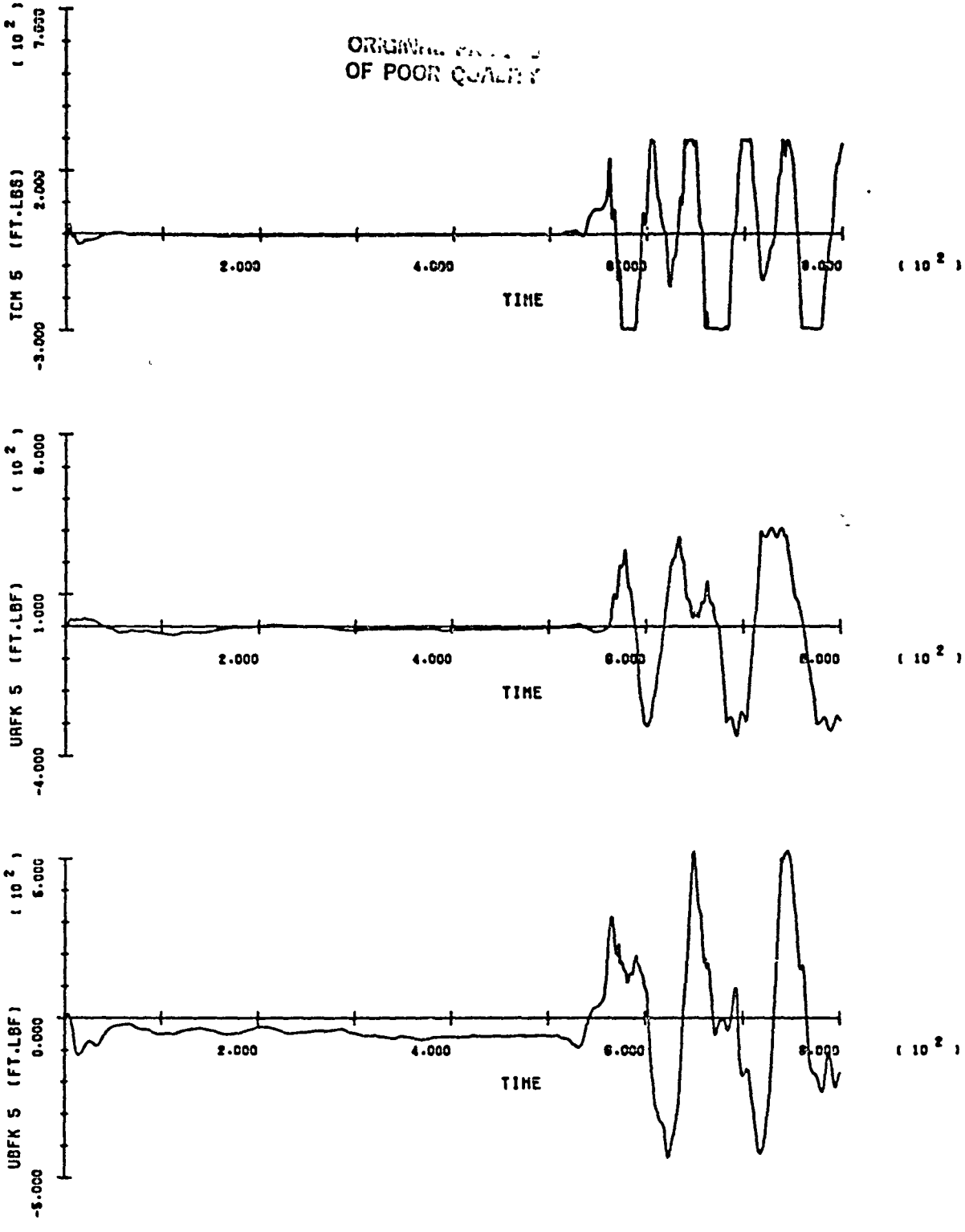


SOC/ORB BERTH - RUN 6

ORIGINAL PAGE IS
OF POOR QUALITY

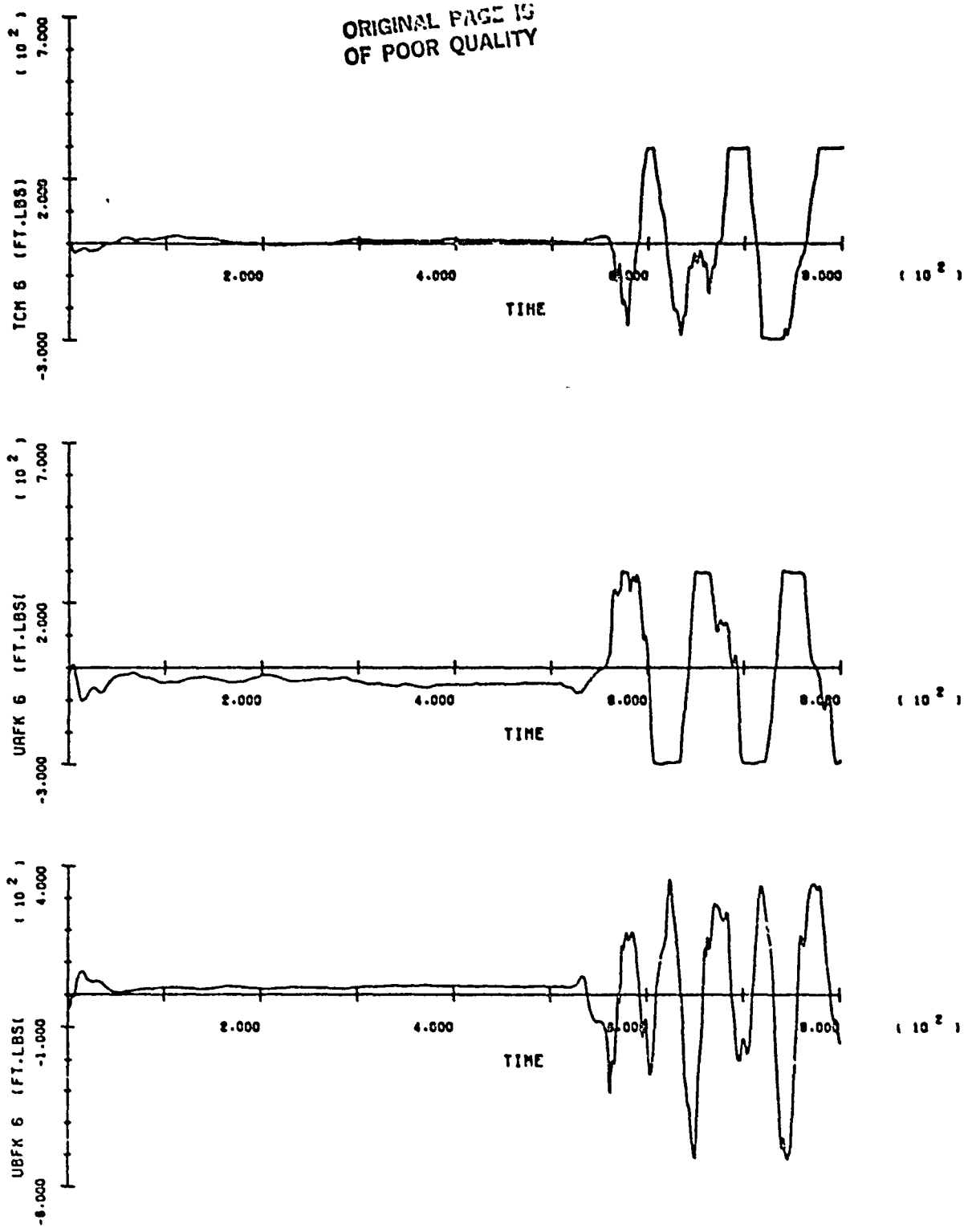


SOC/ORB BERTH - RUN 6

ORIGINAL PAGE IS
OF POOR QUALITY

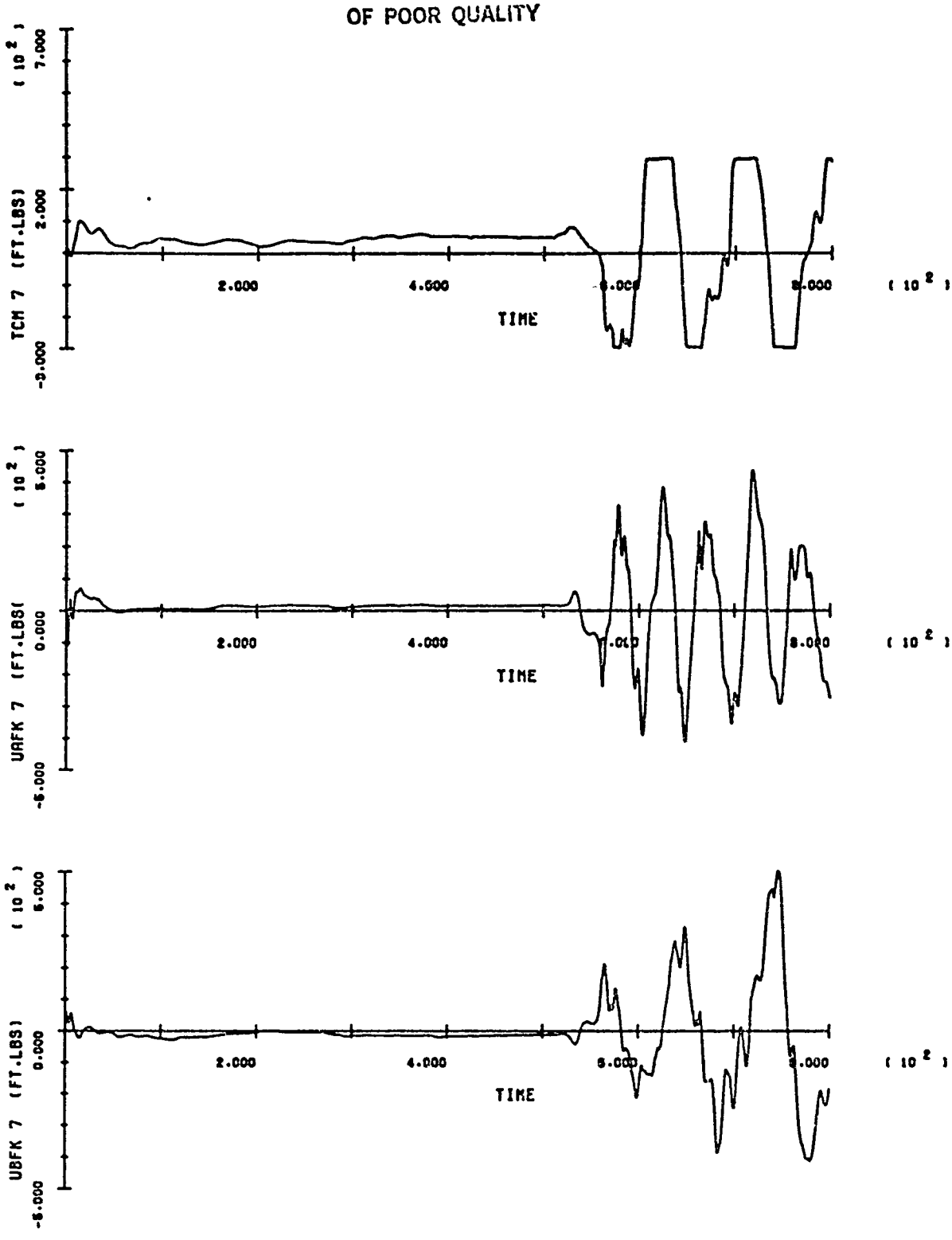


SOC/ORB BERTH - RUN 6

ORIGINAL PAGE IS
OF POOR QUALITY

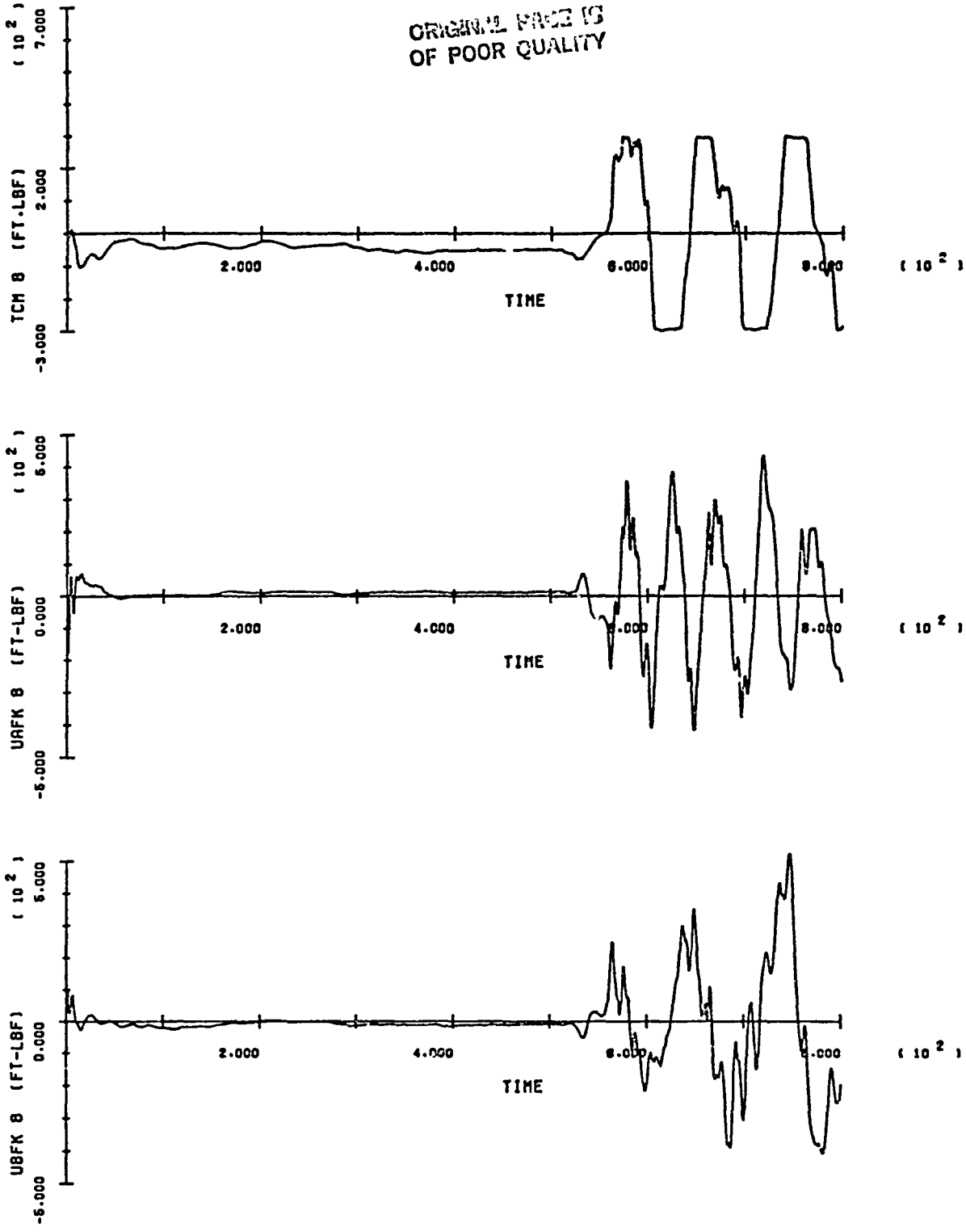


SOC/ORB BERTH - RUN 6

ORIGINAL PAGE IS
OF POOR QUALITY

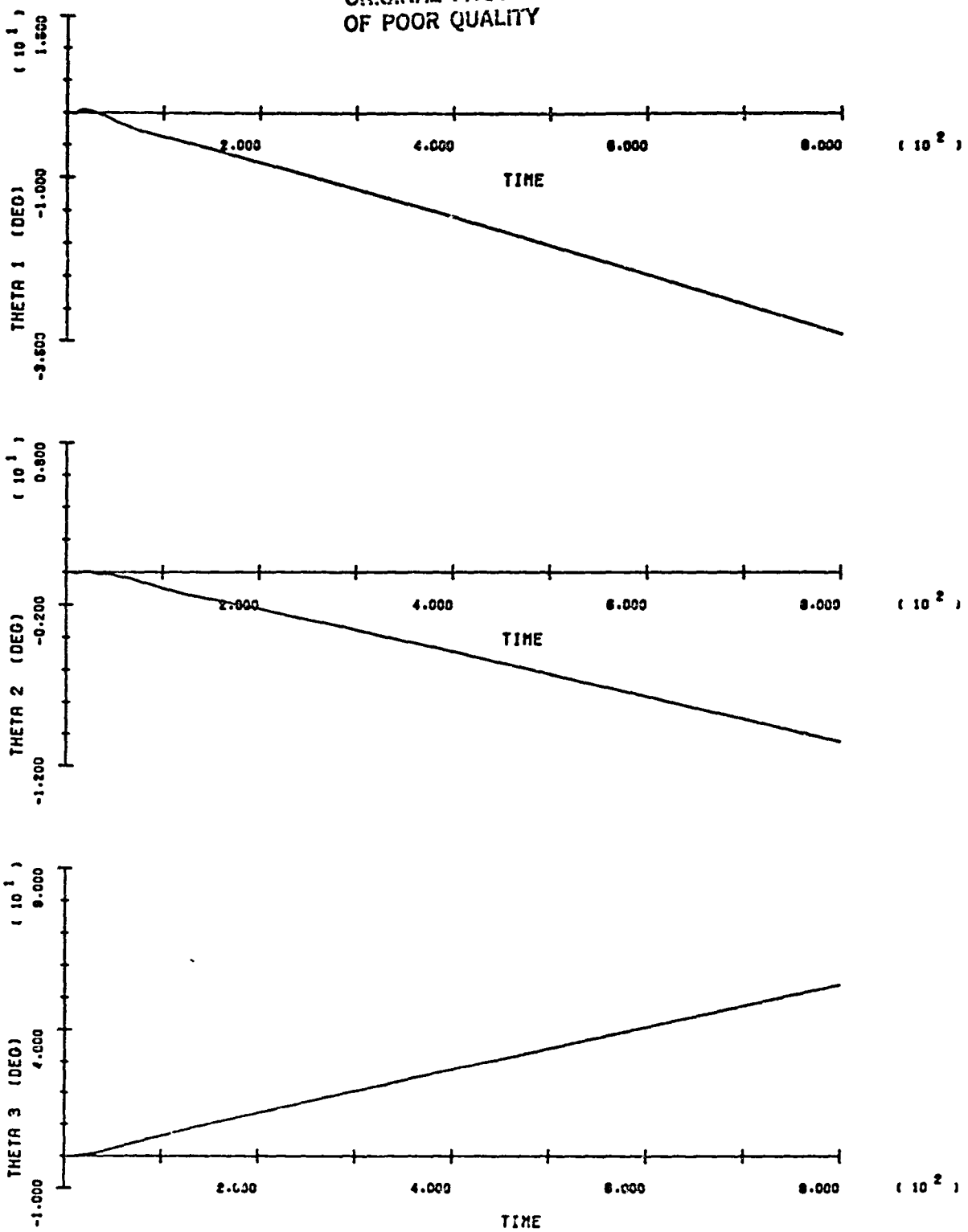


SOC/ORB BERTH - RUN 7

ORIGINAL PAGE IS
OF POOR QUALITY

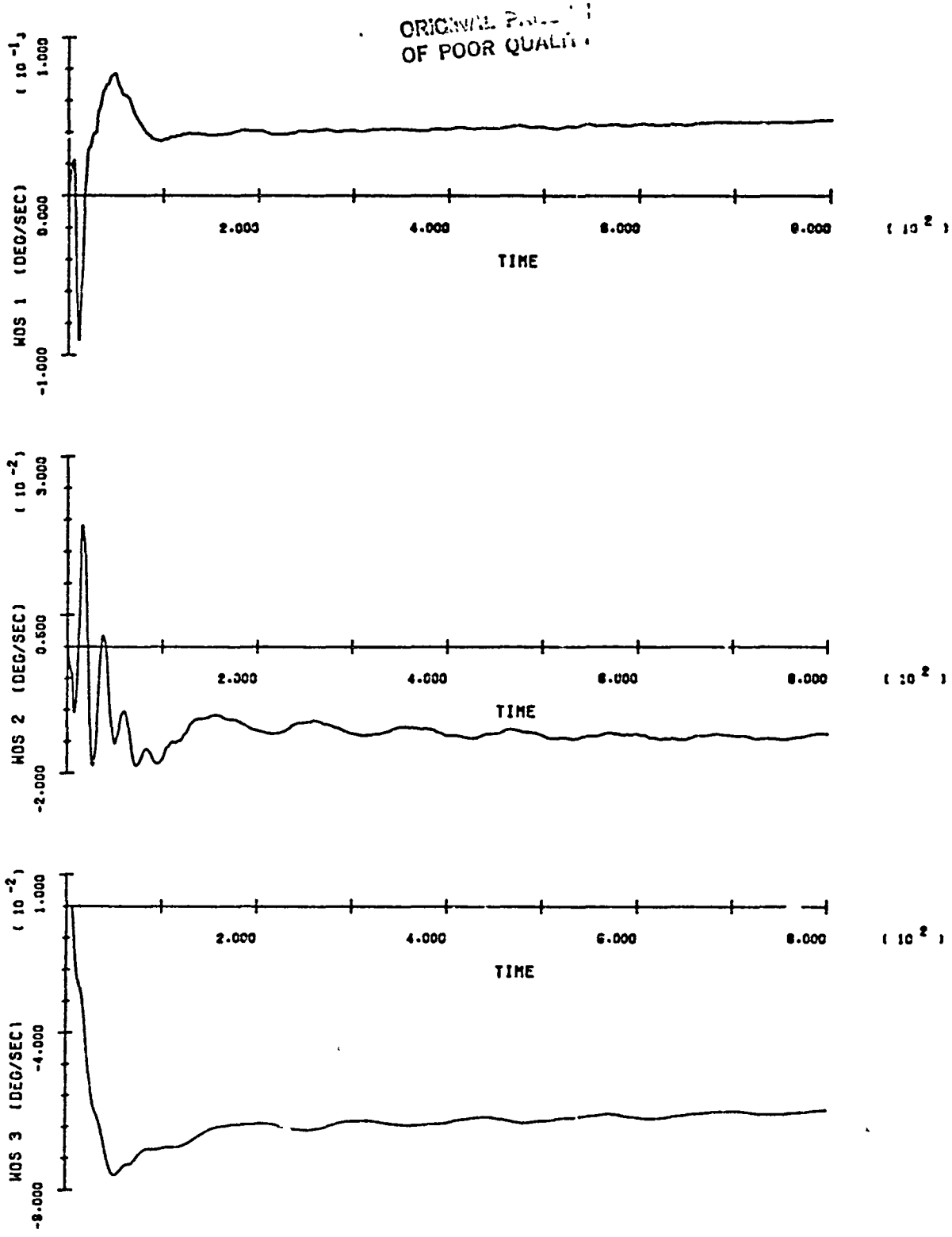


SOC/ORB BERTH - RUN 7

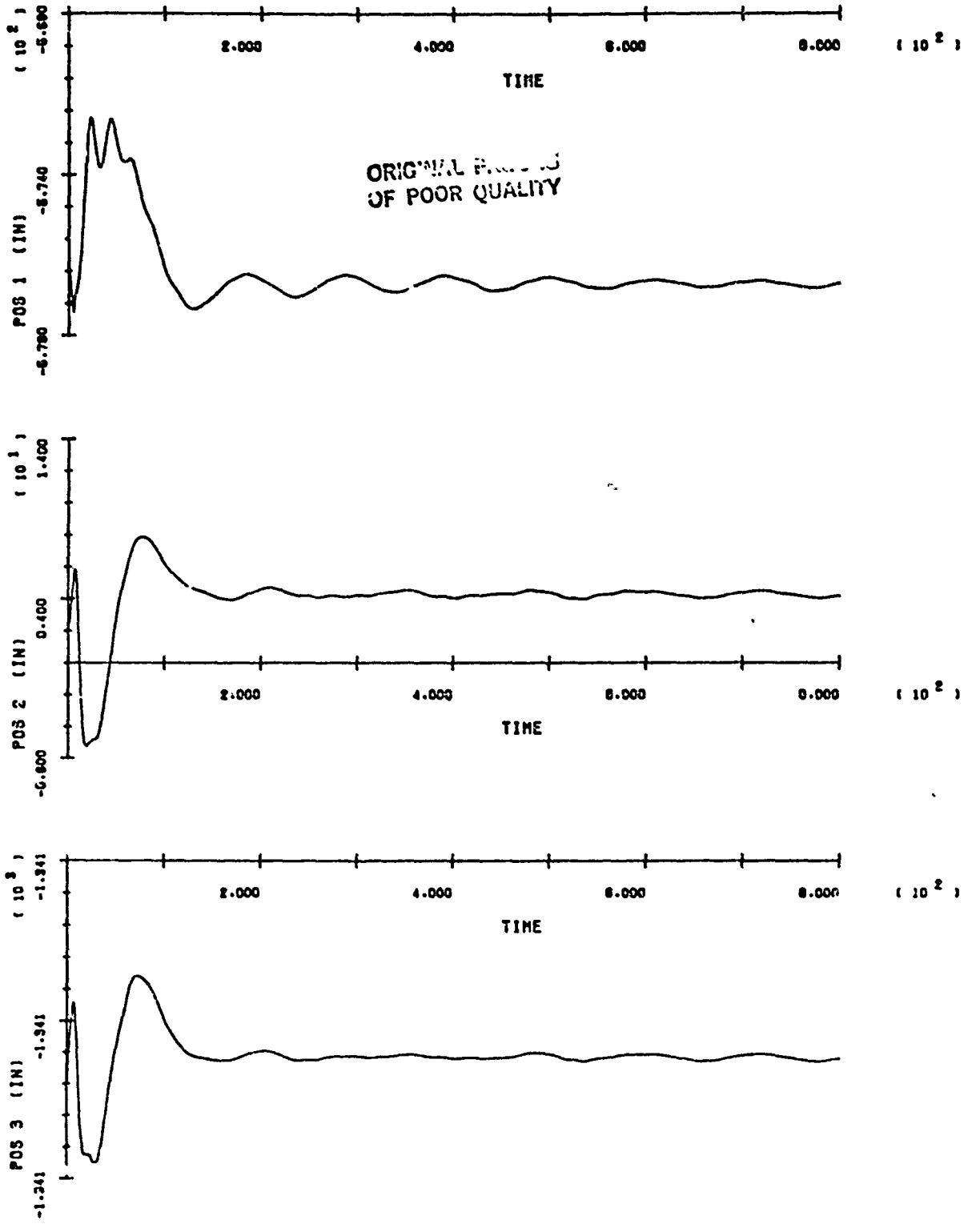


SOC/ORB BERTH - RUN 7

ORIGINAL PAGE IS
OF POOR QUALITY

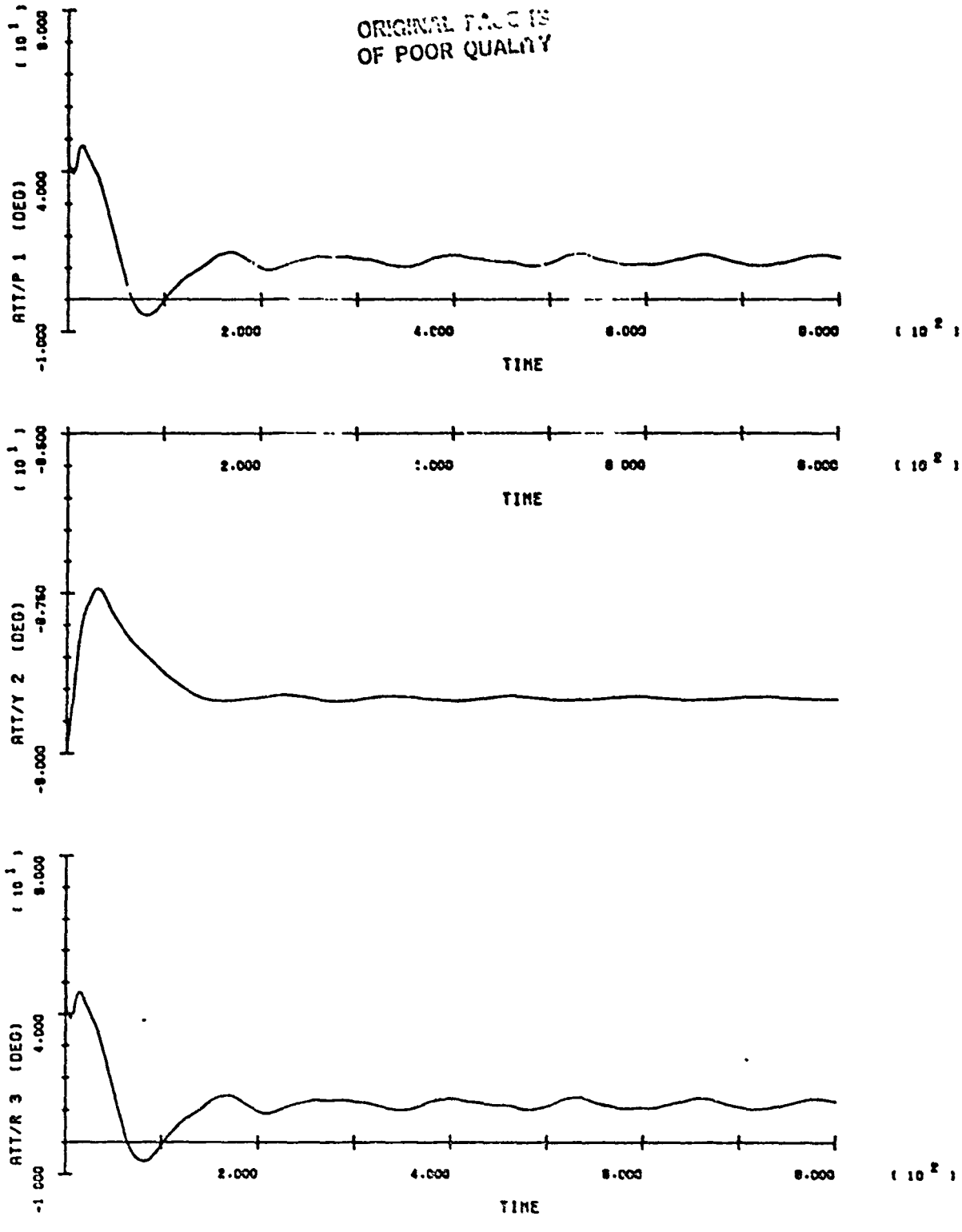


SOC/ORB BERTH - RUN 7

ORIGINAL PAGE IS
OF POOR QUALITY

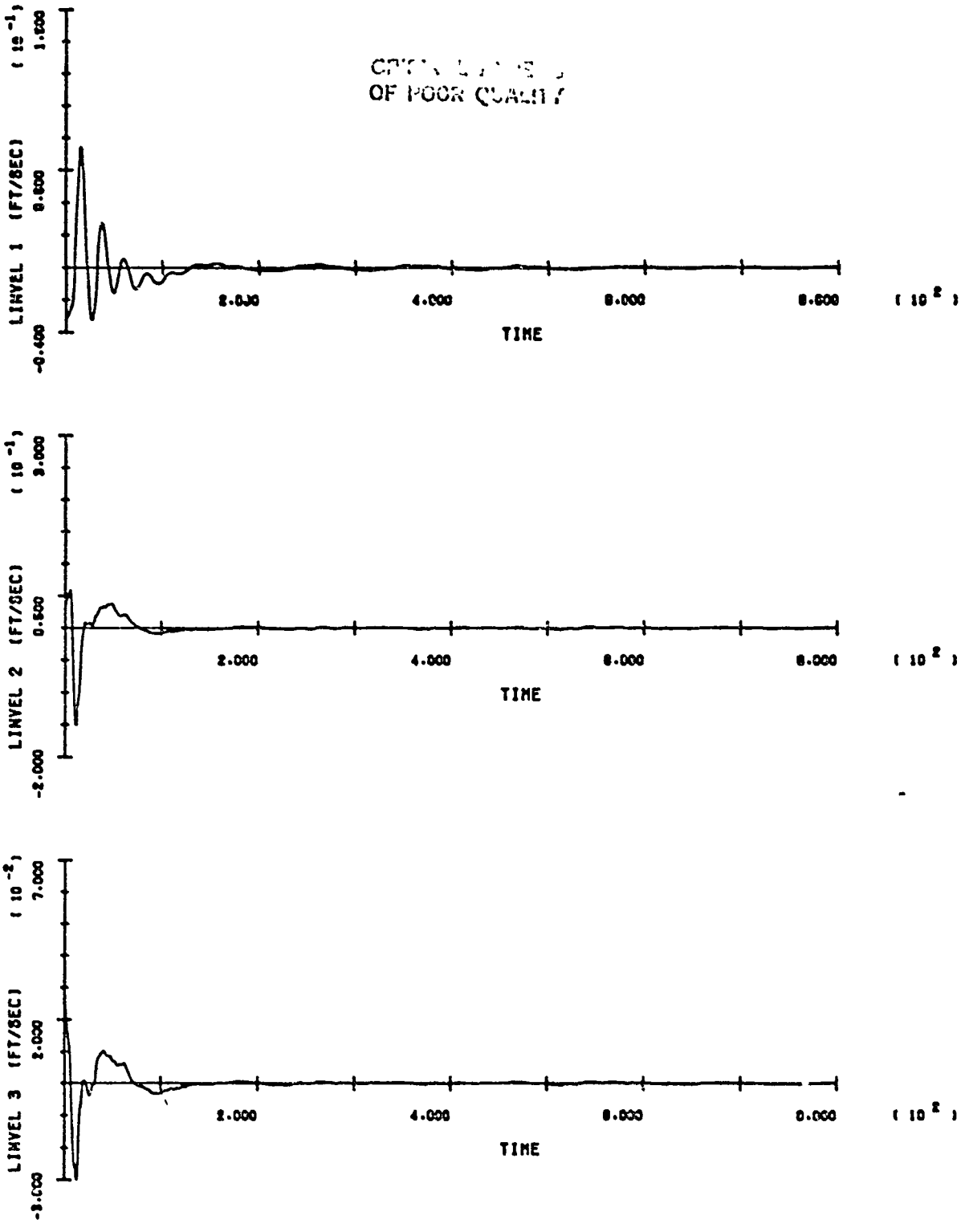


SOC/ORB BERTH - RUN 7

ORIGINAL PAGE IS
OF POOR QUALITY

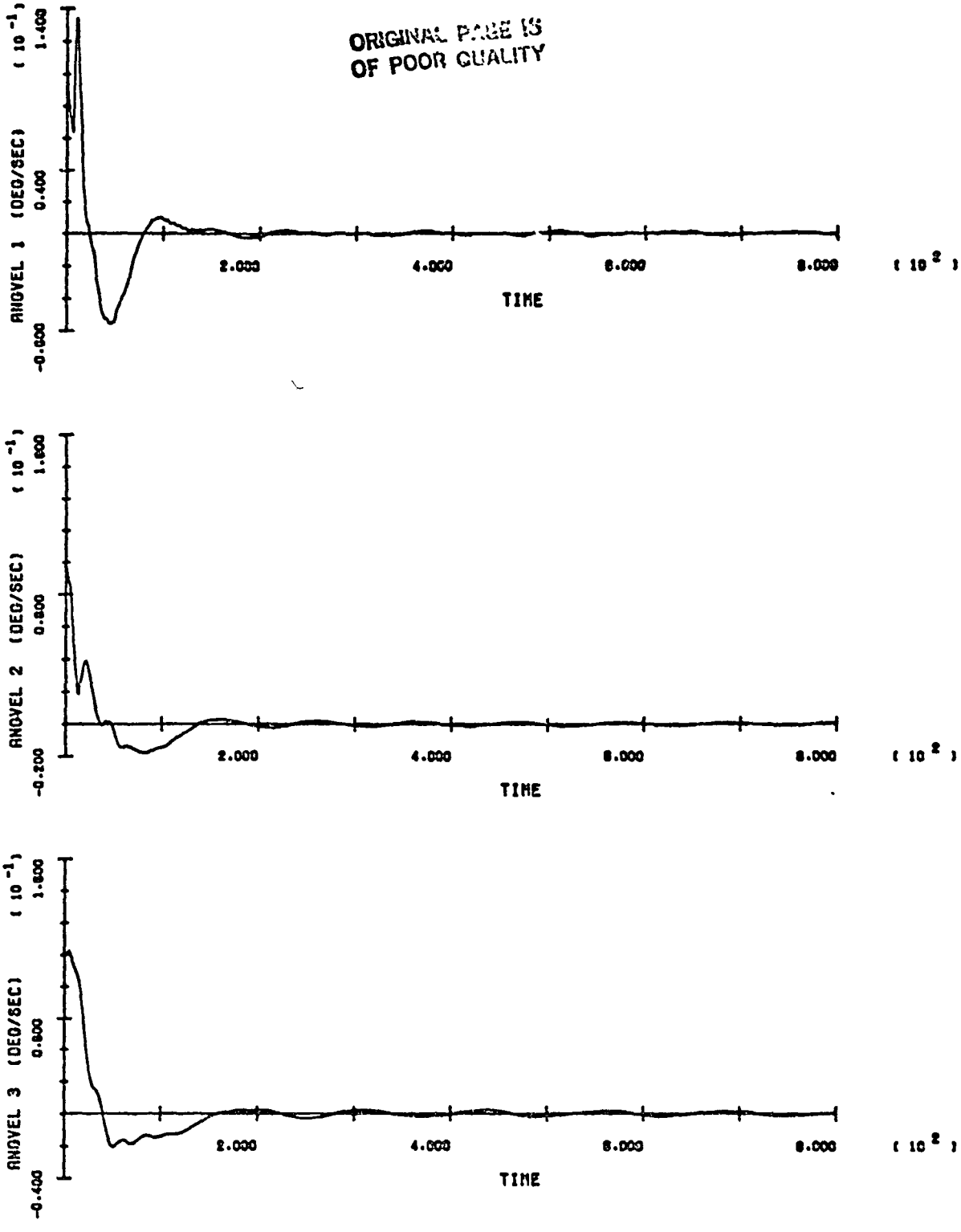


SOC/ORB BERTH - RUN 7

ORIGINAL PAGE IS
OF POOR QUALITY

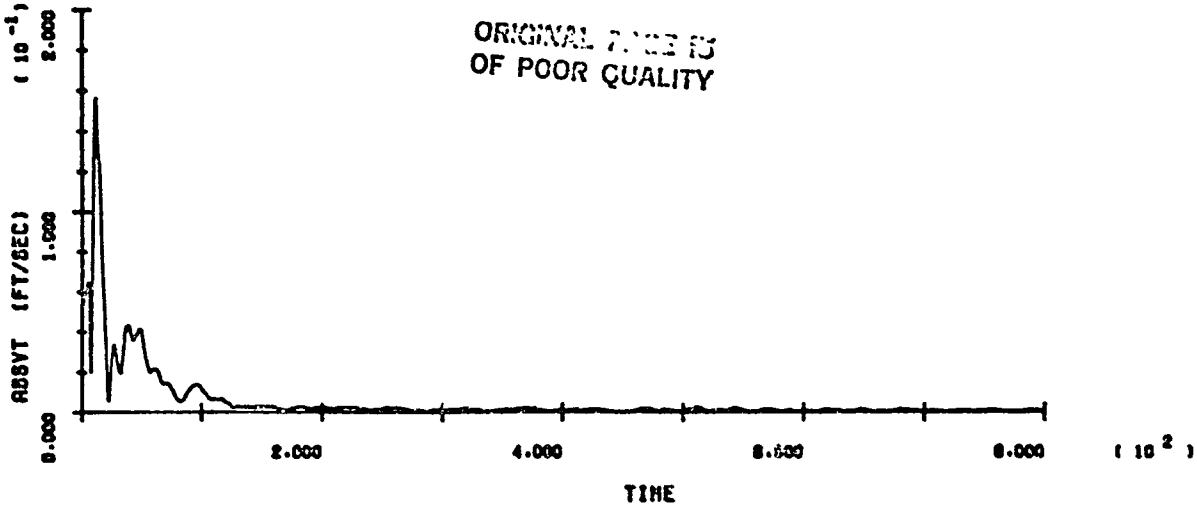


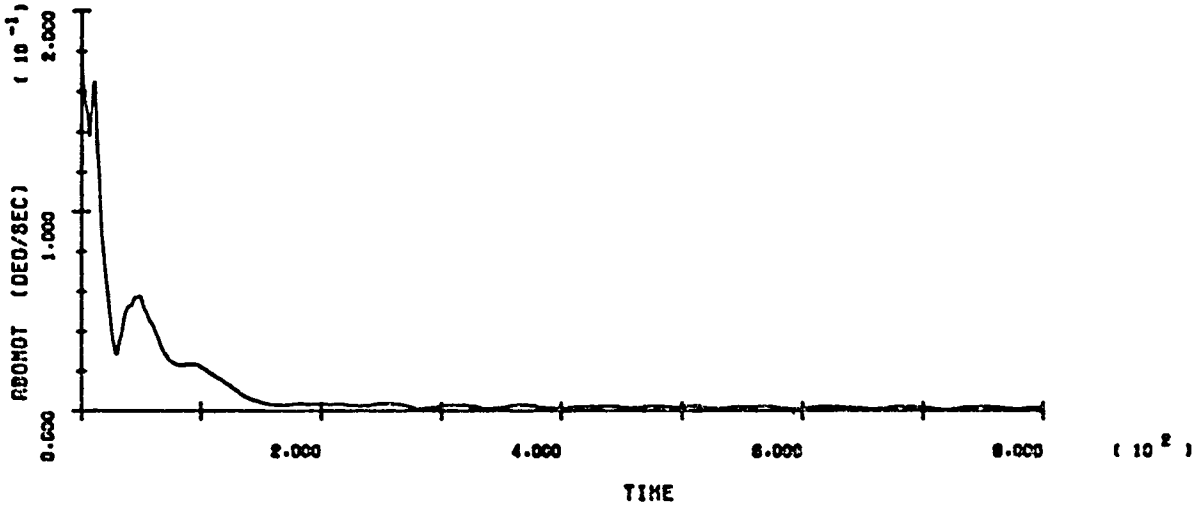


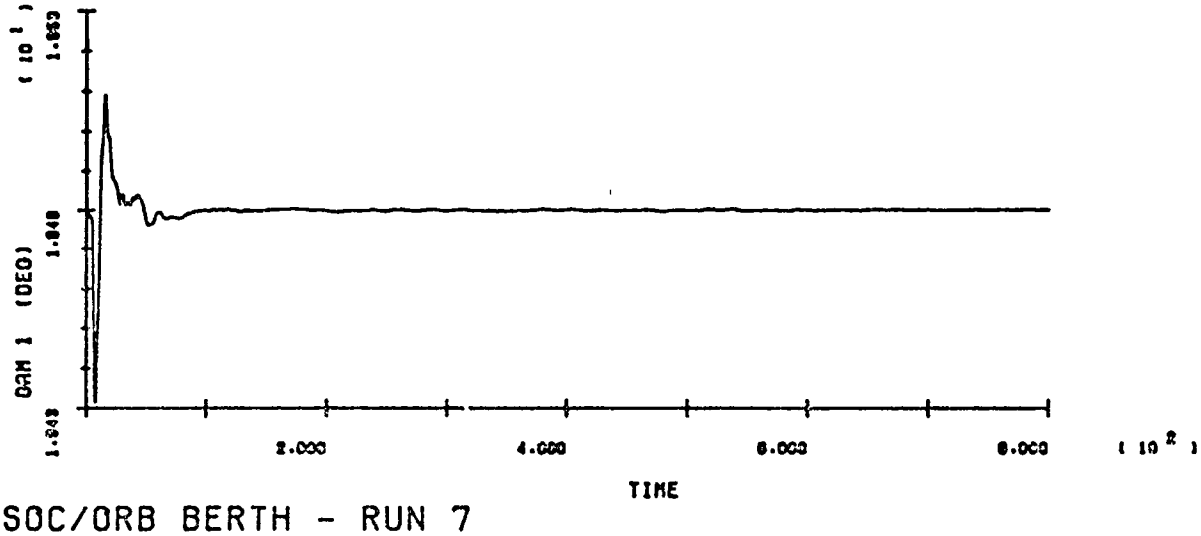


SOC/ORB BERTH - RUN 7

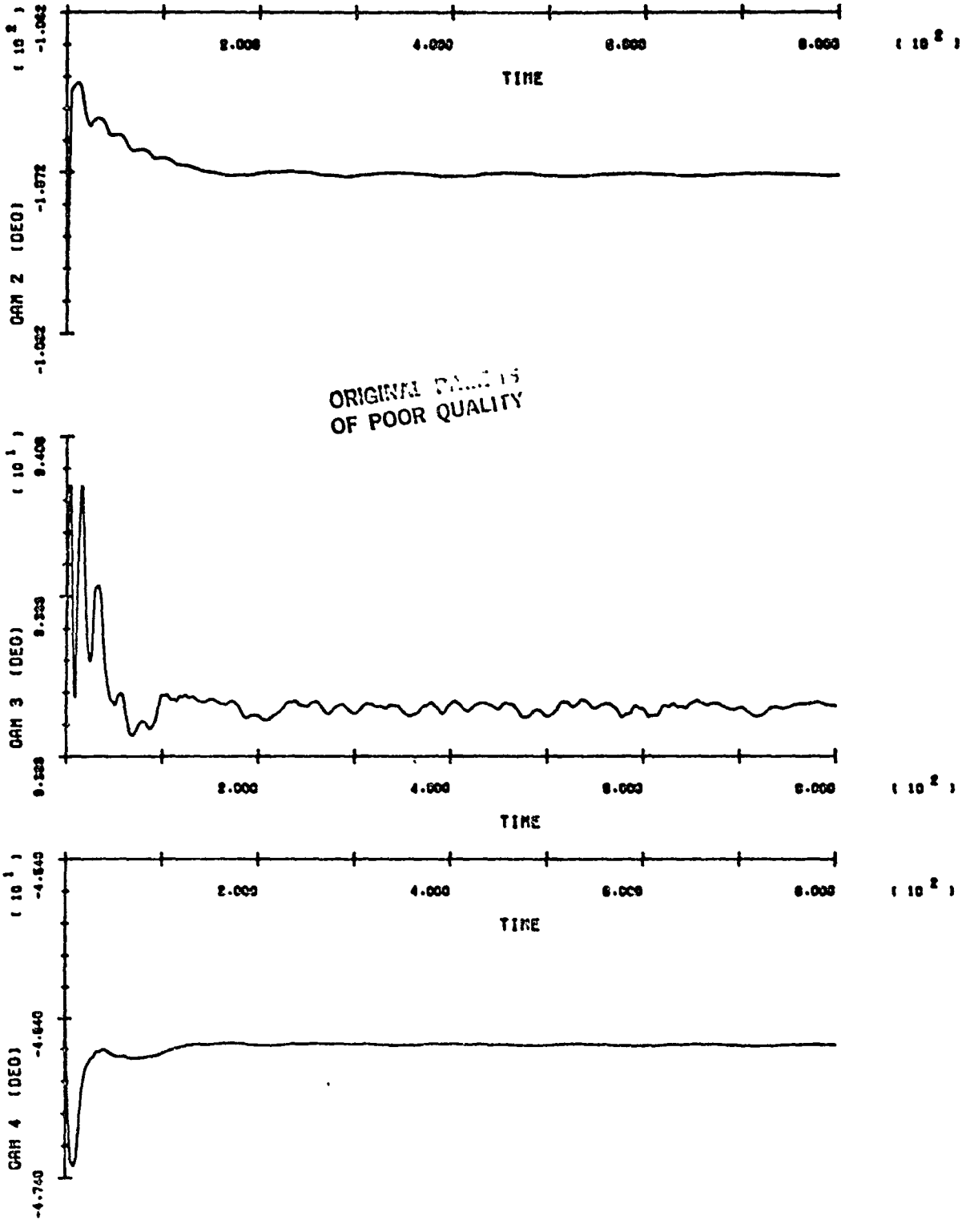


ORIGINAL PAGE IS
OF POOR QUALITY

SGC/ORB BERTH - RUN 7

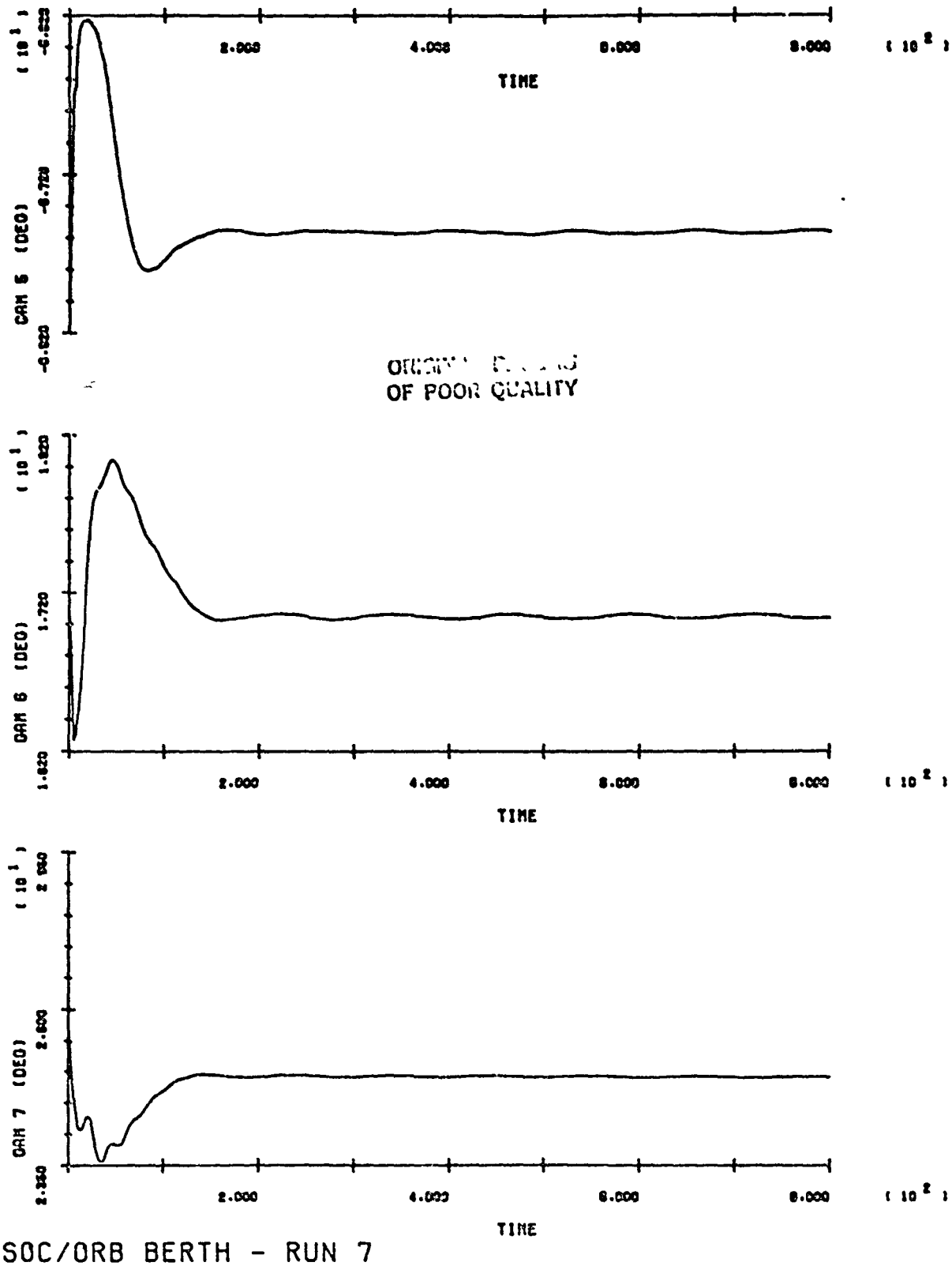


ORIGINAL PAGE IS
OF POOR QUALITY

SOC/ORB BERTH - RUN 7

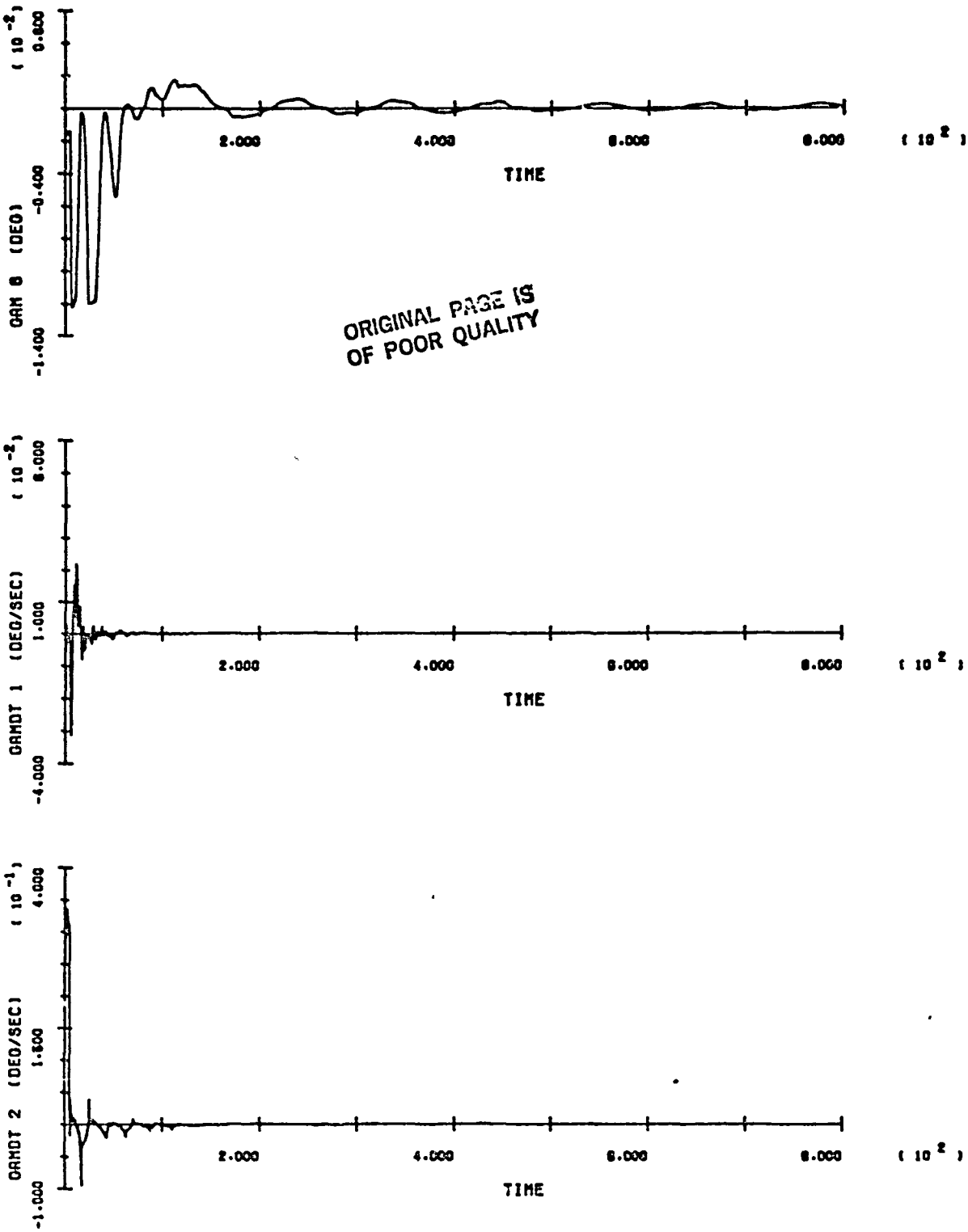


ORIGINAL PAGE IS
OF POOR QUALITY

SOC/ORB BERTH - RUN 7

ORIGINAL PAGE IS
OF POOR QUALITY

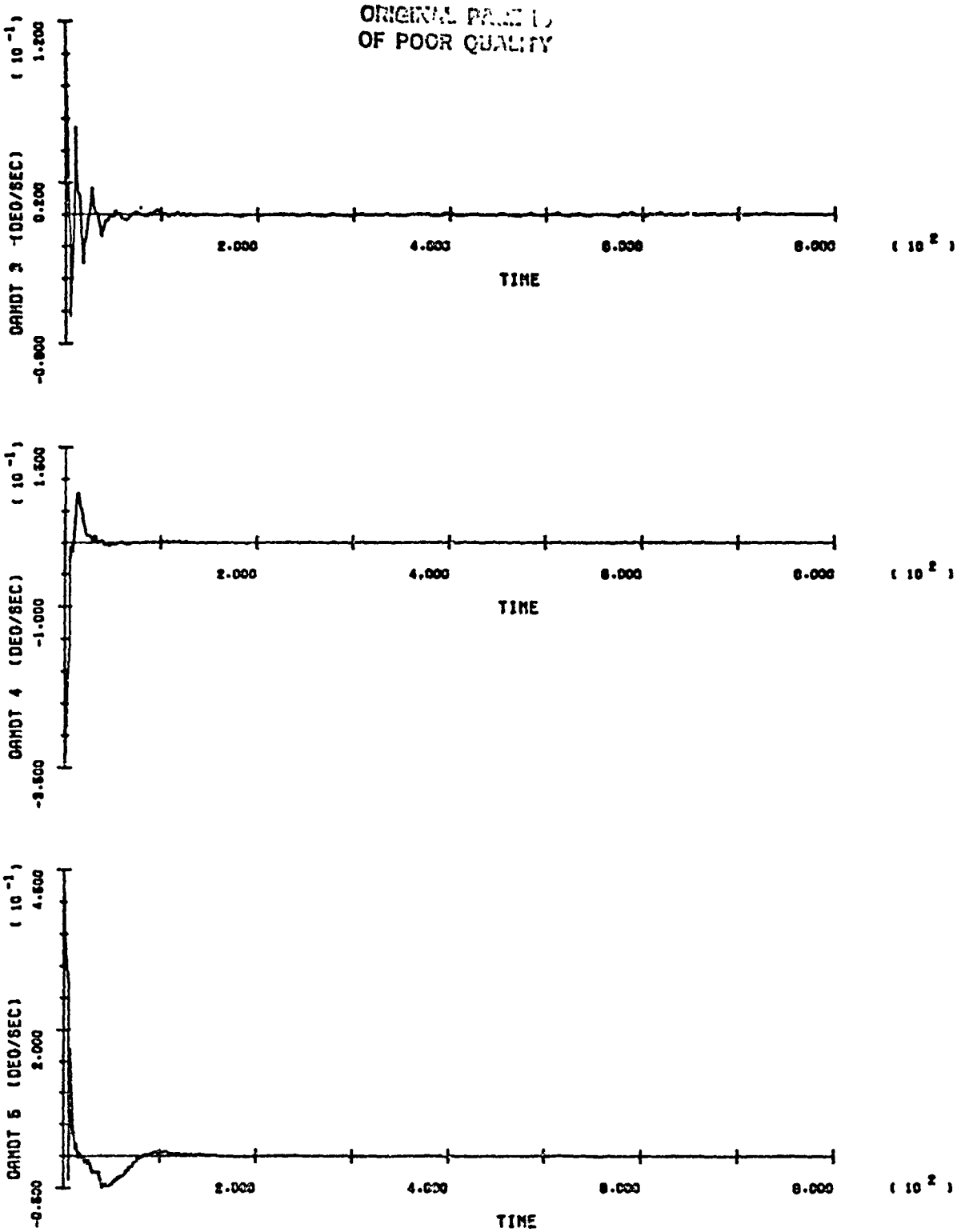


SOC/ORB BERTH - RUN 7

ORIGINAL PAGE IS
OF POOR QUALITY

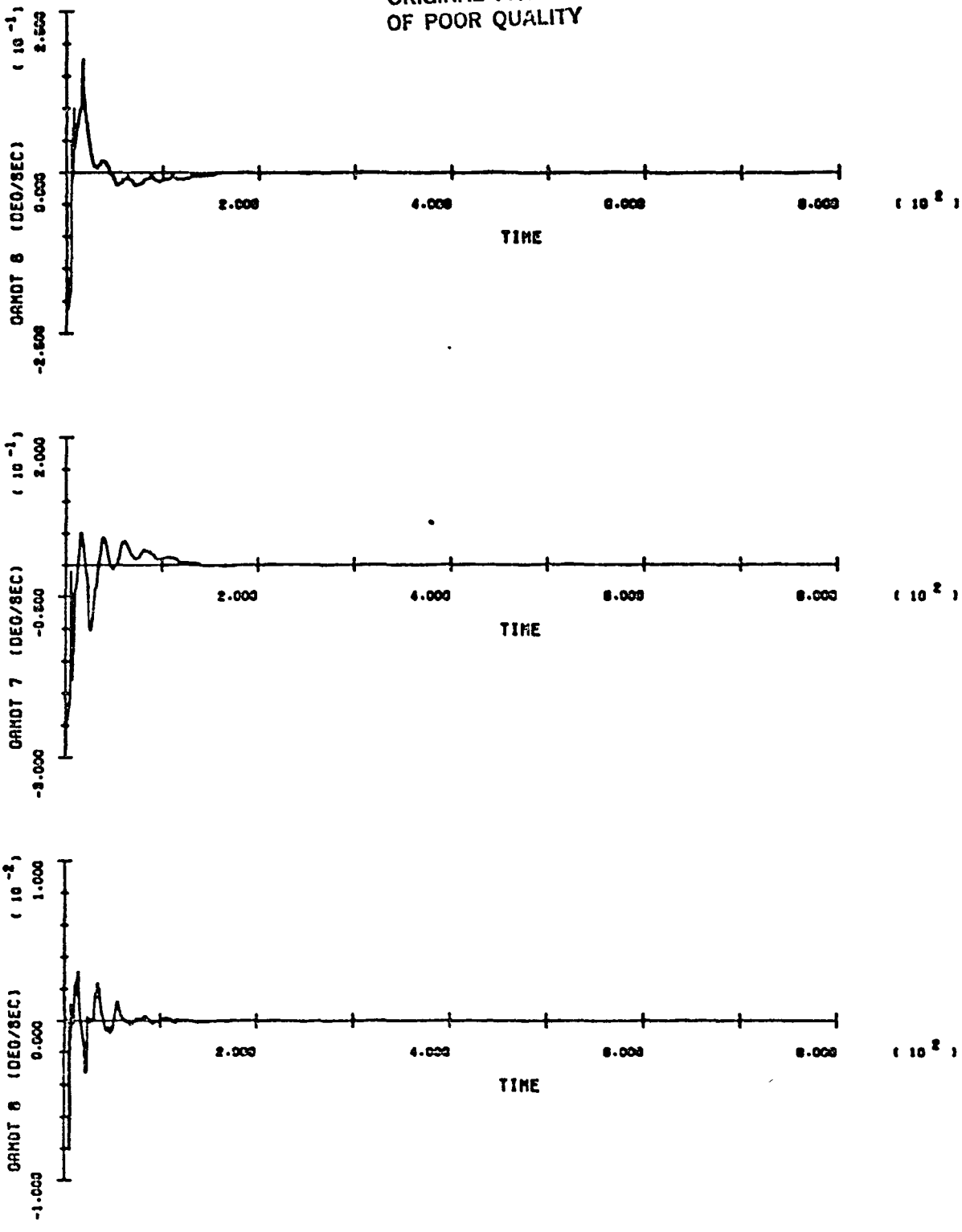


SOC/ORB BERTH - RUN 7

ORIGINAL PAGE IS
OF POOR QUALITY

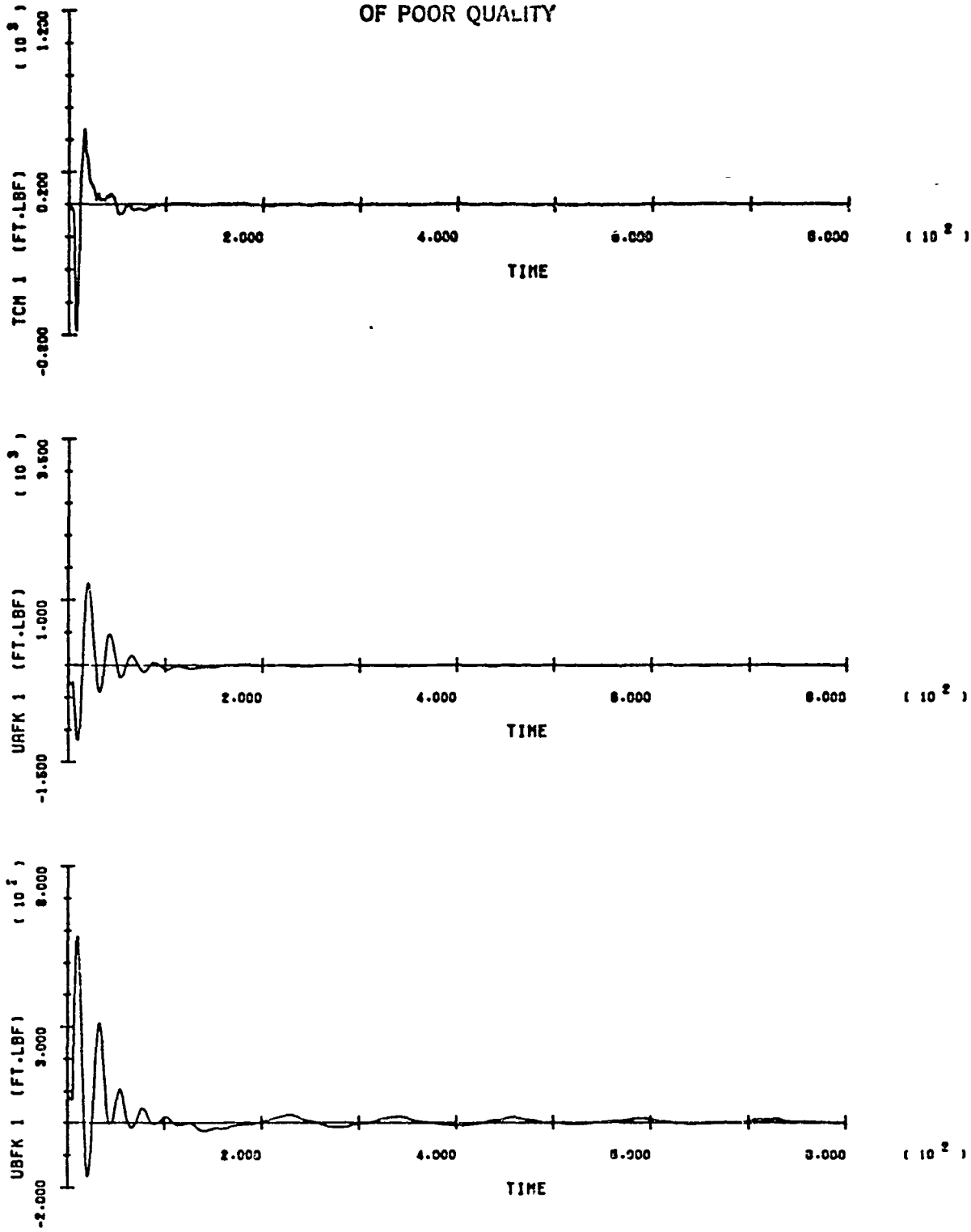


SOC/ORB BERTH - RUN 7

ORIGINAL PAGE IS
OF POOR QUALITY

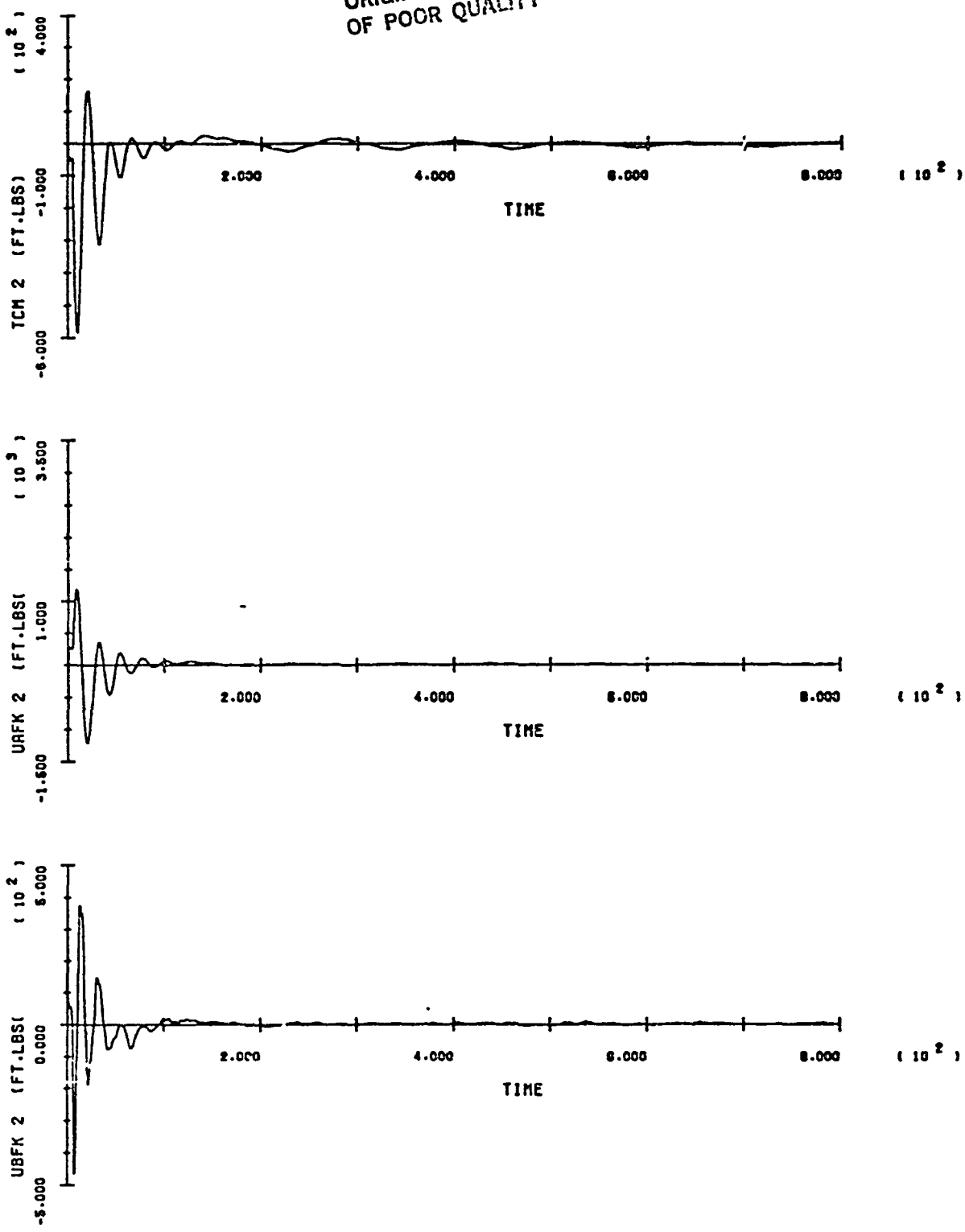


SOC/ORB BERTH - RUN 7

ORIGINAL PAGE IS
OF POOR QUALITY

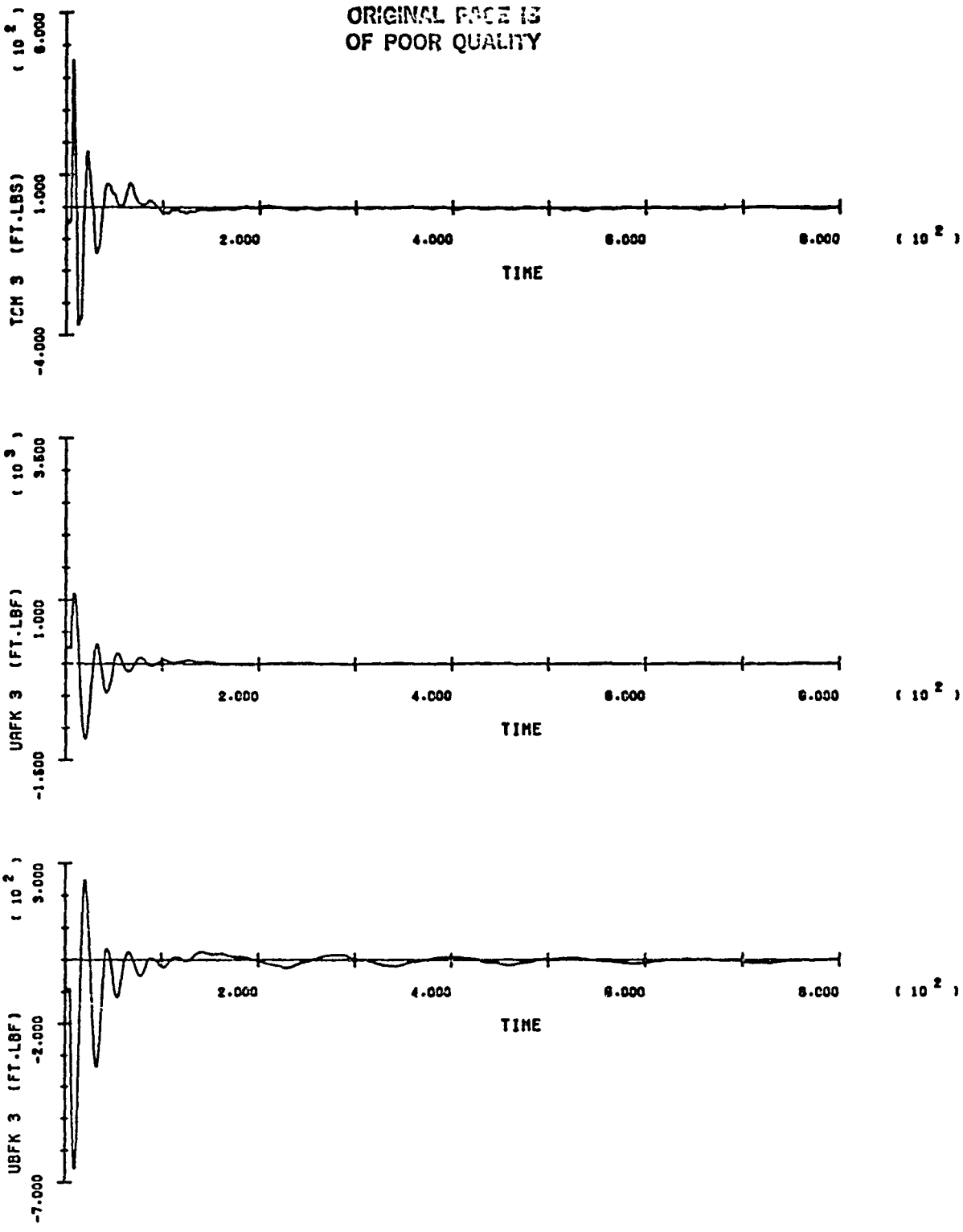


SOC/ORB BERTH - RUN 7

ORIGINAL PAGE IS
OF POOR QUALITY

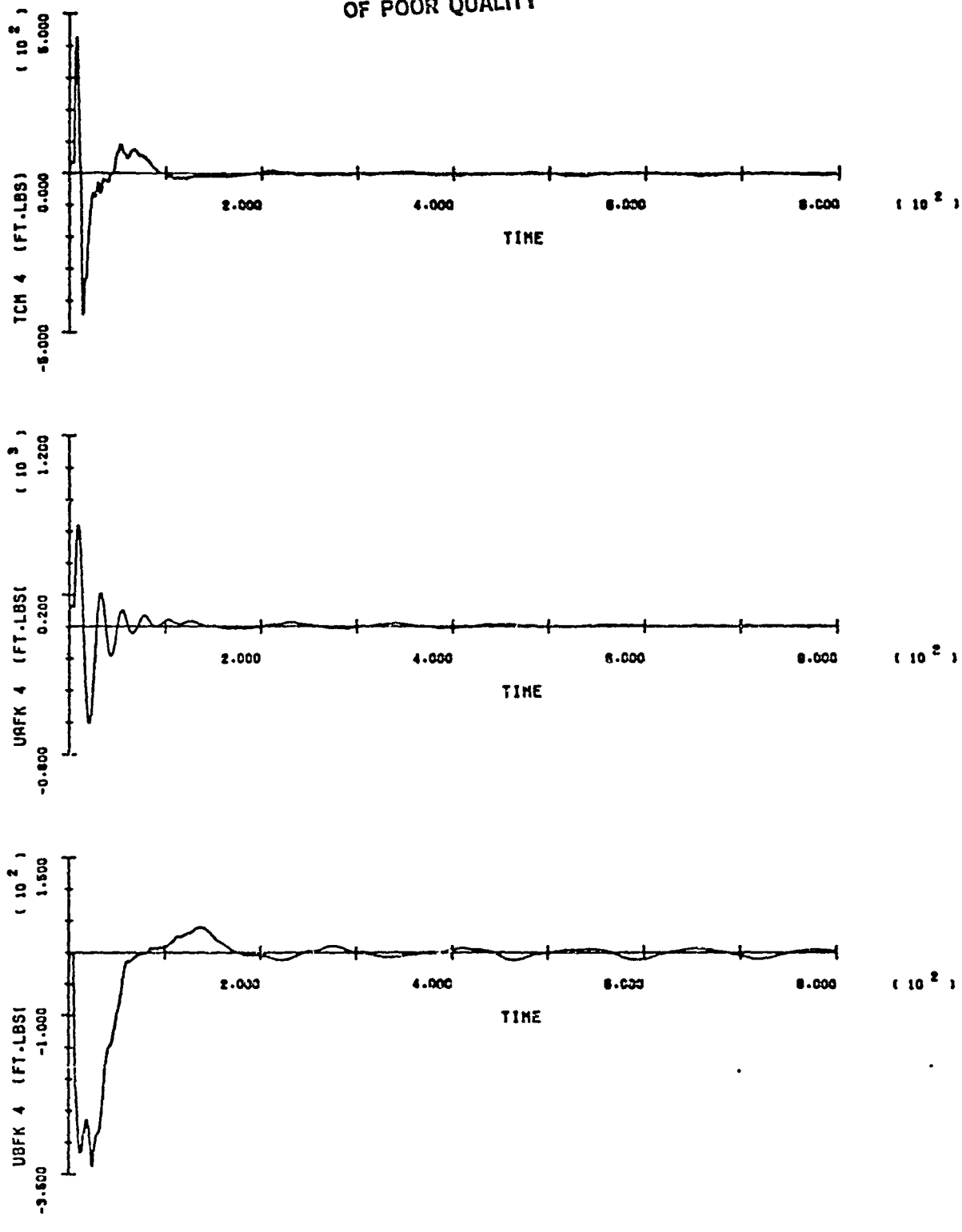


SOC/ORB BERTH - RUN 7

ORIGINAL PAGE IS
OF POOR QUALITY

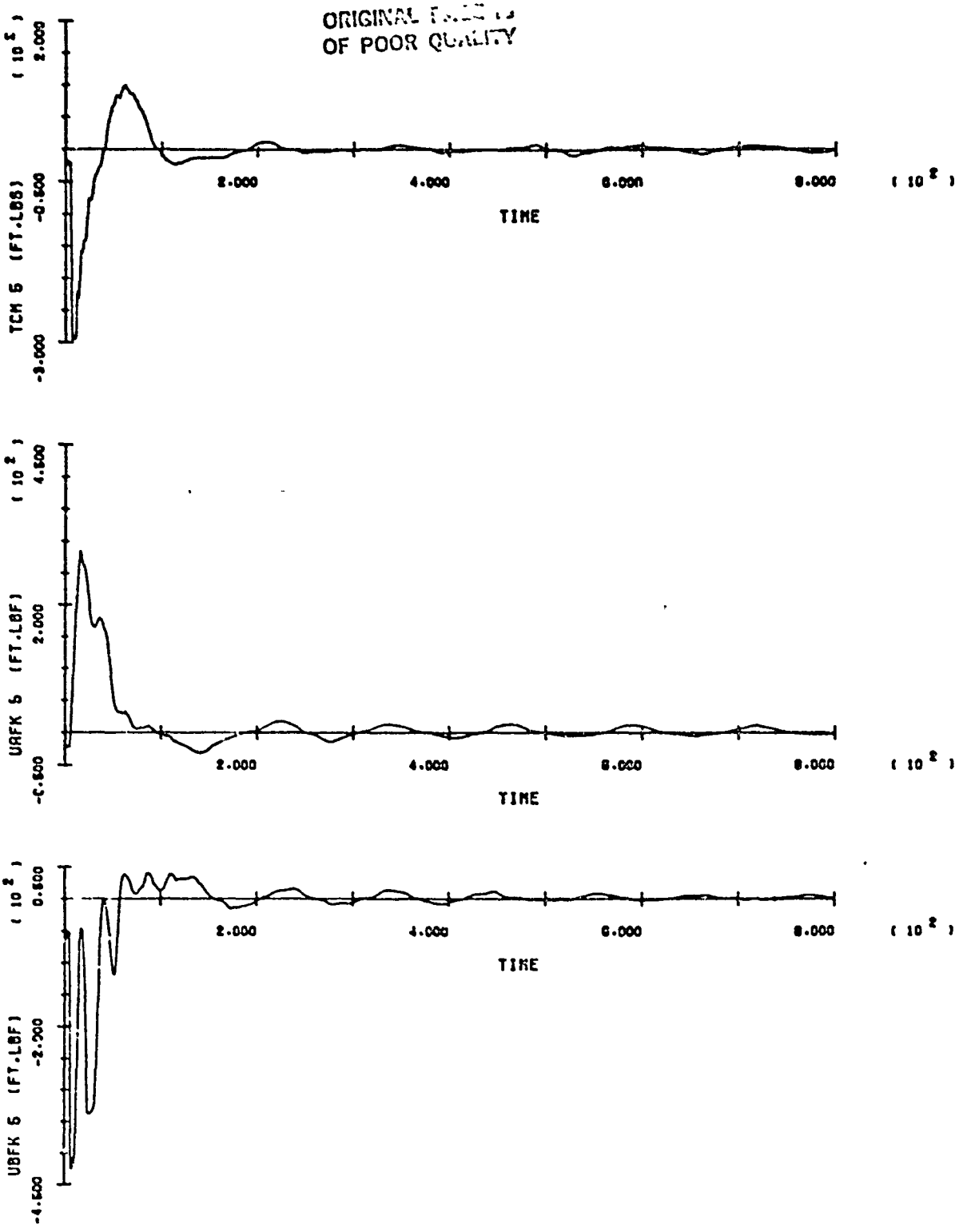


SOC/ORB BERTH - RUN 7

ORIGINAL PAGE IS
OF POOR QUALITY

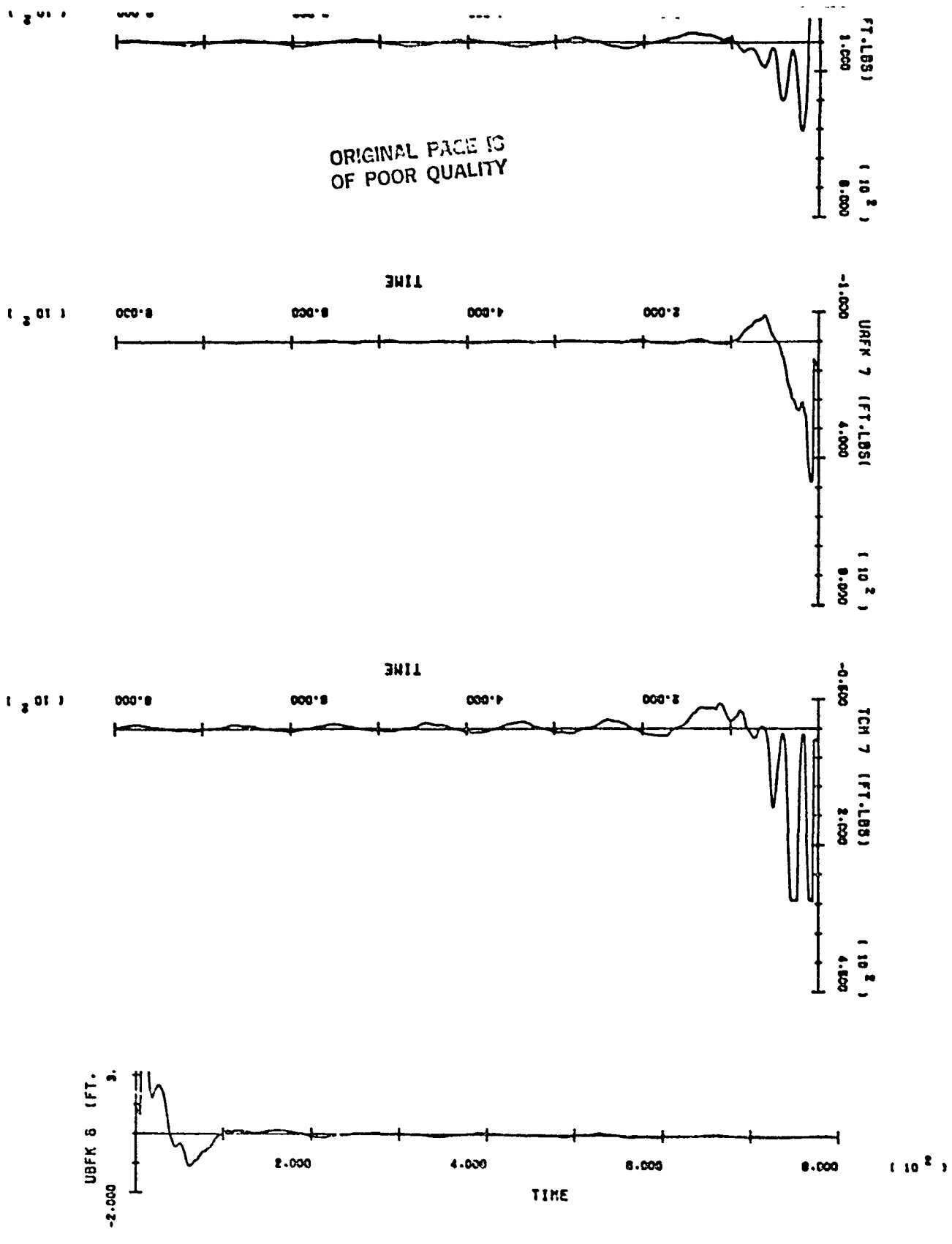


SOC/ORB BERTH - RUN 7

ORIGINAL PAGE IS
OF POOR QUALITY

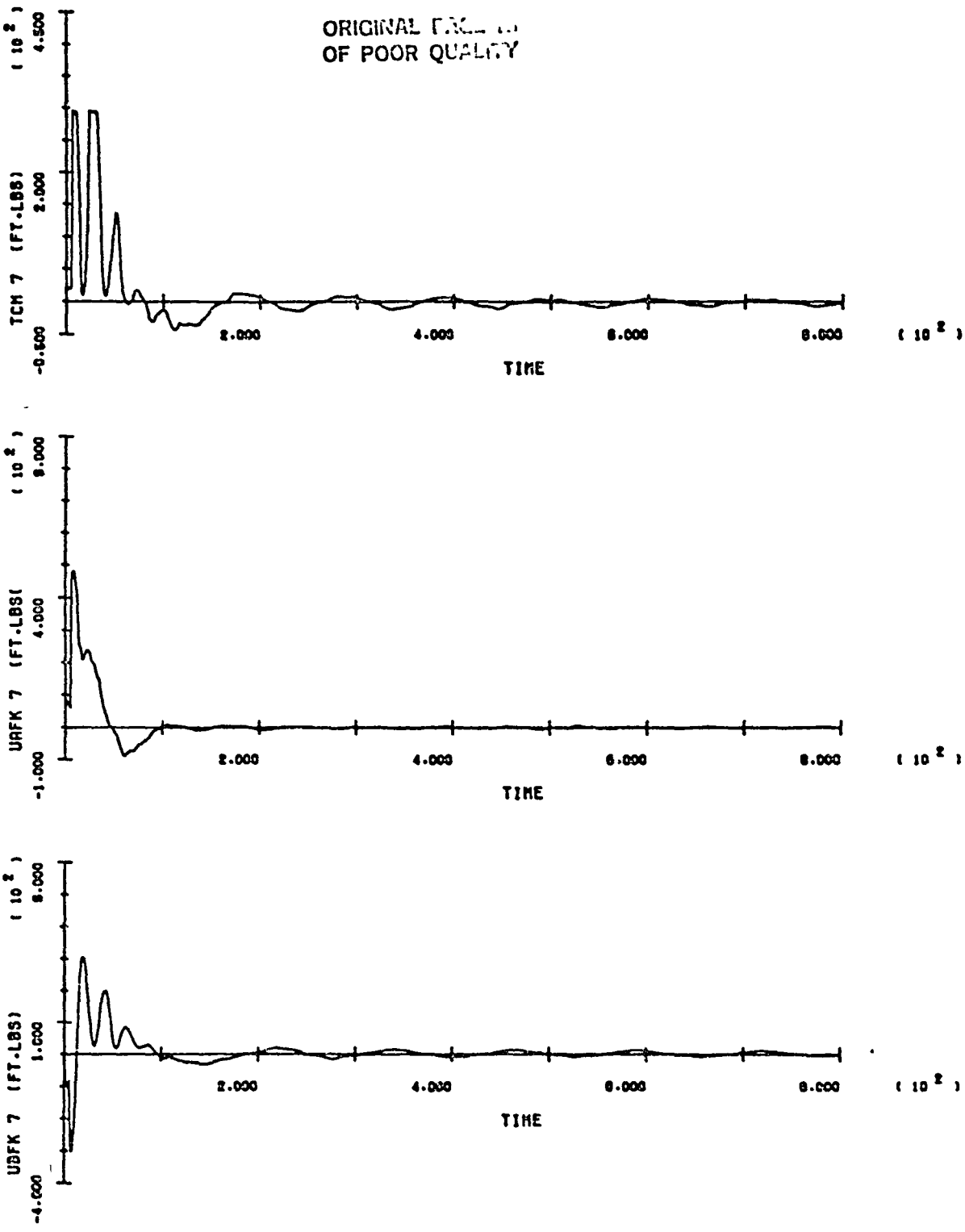


SOC/ORB BERTH - RUN 7

ORIGINAL PAGE IS
OF POOR QUALITY

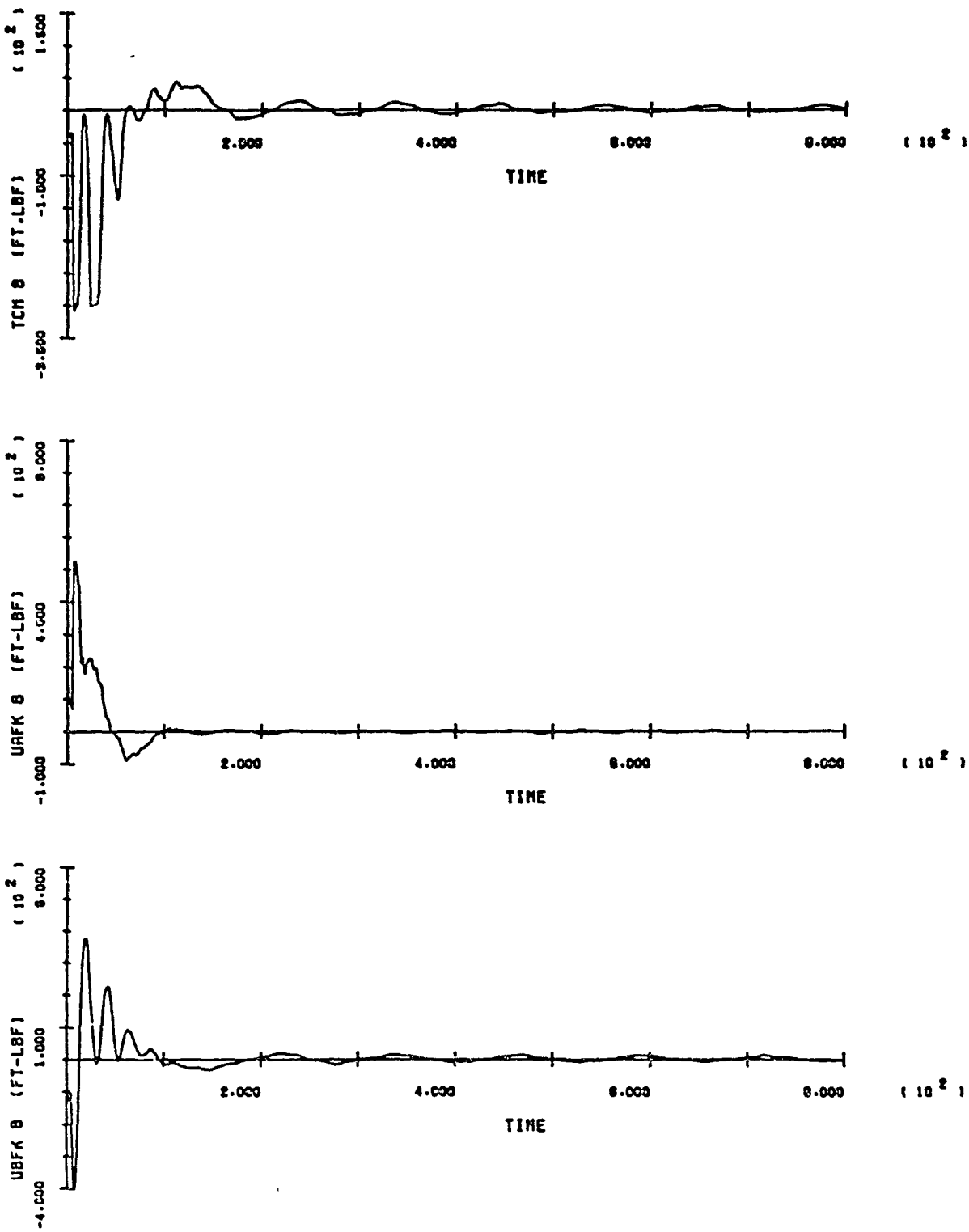


SOC/ORB BERTH - RUN 7

# APPENDIX C

## ON THE ASAD PROGRAM

ORIGINAL PAGE IS
OF POOR QUALITY



At the time of writing this report, the author is in the process of drafing a paper entitled "ASAD - A Non-Real Time Simulation Program for the Shuttle Remote Manipulating System". The paper, to be presented at a July, 1981 conference, contains a short description of the SRMS, ASAD capabilities, assumptions, limitations, software architecture and module description, typical applications and future additions. As such, the author cannot think of a better general description of ASAD. It is hoped that a draft version will be available in time to be made a part of this appendix. If such will not be the case, the paper will be sent as a separate package as soon as possible.

Among the variables plotted and displayed (Appendix B) in this report, there are three Euler angles defining the orientation of $\mathcal{F}_B$ with respect to $\mathcal{F}_I$ (THETA1, THETA2, THETA3). The Euler sequence, bringing $\mathcal{F}_I$ to $\mathcal{F}_B$ is: pitch, then yaw, then roll. At the beginning of each simulation it is assumed that $\mathcal{F}_I = \mathcal{F}_B$. If one denotes the Euler angles by:

$\theta_r$ = Orbiter roll angle (THETA1)

$\theta_p$ = Orbiter pitch angle (THETA2)

$\theta_y$ = Orbiter yaw angle (THETA3)

then the relation between the Euler angular rates and the Orbiter inertial angular velocity $\underline{\Omega}^\circ$ - expressed in $\mathcal{F}_0$ (see Figure A-1) or $\mathcal{F}_S$ - is given by:

$$\dot{\theta}_p = \frac{1}{\cos \theta_y}( \Omega^\circ_y \cos \theta_r + \Omega^\circ_z \sin \theta_r)$$

$$\dot{\theta}_y = \Omega^\circ_y \sin \theta_r - \Omega^\circ_z \cos \theta_r$$

$$\dot{\theta}_r = - \Omega^\circ_x - ( \Omega^\circ_y \cos \theta_r + \Omega^\circ_z \sin \theta_r)$$

ORIGINAL PAGE IS
OF POOR QUALITY



The relative complexity of these relationships is due to the fact that $\dot{\theta}_p$, $\dot{\theta}_y$, $\dot{\theta}_r$ are components in a skewed axis reference frame. If the SRMS manoeuvres 'relatively' small payloads, then $\dot{\theta}_p$, $\dot{\theta}_y$, $\dot{\theta}_r$ are very small angles and the following approximations can be considered:

$$\sin \theta_i \cong 0$$

$$\cos \theta_i \cong 1$$

for i = p, y, r. This approximation is implemented in ASAD. As SOC has large mass and inertia, the Euler angles evolve to significant values; hence the approximation is not valid any more.

Therefore the plotted variables THETA1, THETA2, THETA3 should be regarded as crude approximations.

Fairly precise histories of the Euler angles can, however, be reconstructed from the stored data of all the runs in this report.

# APPENDIX E

## SPAR RMS Berthing Analysis Package

ORIGINAL PAGE IS
OF POOR QUALITY



## SUMMARY

This report has been prepared under R.I. Agreement for Services MIL8GNS-897430M and was jointly funded by Rockwell International Corporation, Downey, California and Spar Aerospace Limited, Toronto, Ontario.

The report is a general feasibility study investigating the use of the Shuttle Remote Manipulator System (SRMS) for berthing the Orbiter at some specially designated station on the Space Operations Centre (SOC). The main investigating tool was ASAD - the SRMS non-real time simulation program developed by Spar. Simulation assumptions, descriptions and results are presented. The report ends with comments on the feasibility of berthing, system limitations and recommendations for future studies.

The report shows that a slightly modified manual mode of operation (Manual Augmented with automatic engagement of Position Hold Mode inhibited) is eminently suited for stopping and manoeuvring payloads with SOC mass and inertia properties. Because the mass of the SOC is well in excess of the upper limit used in the RMS design, the Position Hold Mode is marginally stable or slightly unstable.

It is concluded that, within the assumptions of this study, SRMS-aided SOC/Orbiter berthing is entirely feasible.

ORIGINAL PAGE IS
OF POOR QUALITY



TABLE OF CONTENTS

ORIGINAL PAGE IS
OF POOR QUALITY



## LIST OF FIGURES

END

DATE

FILMED

FEB 18 1983

\

**End of Document**